NTNU – Trondheim
Norwegian University of
Science and Technology

Parameters Governing the Adsorption of Crude and Bunker Fuel Oils to Seawater Suspended Particulate Matter

Lisbet Sørensen

Chemistry

Supervisor: Rudolf Schmid, IKJ
Co-supervisor: Andrew Booth, SINTEF
Alf Glein Melbye, SINTEF

Norwegian University of Science and Technology
Department of Chemistry

Acknowledgements

This thesis is written in collaboration with the Department of Chemistry at NTNU and SINTEF Marine Environmental Technology. It forms a part of the ongoing SINTEF project “Decision support tool for marine oil spills – numerical modelling of fate, and spill response strategies for spilled oil in near-shore water”. The experimental work of the thesis has taken place from September 2011 to March 2012 in the laboratories of SINTEF Sealab in Trondheim.

My thesis would not have reached its completion without the aid of a group of people. First of all, a huge thanks to my supervisors: Andrew Booth, Alf Melbye and Rudolf Schmid. Your talents, knowledge and good humour have inspired me to work through every obstacle I’ve faced during the project work.

Secondly, a warm thanks to the staff at SINTEF Sealab for creating a welcoming environment for me to execute my laboratory practice. I would especially like to thank Marianne Rønsberg, Inger Steinsvik, Kjersti Almås and Siv-Hege Vang for giving me the needed training in the use of instruments, procedures and analytical software. I would also like to thank Trond Nordtug and Anders Olsen, who have developed the oil-droplet generator and provided support during my use of it.

Thirdly, I need to thank all my fellow master students at the Department of Chemistry. Annie, Ingvill, Mari, Marte, Mona, Rune and Stine; I will remember you as my excellent partners in conversation, frustration and procrastination.

At last, a special mention of my parents, who taught me that the only thing separating failure and success, is the power of will.

Gløshaugen, May 15 2012

Lisbet Sørensen

Abstract

In this study, parameters influencing the adsorption of dispersed oil droplets to suspended particulate matter (SPM) in seawater were investigated. The interaction between oil and SPMs can alter the ultimate fate of oil spilled in marine environments, and it is therefore of interest to be able to predict the effect of these interactions. The chosen parameters of this study were sediment type (carbonate sand, quartz sand and clay) and concentration (5-80 g/L seawater), temperature (5-20 °C) and oil type (two crudes, one condensate and a heavy fuel oil). Special attention was given to the effect of adding chemical dispersant to the oil prior to mixing with water and SPMs.

The experimental outline included the mechanical generation of oil droplets using an oil droplet generator. Water with oil droplets were added to a beaker with sediment and a suspension was induced by stirring. After settling and filtration, both the water samples and the sediment samples were subject to extraction, clean-up and analysis by GC-FID. A selection of samples was also analysed by GC-MS.

The study shows that oil droplets adsorb as a bulk to SPM. An absence of water-soluble oil components adsorbed to the sediment was observed. Oil type, sediment size and the use of chemical dispersant stand out as most influencing on the adsorption properties of oil droplets to SPM in seawater. The effect of varying temperature was not considerable compared to the other parameters in this study. Partitioning of oil components to the water column was also monitored in this study, and found not to be influenced significantly by any of the studied parameters.

Sammendrag

I denne studien ble det undersøkt hvordan en rekke parametre ville påvirke adsorpsjon av oljedråper til suspendert partikulært materiale (SPM) i sjøvann. De undersøkte parametrene var sedimenttype (karbonat sand, kvartssand og leire) og konsentrasjon (5-80 g / L sjøvann), temperatur (5-20 °C) og oljetype (to råoljer, et kondensat og en bunkerolje). Spesiell oppmerksomhet ble viet effekten av å behandle oljen med kjemisk dispergeringsmiddel før interaksjon med SPM.

Den eksperimentelle prosedyren inkluderte bruk av en oljedråpegenerator som dispergerte olje mekanisk i sjøvann. Sjøvann med oljedråper ble tilsatt i et begerglass med sediment, og en suspensjon ble indusert ved omrøring. Etter sedimentering og filtrering, ble både vannprøver og sedimentprøver ekstrahert og renset opp. Alle ekstrakter ble analysert ved hjelp av GC-FID. Et utvalg prøver ble også analysert på GC-MS.

Studien viser at oljedråper adsorberes som en bulk til SPM. Fravær av vannløselige komponenter i den sedimentadsorberte fraksjonen ble observert. Oljetype, sedimentstørrelse og bruk av kjemisk dispergeringsmiddel var de parametrene som hadde størst påvirkning på oljedråpenes adsorpsjonsegenskaper til SPM i sjøvann. Effekten av temperaturvariasjoner var ikke betydelig i forhold til de andre parameterne i denne studien. Oppløsning av oljekomponenter i vannsøylen ble også overvåket, men studien viser ingen betydelig effekt av de undersøkte parametrene på konsentrasjonen av oljekomponenter i vannsøylen.

Table of contents

List of abbreviations

A	Area, Analyte
CEN	European Committee for Standardisation
DCM	Dichloromethane
DHNRT	Deepwater Horizon Natural Resource Trustees
DOR	Dispersant to oil ratio
ESGOSS	Ecological Steering Group of the Oil Spill in Shetland
FID	Flame ionization detector
GC	Gas chromatography
HFO	Heavy fuel oil
ITOPF	International Tanker Owners Pollution Federation
LLE	Liquid-liquid extraction
MS	Mass spectrometry
MSD	Mass selective detector
m/z	Mass/charge
pA	Pico ampere
PAH	Poly aromatic hydrocarbons
RIS	Recovery internal standard
RRF	Relative response factor (for a given oil)
PTFE	Polytetrafluoroethylene
SIM	Selective ion monitoring
SIS	Surrogate internal standard
SPE	Solid phase extraction
SPM	Suspended particulate material
SVOC	Semi-volatile organic compounds
TEOC	Total extractable organic compounds
THC	Total hydrocarbons
UCM	Unresolved complex mixture
WAF	Water accommodated fraction
WCOT	Wall coated open tubular
WSF	Water soluble fraction

1 Introduction

1.1 Oil spills

Oil may enter the environment from both natural and anthropogenic sources. The largest proportion of petroleum entering the environment comes from natural sources (Wang and Stout 2007). However, the International Tanker Owners Pollution Federation (ITOPF) report that accidental oil spills have released approximately 5 700 000 tons of oil into our seas since the 1970's (ITOPF, 2011).

ITOPF has collected data on oil spills worldwide since the 1970's and now hold a database including more than 10 000 incidents. The data clearly indicate an improvement over the decades, demonstrating how the number of major (>700 tons) and medium (7-700 tons) oil spills have declined (Figure 1.1).

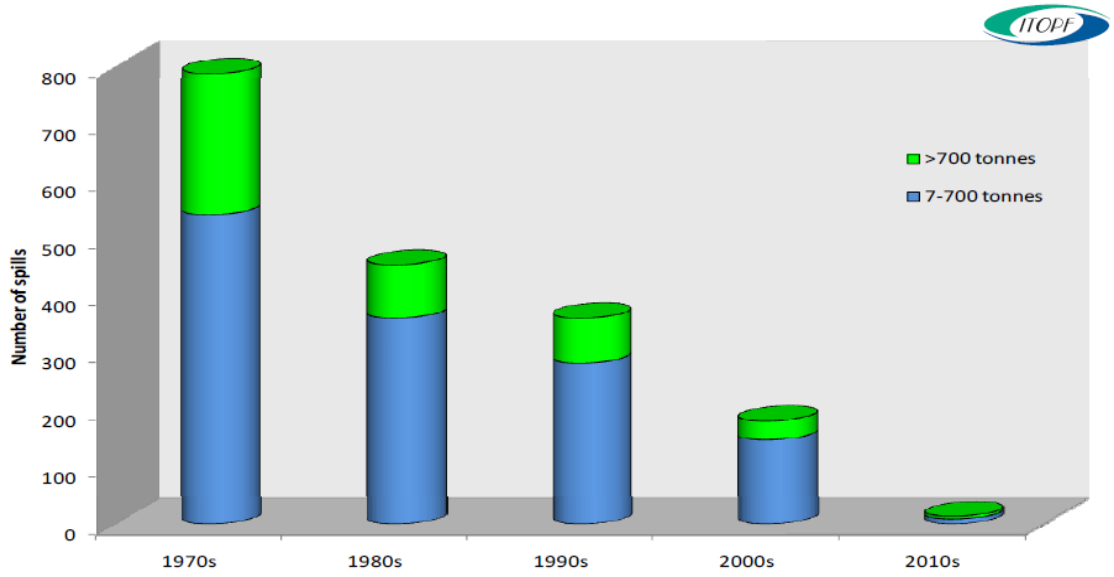

Figure 1.1 - Major and medium oil spill incidents since the 1970's (http://itopf.com/information-services/data-and-statistics/statistics/index.html, Accessed 23.03.12)

During the years 2000-2009, a total of 211 000 tons of oil was spilled at sea. In 2010 12 000 tons were spilled, representing four different large-scale releases from vessels. This does not include the Deep Water Horizon disaster in the Gulf of Mexico, where it is estimated that nearly 800 million litres of oil were spilled during a underwater blow-out (DHNRT, 2011).

2011 represents a historical low, with only one major oil spill incident recorded, and the amount of oil spilled 1 000 tons (ITOPF, 2011)

Sizeable oil spill events receive broad media coverage due to the possible environmental implications, e.g. on the local fauna. It is evident that pictures such as Figure 1.2 and 1.3 will evoke interest and emotions in the public.

Figure 1.2 - Bird covered in oil (http://oilgastrends.com/wp-content/uploads/2011/06/oil-spills-effect-on-bird.jpg)

Immense recovery operations are often necessary to restore the shoreline after an oil spill. The picture in Figure 1.3 is shot during the clean-up after stranding of oil from the shipwreck of the tanker Server in Fedje, Norway in January 2007. It is obvious that having correct and efficient countermeasures is important to preserve wildlife and economic interests in exposed areas.

Figure 1.3 - Oil spill on shoreline after the 2007 Server incident in Norway (http://www.aftenposten.no/migration_catalog/article5841707.ece/BINARY/w780/DSC_0057.jpg)

Oil spilled at sea may have a number of “final destinations”. The worst case scenario is often identified as the stranding of oil on shorelines, with the damage to beaches, fauna and human installations this might cause. However, the dissolution and dispersion of oil into the water column (as droplets or individual components) or the sedimentation of oil to the bottom sediments on the seafloor may also cause severe damage on marine eco-systems (Carls et al., 2008, Ho et al., 1999, Neff et al., 1976) .

1.1.1 Concerns for the Norwegian coastline

Despite the statistically declining risk of a major oil spill occurrence, there are growing concerns for acute spills along the Norwegian coastline. This is due to the observed increase in ship traffic during the last decade. Special concern is linked to the increasing number of vessels from Russia, transporting crude oil along the entire Norwegian coast. Also, oil production platforms are now being installed closer to shore and oil resources are explored in deeper water and farther north (closer to ice-covered areas) than before, thus increasing the risk of severe spill incidents (Daling et al., 2002).

The effective length of the Norwegian coastline, characterized by its long fiords, archipelago and islets, is vast. Due to Norway being sparsely populated, the local infrastructure of coastal regions may often be insufficient in the case of a major oil spill event demanding fast response and extensive allocation of personnel and supplies (Daling and Brandvik, 2010).

1.1.2 Oil spill modelling – predicting the fate of oil spills

It is desirable to be able to predict the fate of oil spilled at sea in order to choose the correct means of oil spill response, both for operation at sea and for shore-line clean-up. Also, the forecasting of oil spills is important to be able to assess the environmental impact they might lead to. Numerical oil spill models have been developed, and are used to predict the fate, and hence the impact, of present and future oil spills (Reed et al., 1995).

A numerical model is based on the experience gained in a series of bench-scale studies, some meso-scale studies and a few full scale studies. As many parameters as practically possible are varied, in order to be able to model any kind of spill situation (Daling and Strøm, 1999).

When planning oil spill response strategies one must often compromise between what is most ecologically and economically beneficial. A relatively new approach, the use of chemical dispersants to break up surface oil slicks is regarded as a cost-efficient response method (Li et al., 2009). But there is still need for a deeper understanding on how dispersants and dispersed oil droplets will behave in the marine environment (Fingas, 2011).

1.2 Weathering of oil

When oil is spilled at sea, it will undergo numerous chemical, physical and biological processes. These processes are collectively referred to as weathering. The most important weathering processes include spreading, evaporation, dissolution, dispersion into the water column, water-in-oil emulsification, photochemical oxidation, microbial degradation, adsorption to suspended particulate matter and stranding on the shore or sedimentation to bottom sediments (Wang and Stout, 2007). Figure 1.4 describes these processes. The processes marked with yellow are of importance to this study.

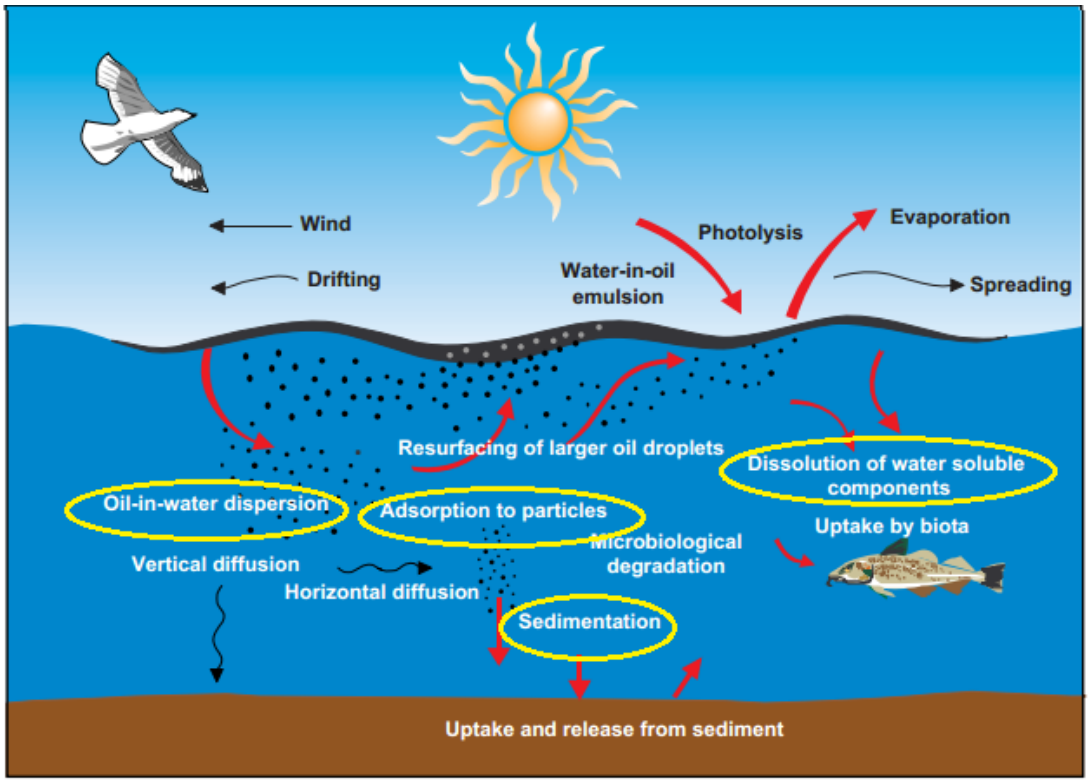

Figure 1.4 - An overview of processes that influence the weathering of oil at sea (SINTEF Materials and Chemistry).

Evaporation and dissolution will significantly alter the composition of the oil, as volatile and water-soluble components are lost from the bulk. Along with emulsification, these processes will also alter the physical properties of the bulk oil, such as its density and viscosity, and this will affect its further fate in the environment.

The time-scale of domination of different weathering processes' varies greatly. Evaporation will affect the spill immediately and remain an important factor for the time span of a few days to a couple of weeks. At the other extreme, microbial degradations is slow and can be of influence several years after the spill incident (Wang and Stout, 2007).

Some processes (e.g. spreading) do not directly alter the composition of the oil, but will influence on the rate of other processes. When making an oil spill model (see Chapter 1.1.2), it is important to consider all relevant weathering processes, that can alter the fate of oil in the environment (Daling and Strøm, 1999). In the following sections, the dispersion and sedimentation of oil is reviewed.

1.3 Dispersion of oil

1.3.1 Natural dispersion of oil

One of the most significant natural processes that affect oil spilled at sea is *mechanical dispersion* into the water column. Oil spills often coincide with poor weather conditions. Heavy wind causes turbulent conditions at the sea surface (wave action) and this might lead to the breaking up of oil slicks into small droplets (<100 µm). These droplets become dispersed into the water column (Muschenheim and Lee, 2002). As a consequence of dispersion, the surface area of the oil increases and this makes the rate of other weathering processes increase (Venosa and Holder, 2007, Fiocco and Lewis, 1999, Chapman et al., 2007).

1.3.2 Chemical dispersion and dispersants

Chemical dispersants especially designed to disperse oil slicks have been developed and become a part of current oil spill response strategies. The aim of the dispersant is to prevent the surface oil reaching coastlines by dispersing it in the water column.

The application of chemical dispersants to an oil slick will result in the formation of more oil droplets and droplets of reduced size, when compared to naturally/mechanically dispersed oil (Khelifa et al., 2008, Li et al., 2007, Li and Garrett, 1998, Li et al., 2009).

Studies have seen that oil treated with dispersants more easily biodegraded than un-treated oil. A plausible explanation for this observation is the reduction in oil droplet size (increase in surface area) (Zahed et al., 2010, Venosa and Holder, 2007, Swannell et al., 1997).

Due to rapid dilution, dispersed oil droplets have not been observed to have significant detrimental effects on marine organisms. In the case of minor effects, biological recovery has been rapid. The maximum observed concentration of oil in water after dispersion is 10-40 ppm (close to the surface). It is not observed that chemically dispersed oil sink (Lessard and DeMarco, 2000).

The chemistry of dispersants

Chemical dispersants used in oil spills are a mixture of surfactant in a solvent, and therefore not so different from any household detergent (see Figure 1.5).

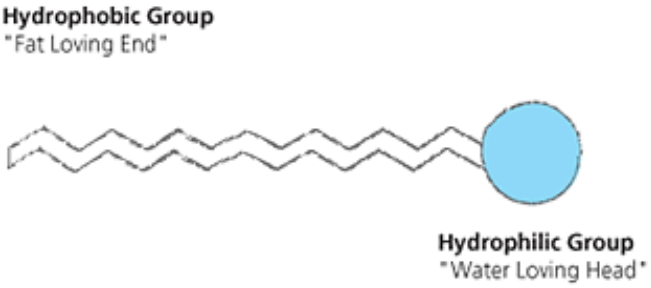

Figure 1.5 - Surfactant molecule, with a long hydrophobic, unpolar chain and a hydrophilic polar "head". (http://www.scienceinthebox.com/en_UK/glossary/surfactants_en.html)

Common solvents for the dispersant surfactants include water and glycol. The solvents function is to behave as a liquid carrier for the surfactants. The percentage of solvent to surfactant ranges from 20-80 % (Fingas, 2011, Lessard and DeMarco, 2000, Fiocco and Lewis, 1999).

How does dispersants work?

Figure 1.6 illustrates what happens when a dispersant is sprayed on an oil slick. The dispersant reduces the surface tension of the oil and stabilizes the formation of droplets, normally sized 10-15 µm (Fingas, 2011, Lessard and DeMarco, 2000, Fiocco and Lewis, 1999).

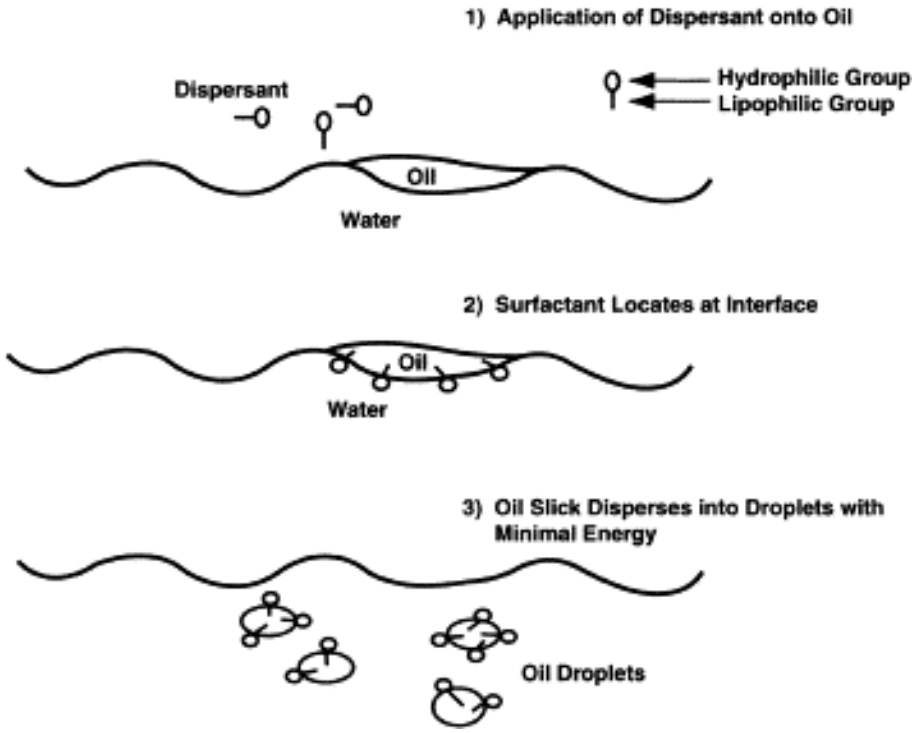

Figure 1.6 - Dispersant effect on oil slick. 1) Oil and water do not mix. Dispersant is added 2) Dispersant surfactants align along the oil-water interface with polar end in water. 3) Oil slick is dispersed as droplets stabilized in the water by the surfactants (Lessard and DeMarco, 2000).

In the case of an oil spill, the decision to apply oil spill dispersants must be determined by a Net Environmental Benefit Analysis (NEBA), which is defined as follows (Fiocco and Lewis, 1999, Daling et al., 2002):

"Weighing of advantages and disadvantages of alternative oil spill responses for all aspects of environmental effects compared with no response."

Historically, oil spill dispersants have not been used much. This is due to potential ecological damage caused by overdose treatments and the use of dispersants those themselves proved to be toxic. Through the development of better products, it has become more accepted to use dispersants over the last ten years. In addition to being less toxic, the "new" dispersant are also more effective (less dispersant per amount of oil necessary). More efficient tools for application (e.g. from vessels or plain) have also been developed (Daling et al., 2002). Normal dosage of dispersant today is 1-5 % of the oil slick (Fiocco and Lewis, 1999). The

efficiency of chemical dispersants has been shown to be related to the dispersant type, water temperature, oil type and weathering degree of the spilled oil (Fingas, 2011, Li et al., 2010). Dispersants have been used with great success in several events, amongst them the Sea Empress incident in the UK in 1996 (Lessard and DeMarco, 2000).

1.4 Sedimentation of oil

There are three different routes that may lead oil to sink and be incorporated into bottom sediments. Firstly, if weathering processes make the oil's density exceed 1 g/L, the oil will submerge and sink. Secondly, the oil can be ingested by organisms and transported to the bottom by these. Thirdly, oil can interact with suspended particulate materials (SPM) to form agglomerates and sink when the combined density of oil and particulates is high enough (Boehm et al., 1982). Sedimentation of oil has been observed empirically after several oil spill incidents, and two cases are presented here.

Tsesis oil spill (1977)

The tanker Tsesis grounded in the Swedish archipelago on 26 October 1977 and spilled 300 tons of fuel oil into the environment. It has been estimated that 10-15 % of this oil was incorporated into bottom sediments by sedimentation with suspended particulates (Boehm et al., 1982, Johansson et al., 1980, Payne et al., 2003). Studies by Johansson et al. (1980) and Boehm et al. (1982) demonstrated that the sedimentation of the oil impacted both the weathering rate of the oil (increased) and the negative impact on organisms, which was lower than expected.

Braer oil spill (1993)

On 5 January 1993, 85 000 tons of Gullfaks crude oil was spilled off the coast of Shetland. The rough weather conditions with heavy wind made the oil quickly disperse completely into the water column, and no oil was stranded. It is estimated that approximately 35 % of the oil ended up in sediments. Following the spill, several studies of its environmental impact have been carried out, and the general outcome is that ecosystems received little impact, and

were restored to normal within a year of the release (ESGOSS, 1994a, ESGOSS, 1994b, Edgell, 1994, Law and Moffat, 2011, Thorpe, 1995, Turrell, 1994).

Once oil has been incorporated in still sediments, experiences show that biodegradation and weathering rates decline considerably. This is due to the oil being enclosed in the sediment, and therefore protected from erosion, evaporation and other ambient processes. Oxygen supply is at a minimum, and this inhibits microbial degradation (Muschenheim and Lee, 2002, Taylor and Reimer, 2008, Atlas, 1981, Garcia de Oteyza and Grimalt, 2006).

1.5 Interactions between oil and suspended particulate matter

Particulate material present in aqueous environments is a known pollutant scavenger through the routes of adsorption, flocculation and complexation. Compounds that are insoluble in water will have a greater affinity for particle surfaces. The interaction between a pollutant and particulates might significantly alter its bioavailability (Stumm and Morgan, 1996, Manahan, 2005, Skoog, 2004). These interactions will also lead to the transportation of pollutants to the seafloor, and reduced residence time in the water column has been observed for pollutants in waters with high SPM-loads (Boehm, 1987). Hence, areas of high sediment deposition will experience a concentration of pollutants within the sediments.

Using a numerical model, Bandara et al. (2011) showed that more than 80 % of spilled oil can interact with suspended particulate materials (SPM), and that up to 65 % of released oil may be removed from the water column as oil-sediment aggregates. In contrast, Muschenheim and Lee (2002) have reviewed field and enclosure studies and noted that the general opinion is that a maximum of 20-30 % of the spilled oil can be sedimented. Payne et al. (2003) emphasize the importance of considering the sources of both SPM and oil droplets when modelling their interactions. Organic and inorganic particles of both natural and anthropogenic origin will be present in marine waters, of which this text will focus on natural, inorganic particles (sediments). Some important sources of inorganic SPMs are the following (Payne et al., 2003):

- resuspension of bottom sediments
- advective input from rivers, streams and glaciers
- physical scouring of shoreline sediments by wave turbulence
- aerolian transport

Oil droplets may be formed by turbulence at the sea surface where oil is spilled or by dispersion of whole oil-droplets from oil-in water emulsions Also, individual oil components may be dissolved both from oil droplets and from oil at the water surface, and these may adsorb to SPM on a molecular level (Payne et al., 2003, Bandara et al., 2011).

1.5.1 Mechanism for incorporation of oil in suspended sediments

The generally accepted model states that oil-SPM aggregates form when oil droplets collide and adhere to suspended matter in aqueous environments (Ajijolaiya et al., 2006, Payne et al., 2003). Guyomarch et al. (2002) suggest that formation of oil-mineral aggregates is caused by interactions between polar oil compounds and negatively charged sediment particles.

When turbulence in the water column is not sufficient to maintain a suspension of oil droplet-SPM agglomerates, the oil laden particles will sink and hence the oil is incorporated into the bottom sediment (Payne et al., 2003).

Payne et al. (2003) insists on a limited time-window for the incorporation processes to take place after a spill incidence. Weathering processes (evaporation, dissolution, formation of emulsions) will act upon the oil to increase its viscosity. It was found that the first 48-hours were the most important period for oil-SPM interactions. After this time, the increased viscosity of the oil will make the interactions less effective.

Several studies have looked at the influence of water salinity on the formation of oil-SPM agglomerates. Guyomarch et al. (2002) found that increasing salinity required increasing concentration of SPMs to maintain a constant number of aggregates formed. Still, the highest rate of oil-SPM aggregate formation is achieved at lower intermediate salinity ranges. Freshwater demonstrates the least inviting environment for aggregation. (Bassin and Ichiye, 1977, Khelifa et al., 2005a, Muschenheim and Lee, 2002).

1.5.2 Factors determining droplet-particle interaction and adsorption kinetics

From empirical studies, Kirstein (in Payne et al. (1989)) derived a mathematical description (Equation 1.1) for the rate of loss of free oil droplets from the water column, as they collide and adhere to SPM (*C*: concentration of oil droplets (mg/L); *S*: concentration of SPM (mg/L);

α: an SPM "shape, size and sticking" coefficient; ε: the energy dissipation rate (per mass of fluid); v: the kinematic viscosity of the water).

$$dC / dt = -1.3\alpha\sqrt{\frac{\varepsilon}{v}}CS \qquad (1.1)$$

The equation is meant to describe the well-mixed reaction conditions that are encountered in the near-shore/surf-zone waters with high SPM loads (Payne et al., 1989). From a qualitative point of view, the equation demonstrates that both oil droplet concentration, SPM-concentration and SPM-characteristics will be of importance to the adhesion of oil droplets to sediment. A linear relationship between the amounts of oil sorbed (lost from the water column) and the SPM-load in the water column is expected. Sediment characteristics (such as size) are also expected to be linearly related to the amount of oil sorbed.

1.5.3 The transport of oil to bottom sediments

Boehm (1987) describes how different SPM loads influence the transportation of oil to the seabed. He concludes that in order to sediment a significant fraction of the oil, a SPM load of > 100 mg/L is necessary. When the load is less than 10 mg/L, no transport is observed. The transport abilities of intermediate loads depend on conditions that promote oil-SPM interactions, such as turbulent mixing. Hence, the interactions will probably not be significant for transport of oil at open sea, but can be of influence in shallow water, especially with turbulent conditions whirling up sediments (Payne et al., 2003). This is illustrated by Figure 1.7.

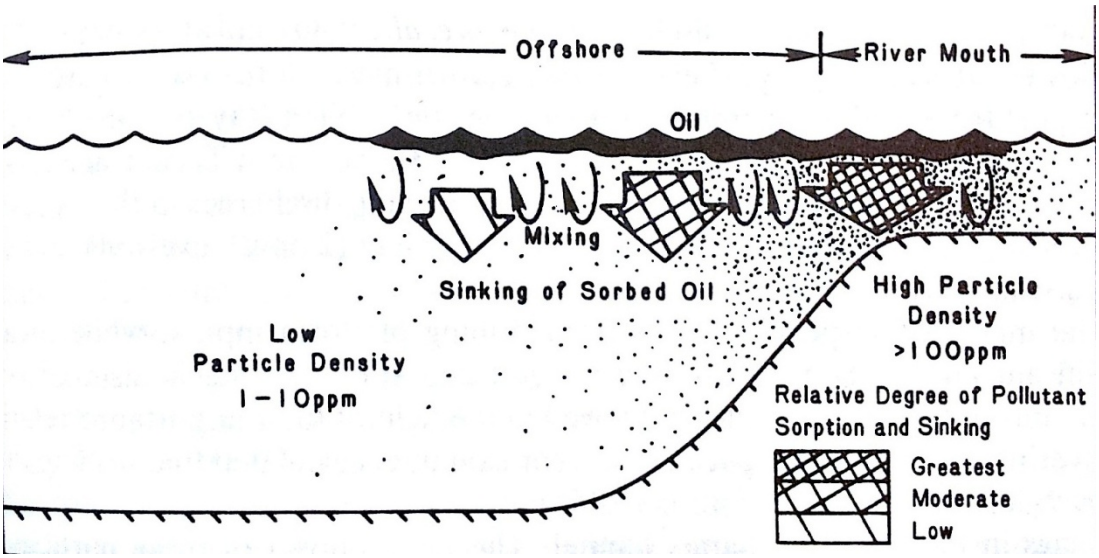

Figure 1.7 - Illustration of how increased concentration of suspended particulate material (SPM) promotes sorption and sedimentation of oil from a spill source. Facsimile from Boehm (1987).

1.5.4 Appearance of oil adhered to sediment

The physical behaviour of oil when adhered to sediment can be of importance to its further fate, such as weathering and sinking to the bottom. Delvigne (2002) studied the physical appearance of oil in oil-contaminated sediment. It was suggested that the parameters governing the physical characteristics of oil in sediment are:

- the interaction mechanism between oil and sediment
- the oil type
- the sediment type
- the concentration of oil
- degree of weathering of oil

Using both natural, contaminated sediment and simulated sediment, he found that the oil might be present in three different phases: as droplets, coated on sediment particles and as “oil patches”. The droplets were either covered with sediment particles or encapsulated in the sediment mass as agglomerates. Delvigne (2002) concluded that the majority of oil in subtidal sediments exists as discrete droplets. The size distribution of these droplets will depend upon oil type and the turbulent energy at the sea surface.

1.6 Effects of chemical dispersants on the formation of oil-SPM-aggregates

The formation of aggregates between SPM (suspended particulate material) and mechanically dispersed oil is described in Chapter 1.5. This chapter will describe what is known about the influence of chemical dispersants on the formation of oil-SPM aggregates.

Existing studies show conflicting results on how dispersants affect adsorption properties of oil droplets. (Mackay and Hossain, 1982) found that chemically dispersed oil associated less with mineral matter than naturally dispersed oil would. However, others, e.g. (Guyomarch et al., 2002, Khelifa et al., 2008, Khelifa et al., 2005a, Sun et al., 2010), have found that oil and suspended material will form aggregates efficiently despite dispersant being added.

Khelifa et al. (2008) studied the sedimentation of oil-SPM-aggregates with and without dispersant for different concentrations of particulates (fine clay in the range 0,1-10 µm). It was found that the formation of oil-SPM aggregate formation was the same, regardless of dispersant application, and concluded that chemical dispersants did not form a barrier to oil-SPM aggregation. Actually, for low particle loads (< 25 mg/L) the dispersant increased oil sedimentation with a factor of 3-5.

Khelifa et al. (2008) points to three important reasons for expecting chemical dispersants to alter the formation and fate of oil-SPM-aggregates, namely:

- the reduction in size and increase in concentration of oil droplets in the water column,
- the alteration of surface properties of the oil droplets
- that the smaller, chemically dispersed droplets will require less solid material (fines, clay) in order to sink

Simulations by Bandara et al. (2011) showed that the presence of smaller droplets (< 0,1 mm) increased the predicted amounts of oil-SPM aggregates formed. The suggested explanation for this is that the droplet residence time in the water phase is prolonged due to the decreased buoyant velocity of smaller particles, and this allows for more interactions with suspended matter.

Lessard and DeMarco (2000) present one of the advantages of dispersant application as the reduction of “stickiness” of the oil. Therefore, it is seen as less likely that the chemically dispersed oil droplets will adhere to suspended sediments and other solids.

1.7 This study

At present there is still a knowledge gap concerning the fate of (chemically) dispersed oil in the marine environment. Adsorption onto suspended particulate matter is one potentially important route of fate for such dispersed oil droplets. This study will focus on the parameters governing oil-SPM interactions, with the use of dispersant as one of the parameters. The influence of other relevant parameters, including oil type, type of adsorbing particulate matter (sediment characteristics), and temperature are also investigated in this study.

Sediment

Processes governing adsorption of oil to sediment will be different for scenarios in open water and near shore. The depth of water and the amount of sediment dispersed in the water column will differ significantly for these two scenarios (Boehm, 1987, Payne et al., 2003). In this study, the focus will be on the coastal region, from the shoreline and islets to some hundred meters ashore.

Near-coast areas can be characterized by the energy from wave and wind action that they are exposed to. In high energetic areas, larger mineral particles of sands and carbonate will be drawn up into the water column. In lower energy areas, smaller particles, such as silt and clay might exist in suspension equilibrium (Bjerkli, 2011). The experiments conducted in this thesis are designed to be of sufficient energy for the suspension of particles with a size up to 2mm. Clay, quartz sand and carbonate sand is used in the study in order to see if particle characteristics such as size and mineral composition make a difference in the bulk amount of oil adsorbed. Different sediment concentrations are also tested.

Oil

Four different oil types are chosen for the study, comprising two crude oils, one condensate and one heavy fuel oil. All oils, except the fuel oil, are weathered synthetically in the laboratory prior to use in the study.

A crude oil is used for the main section of the experiments, and its adsorption is compared to that of the other oils. It is suggested that the difference in content of heavier components, such as asphaltenes will be of importance to the bulk adsorption. It is also investigated whether this difference can be spotted by component analysis by GC-MS.

Throughout the experiments, the oil concentration (generated droplets in the water) was held constant at 20 mg/L.

Temperature

Throughout the year, the Norwegian coastline is characterized by great diversity in seawater temperatures. Therefore the temperature of the experiments in this study was varied from 18-20 °C (shallow water in warm summers) to 4-5 °C (deeper water and/or winter temperatures).

Dispersant

The chemical dispersant used in this study was “Dasic Slickgone NS 2011-0300”, at two different ratios of dispersant to oil (1 % and 5 % by volume). The ratios were chosen as the minimum and maximum concentrations that are part of current government recommendations for spill scenarios.

1.7.1 Project aim and objectives

The aim of the project is to study the adsorption of dispersed oil droplets to particulate materials when oil is released into the marine environment.

There are two main objectives to this thesis.

- To determine which petroleum derived compounds preferentially adsorb to the surface of particulate material and which remain in solution.
- To assess the effects on the adsorption process by varying a selection of parameters.

2 Theoretical background

2.1 Crude oil

Petroleum (Latin; Petra: rock; oleum: oil) is a naturally occurring, complex mixture of hydrocarbons and organic compounds. More than 97 % of petroleum is composed solely of hydrogen and carbon. Sulphur, nitrogen, oxygen and some trace metals (e.g. vanadium and nickel) comprise the smaller fraction of elements present in petroleum (Hunt, 1996).

Petroleum is commonly divided into four main sub-categories, namely crude oil, natural gas/condensates, solid bitumens and oils sand (Wang and Stout, 2007). This text will focus on crude oil.

Crude oil is a liquid mixture that includes a huge variety of different compounds, ranging from the smallest and simplest molecules (e.g. methane) to large and very complex molecules, such as the asphaltenes (Wang and Stout, 2007). All crude oils contain both aliphatic and aromatic hydrocarbons, as well as non-hydrocarbons, but the proportions of each, and distribution of compounds within each class might vary extensively between different crude oils (Tissot and Welte, 1984). This variation in composition is due to the corresponding variation in natural processes and conditions that govern the formation of crude oil. This means that no crude oil has the same “chemical fingerprint” (Wang and Stout, 2007).

2.1.1 Formation of crude oil

Petroleum originates from biological material, such as bacteria, algae, higher plants and dead animals. Through the complex process called thermal maturation, these materials are broken down. There are three main processes governing the outcome of thermal maturation, namely diagenesis, catagenesis and metagenesis, where the two former are responsible for the formation of petroleum (Hunt, 1996, Tissot and Welte, 1984, Wang and Stout, 2007).

Diagenesis consists of two phases. In the first phase, biological material is buried by sedimentation. Next, temperature and pressure acts on the material in order to break down the organic compounds it consists of. Also, biodegradation of the oil by bacteria and chemical reactions such as oxidation, dehydration and decarboxylation will assist in the

transformation of the material. The primary products of diagenesis are called kerogen and bitumen.

Kerogen is a mix of preserved and resistant cellular organic materials from algae, pollen, spores, leaf cuticles and degraded residues of less resistant organic matter. It is the variation in kerogen composition, determined both by the starting biological material and the parameters governing diagenesis that form the basis of the crude oils composition (Tissot and Welte, 1984).

The cracking process that transforms kerogen into liquid or gaseous hydrocarbons is called catagenesis. The process takes place in the temperature range of 50-250 °C, and results in the formation of the main hydrocarbons of oil and gas (Tissot and Welte, 1984).

2.1.2 Crude oil composition

Petroleum is a mixture of several different groups of organic compounds, where hydrocarbons, aliphatic and aromatic, constitute the major component of crude oil.

Hunt (1996) sub-divide the constituents of petroleum into five groups based on molecular structure. The following will describe these groups. Petrology terms for the chemical groups are given in headline parentheses'.

Alkanes (Paraffins)

The first group of saturated hydrocarbons is known as the alkanes, and consists of the *n*-alkanes (straight chain) and branched alkanes (*iso*-alkanes). One important sub-group of paraffins are waxes (straight chain alkanes of more than 20 carbon atoms). The normal content of wax in crude oil is 2-15 % (CEN, 2006). The general molecular formula of alkanes is C_nH_{2n+2}, and some examples of structure are given in Figure 2.1.

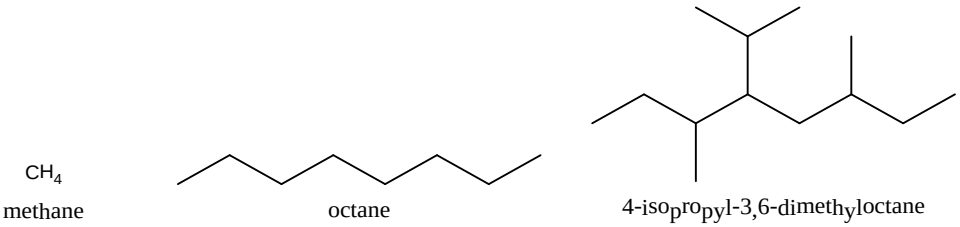

Figure 2.1 - Examples of alkanes

Cycloalkanes (Naphthenes)

Aliphatic compounds of cyclic structure are known as cycloalkanes, and some examples of these are given in Figure 2.2. The general molecular formula of cycloalkanes is C_nH_{2n}. Due to stability constraints, cycloalkanes normally consist only of 5-6-membered rings. The average crude oil consists of 50 % naphthenes (Hunt, 1996).

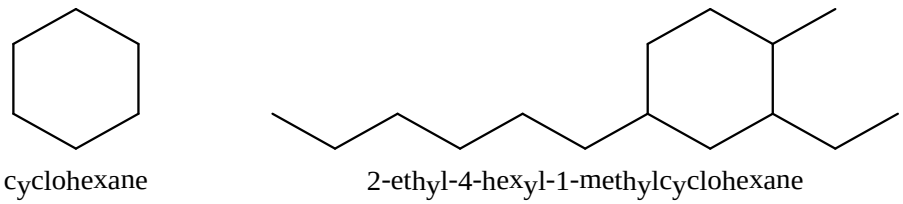

Figure 2.2 - Examples of cycloalkanes

Alkenes (Olefins)

Alkanes and cycloalkanes are known as saturated compounds, since all available carbon bonds are saturated with hydrogen. However, this is not the case for alkenes, which contain one or more double between carbon atoms and are therefore unsaturated with hydrogen. This unsaturation means that the alkenes are much more reactive than the saturated compounds (Hunt, 1996). This instability makes small alkenes rare in crude oil (Tissot and Welte, 1984)

Arenes (Aromatics)

Aromatics molecules usually include 1-5 aromatic rings (like the benzene ring in Figure2.3), and homologues with side chains of straight or branched nature. Aromatics with two or more aromatic rings are known as polycyclic aromatic hydrocarbons (PAH). Two examples of PAHs (benzo[a]pyrene and phenanthrene) are given in Figure 2.3. Crude oil normally contains a maximum of 15 % aromatics, but the group is often concentrated in more heavy oil fractions (Hunt, 1996, Tissot and Welte, 1984).

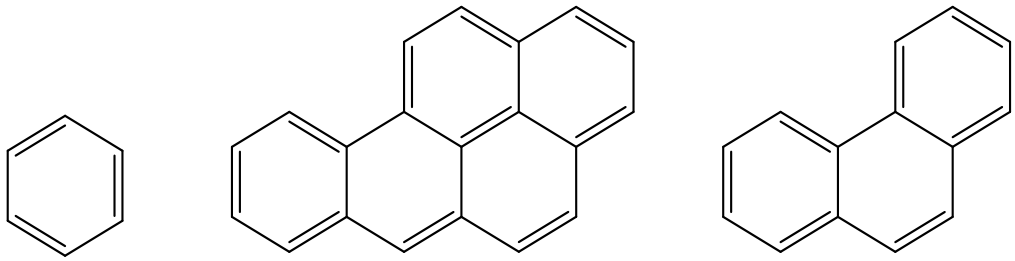

Figure 2.3 - Examples of aromatics

NSO-compounds and asphaltics

Compounds containing the elements nitrogen, sulphur and oxygen are known as NSO-compounds. Examples of small NSO's are given in Figure 2.4. NSO-compounds of high molecular weights (>700) are known as resins. Resins are surface active compounds, like carboxylic acids and phenol-like compounds (CEN, 2006).

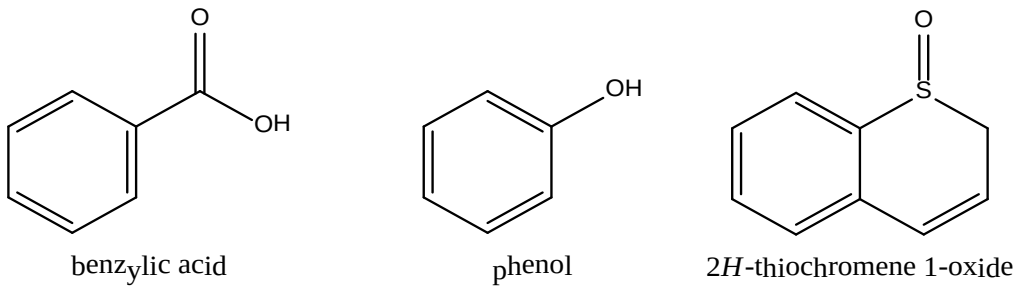

Figure 2.4 - Examples of NSO-compounds

Along with the resins, asphaltenes make up the group known as asphaltics. Asphaltenes are large molecules (molecular weight>1000) that consist of condensed PAHs. Asphaltenes are regarded as the most polar constituents of crude oil (CEN, 2006, Jamialahmadi et al., 2009).

UCM's

All crude oils and especially weathered oils will contain what is known as an unresolved complex mixture (UCM). In a chromatogram (see Chapter 2.6), the UCM is visible as a raised baseline hump. The chemical composition of the UCM will vary extensively between oils due to their previously described differing formation processes. Degradation of the oil by weathering (see Chapter 1.2) will enhance the UCM-proportion of the oil.

Killops and Aljuboori (1990) found that a typical UCM contained mainly aliphatic compounds, a large proportion of them cyclic. Later studies have discovered the variation in UCM's between crudes is vast and that the contribution from aromatic compounds and polar compounds can be significant (Booth, 2004, Booth et al., 2007, Melbye et al., 2009). The UCM is thought to comprise hundreds of thousands of alkylated analogues of well established crude oil compounds, such as benzenes, naphthalenes, phenanthrenes etc.

The reason for the overlapping nature of the UCM in chemical analysis is that the boiling points of the individual components are similar and therefore irresolvable (Frysinger et al., 2003, Killops and Aljuboori, 1990, Wang and Stout, 2007).

2.2 Refined oil products

Crude oil is a complex mixture, and therefore oil refineries fractionate the hydrocarbon constituents in a way that allows for a more efficient utilization of the compounds energetic properties. Distillation (atmospheric and/or vacuum) is one of the central operations in crude oil refining. During this process, the oil is fractionated by boiling point ranges (Speight, 2007).

2.2.1 Heavy fuel oil (HFO)

The highest boiling compounds (t>350 °C), heavy gas oil and the distillation residue are combined to what is known as heavy fuel oil (HFO). The composition of HFO depends on the refining process, and is therefore individual for fuel oils from different refineries. HFOs are classified by IFO-grades (Intermediate Fuel Oil), where the oils are graded after their viscosity, measured in centistokes (cSt), at 50 °C. Thus, IFO 380 has a viscosity of 380 cSt (at 50 °C). Heavy fuel oils are used as fuel in ships and on thermal and power plants on land (CEN, 2006, Speight, 2007).

2.3 Properties of oil

As oils vary in chemical composition, their physico-chemical properties will vary consistently. Some important properties are described here.

2.3.1 Boiling point

The lighter the oil, the more volatile the major proportion of components in the oil. Small, straight chain hydrocarbons often have the lowest boiling points. The proportion of volatile compounds in oil will determine the evaporative loss in an oil spill incident. This loss can be simulated in the lab by “topping” the oil, which means a stepwise distillation until a specific temperature (100-250 °C) is reached. A oil that is “topped 250+” should have suffered evaporative loss equal to 5 days at open sea (Daling et al., 1997).

2.3.2 Solubility

Although most hydrocarbons are regarded as “insoluble” in water, all molecules will dissolve to some extent. How soluble a specific compound is, depends on its structure. Generally, small molecules with polar functional groups are more soluble than more complex molecules. Also, small aromatics tend to be relatively more soluble than other heavy oil components (Booth, 2004, Carey, 2006). Within a homologous series, higher substitution will reduce the water solubility (Tolls et al., 2002).

A simple overview of the relative solubility of oil component groups is found in (CEN, 2006), and cited here:

Hetero compounds > aromatic hydrocarbons > saturated hydrocarbons

To describe how a given molecule will distribute between water and a non-polar environment, the octanol-water coefficient (K_{OW}) is an established surrogate. The coefficient of a compound (A) is determined experimentally using a two-phase system consisting of water and *n*-octanol. Equation 2.1 below describes the calculation, where [$A_{octanol}$] is the concentration of A in *n*-octanol and [A_{aq}] the concentration in water. Values for octanol-water partition are often given as log K_{OW}, where the higher value the less water soluble a compound is.

$$K_{OW} = \frac{[\mathrm{A}_{\mathrm{octanol}}]}{[\mathrm{A}_{\mathrm{aq}}]} \qquad (2.1)$$

Raoult's law (Equation 2.2) describe the concentration (C_{AW}) of a given compound (A) dissolved in the aqueous phase, based on its solubility in water (C_{AW}*) and the molar fraction (X_{OW}) of A in a solid or liquid that shares an interphase with water (Helbæk and Kjelstrup, 2006). Sterling Jr et al. (2003) and Faksness et al. (2008) use the equation to describe the dissolution of individual compounds from oil in the water (surface slick or droplets).

$$C_{AW} = C^{*}_{AW} \cdot X_{AO} \qquad (2.2)$$

2.3.3 Density

Density (weight/volume) can be seen as an indication of an oils composition. Oils of low density (~0,7-0,8 g/mL) are often rich in paraffinic components of low molecular weight. Oils

with high content of aromatics, naphtenes and asphaltenes will have higher densities (up to 0,99 g/mL) (Speight, 2007).

2.3.4 Viscosity

Viscosity is defined as a liquids inner friction (resistance to flow). The viscosity of an oil type depends on the viscosity of its components, where low molecular weight compounds tend to have the lowest viscosity and vice versa. Viscosity is measured in Poise (1 P = 1 dyn*sec/cm^3) (Speight, 2007).

2.4 Geology 101

The aim of this section is not to go in detail on geological phenomena, only to clarify some definitions relevant to the experimental work conducted as part of this thesis.

Most rocks are aggregates of minerals, where the silicate minerals are the most common. Another important class of minerals are the carbonates. Table 2.1 gives an overview of the common particulates found in marine environments, and their typical size distributions.

Table 2.1 - Size of different inorganic particulates (Adapted from Pipkin et al. (2005)).

Particulate	**Size**
Gravel	> 2 mm
Sand	62 µm – 2 mm
Silt	4 µm – 62 µm
Clay	< 4 µm

An important constituent of sand and silt is the mineral quartz (SiO_2). Clay has a different chemical composition, and its main components are different hydrous alumina silicates (Pipkin et al., 2005, Manahan, 2005). Many oxides, carbonates and silicates present in waters and sediments exhibit a surface charge, which, at the pH of natural marine waters, often is negative. The charge properties will influence how the particles interact with other water-borne species (Stumm and Morgan, 1996).

2.5 Sample preparation

Even the simplest environmental samples (e.g. water) are most often unsuitable for direct chemical analysis, and hence some kind of sample preparation is necessary in order to deal with concentrations issues, contamination and unwanted components or sample incompatibility with the analysis instrument. Sample preparation is regarded the "bottleneck" of analytical methodologies, as it is still among the most time-consuming steps and also an important source of error (Luque de Castro and Luque-Garcia, 2002).

2.5.1 Liquid-liquid extraction

Liquid-liquid extraction is based on the partitioning of a solute between two immiscible phases, often water and an organic solvent. The purpose of the technique is to transfer a desired analyte from one solvent to another, and remove it from components mainly soluble in the other phase. The equilibrium of distribution of the solute A between the two phases may be described as (Skoog, 2004)

$$A_{aq} \rightleftharpoons A_{org}$$

The distribution constant *K* is described by Equation 2.3 (*a*: activity in the given phase, [A]: concentration of A in the given phase).

$$K = \frac{(a_A)_{org}}{(a_A)_{aq}} \approx \frac{[A]_{org}}{[A]_{aq}} \qquad (2.3)$$

The distribution constant is useful, as it makes it possible to calculate the concentration of analyte remaining in a solution after a certain number of repeated extractions, and thus acts as a guide towards the most efficient way to perform an extractive separation. Equation 2.4 describes this principle for the extraction of a water sample with *i* portions of organic solvent, each of volume V_{org}, and thus the remaining concentration of A in the aqueous solution ($[A]_i$).

$$[A]_i = \left(\frac{V_{aq}}{V_{org}K + V_{aq}}\right)^i [A]_0 \qquad (2.4)$$

Improved efficiency of multiple extractions will decrease rapidly (Skoog, 2004), often one uses three repeated extractions. The negative aspects of liquid-liquid extraction are a relatively large solvent consumption, and that the process (when manually handled) is slow and tedious (Skoog, 2004).

2.5.2 Solid sample treatment

Most analytical instruments cannot handle solid samples, and hence the target analytes must be transferred to a liquid phase. There are several ways to achieve this, but solvent extraction (solid-liquid extraction, leaching) represents one of the oldest techniques. The analyte compounds are separated from their insoluble matrix, but also potentially from other compounds that might interfere in the analysis (Luque de Castro and Priego-Capote, 2010).

2.5.3 Soxhlet extraction

Soxhlet extraction was developed in 1879, and for a long time has been the most widely used technique for the extraction of chemicals from solid matrices. Today, several modifications to the conventional Soxhlet method have been developed, including the use of high pressure, ultrasound-assistance, micro-wave-assistance and automation. Only conventional Soxhlet extraction will be described here.

The sample is placed in a solvent-permeable thimble (e.g. made of cellulose), and the thimble is placed in thimble-holder above a distillation flask in a heat source (as shown in Figure 2.5). Fresh, condensed solvent gradually fills the thimble-holder until it reaches the over-flow-level. The siphon aspirates the solution from the thimble-holder and back into the distillation flask, thus carrying the extracted analytes into the bulk liquid. The operation is

repeated until complete extraction is accomplished (Luque de Castro and Priego-Capote, 2010).

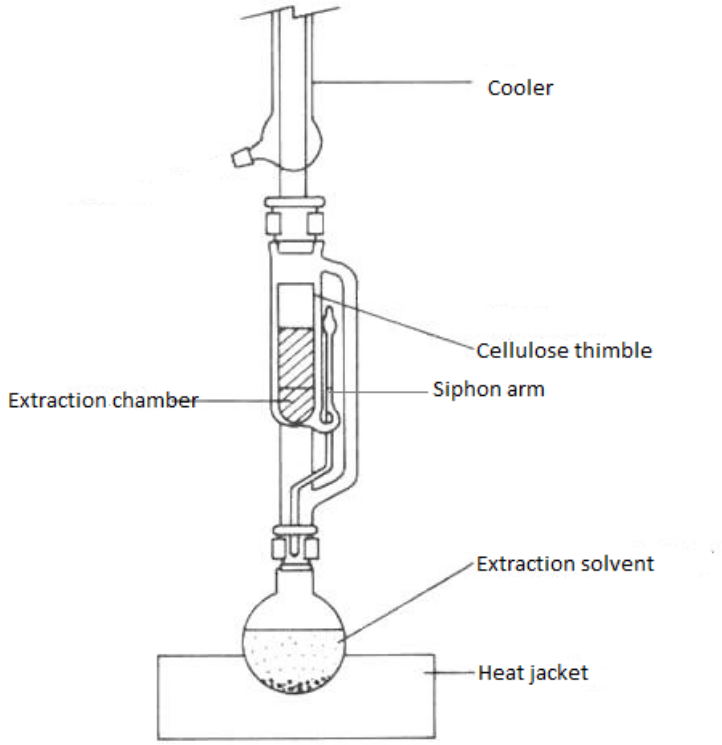

Figure 2.5 - Illustration of the Soxhlet apparatus (Adapted from http://www.oxbo.nl/chemie/scheidingsmethoden/extractie/extractie-1.htm)

There is seemingly no matrix effects hindering Soxhlet extraction, it is a simple and easy to learn technique. Soxhlet extraction is capable of extracting more sample than competing techniques. The two main disadvantages of Soxhlet extraction is the protracted leaching process and the large solvent consumption. Also, since the sample is kept at the solvent boiling point over long periods of time, thermal decomposition of thermo labile components might occur (Luque de Castro and Priego-Capote, 2010).

2.5.4 Solid phase extraction (SPE)

Solid phase extraction, also known as liquid-solid extraction, employs the partitioning of a compound between a liquid and a solid material. The solid is often referred to as the sorbent, and might be both polar and non-polar, depending on the separation problem

(Greibrokk et al., 1984). The sorbent can be packed in a cartridge, a syringe, in the form of a membrane or some other suitable device (Skoog, 2004).

The general procedure for solid phase extraction is composed four steps, as illustrated below (Figure 2.6):

1. Conditioning with solvent
2. Application of sample
3. Washing with solvent
4. Elution using the same or a stronger solvent than during the washing step

In some procedures, steps 3 and 4 are combined, so that only impurities are retained in the sorbent, while compounds of interest pass through at once (Skoog, 2004).

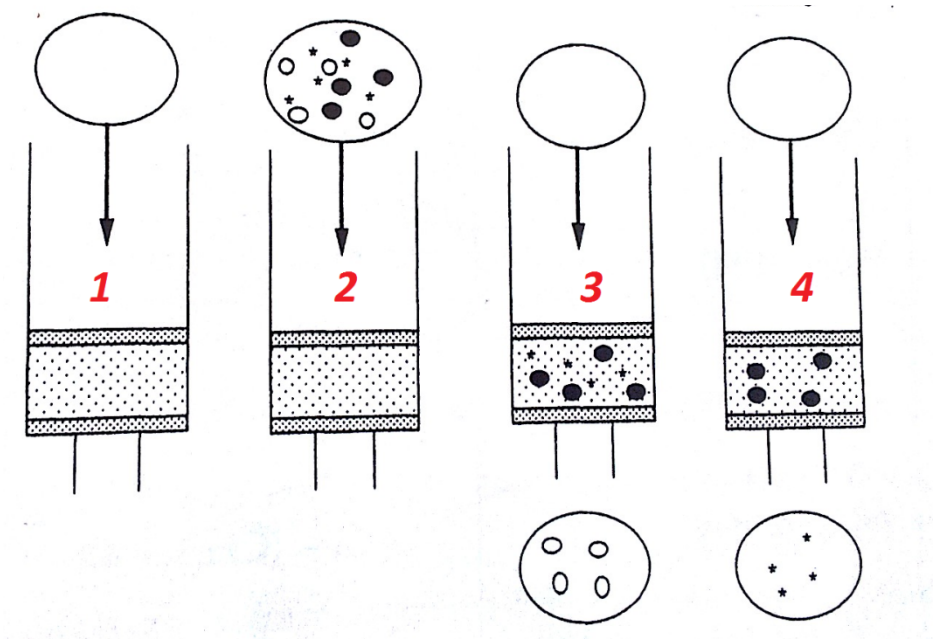

Figure 2.6 - The four steps of solid phase extraction. 1) Conditioning of the column with solvent. 2) Sample application. 3) Washing with solvent. 4) Elution of analyte compounds (Adapted from Greibrokk, 1984).

2.6 Chemical analysis of oil

2.6.1 Chromatography – a separation technique

Chromatography (from Greek chromos: colour, graphein: to write) is a collective term used for separation techniques employing two phases, where one is stationary and the other

mobile. The analytes will partition between the two phases according to their physical and/or chemical properties, and this is basis for their separation (Greibrokk et al., 1984). Compounds which prefer to stay in the mobile phase will travel through the system faster than compounds which prefer the stationary phase, and thus they are separated.

A chromatographic system might be either planar or in form of columns of different sizes, where the latter is more common in analytical chemistry. Columns might be packed or open, depending on their application.

The different chromatographic methods used in analytical chemical techniques are characterized as gas chromatography (GC), liquid chromatography (LC) or supercritical fluid chromatography (SFC), based on the nature of their mobile phase. The stationary phase might be a solid or a liquid (possibly placed on a solid carrier) (Greibrokk et al., 1984).

Retention time

The time it takes for a specific analyte to travel through a chromatographic system, is known as the retention time (t_R). Under constant conditions, the retention time of an analyte will remain unchanged. Therefore, retention time is an important parameter for identification of the separated compounds (Greibrokk et al., 1984).

Band broadening

Although a sample is introduced as a sharp, rectangular pulse into the column, the separated compounds will leave the column as a broadened band with a maximum at their retention time. This phenomenon is known as band broadening, and results from kinetic factors acting upon the sample inside the column. The factors contributing to band broadening include eddy diffusion, longitudinal diffusion and resistance to mass transfer (Poole, 2003).

Eddy diffusion is especially a problem in packed column chromatography, and is caused by individual molecules taking different routes through the column. These routes might be of different length, and hence the analyte zone is broadened. Longitudinal diffusion is caused by the diffusion of analytes in the mobile phase (Greibrokk et al., 1984).

Resistance to mass transfer is the limitations of diffusion between the mobile and stationary phases. Molecules close to the phase boundary might cross this boundary quickly, whilst those farther away will require more time. During this time, the molecules might move some distance in the mobile phase, causing broadening of the band (Poole, 2003).

Plate number

Chromatographic efficiency is determined by the extent of band broadening in a given system. Efficiency, in the chromatographic sense, is expressed as either the number of theoretical plates (N), the height equivalent to a theoretical plate (HETP) or plate height (H). The chromatographic system will ideally function as a Gaussian operator, and the chromatographic peaks (amount of analyte eluted from the column, plotted as a function of time) will be Gaussian (Poole, 2003). This is described by Figure 2.7 below.

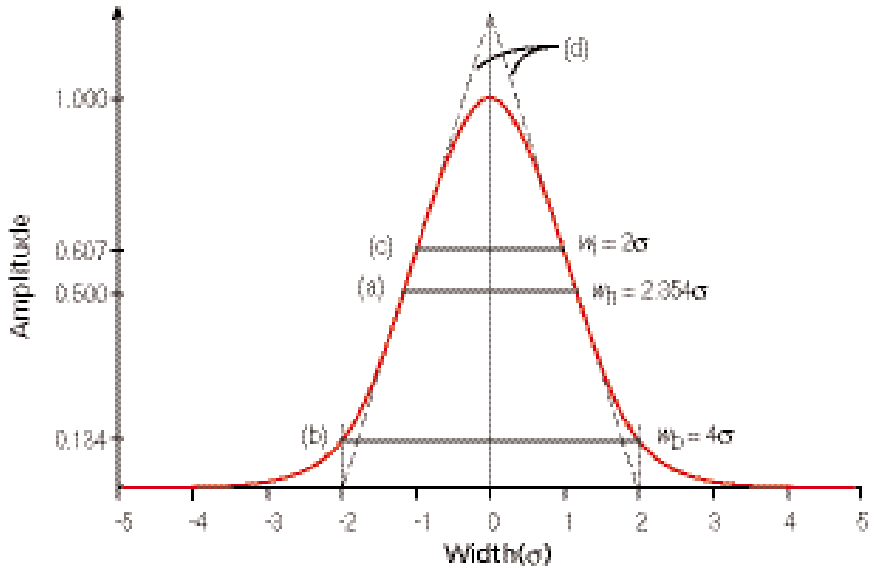

Figure 2.7 - Description of Gaussian chromatographic peak. *w* is the width of the peak, described at different heights by *σ*, which represents the standard deviation (Hinshaw and Ettre, 1994).

The efficiency is described mathematically by the equations below (2.5 and 2.6), where L is the length of the column, t_R the retention time and σ_t is the standard deviation of the peak with the shape of a Gaussian curve (Greibrokk et al., 1984).

$$N = (\frac{t_R}{\sigma_t})^2 \qquad (2.5)$$

$$H = \frac{L}{N} \qquad (2.6)$$

Resolution

The objective of chromatography is to separate two or more compounds, and the resolution (R_S) is the measure of how well this is achieved. To have a baseline separation (see Figure 2.8), R_s has to be 1,5 or greater (Greibrokk et al., 1984).

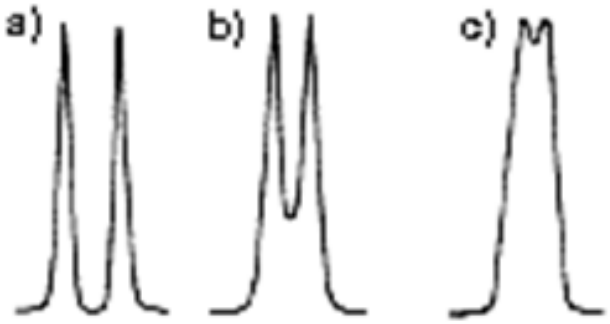

Figure 2.8 - An illustration of chromatograms where two compounds elute at close time intervals. In this example, only the first two peaks (a) have baseline separation (http://www.shodesx.net/index.php?seitenid=1&applic=1473).

The resolution between two peaks can be calculated by Equation 2.7, where w_b represents the average peak width at the base and t_i is the retention time of compound *i*.

$$R_S = \frac{t_{i+1} - t_i}{\frac{1}{2} w_b} \qquad (2.7)$$

Applications of chromatography

Chromatographic techniques find many applications in the fields of analytical chemistry, organic chemistry and biochemistry. For the analysis of oil, the most widely used techniques are high-resolution capillary GC with a flame ionization detector (GC-FID) and GC coupled with a mass spectrometry (GC-MS) (Wang and Fingas, 1997).

2.6.2 Gas chromatography (GC)

A schematic illustration of a GC-instrument is shown in Figure 2.9 below.

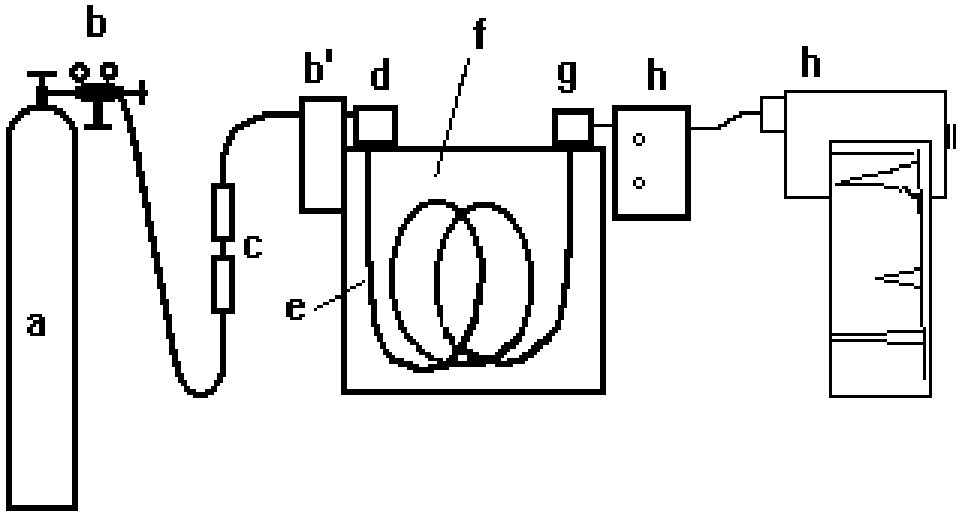

Figure 2.9 - Schematic illustration of the gas chromatograph (a: carrier gas supply, b: pressure-and gas-flow regulator, c: gas purification, d: injection, e: column, f: temperature regulation, g: detector, h: signal processing) (Schmid, 2010).

There are two types of gas chromatography, gas-solid chromatography (GSC) and gas-liquid chromatography (GLC), where the latter has the widest range of applications. In GLC, the stationary phase is a liquid that is spread on an inert support or coated as a thin film on the internal wall of a capillary column. There are five types of columns in GC, where three are packed, and the two remaining are open tubular columns. The column is “open” because there is an open passageway through the center of the column (Poole, 2003).

One type of open tubular column, and the first choice for analytical separations in GLC, is the WCOT (wall-coated open tubular) column. In these types of columns, the liquid phase is coated directly on to the internal column wall. The wall is either smooth, or has been chemically etched. WCOT columns have a much higher permeability than packed columns, and therefore provide the opportunity of more rapid separations at constant temperatures (Poole, 2003).

Stationary phases in GLC

Practical requirements of the stationary phase in GLC mean that the liquid should be unreactive, non-volatile, have good coating characteristics and reasonable solubility in some common volatile organic solvents. The stationary phase should also be thermally stable, as the operating temperature range of GC is -60 ° - 400 °C (Poole, 2003). The stationary phase should also provide the desired separation without reacting irreversibly with the sample (Greibrokk et al., 1984) . Some of the most common stationary phases today include methyl siloxanes and phenyl methyl siloxanes (Schmid, 2010) .

Mobile phases in GC

The three most common mobile phases in gas chromatography are hydrogen, helium and nitrogen. These gases are non-solvating and behave close to ideally at the conditions applied in GC. The primary function of the gas in GLC is to carry the sample through the column, hence the name “carrier gas” (Poole, 2003). The gas will normally not influence the selectivity of the separation. The choice of carrier gas depends on the cost, need for purity, safety and control of reactivity. Compatibility with the detector is also an important consideration. Nitrogen will be the cheap alternative, but helium and hydrogen provide a better efficiency at higher carrier gas velocities, as illustrated by the Van Deemter plot in Figure 2.10.

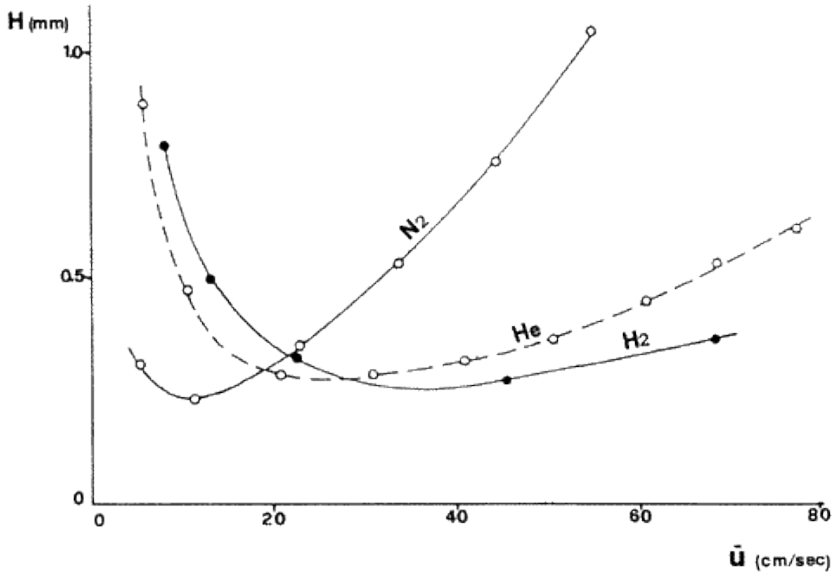

Figure 2.10 - Van Deemter plot for GC, comparing efficiency (plate height, H) at different gas phase velocities (u) for N_2, He and H_2 (Bruner, 1993).

Temperature

By far, the most important factor controlling the separation in gas chromatography is the temperature, as it determines the samples vapour pressure (Schmid, 2010). A practical rule of thumb is that an increase in column temperature of 30 °C, will reduce the retention time for any given analyte by approximately 50 %. Analyses with GC can be performed both isothermally and with a temperature program, where the latter is most common in analytical applications.

2.6.3 Flame Ionization Detector (FID)

The flame ionization detector is the most widely used detector for gas chromatography. It is a nearly universal detector, which means that it will give a response for practically all organic substances. It will however not give response for small inorganic molecules, such as He, N_2, H_2O, O_2, CO_2 (Greibrokk et al., 1984).

The flame ionization detector is based on the principle that the electrical conductivity of a gas is proportional to the concentration of charged particles in the gas. The effluent from the GC-column is directed into a flame consisting of air and hydrogen, which causes some of the

organic compounds to be ionized. A voltage (~300 V, (Greibrokk et al., 1984)) is applied between the burner tip and a collector electrode. The collector electrode will collect the anions and electrons that are produced in the flame, and the resulting current is measured with a picoammeter (Skoog, 2004). The flame ionization detector is highly sensitive (~10^{-3} g/s), has a vast linear response range (~10^{7}) and low noise. Its main disadvantage is that its combustion process is destructive towards the sample. This detection method is also unable to directly provide any way of characterizing unknown compounds. A schematic overview of the detector is presented in Figure 2.11.

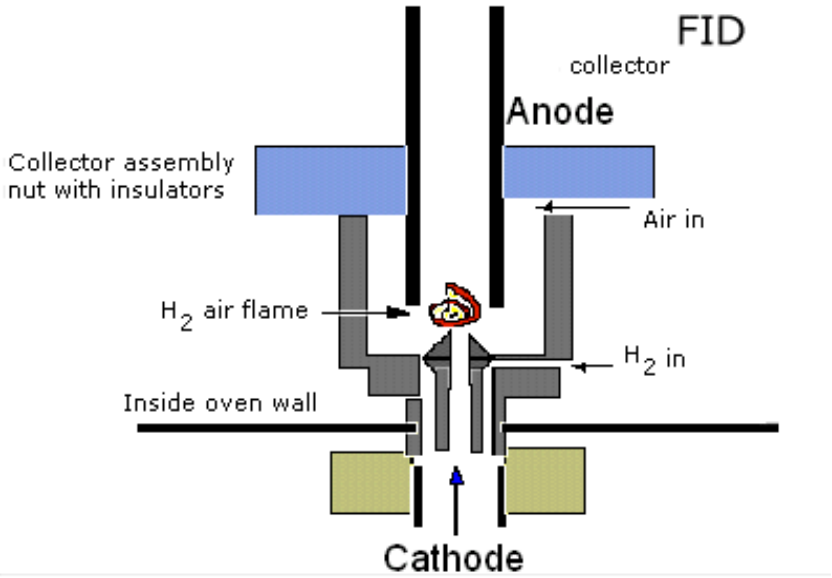

Figure 2.11 - Schematic illustration of a Flame Ionization Detector, the cathode is earthed (http://www.osha.gov/dts/ctc/gas_detec_instruments/slide21.html).

2.6.4 Mass spectrometry (MS)

Mass spectrometry is an analytical tool that can be used alone, or coupled to a separation step, such as chromatography. It can be used to determine both inorganic and organic species, and is also commonly used for elemental analysis. The principle of mass spectrometry is the separation of ions based on their mass to charge ratio (m/z) (Gross, 2004).

The scheme of a mass spectrometer is illustrated by Figure 2.12. After the sample is introduced into the mass spectrometer, the analytes are ionized and the ions are separated by the mass analyser and subsequently detected.

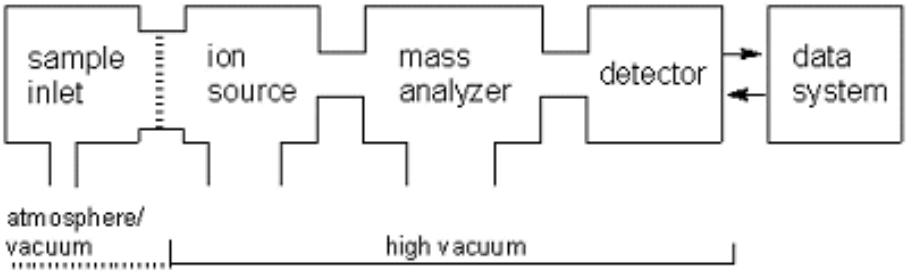

Figure 2.12 - General scheme of the mass spectrometer (Gross, 2004)

After detection, the data system provides a mass spectrum, which relates signal intensities (directly related to abundance) to the respective m/z-values. Often, the ion charge is equal to 1, and the m/z-scale can be read directly as a mass-scale. Still, it is important to note that this is not always the case. Some molecules and ionization conditions will preferably yield ions with multiple charges (Gross, 2004, Hoffmann and Stroobant, 2007).

Ionization

There exists a variety of ionization techniques that are used for mass spectroscopy. Different ionization methods can be divided into three main groups of methods; gas-phase ionization, desorption ionization and evaporative ionization methods. The main difference between these three is the physical state of the sample at introduction (Silverstein et al., 2005).

The choice of ion source suitable for a specific application depends on several aspects, such as the thermolability of the sample and its volatility. There are two main categories of ion sources. The highly energetic ones, that induce extensive fragmentation of the analyte molecules, and the more “soft” techniques that only produce ions of the molecular species (Hoffmann and Stroobant, 2007).

Electron ionization (EI, also known as electron impact) is a widely used ionization technique that causes extensive fragmentation. In the EI source, a heated filament gives off high

energy electrons that are accelerated (normally 70 eV) towards an anode. A beam of gaseous analyte molecules are directed perpendicularly through the beam of electrons, and thus the two will collide (Hoffmann and Stroobant, 2007).

The collision will cause the sample molecule to eject one of its electrons and hence produce a radical cation (the molecular ion). The relatively high energy at which the ionization takes place often causes covalent bonds in the molecule to break (fragmentation). The fragmentation pathway of a given molecule under specific conditions is highly reproducible and presents the analyst with the possibility to identify compounds from an unknown sample. A drawback with the electron impact method is that the fragmentation often makes it impossible to detect the molecular ion (Silverstein et al., 2005).

Other ionization techniques are chemical ionization (soft technique, provides a quasi-molecular ion, e.g. a protonated molecular ion), several types of desorption ionization (for desorbing ions from solid samples), fast atom bombardment (desorbing molecules from an involatile liquid matrix), and a variety of atmospheric pressure ionization methods (for analytes that are thermally labile or of low volatility) (Hoffmann and Stroobant, 2007).

Mass analysers

From the ion source, the ions pass through a slit or lenses and into the mass analyser. The analyser is the part of the MS-instrument where the ions of different m/z-ratio are separated. Different types of mass analysers will differ in the principle of ion separation. Examples of such include separation by time-of-flight (ToF), separation by momentum in a magnetic field (magnetic sector) and separation by cyclotron frequency in magnetic field (ion cyclotron resonance).

One of the most common mass analysers is the quadrupole. The principal of quadrupole mass separation is electrostatic attraction, where opposite charges attract and equal charges repel each other. A quadrupole consist of four hyperbolic or circular rods, arranged parallel to each other. The rods are imposed with a direct voltage (DC) and an alternating voltage (AC). Ions are separated by the difference in stability of their trajectories in the oscillating

electric fields that are applied to the rods (Gross, 2004). Figure 2.13 show a schematic illustration of the quadrupole.

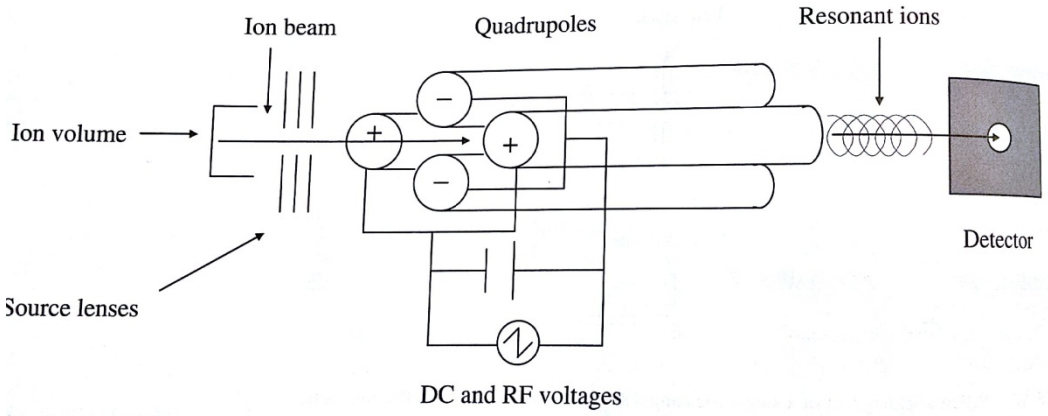

Figure 2.13 - Schematic overview of the quadrupole mass analyser. Facsimile from Hoffmann and Stroobant (2007).

GC-MS

In order to analyse a complex mixture such as crude oil, the mass spectrometer is usually coupled with a separation technique, often gas chromatography. Capillary GC-columns with flow rates of approximately 1 mL/min can be directly connected to EI/CI ion sources.

The obvious advantage of coupling GC and MS is that offers an added dimension of information. One example of such is the possibility of monitoring specific target components during the separation. The operation mode of GC-MS known as selected ion monitoring (SIM) allows for the repetitive scanning of one or more masses. An alternative to SIM-mode is the full scan mode, where the entire eluent flow from the GC is scanned for m/z-values in a given range (Gross, 2004).

2.6.5 Treatment of analytical data

Sources of error

Chemical analysis may be affected by three types of errors. *Random errors* have a variety of sources, and will ideally lead to the symmetrical scattering of data around a mean value. *Systematic errors* are caused by a continuous fault in the experimental set-up or the

instrument. These errors cause all data to differ from the correct value in the same direction. The third type of errors is known as gross errors. Gross errors are often caused by human errors or temporary system failure. *Gross errors* will lead to data points differing largely from the trend (outliers).

There are different approaches to dealing with the different types of errors. Outliers in data sets should, in some way, be identified and omitted from the data analysis. Systematic errors can be found and corrected for by periodic analysis of standards and blank samples. Systematic errors that can't be removed can be handled by external calibration of instruments.

Random errors are difficult to avoid, and must therefore be dealt with in some way. The common approach is statistics. Performing a sufficient number of repeated analyses will give statistical ground to treat the mean value as the correct value, and it will also give an estimate of the (expected) precision of the experimental value (Skoog, 2004).

Statistics

A set of values describing the results of identical experiments is called a population. The average of a population can be calculated using Equation 2.8, where x_i represents the result of parallel *i* and *n* is the number of parallels. Often, the average will be a better description of results, as it will compensate for variation due to random errors.

The standard deviation is a value that complements the average, as it describes how individual values deviate from the calculated average. Standard deviation (*s*) of a population can be calculated using Equation 2.9 (Skoog 2004).

$$\bar{x} = \frac{\sum x_i}{n} \qquad (2.8)$$

$$s = \sqrt{\frac{\sum (x_i - \bar{x})^2}{n-1}} \qquad (2.9)$$

If a result is calculated from two or more experimental data points, the coherent standard deviation must be estimated. Equations 2.10 and 2.11 show the estimation of standard deviation of a sum and a product, respectively (Løvås, 2004, Skoog, 2004).

$$s_{\Sigma a_i x_i} = \sqrt{\Sigma (a_i s_{x_i})^2} \qquad (2.10)$$

$$s_{\Pi (a_i x_i)} = \Pi (a_i s_{x_i}) \sqrt{\Sigma (\frac{a_i s_{x_i}}{x_i})^2} \qquad (2.11)$$

3 Method

3.1 Chemicals and materials

Table 3.1 specifies the solvents and equipment used in the study.

Table 3.1 - Specifications of the solvents and equipment used in the study

Equipment	Type	Comments
Water pump	CeramPump® QG Valve pump	
Oil pump	Aladdin AL-2000 syringe pump	
Overhead stirrer	VWR VOS 16	Equipped with a PTFE rod and blade (65 mm width, 25 mm height)
Absorbent pad	Hazmat	
Soxhlet thimble	Whatman standard cellulose, type 603	Rinsed with three portions of DCM before use
Cotton wool	Whatman Bilson	Rinsed with three portions of DCM before use
Filter paper	Whatman GF/C (1,2 µm)	Rinsed with three portions of DCM before use
Dry-bath	Thermolyne type 16500 Dri-Bath	Set to 35 °C
TurboVap®	Zymark TurboVap® 500	Water bath set to 35 °C
Vacuum chamber	Supelco Visiprep D-L™	
SPE columns	Supelco Bond-Elut silica columns	500 mg
Glassware	Various	Baked (> 400 °C) and/or rinsed with DCM before use
Dichloromethane (DCM)	Merck, 99 % HPLC grade	
n-hexane	Fluka, 99 % HPLC grade	

Authentic sea water was supplied from a depth of 90 meters in the Trondheim fiord (63°26'N, 10°26'E) through a continuous pipeline seawater system with built-in filters (50 µm). The salinity of the water is (33,5 ± 0,2) ‰. Before use in the experiments, seawater was allowed to adjust to the correct experimental temperature over night by storing it in plastic cans near the experimental set-up. Six blank samples of seawater were extracted and analysed to determine the background concentration of hydrocarbons in the water.

To enable accurate quantification in the chemical analysis of the oil samples, both surrogate internal standards (SIS) and recovery internal standards (RIS) were added to the samples. The standards are described in Table 3.2. The SIS-standards were added prior to extraction of both water and sediment samples, whilst the RIS-standards where added before the chemical analysis by GC. THC standards were used for quantification in GC-FID analysis; PAH standards were used for quantification in GC-MS analysis. Throughout the project, 100 µL of each standard was added to every sample.

Table 3.2 - Recovery (RIS) and surrogate (SIS) internal standards used in the experiments. THC standards are used for quantification in GC-FID analysis; PAH standards are used for quantification in GC-MS analysis.

Name	Compounds and their concentrations
RIS-PAH	fluorene-d10 (1,003 µg/mL in DCM)
RIS-THC	5-α-androstane (10 µg/mL in DCM)
SIS-PAH	naphthalene-d8 (25,14 µg/mL in DCM) phenantrene-d10 (5,02µg/mL in DCM) chrysene-d12 (4,98 µg/mL in DCM)
SIS-THC	*ortho*-terphenyl (10 µg/mL in DCM)

3.1.1 Oil types

Four different oils were applied in the study. A summary of their physico-chemical properties is given in Table 3.3. “Topped 250+” means that the oil is a residue of a fresh oil that has been distilled until the temperature reached 250 °C. This is done to simulate the loss of volatile components due to evaporation. The fresh oil has not been altered this way.

Table 3.3 - Physico-chemical properties of the four test oils used in the study

Name	Type of oil	Sintef batch ID	Density [g/cm^3]	Viscosity, 13 °C [cP]	Asphaltene content [wt%]	Wax content [wt%]
Troll	Crude oil, topped 250+	2007-0287	0,9296	247[1]	0,08[1]	1,93[1]
Avaldsnes	Crude oil, topped 250+	2011-0444	0,9353	2044	2,2	3,7
Kvitebjørn	Condensate, topped 250+	2009-0239	0,8534	4090	0,15	9,18
IF 380	Fuel oil, fresh	2006-1125	0,9631	N/A	N/A	N/A

3.1.2 Chemical dispersant

The chemical dispersant that was applied in the experiments was “Dasic Slickgone NS 2011-0300”. A sample of the dispersant, along with some of the oils is shown in Figure 3.1. Two different dispersant-oil ratios (DOR) were used, 5 % (1:20) and 1 % (1:100). The dispersant ratios were chosen to span the range of dispersant dosage that is part of present-day recommendations (see Chapter 1.3.2).

Figure 3.1 - Troll oil, Kvitebjørn oil, dispersant Dasic Slickgone, IF 380 oil (Lisbet Sørensen, 22.11.2011)

[1] Measured for Troll blend 2005-0845

Procedure for mixing of oil and dispersant

Dispersant (50 µL for DOR 1 % and 250 µL for DOR 5 %) was added to a vial using an auto-pipette. Oil (5 mL) was added to the same vial using a graduated syringe. The vial was then treated as follows:

- Heated at 50 °C for 5 minutes
- Shaken vigorously for 1 minute
- Sonicated in an ultrasonic bath for 5 minutes
- Shaken vigorously for 1 minute

The oil-dispersant mixture was added to the system using the same syringe pump as for the pure oil.

3.1.3 Sediment

Three different, natural sediments were applied in this study. These sediments were found and collected at three different locations in Sør-Trøndelag (see map in Figure 3.2). To remove any unwanted particles and possible contaminants, the sediments were flushed with large amounts of clean seawater and dried at 100 °C before use in experiments. The sediments were stored in aluminium containers, covered by aluminium foil. Laboratory blanks of the sediments were extracted and analysed similarly to sediment from the experiments.

Carbonate sand from Grandefjæra

The first sediment, which was used as the standard sediment in all experiments except those specifically investigating the effect of sediment type, was a carbonate rich sand collected at Grandefjæra in Ørland (+63°40'N, +9°32'E). Its grain size distribution was determined using SINTEF procedure KS 66-21-A-220, and the result of this is given in Chapter 4.1 and Appendix C. The procedure fractionates the particulates using number of connected sieves with filters in the range 63 µm – 2 mm. After adding the sediment to the top sieve (2 mm), the sieving system is shaken for 10 minutes to ensure that all particles collect at the correct level. The

individual fractions are then weighed. The grain size distribution was repeated for three parallels.

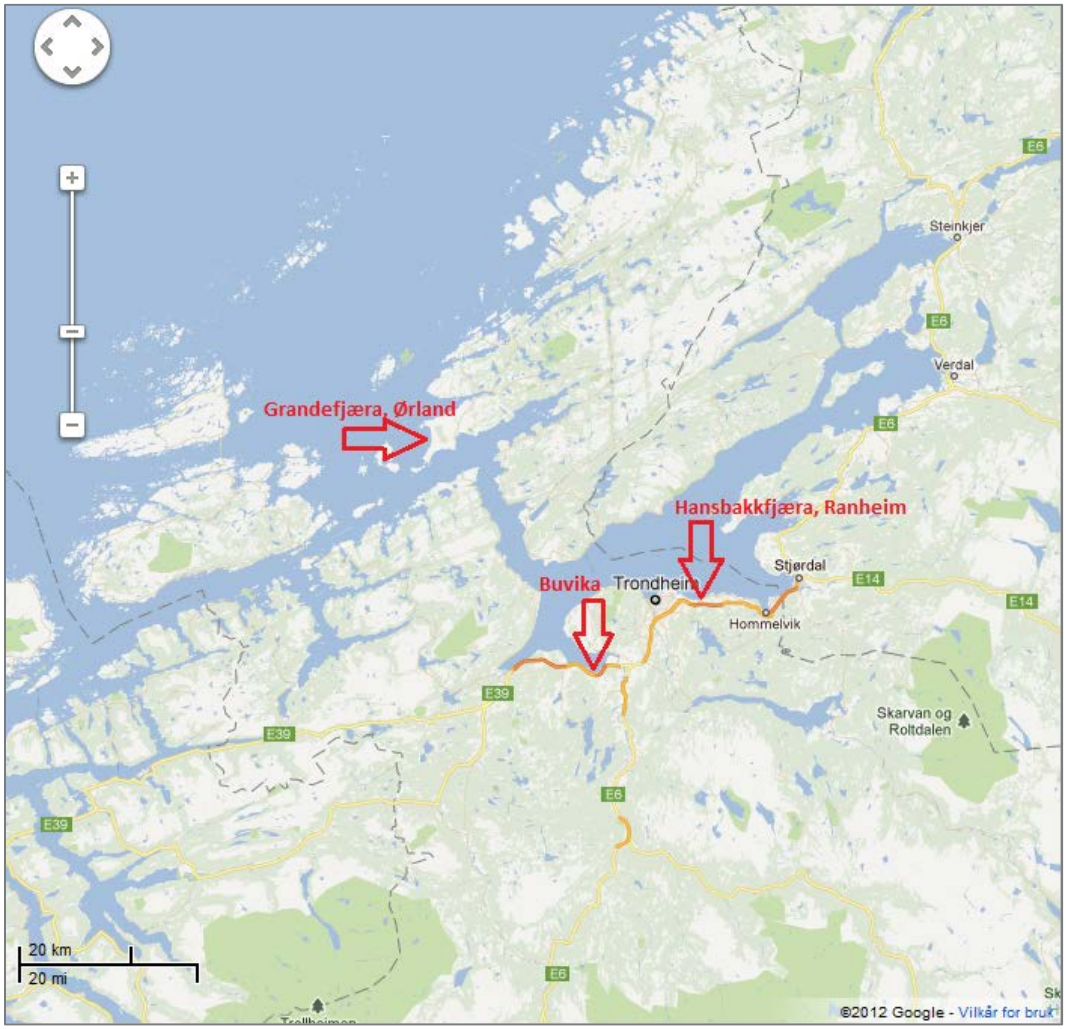

Figure 3.2 - Locations where the three natural sediments used in the study was collected (Google Maps, adapted by Lisbet Sørensen)

Sand from Ranheim

The second sediment was sand collected at Hansbakkfjæra in Ranheim in Trondheim (+63°25'N, +10°32'E). The original sediment contained some larger pebbles, and thus it was chosen to sieve the sediment to eliminate all particles larger than 2 mm. The grain size distribution of the remaining sand was determined using SINTEF procedure KS 66-21-A-220, and the result of this is given in Chapter 4.1 and Appendix C.

Hansbakkfjæra is a popular beach used for recreation, and hence the sediment could contain some coal from barbequing that might interfere with analysis. Thus, the sediment was cleaned 3 times by adding 100 mL DCM, stirring and sonicating on an ultrasonic bath for 5 minutes.

Clay from Buvika

The final sediment was clay collected at Buvika (+63°18'N, +10°10'E), with all particles <63µm. After drying at 100 °C over night, the clay was powdered into fine particles using a porcelain pestle and mortar, as seen in Figure 3.3:

Figure 3.3 - Grinding of dried clay from Buvika to make a fine powder for use in the experiments (Lisbet Sørensen, 22.02.2012)

3.2 Experimental set-up

3.2.1 Generation of the oil-in-water dispersion

In order to simulate mechanically dispersed oil droplets, an oil droplet generator comprising two pumps, one for oil and the other for water, were applied. The water pump was adjusted to deliver sea water from a reservoir at a rate of 160 ml/min. The second pump, a syringe pump, delivered oil to the system. The rate of oil delivery was adjusted to match the density of the oil in use, in order to deliver a fixed amount based on weight. In a SINTEF-developed mixing tube, the oil and water was mechanically mixed to generate small droplets of oil dispersed in the sea water. Figure 3.4 shows the pumps and generator.

The initial recommendation given was to give the system 5 minutes to condition/equilibrate before using the oil-in-water dispersion in the experiments (Nordtug and Vang, 2011). This necessity was supported by laboratory observations in the early phase of the project. It was therefore decided to let the generator equilibrate for a minimum of 10 minutes. Some time into the project, staff of NTNU Centre of Fisheries and Aquaculture, gave feedback on some of their recent experiences using an identical system. They had measured the oil droplet distribution at the outlet of the generator and found that a stable output of droplets (number and size) was reached only after operation for 2-3 hours (Olsen, 2012). In this study, the stability of output (of oil) from the syringe pump was tested and it was demonstrated good stability over time (see Appendix B).

The system would generate oil droplets in the size range of 2 – 20 µm (Nordtug and Vang, 2011). The desired concentration of oil in water was 20 mg/L. Appendix B describes how the syringe pump was tested and set to deliver the required amounts of oil.

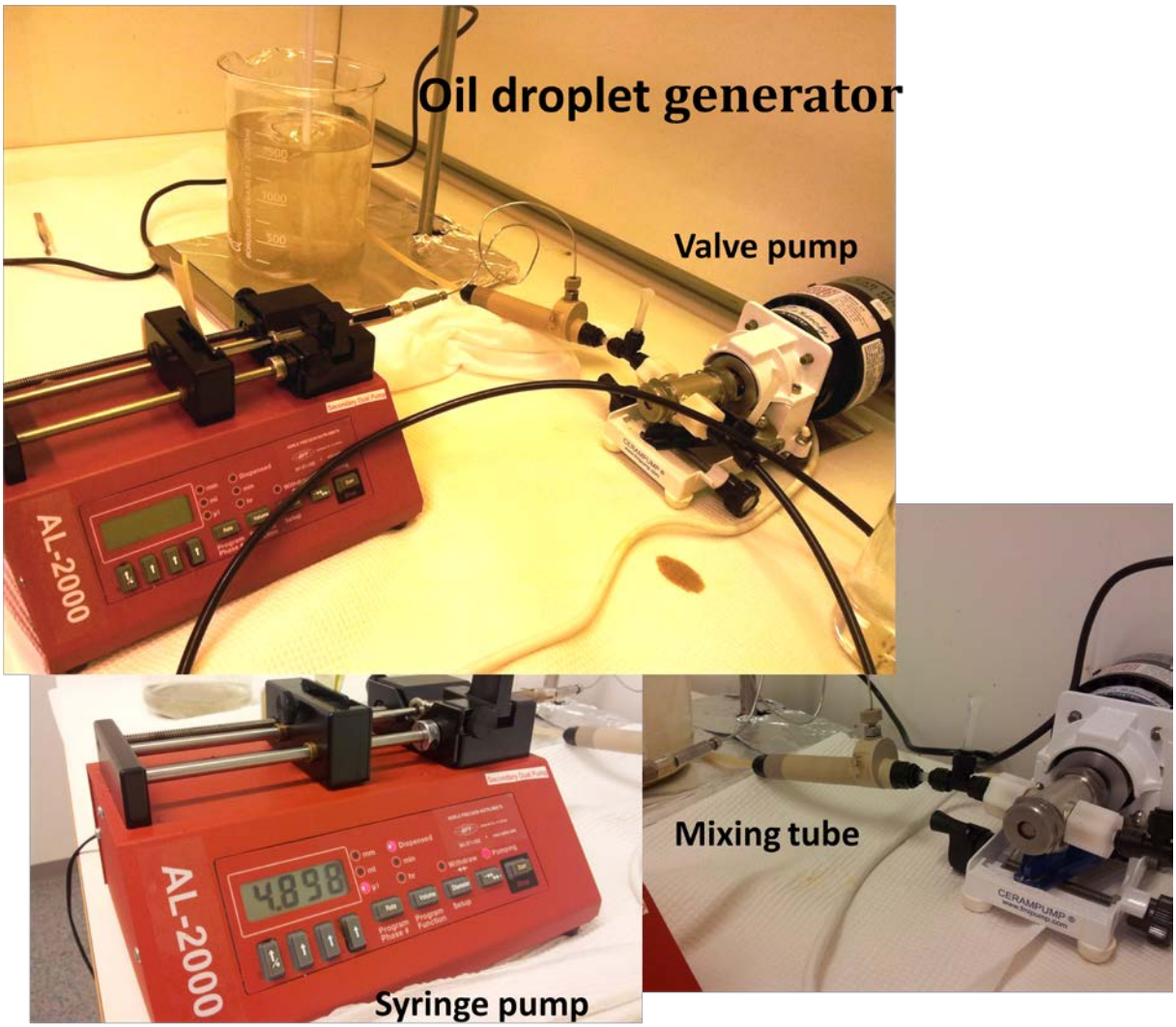

Figure 3.4 - Overview of the oil droplet generator system, with a CeramPump® QG valve pump for water delivery, an Aladdin AL-2000 syringe pump for oil delivery and a mixing tube for generation of oil droplets in the water (Lisbet Sørensen, 13.10.2011).

3.2.2 Sediment suspension and exposure to oil dispersion

Accurately weighed sediment was added to a glass beaker and seawater with dispersed oil (20 mg/L) was added by the oil-droplet generator. The system was stirred by an overhead stirrer for 55 minutes at ~250 rpm, followed by 5 minutes stirring at ~50 rpm (see Figure 3.5). The overhead stirrer offered the advantage of optimizing and reproducing the stirring speed. The speed was chosen by visual observation of the speed that allowed for suspension of all sediment without adding a torque. Payne et al. (2003) employed a similar design when studying the kinetics of oil-SPM interactions.

After removing the stirrer, the beaker was covered by aluminium foil and the sample was allowed to settle for 24 hours.

Residual oil on the water surface and glass walls was removed by using a absorbent pad. The sample was filtrated on a Buchner funnel with a filter paper. The sediment was flushed three times on the filter paper with 30 mL of clean sea water, left to dry at room temperature and then transferred to aluminium containers and covered by aluminium foil.

The water phase was transferred to 2 L glass bottles.

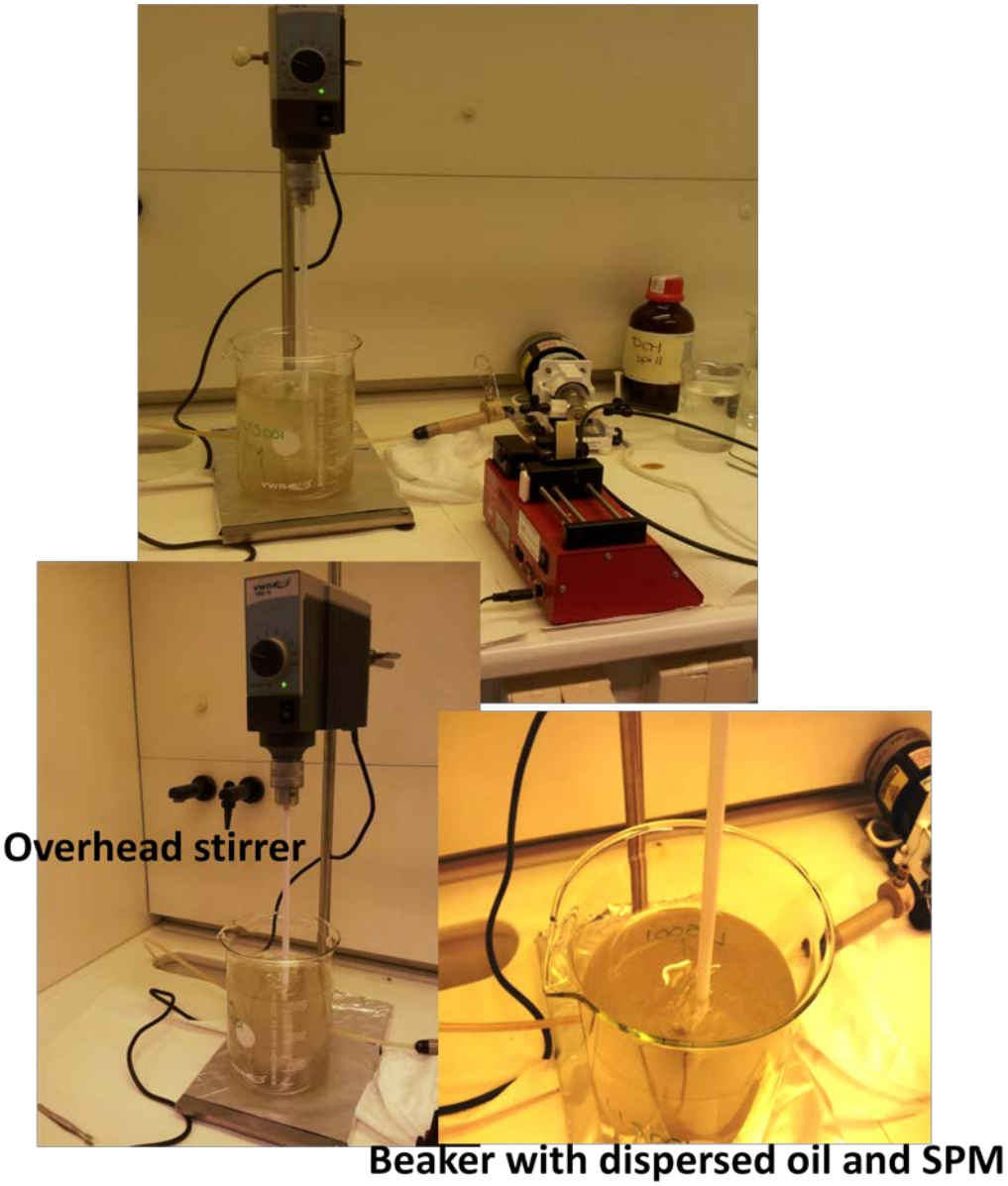

Figure 3.5 – An overview of the experimental set-up with the oil-droplet generator, overhead stirrer and the beaker containing the mix of dispersed oil in seawater and suspended particulate matter (SPM) (Lisbet Sørensen, 13.10.2011).

3.2.3 Storage of samples

To prevent an alteration in chemical composition of the water and sediment samples after fractionation, care was taken in storing them safely. All samples were kept in closed containers, and in constant cool conditions (4 °C). Water samples were acidified by adding hydrochloric acid (HCl, 15 %, 10 mL) as recommended by SINTEF procedure KS 66-21-L-235 (Faksness, 2000). No sample was stored for more than 7 days prior to extraction.

3.3 Sample extraction and clean-up

3.3.1 Comparison of techniques for the extraction of oil from sediment

Soxhlet extraction and alkaline saponification represent two common techniques for extraction of oil from sediment. In a preliminary study, the efficiency of these two methods was tested, in order to determine which gave the best recovery of oil. It was also interesting to see whether the techniques would give the same GC-FID profile.

Soxhlet extraction is described in part 6.2 of SINTEF internal procedure KS 66-21-A-248 (Sørheim, 2005). The Soxhlet thimble was fitted and rinsed three times with DCM. The sample was transferred to the thimble and covered with cotton wool. Internal standards SIS-PAH (100 µL) and SIS-THC (100 µL) were added to the thimble. The thimble was placed in the Soxhlet glassware (see Figure 3.6),

DCM (50 mL) was added to a round bottomed flask and the flask was connected to the Soxhlet glassware with a Liebig cooler and placed in a heat jacket. The extraction time was 7 hours. The flask with the extract was cooled and filtered through Bilson cotton and anhydrous sodium sulphate (Na_2SO_4, baked) in to TurboVap® glassware and reduced to approximately 0,5 mL by evaporation of solvent, using TurboVap®, and reduced to approximately 0,5 mL. The samples were transferred to 4 mL sample vials. The TurboVap® glassware was rinsed three times with DCM, and this was also transferred to the GC vials.

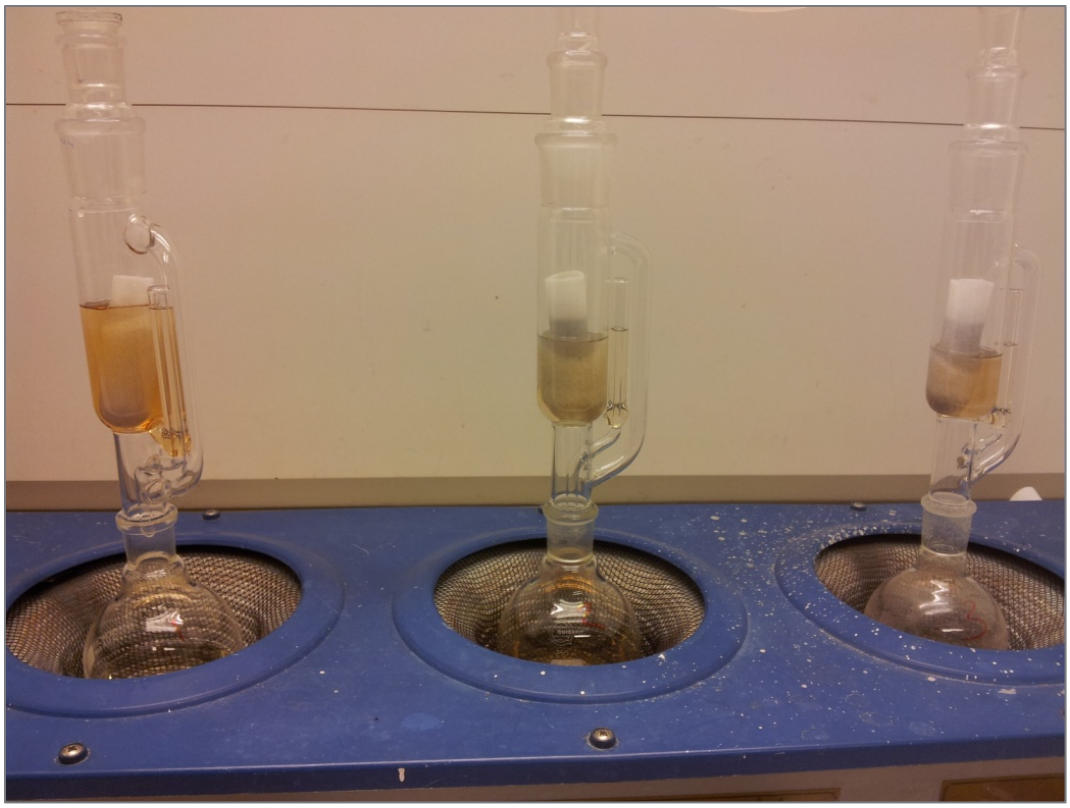

Figure 3.6 - Soxhlet extraction of sediment samples from experiments using oil type IF 380 Fresh. The picture shows the Soxhlet glassware with cellulose thimble, and round bottomed flasks placed in the heat jacket. (Lisbet Sørensen, 16.11.2011)

Alkaline saponification is described in SINTEF internal procedure KS 66-21-A-204 (Faksness, 2001b), but this procedure assumes a sediment amount of 100 g. Therefore the procedure was adjusted to fit the smaller amount of sediment used in these experiments.

The sediment was transferred to a round-bottomed flask (100 mL) and methanol (25 mL), potassium hydroxide (KOH, 1 g) and anti-bumping granules were added. Internal standards SIS-PAH (100 µL) and SIS-THC (100 µL) was also added. The mixture was boiled for two hours on a heat jacket with reflux. After cooling, the sample was filtered through a filter paper on a Buchner funnel. The sediment on the filter was washed with DCM (3x10 mL). The filtrate was transferred to a separating funnel (250 mL) and distilled water (25 mL) was added. The funnel was shaken vigorously for 2 min and after the two phases had separated, the lower phase (DCM) was transferred to a conical flask. The extraction was repeated two times with 15 mL of DCM each time.

The combined organic phases were returned to the empty separating funnel and distilled water (20 mL) and saturated sodium chloride (NaCl, 2 mL) was added. It was shaken for 2 min and left for 15 min for phase separation. The lower phase (DCM) was drained into a conical flask containing sodium sulphate, shaken for ½ min and left for 1 hour to remove any remaining water. The sample was filtered through cotton wool in a glass funnel and into TurboVap® glassware and subsequently reduced to approximately 0,5 mL on the TurboVap®. The samples were transferred to 4 mL sample vials.

The results from the method development are described in Chapter 4.2. The method chosen to be used for the main experiments was Soxhlet extraction, using DCM-volumes as specified in Table 3.4. Due to practical considerations, the extraction time was reduced to 6 hours. See also the discussion in Chapter 5.7.4.

Table 3.4 - Volume of DCM used for Soxhlet extraction of sediment samples

Amount of sediment for extraction [g]	Volume of DCM in Soxhlet extraction [mL]
7,5	50
15	120
30	120
60	120
120	240

3.3.2 Extraction of oil from the water phase

The water phase was extracted using liquid-liquid extraction, as described by SINTEF Internal Procedure KS 66-21-L-235 (Faksness, 2000). The pH of the samples was adjusted to <2 (checked with pH strips) using HCl (15%). The samples were transferred to 2 L separation funnels, and internal standards SIS-THC (100 µL) and SIS-PAH (100 µL) added. The sample

bottles were rinsed with 120 mL (90+30 mL) DCM and this was also added to the separation funnel.

The separation funnel was sealed and shaken vigorously for 2 minutes. After 10 minutes standing to allow the aqueous and organic phases to fully separate, the organic phase was transferred to an Erlenmeyer flask. The extraction was repeated two more times, using 2x60 mL DCM. The three organic extracts were combined and anhydrous sodium sulphate was added. The flask was shaken, and the sodium sulphate was allowed to rest for ½ h. See Figure 3.7 for a picture describing the liquid-liquid extraction set-up.

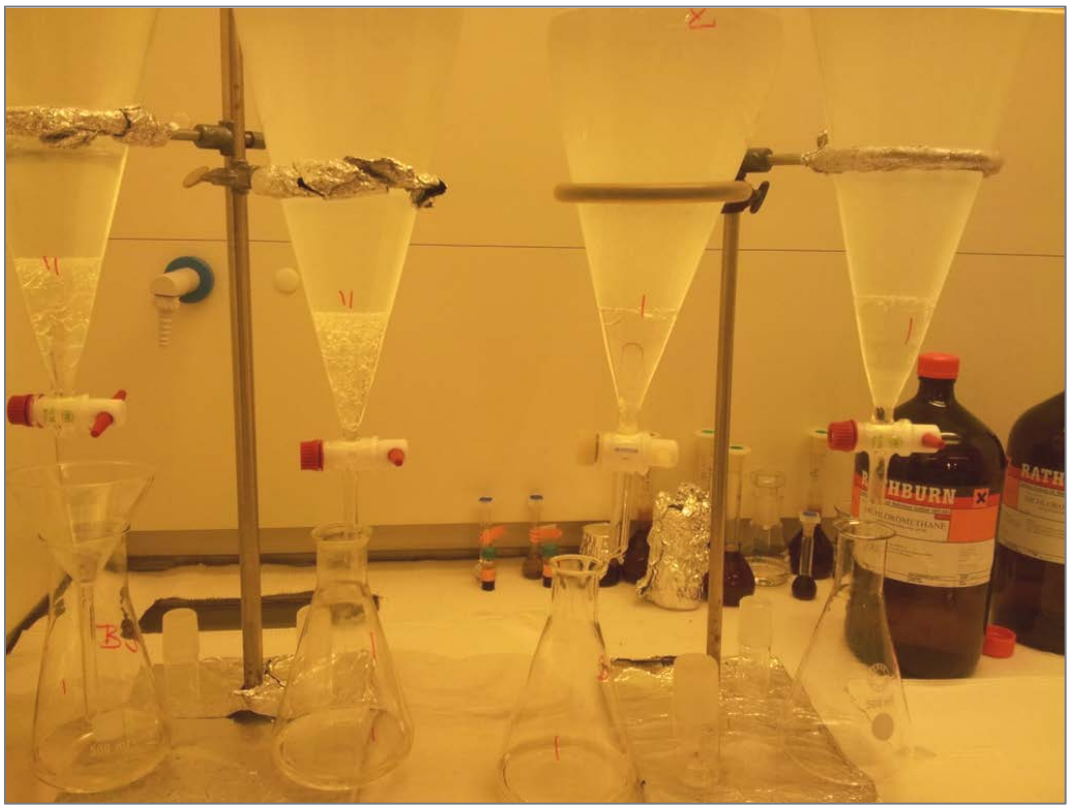

Figure 3.7 - Equipment set-up for liquid-liquid extraction of seawater samples (Lisbet Sørensen, 24.11.2011).

3.3.3 Sample concentration and clean up

All sediment and seawater extracts were transferred to TurboVap® glassware and reduced to approximately 0,5 mL by evaporation of solvent, using a TurboVap®. The extracts were transferred to 2 mL GC vials. The TurboVap® glassware was rinsed three times with DCM, and this was also transferred to the GC vials.

In the case of the water extracts, the volume was adjusted to 0,8 mL using N_2 blow down technique on a dry-bath se. Finally, internal standards RIS-PAH (100 µL) and RIS-THC (100 µL) were added to each sample to give a total sample volume of 1 mL ready for analysis.

As the sediment extracts contained high concentrations of biogenic compounds, these were subject to sample clean-up prior to analysis. The clean-up procedure is described fully in SINTEF internal procedure KS 66-21-A-211 (Faksness, 2001a). The sample solvent was changed from DCM to *n*-hexane, and then the sample was eluted through a silica-column in a vacuum chamber using 3x2 mL *n*-hexane. The biogenic compounds were retained on the silica column whilst the target oil compounds eluted in the solvent. The samples were reduced to 0,8 mL using N_2 blow-down technique on a dry-bath. Internal standards RIS-PAH (100 µL) and RIS-THC (100 µL) were added to each sample. An illustration of the equipment for sample clean-up is shown in Figure 3.8.

Figure 3.8 - Bond-Elut clean-up of sediment extracts on a 500 mg Si-column, *n*-hexane used as solvent and eluent (Lisbet Sørensen, 30.09.2011).

3.4 Chemical analysis

3.4.1 GC-FID

To determine the total extractable organic compounds (TEOC) in the sediment and water samples, all extracts were analysed by GC-FID. The GC-FID system comprised an Agilent 7890A GC equipped with a 7683B series auto-sampling injector. The GC was fitted with an Agilent J&W HP-5 fused silica capillary column (SF: 5 % diphenyl 95 % dimethylpolysiloxane), with dimensions 30 m length, 0,25 mm internal diameter and film thickness 0,25 µm. The carrier gas was helium (grade 4.6), at a constant flow of 1,5 mL/min. 1 µL of sample was injected using pulsed splitless injection. The column oven provided the following temperature program: 40 °C for 1 minute, the 6 °C/min until 315 °C, hold at 315 °C for 15 minutes. The detector temperature of the FID was 330 °C.

The TEOC-content of each sample was quantified by use of internal standard. A calibration curve for each oil type was constructed by analyzing four standards of each with different concentrations (1 µg/mL, 2,5 µg/mL, 5 µg/mL and 10 µg/mL oil in DCM). An internal standard (RIS-THC, 100 µL) was added to each oil standard (0,9 mL). The calibration curves can be seen in Appendix D.

3.4.2 Quantification of results from GC-FID

Every chromatogram was integrated from 8 minutes to 48 minutes (corresponding to the range of *n*-alkanes C_{10} to C_{40} (Almås, 2011). To estimate the background baseline (and drift in baseline) due to column bleeding, blank samples of sample solvent (DCM, *n*-hexane) were analysed at intervals of every 10-15 sample injections. Also, an *n*-alkane standard (5 µg/mL) was analysed repeatedly at the same intervals to ensure that the instrument was stable.

The relative response factors (RRF) for each of the four oils was calculated using Equation 3.1, at every concentration, and an average value of RRF was calculated. The criteria for use of the average relative response factor was that the average relative standard deviation for every analyte was less than 15 % (Almås, 2011).

$$RRF = \frac{A_{std} \times C_{RIS}}{A_{RIS} \times C_{std}} \qquad (3.1)$$

A_{std} is the total area/response of the oil components in the standard

A_{RIS} is the area/response of the RIS-THC component in the standard

C_{std} is the concentration of the oil in the standard

C_{RIS} is the concentration of the RIS-THC component in the standard

The true response of the total hydrocarbon (THC) was calculated by subtracting the area of internal standards (SIS-THS and RIS-THS) and the area due to column bleed from the total area of the chromatogram, as described in Equation 3.2.

$$A_{THC} = A_{tot} - (A_{blank} + A_{std}) \qquad (3.2)$$

The concentration of THC in the extract was calculated using Equation 3.3.

$$C_{THC} = \frac{A_{THC} \times C_{RIS}}{A_{RIS} \times RRF} \qquad (3.3)$$

Note that the samples had not been diluted prior to analysis.

All data was subsequently corrected for extraction (LLE, Soxhlet) variations by the recovery of surrogate internal standard (SIS-THC) (see Tables G.1 and G.2 of Appendix G).

For a number of the sediment extracts, the *o*-terphenyl (SIS-THS, internal standard) co-eluted with a naturally occurring oil component (*n*-alkane C_{19}), and could not be integrated directly. Discussion with the technical staff at SINTEF (Almås and Rønsberg, 2012) led to the realization that this is a common problem, especially for complex samples. The

recommended solution was to calculate an average response (area) of *o*-terphenyl from the samples where co-elution was not a problem, and use this to estimate the response (and hence, the recovery) of the remaining samples. This estimation is given in Appendix G, and used in further calculation of the results presented in Chapter 4.

3.4.3 GC-MS

Three experiments were chosen to be analysed by GC-MS to determine component group distribution of C_{10+} saturates, naphthalenes, 2-3 ring PAHs and 4-6 ring PAHs (in the text also referred to as semi-volatile compounds (SVOCs)). The experiments chosen were:

- Troll 250+ oil, Grandefjæra carbonate sand, 18-20 °C, no dispersant (LIS002)
- IF 380 Fresh oil, Grandefjæra carbonate sand, 18-20 °C, no dispersant (LIS009)
- Troll 250+ oil, Grandefjæra carbonate sand, 18-20 °C, 1 % dispersant (LIS010)

Three parallels of both sediment and water extracts were analysed.

The GC-MS system comprised an Agilent 6890N GC equipped with an Agilent 5975B quadrupole mass-selective detector (MSD). The GC was fitted with an Agilent J&W HP-5MS fused silica capillary column (SF: 5 % diphenyl 95 % dimethylpolysiloxane), with dimensions 60 m length, 0,25 mm internal diameter and film thickness 0,25 µm. The carrier gas was helium (grade 6.0), at a constant flow of 1.2ml/min. 1 µL of sample was injected at 310 °C using pulsed splitless injection. The column oven provided the following temperature program: 40 °C for 1 minute, raised by 6 °C/min and held at 315 °C for 15 minutes. The MSD ion source used electron ionization (EI) at 70 eV, and held a temperature of 230 °C.

MSD ChemStation (version D.03.00.611) software monitored and recorded the chromatograms. Appendix H specifies the monitored compounds and their quantification ions.

3.4.4 Quantification of results from GC-MS

Prior to analysis, eight standards were analysed in order to find response factors of the different components for external calibration. Average response factors for the different component groups (see Appendices H and I) were calculated using Equation 3.4.

$$RF = \frac{A_t \times C_i}{A_i \times C_t} \qquad (3.4)$$

A_t is the total area of quantification ion for the target analyte in the standard

A_i is the total area of quantification ion for the internal standard in the standard

C_t is the concentration of target analyte in the standard

C_i is the concentration of internal standard in the standard

The concentration of target analytes is determined using Equation 3.5.

$$C_a = \frac{A_a \times Amt_i}{A_i \times RF_i \times V_a} \qquad (3.5)$$

C_a is the concentration of target analyte

A_a is the total area of quantification ion for the target analyte

A_i is the total area of quantification ion for the internal standard

Amt_i is the amount of internal standard added to the sample

RF_i is the average RF for the analyte, determined from initial calibration

V_a is the sample size

3.5 The experimental series

A total of 19 experiments were conducted with 3-7 parallels each.

The parameters that were varied throughout the experimental series were

- type of particulate matter
- concentration of particulate
- temperature
- method of dispersion (with/without dispersant, time in water before allowing contact with sediment)
- oil type

The parameters were varied one by one from a standard set of conditions defined at the start of the study. In the standard conditions, the type of particulate was carbonate sand from Grandefjæra in a concentration of 10 g/L sea water. The temperature was 18-20 °C, and the oil type was Troll 250+ without chemical dispersant. Table 3.5 describes the experimental design. Appendix A describes the experimental data for all parallels of every experiment. For all experiments, the oil concentration was 20 mg/L seawater, and the exposure time was 25 hours (1 hour suspension induced by stirring followed by 24 hours settling time).

Two series of experiments (LIS014 and LIS015) attempted to test the combined effect of varying temperature and adding dispersant simultaneously. As it is shown in the chromatograms in Appendix F, the quantification in Appendix G and seen by observations in the laboratory, these experiments suffered from a system failure. The syringe of the syringe pump was not able to displace the low-viscosity mix of oil and dispersant when influenced by low temperature. Therefore, little or no oil was added to the system. Thus, these results are neither presented nor discussed further.

Table 3.5 - Description of parameter variation in the experimental series of this study

Experiment ID	Type of particulate	Concentration of particulate [g/L]	Temperature [°C]	Dispersant added	Oil type
LIS001	Carbonate sand	5	18-20	No	Troll 250+
LIS002	Carbonate sand	10	18-20	No	Troll 250+
LIS003	Carbonate sand	20	18-20	No	Troll 250+
LIS004	Carbonate sand	40	18-20	No	Troll 250+
LIS005	Carbonate sand	80	18-20	No	Troll 250+
LIS006	Carbonate sand	10	4-5	No	Troll 250+
LIS007	Carbonate sand	10	10-11	No	Troll 250+
LIS008	Carbonate sand	10	18-20	No	Kvitebjørn condensate 250+
LIS009	Carbonate sand	10	18-20	No	IF 380 Fresh
LIS010	Carbonate sand	10	18-20	1 %	Troll 250+
LIS011	Carbonate sand	10	18-20	5 %	Troll 250+
LIS012	Carbonate sand	10	18-20	1 %, Time 10 min	Troll 250+
LIS013	Carbonate sand	10	18-20	1 %, Time 30 min	Troll 250+
LIS014	Carbonate sand	10	10-11	1 %	Troll 250+
LIS015	Carbonate sand	10	4-5	1 %	Troll 250+
LIS016	Carbonate sand	10	14-15	No	Troll 250+
LIS017	Clay	10	18-20	No	Troll 250+
LIS018	Carbonate sand	10	18-20	No	Avaldsnes 250+
LIS019	Sand	10	18-20	No	Troll 250+

4 Results

All GC-FID chromatograms from the analysis of water extracts and sediment extracts of samples and blanks are given in Appendix F. Detailed calculation of quantitative results is described by Appendix G. Results from quantification of GC-MS results are given in Appendix I. In this chapter, the averages of all valid parallels of an experiment are presented. Parallels were disregarded from calculations if some experimental conditions made the results of the experiment questionable. Error bars in graphs represent standard deviation. The maximum relative standard deviation for quantification of GC-FID results for water extracts is 31 %, and the average relative standard deviation for all water extracts is 13 %. The corresponding numbers for sediment extracts is 22 % (maximum) and 13 % (average).

4.1 Grain size distribution of sediments

The results of the grain size distribution determination (see Chapter 3.1.3) of sediments are given in Appendix C, and presented graphically below (Figure 4.1). The carbonate sand from Grandefjæra has most particles in the size range of 125 – 355 µm. The sand from Ranheim has most particles in the size range of 180 – 500 µm. A great portion of particles of Ranheim sand are also up to 2 mm. The grain size of the Buvika clay particles were all < 63 µm, and no grain size distribution diagram was made for this sediment.

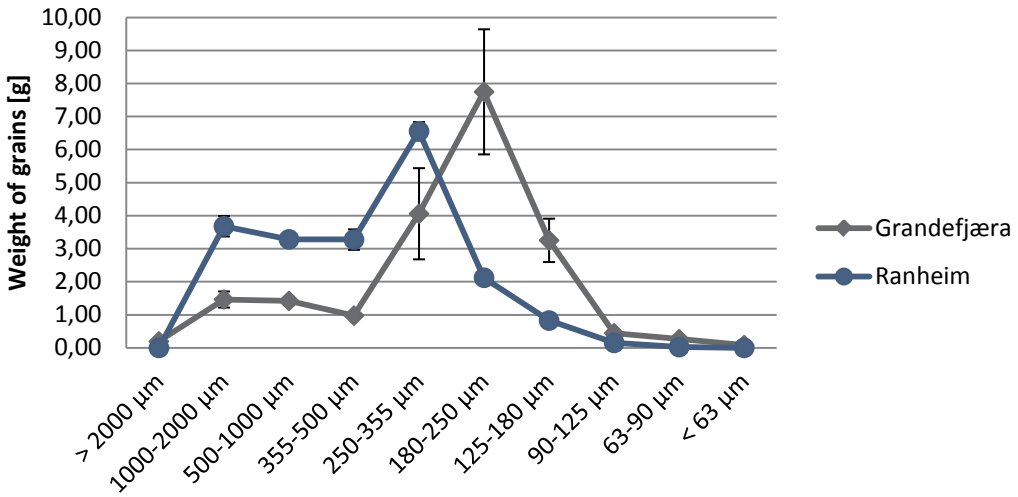

Figure 4.1 - Grain size distribution of sediments from Grandefjæra and Ranheim (Error bars represent standard deviation for, N=3).

4.2 Comparison of Soxhlet extraction and alkaline saponification

The results from the comparison of Soxhlet extraction and alkaline saponification are given in Appendix E. Two parallels of each extract gave quantifiable results from GC-FID analysis. A comparison of amount of oil recovered by the two techniques is shown in Figure 4.2. The results indicate that Soxhlet extraction is the most efficient technique with regards to recovery of oil. The GC-FID profiles (see Appendix E) of the compared extracts do not differ in any other way than peak height, which can be directly interpreted as a measure of extraction efficiency.

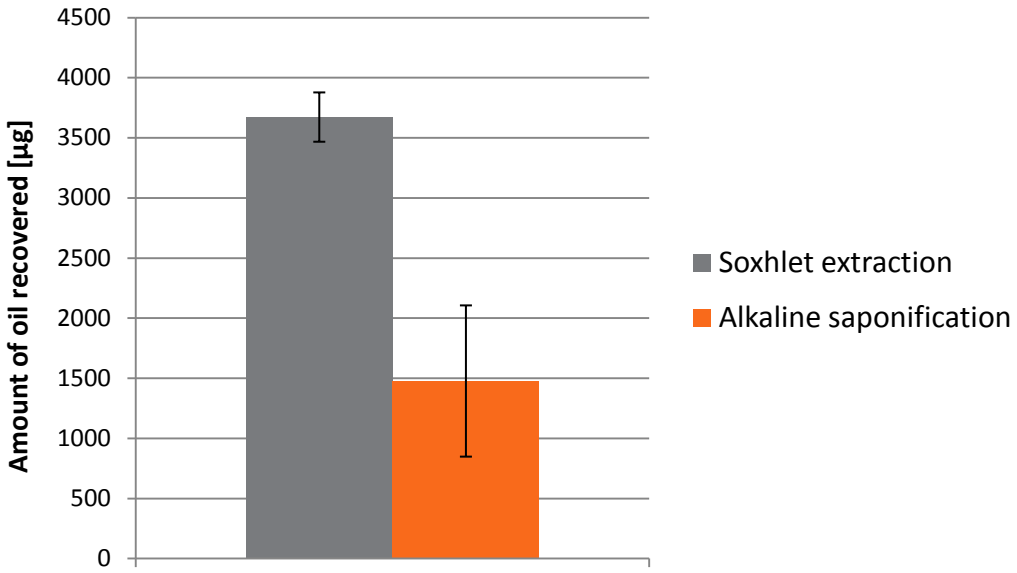

Figure 4.2 - Comparison of efficiency recovery of Soxhlet extraction and alkaline saponification (Error bars represent standard deviation).

4.3 Adsorption studies – sediment extract samples

Figure 4.3 shows a comparison of chromatograms of the pure oils used in this study with corresponding sediment extracts from the experiments (10 g sediment/L water, 18-20 °C, no dispersant). A general trend that can be observed is the loss of components eluting before 20 minutes in the sediment extracts compared to the pure oils. In addition, there is a relative increase in the concentration of the heavier and larger oil components which elute after 35 minutes in the GC-FID chromatograms.

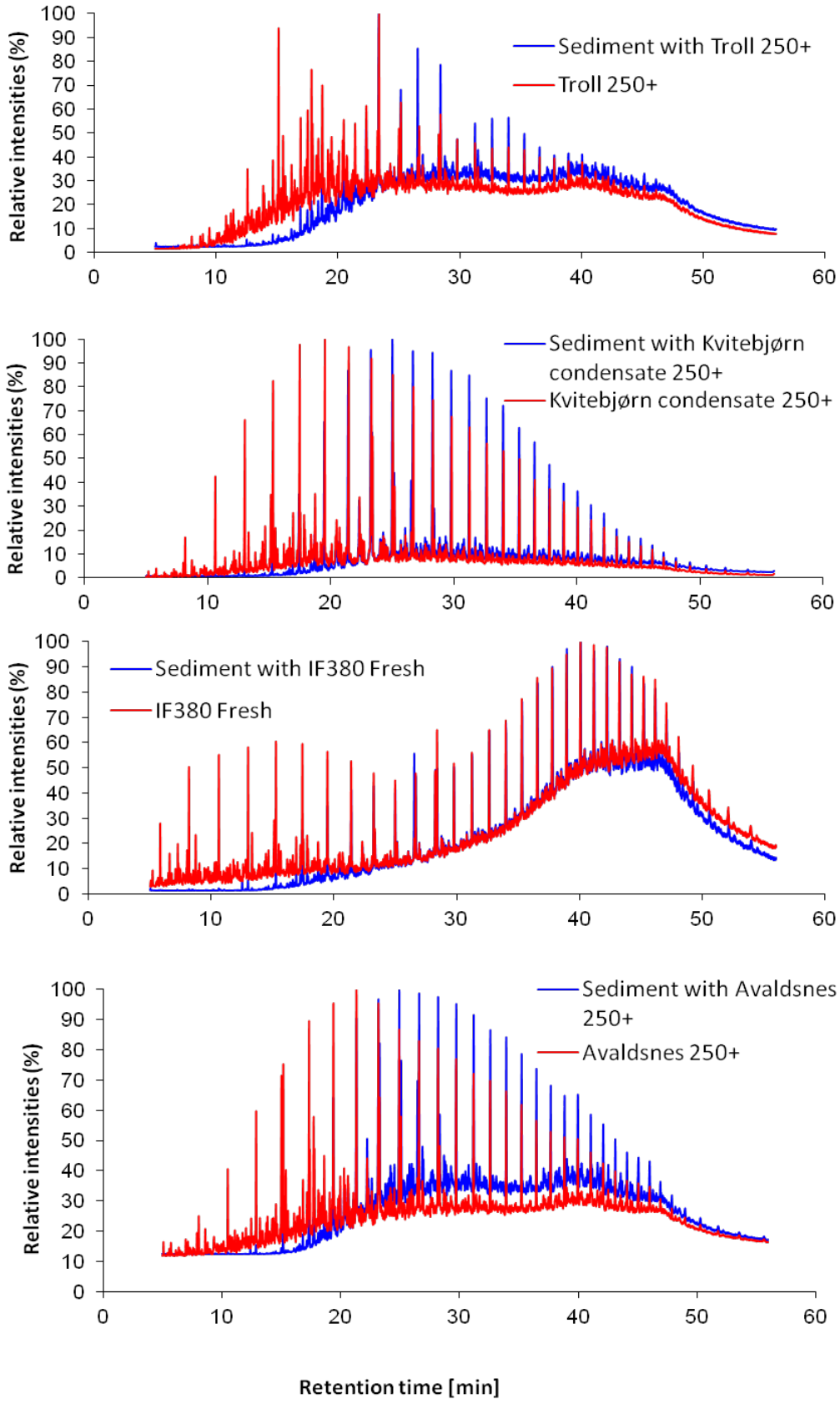

Figure 4.3 - Overlay comparison of chromatograms for all four oil standards (10 µg/mL in DCM) and representative sediment extracts of experiments where the oils have been applied.

Figure 4.4 shows a comparison of the chromatogram of a sediment extract from an experiment with Troll 250+, carbonate sand, 18-20 °C and no dispersant added with a sediment extract where dispersant has been added (1 %). The concentration of oil in the sediment extract where dispersant has been used is clearly lower than in the experiment with no dispersant added. Whilst the chromatograms show differences in response between the two samples, they appear to exhibit the same pattern and ratio of different components.

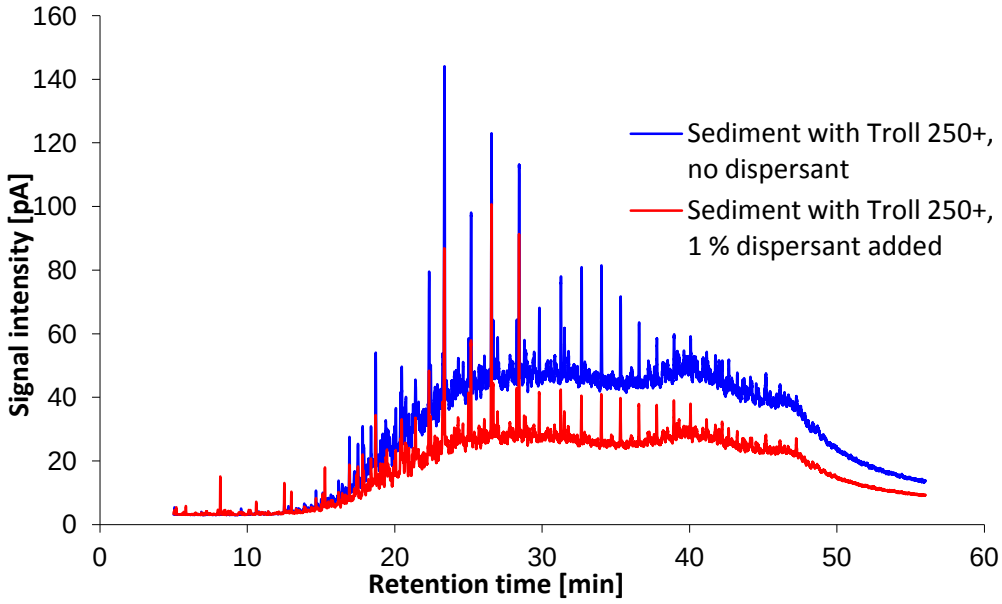

Figure 4.4 - Overlay comparison of chromatograms for sediment extracts of experiments with Troll 250+ with 1 % dispersant and without dispersant added.

4.3.1 Sediment concentration

The results from varying sediment concentrations (investigated using the carbonate sand) in the water are shown in Figure 4.5. It is apparent that the increase in sediment amount increases the amount of oil removed from the water phase. A linear curve is fitted to the data, and the R-squared value for this fitting is 0,6996. A logarithmic curve is also fitted to the same data, and the R-squared value for this fitting is 0,8633.

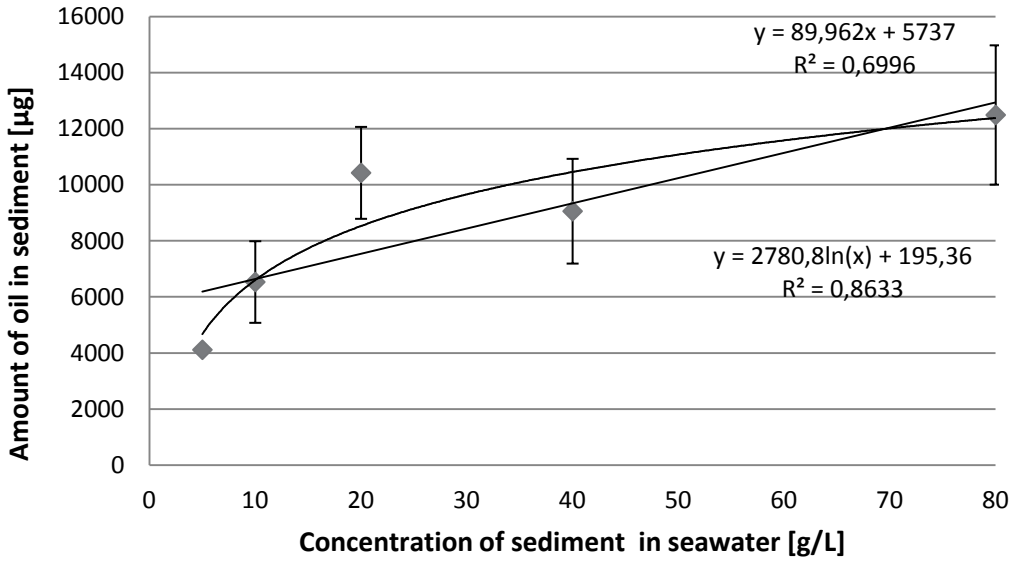

Figure 4.5 - Graph displaying the variation in oil uptake (µg) in sediment as a function of sediment concentration (Error bars represent standard deviation). The data is fitted with both a linear and a logarithmic curve.

Figure 4.6 plots the concentration of oil in the sediment as a function of increasing sediment concentration in the water column. The plot clearly demonstrates the oil-SPM ratio decrease when the amount of sediment is increased. A logarithmic curve is fitted to the data, and the R-squared value for this fitting is 0,9733.

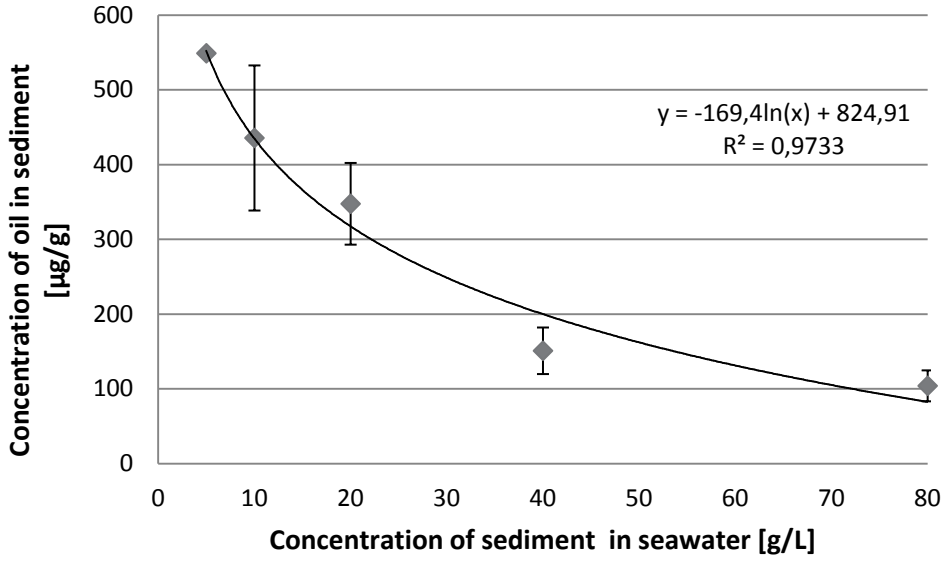

Figure 4.6 - Graph displaying the variation in oil concentration in sediment (µg oil/g sediment) as a function of sediment concentration (Error bars represent standard deviation). The graph is fitted with a logarithmic curve.

4.3.2 Sediment type

A bar chart displaying the results from the variation of sediment type is given in Figure 4.7. In these experiments, the effect of sediment type on adsorption of oil was assessed using the defined standard conditions of 10 g/L sediment concentration, temperature of 18-20°C, Troll 250+ crude oil and no dispersant. Only the sediment type was varied in the study. The quantitative amount of oil (Troll 250+) adsorbed to the clay is 2-3 times the amount adsorbed to any of the sands.

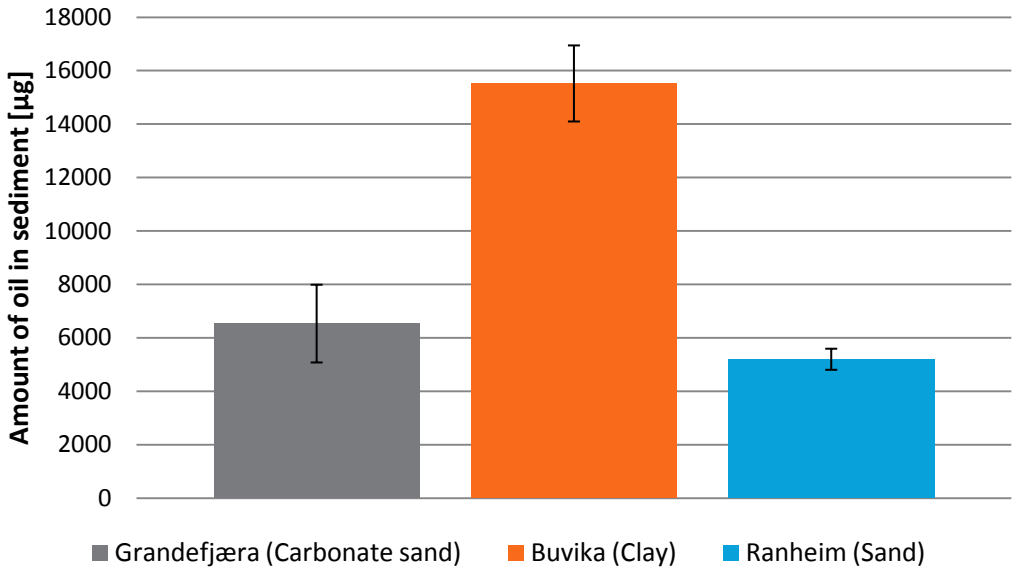

Figure 4.7 - Bar chart displaying the variation in oil uptake (µg) in sediment as a function of sediment type (Error bars represent standard deviation, N=7; 4; 3).

4.3.3 Oil type

A bar chart displaying the results from the variation of oil type is given in Figure 4.8. In these experiments, the effect of oil type on adsorption of oil to sediment was assessed using the defined standard conditions of carbonate sand sediment, 10 g/L sediment concentration, temperature of 18-20°C and no dispersant. Only the oil type was varied in the study. It is indicated that the "heavier" oils (IF 380 and Avaldsnes 250+) are adsorbed to the sediment in higher quantities than the other oils in the study.

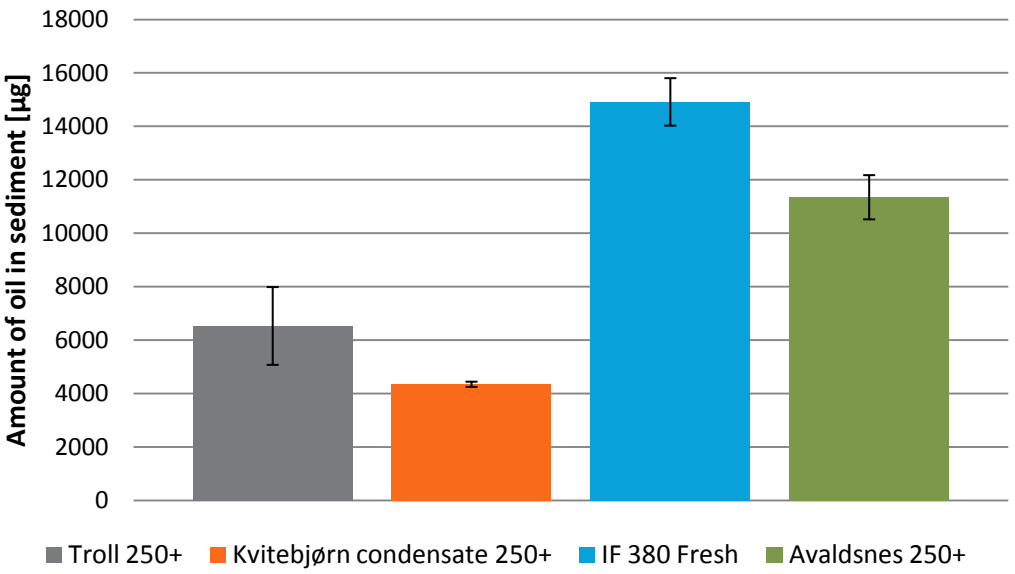

Figure 4.8 - Bar chart displaying the variation in oil uptake (µg) in sediment as a function of oil type (Error bars represent standard deviation, N= 7; 3; 3; 3).

4.3.4 Temperature

The results from varying temperatures are shown in Figure 4.9. In these experiments, the effect of temperature on adsorption of oil to sediment was assessed using the defined standard conditions of carbonate sand sediment, 10 g/L sediment concentration, Troll 250+ crude oil and no dispersant. Only the temperature was varied in these experiments. It is apparent that the increase in temperature decreases the amount of oil adsorbed to sediment. A logarithmic curve is fitted to the data, and the R-squared value for this fitting is 0,8616.

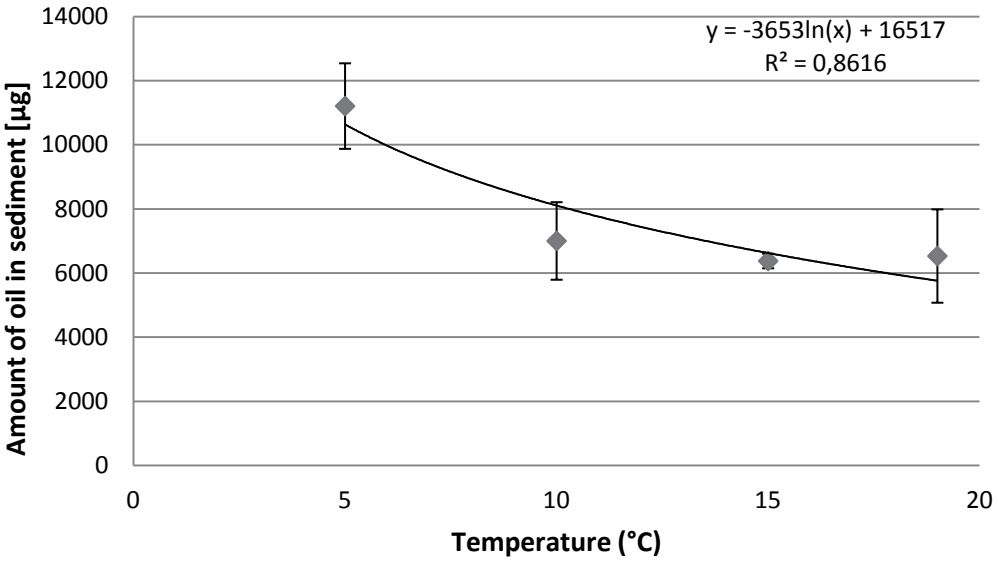

Figure 4.9 - Graph displaying the variation in oil uptake (µg) in sediment as a function of temperature (Error bars represent standard deviation, N=3; 5; 4; 7).

4.3.5 Use of chemical dispersant

Amount of dispersant used

The results from varying the ratio of dispersant to oil (DOR) are shown in Figure 4.10. In these experiments, the effect of chemical dispersant on adsorption of oil to sediment was assessed using the defined standard conditions of carbonate sand sediment, 10 g/L sediment concentration, temperature of 18-20°C and Troll 250+ crude oil. Only the use and quantity of chemical dispersant was varied in the study (0-5 %). It is apparent that the increase in DOR decreases the amount of oil adsorbed to sediment. A linear curve is fitted to the data, and the R-squared value for this fitting is 0,8248. An exponential curve is also fitted to the same data (this is speculative, see Discussion), and the R-squared value for this fitting is 0,9587.

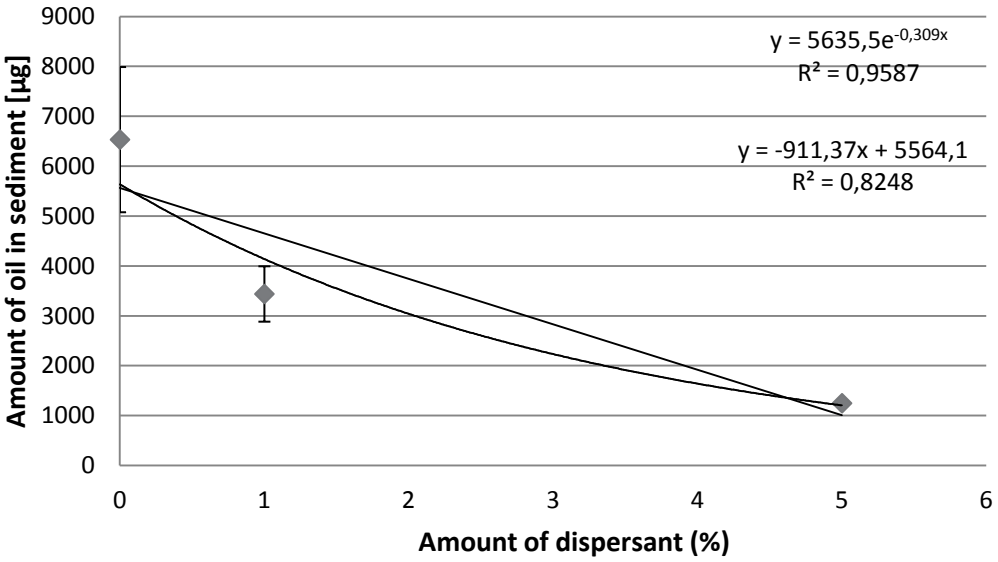

Figure 4.10 - Graph displaying the variation in oil uptake (µg) in sediment as a function of amount dispersant added (Error bars represent standard deviation, N= 7; 5; 3).

Residence time

It was attempted to see if any difference in adsorption of oil to sediment would be observed if there was a time-delay between addition of the oil-in-water dispersion and the addition of sediment to the system. In this study, the defined standard conditions of carbonate sand sediment, 10 g/L sediment concentration, temperature of 18-20°C, Troll 250+ and 1 % dispersant were used. The results are given in Figure 4.11. No clear trend can be seen from the data, but it is indicated that the adsorption of oil to sediment is least effective when the chemically dispersed droplets have been in the water column 10 minutes prior to introduction of sediment.

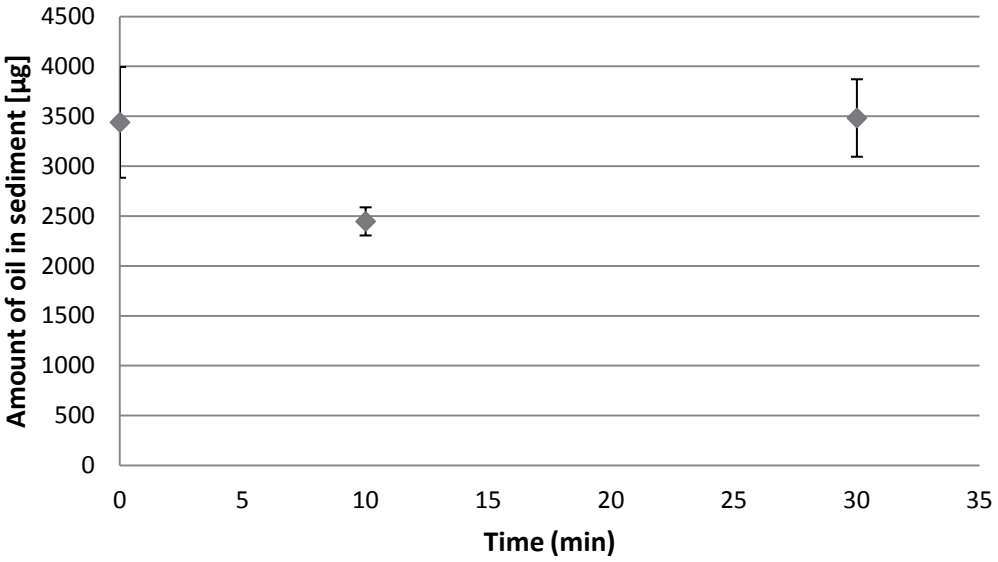

Figure 4.11 - Graph displaying the variation in oil uptake (µg) in sediment using 1 % dispersant as a function of hold-up time before adding the sediment to the system (Error bars represent standard deviation, N= 5; 3; 3).

4.4 Components partitioned to the water column

The following will focus on the seawater extracts from the water column corresponding to the sediment extracts presented in Section 4.3. Figure 4.12 show an example of a GC-FID chromatogram of the water extract from an experiment with Troll 250+ oil, carbonate sand, 18-20 °C and no dispersant added. The chromatogram contains a large number of resolved compounds with no observable UCM. Appendix F.2 presents the GC-FID chromatograms of all seawater extracts.

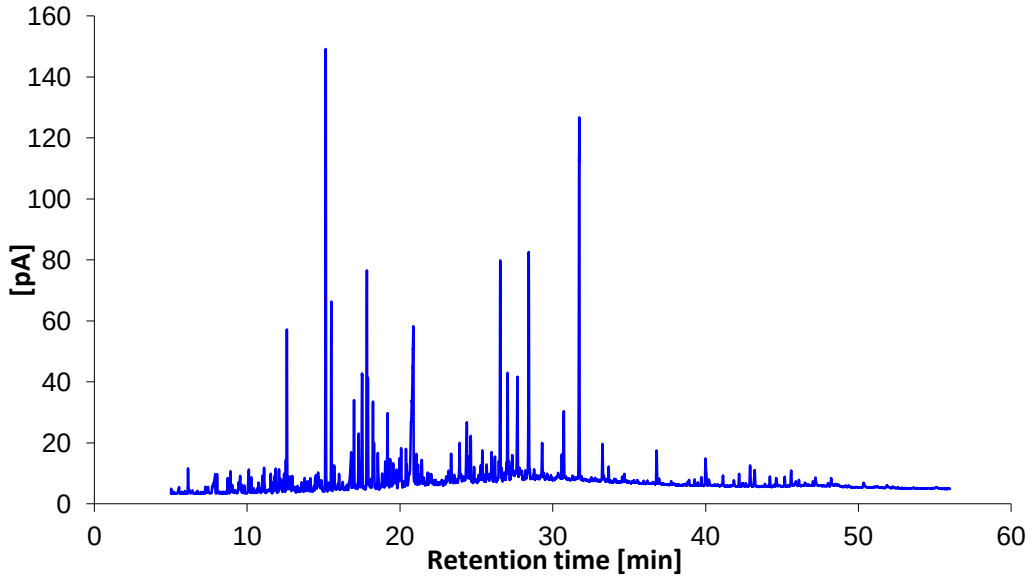

Figure 4.12 - GC-FID chromatogram of water extract from experiment with Troll 250+, no dispersant added.

4.4.1 Sediment concentration

The effect of varying sediment concentration on the dissolved components in the water phase demonstrates no clear trend (Figure 4.13).

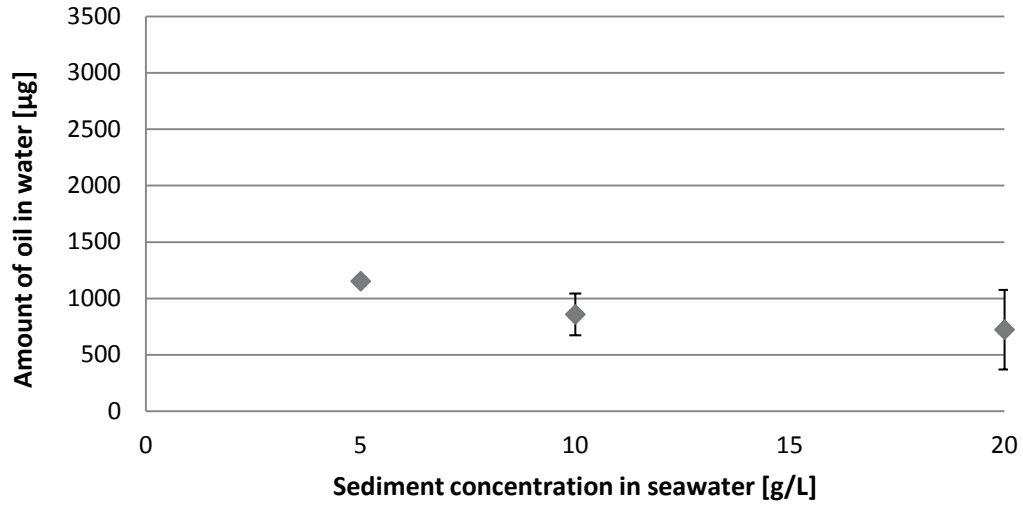

Figure 4.13 - Graph displaying the variation of oil in the water phase (µg) as a function of sediment concentration (Error bars represent standard deviation, N= 3; 6; 3).

4.4.2 Sediment type

The sediment type does not appear to result in any significant difference in the total amount of oil present in the water phase, given the relatively high standard deviations seen in Figure 4.14.

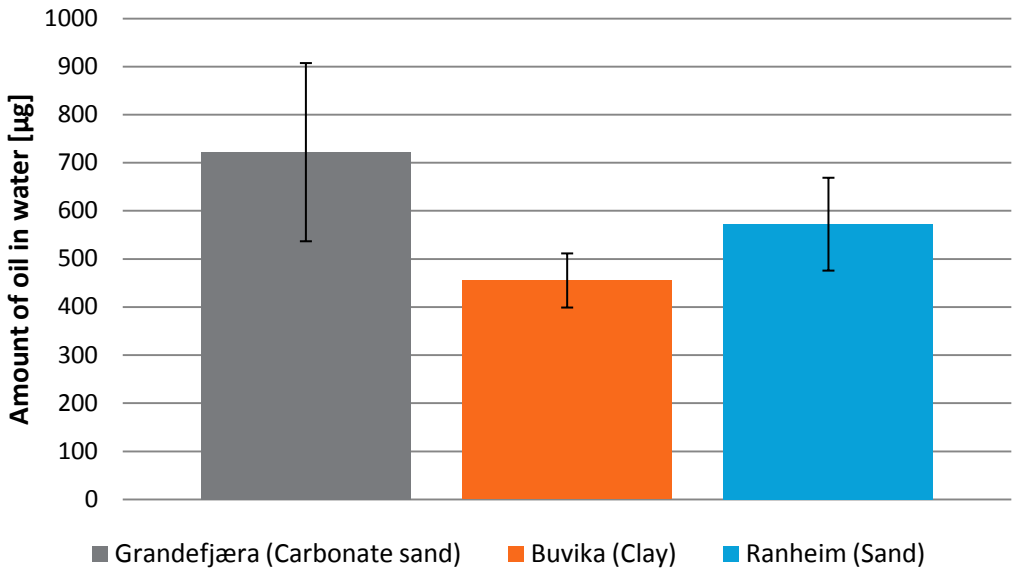

Figure 4.14 - Bar chart displaying the variation of oil in the water phase (µg) as a function of sediment type (Error bars represent standard deviation N= 6; 4; 4).

4.4.3 Oil type

A significant difference of partitioning of oil components to the water phase for the four test oils is not observed (Figure 4.15).

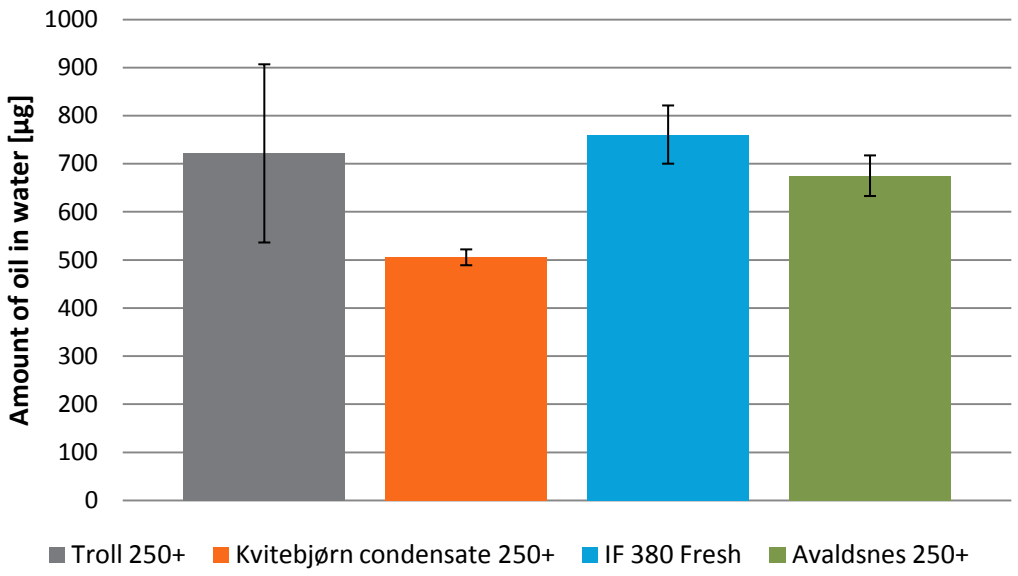

Figure 4.15 - Bar chart displaying the variation of oil in the water phase (µg) as a function of oil type (Error bars represent standard deviation, N= 6; 3; 3; 4).

4.4.4 Temperature effects on dissolved oil fraction

Figure 4.16 demonstrates the variation in oil dissolution as a function of temperature. The data does not indicate any clear trend.

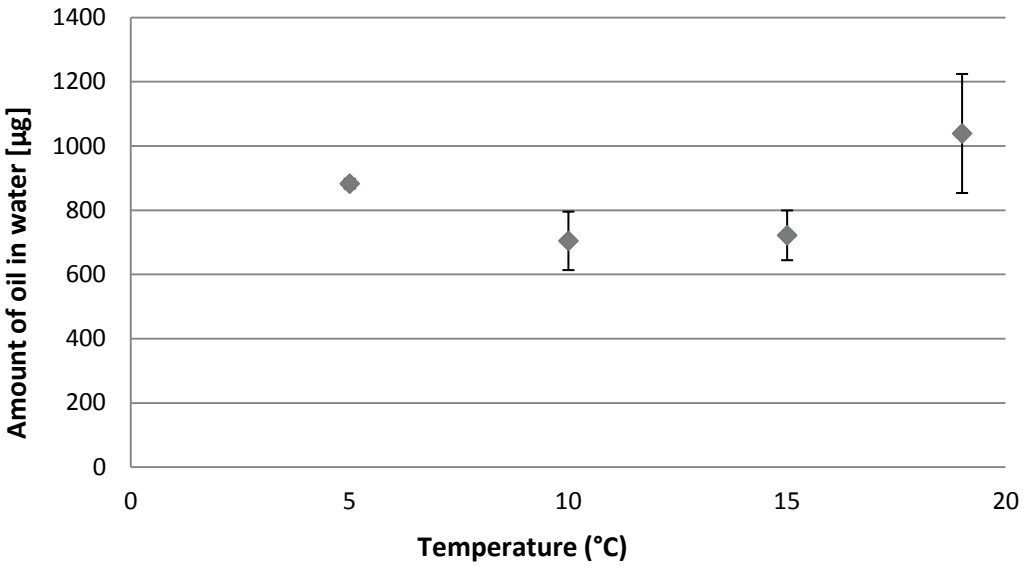

Figure 4.16 - Graph displaying the variation of oil in the water phase (µg) as a function of temperature (Error bars represent standard deviation, N= 3; 4; 4; 6).

4.4.5 Use of chemical dispersant

Figure 4.17 suggest that adding dispersants to the oil does not alter the amount of oil dissolved to the water phase, as there is not observed any change in amount of oil extracted from the water phase of experiments with 0, 1 or 5 % dispersant added.

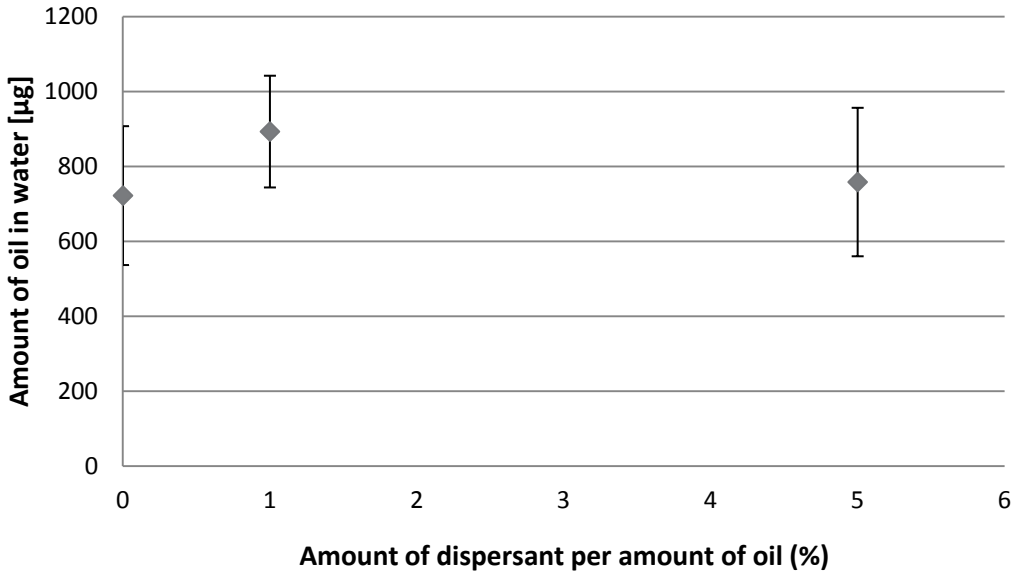

Figure 4.17 - Graph displaying the variation of oil in the water phase (µg) as a function of dispersant amount (Error bars represent standard deviation, N= 6; 4; 5).

Residence time

Figure 4.18 demonstrates that altering the residence time of oil droplets prior to addition of sediment does not alter the amount of oil dissolved to the water phase. There is no observed change in the amount of oil extracted from the water phase of these experiments.

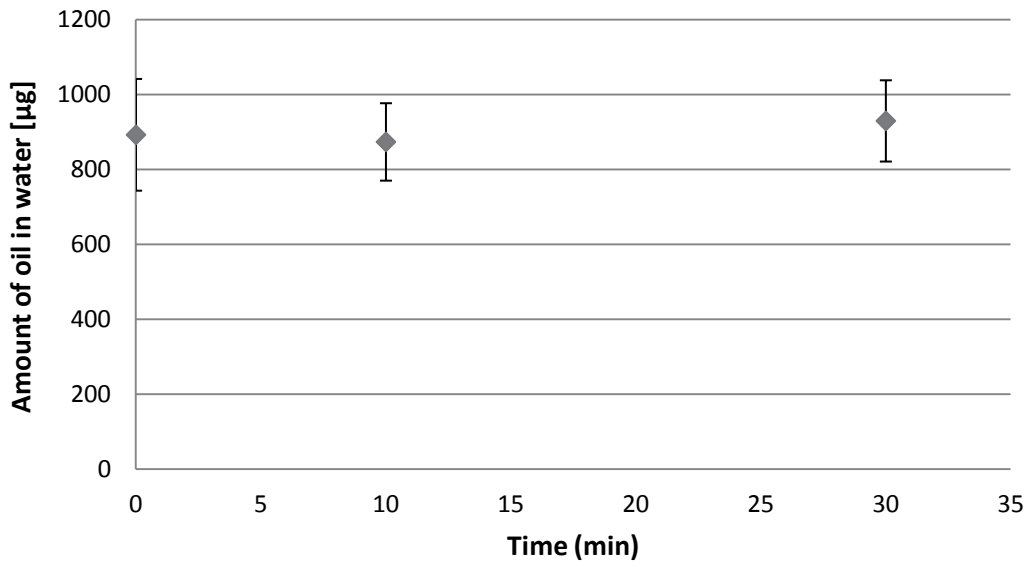

Figure 4.18 - Graph displaying the variation of oil in the water phase (µg) using 1 % dispersant as a function of hold-up time before adding the sediment to the system (Error bars represent standard deviation, N= 4; 3; 3).

4.5 Results of SVOC-analysis

Three parallels of both sediment extracts and water extracts from experiments with Troll 250+ oil and no dispersant, Troll 250+ oil with 1 % dispersant and IF 380 Fresh (no dispersant) were analysed by GC-MS to quantify the distribution of semi-volatile organic compound groups (SVOCs). Table 4.1 shows the sum of SVOCs quantified for each sample extract (µg/sample). Appendix H show an overview of the ions monitored and detected (SIM).

Table 4.1 - Sum of SVOCs determined by GC-MS analysis of pure oil and sample extracts.

	Pure oil		Sediment extract			Water extract		
	Troll 250+	IF 380 Fresh	Troll 250+	IF 380 Fresh	Troll 250+ 1 % dispersant	Troll 250+	IF 380 Fresh	Troll 250+ 1 % dispersant
Average (µg/ sample)	19	6	73	78	41	77	11	81
Standard deviation (µg/ sample)	2	1	6	5	1	22	2	19

Figure 4.19 shows the distribution of SVOCs in Troll 250+ and IF 380 Fresh oils. Both oils have a low content of C_{10+} saturates. Troll 250+ is dominated by naphthalenes (~60 %), and 2-3 ring PAHs (~30 %) is the second most abundant component group. IF 380 Fresh is dominated by 2-3 ring PAHs (~45 %), and have almost equal content of naphthalenes and 4-6 ring PAHs (~25 %).

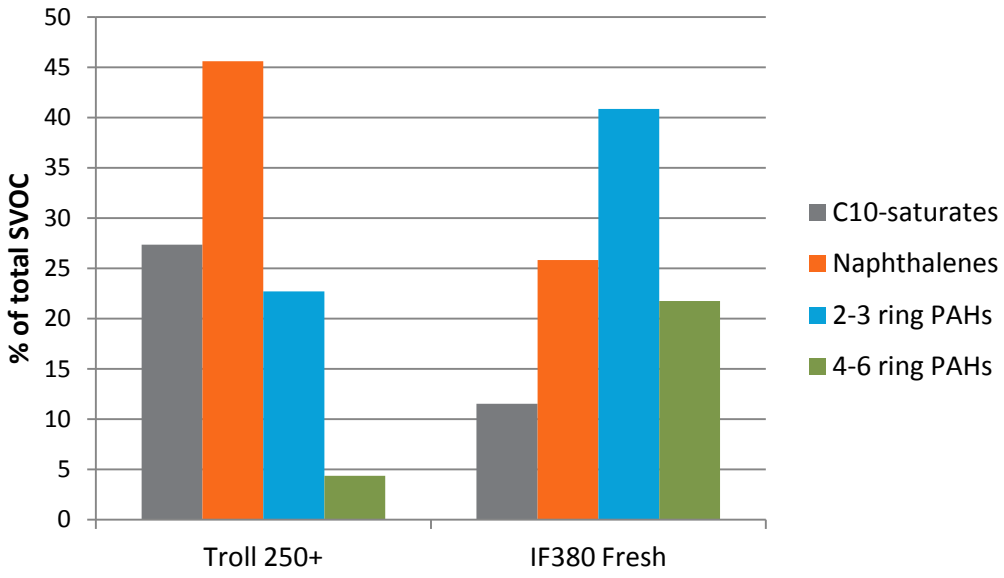

Figure 4.19 - Component group distribution of SVOCs in Troll 250+ and IF 380 Fresh

Figure 4.20 demonstrates the component group distribution of the proportion of Troll 250+ and IF 380 Fresh that adhered to the sediment (Grandefjæra carbonate sand). Figure 4.21 shows the same for the corresponding water columns. By comparing these graphs to those in Figure 4.19, one can see how naphthalenes are enriched in the water column compared to the parent oil but less abundant in the sediment extracts. In contrast, the 2-3 and 4-6 ring PAHs are enriched in the sediment extracts but reduced in the aqueous extracts.

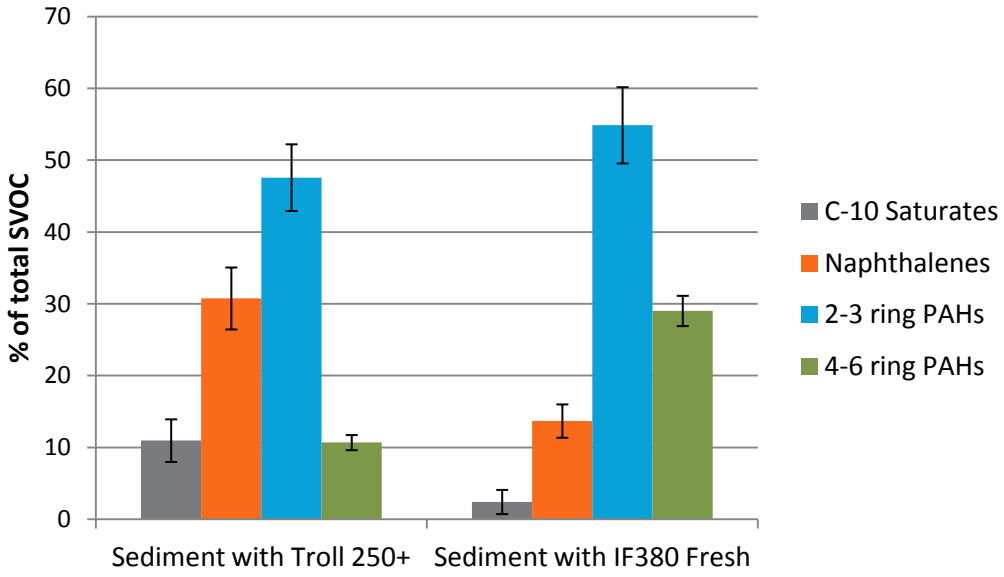

Figure 4.20 - Comparison of component group distribution (SVOC) in the sediment extracts of the experiments where Troll 250+ and IF 380 Fresh were added (Error bars represent standard deviations, N=3).

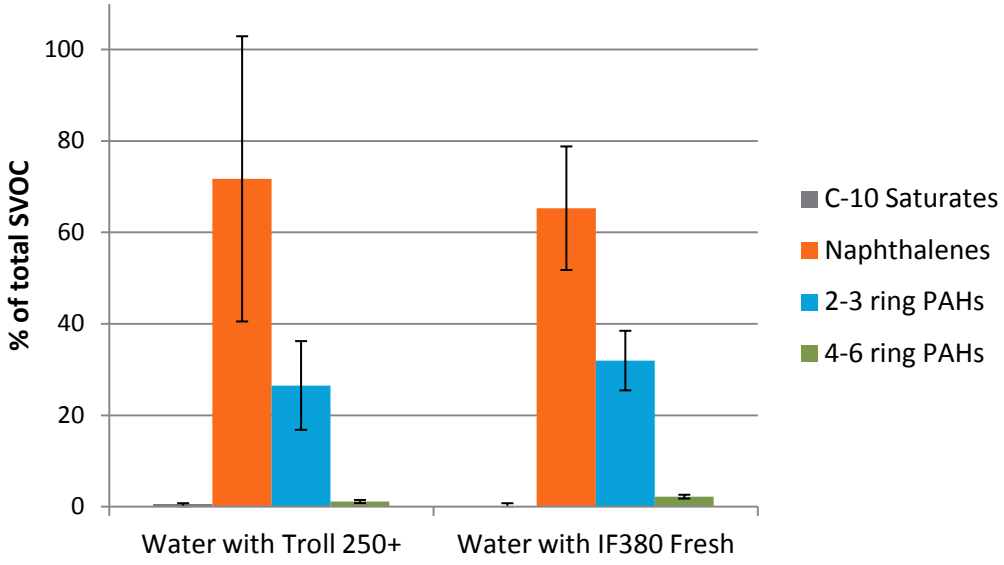

Figure 4.21 - Comparison of component group distribution (SVOC) in the water extracts of the experiments where Troll 250+ and IF 380 Fresh were added (Error bars represent standard deviations, N=3).

Figure 4.22 compares the component group distribution of SVOCs for Troll 250+ with the proportion of oil adhered to sediment in experiments with and without chemical dispersant added. Figure 4.23 compares the component group distribution of SVOCs for Troll 250+in the corresponding aqueous extracts. Again, it is clear that naphthalenes are enriched in the

water column and PAHs are enriched in the sediment. However, the addition of dispersant does not appear to cause any significant affect on either the component distribution profiles in the sediment and water extracts or amounts adsorbed/dissolved.

Figure 4.22 - Comparison of component group distribution (SVOC) in the in Troll 250+ with sediment extracts of the experiment with Troll 250+ (no dispersant) and the experiment with Troll 250+ with 1 % dispersant (Error bars represent standard deviations, N=3).

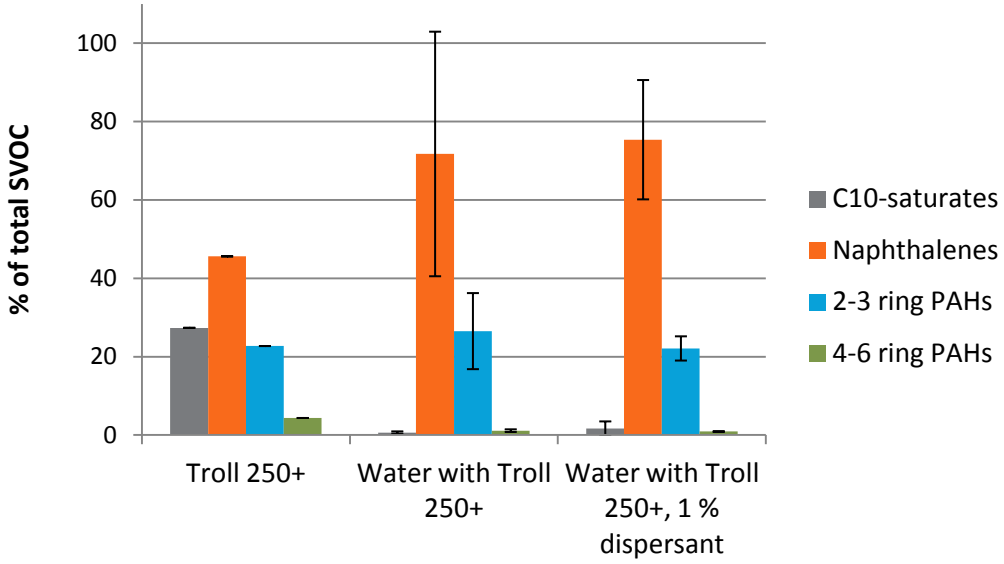

Figure 4.23 - Comparison of component group distribution (SVOC) in the in Troll 250+ with water extracts of the experiment with Troll 250+ (no dispersant) and the experiment with Troll 250+ with 1 % dispersant (Error bars represent standard deviations, N=3).

5 Discussion

In the case of an oil spill, it is of interest to be able to predict the environmental fate of the spilled oil. One possible route of fate for aqueous contaminants is the interaction with suspended particulate materials (SPM) present in the marine environment, and subsequent transport to the seafloor.

In this study, the influence of different parameters on the adsorption of oil to SPMs in seawater was examined. Oil droplets were generated mechanically by an oil-droplet generator. Seawater with oil droplets (20 mg/L) was added to a beaker with sediment and a suspension was induced by stirring.

The parameters investigated were sediment type (carbonate sand, quartz sand and clay) and concentration (5-80 g/L seawater), temperature (5-20 °C) and oil type (two crudes, one condensate and a heavy fuel oil). Special attention was given to the effect of adding chemical dispersant to the oil prior to mixing with water and SPMs.

Dissolved oil components in the water column were monitored in all the experiments. The dissolved fraction of oil is also of environmental interest, and it was of interest to see whether the parameters investigated in this study would also influence the dissolution process.

Extracts of water and sediment were analysed by GC-FID and GC-MS.

5.1 General partitioning patterns

The results from GC-FID analysis of the sediment extracts from samples containing the four test oils of the study (demonstrated by the chromatograms in Figure 4.3) show a loss of the earliest eluting components (the first 20 minutes of the temperature program). This trend is consistent for all the oils. This reduction in the lighter components also corresponds to a relative enrichment of the heavier oil compounds in the sediment adsorbed samples. No other change in the GC-FID profiles from pure oil to extract than the loss of early-eluting components is observed.

The components eluting early are relatively small and polar, and hence more soluble in water. The reason for their loss in the sediment extracts is therefore probably preferential

partitioning into the water column. The chromatograms from GC-FID analysis of the water extracts show no UCM (see Figure 4.12 and Appendix F.2), but they do show an enrichment of individual components eluting in the (approximate) time range 16-22 minutes. This enrichment is not observed in the blank samples of water, and thus can be caused by oil components dissolved in the water column of the experiments. The GC-FID profiles (Figure 4.3) of the sediment extracts also show a relative increase of the larger and heavier components (eluting after 35 minutes). These components are more hydrophobic, and will therefore prefer partitioning to sediment over dissolution in the water column.

If the experiments had involved the use of fresh oils, the loss of early eluting components could possibly be due to evaporation. The influence of evaporation was deliberately eliminated from the experiments by choosing topped oils (250 °C), where the most volatile components have been effectively removed. The nature of a heavy fuel oil (IF 380) means that it does not contain components volatile enough to evaporate at room temperatures either (see Chapter 2.2).

When compared to pure oils (Figure 4.19), GC-MS analysis of the sediment extracts from the experiments using the oil types IF 380 Fresh and Troll 250+ (Figure 4.20) show that the PAHs (2-6 rings) are preferentially enriched in the sediment, whilst the C_{10+} saturate compounds and naphthalenes are clearly reduced in concentration compared to pure oils. In the corresponding water extracts (Figure 4.21), the naphthalenes are enriched. The water phase is almost free of C_{10+} saturates and 4-6 ring PAHs. This observation is in agreement with the theoretical knowledge the solubility of individual PAHs in water will decrease exponentially with an increase in number of aromatic rings (Neff, 1979). The log K_{OW} value of naphthalene is 3,4. Larger PAHs have higher log K_{OW} values, e.g. benzanthracene and chrysene (4 ring PAHs) which have K_{OW} values in the range 5,3-5,6 (Briggs, 1981, Xing, 1997). This also supports the observation of a higher water fraction of naphthalenes than larger PAHs in the experiments of the current study.

Although the SVOC profiles of pure Troll 250+ and IF 380 Fresh have significant differences (Figure 4.19), the SVOC profiles of extract of water column exposed to droplets of these oils are alike (Figure 4.21). Apart from a depletion of naphthalenes, the profiles of pure oil (Figure 4.19) and sediment extracts (Figure 4.20) appear to have corresponding profiles. These findings show that the oil components that partition more strongly to particulates are

those which have low aqueous solubility. Thus, it appears as the dissolution process takes place independently of the adsorption.

The findings of the current study are supported by results from earlier studies (Payne and McNabb, 1984, Payne et al., 2003, Zurcher and Thuer, 1978), which demonstrate that higher-molecular weight aliphatics and PAH components prefer to partition to SPM in a water-oil-SPM system. Payne et al. (1984) have specifically shown that C_{10}-C_{40+} aliphatics and alkyl-substituted 2-5 ring PAH compounds (log K_{OW} values > 4) prefer to associate with particles rather than dissolve in the water column. The same studies showed that monocyclic aromatics with log K_{OW} values between 2,1 and 3,7, the more volatile C_1-C_{10} aliphatics and some lower molecular weight 2-3 ring PAH's with log K_{OW} values between 3,7 and 4,8 would partition to the water column (Payne et al., 2003).

Faksness et al. (2008) studied the water accommodated fraction (WAF) of nine different oils from Norwegian oil fields. For all the oils, the naphthalenes (along with the phenols) were the dominating group of SVOCs in WAF. Saeed and Al-Mutairi (2000) studied the water soluble fraction (WSF) of ten Kuwait crude oils, and found that of the PAHs, naphthalene and its homologues were the dominating group of all the oils WSFs. These two studies show excellent agreement with the current study, indicating that the naphthalenes will be the dominant hydrocarbon species in the water column near an oil spill (dispersed droplets or slick).

Contamination of water extracts

Some of the GC-FID chromatograms of water extracts show an enrichment of compounds eluting before 15 minutes. This trend is observed for some of the blank samples as well (see Appendix F.2.2). Contamination of the sea water or of glassware is the suggested cause of these otherwise unexplainable trends, as they do not show any coherence with experimental variables. Therefore, trends of compounds eluting before 15 minutes are not discussed.

5.2 Comparison of Soxhlet extraction and alkaline saponification

From a qualitative interpretation of the GC-FID results from the initial comparison of extraction techniques (given in Appendix E), it is apparent that the Soxhlet extraction is the most efficient technique with regards to recovery of oil from contaminated sediment. Figure 4.2 indicates that Soxhlet extraction recovers more than double the amount of oil than alkaline saponification. The two techniques do not give GC-FID profiles that differ significantly in any other way than amount. This indicates that there is o discrimination towards particular compound types between the two extraction techniques.

From a time-frame perspective, Soxhlet and alkaline saponification both require the same amount of time to be completed. However, the Soxhlet apparatus runs unsupervised, whilst the saponification requires more hands-on work. This also supports the choice of using Soxhlet in a project with a limited time frame.

Luque de Castro and Priego-Capote (2010) have compared Soxhlet extraction to other conventional techniques for extraction from solid materials. In terms of efficiency, it was found that Soxhlet was superior to any of the other techniques. The main disadvantage of Soxhlet was in fact related to the environmental issues caused by the high consumption of solvent that the technique requires.

5.3 Sediment characteristics

5.3.1 Sediment concentration

Figures 4.5 and 4.6 in Chapter 4.3.1 show that total oil adsorption increases with increasing amount of sediment. This trend was expected, as higher loads of sediment should provide an increased surface area available for adsorption of dispersed oil.

In Figure 4.5, both a linear curve (R^2=0,6996) and a logarithmic curve (R^2=0,8633) is fitted to the data set. The logarithmic curve is more speculative due to the limited number of data points, but appears to demonstrate a better fit. The fact that the relationship is clearly not linear indicates that doubling sediment concentration does not double the amount of oil partitioned to the suspended sediment. From the same experimental data, the concentration of oil in sediment (mg/g) is calculated and plotted against sediment concentration (g/L) in the water column (Figure 4.6). This clearly demonstrates how the

oil/SPM ratio of the extracted sediment decreases with increasing loads of SPM in the water column.

The good fit of the logarithmic curve in Figure 4.6 (R^2= 0,9733) indicates that the oil components in the water phase will not fully partition to the particulates (for a sediment type of the given characteristics; carbonate sand, grain size distribution as shown in Figure 4.1). These data indicate that for a given sediment type, there will exist an SPM-load where there is no further partitioning of oil droplets from the water column. Thus, a full equilibrium of oil partitioning between water and SPM is achieved.

For the experiments using Troll 250+ oil and carbonate sand, the maximum observed adsorption of oil is 15 mg (in one parallel where the SPM load was 80 g/L seawater). This is close to the amount of oil adsorbed to 10 g/L of clay from Buvika (see Figure 4.7). It is probable that a higher load of clay particles would lead to a higher fraction of adsorbed oil, but this can't be directly derived from the results of this study. Chapter 5.2.2 will further discuss the observed adsorption differences between sand and clay.

High relative standard deviations are observed for the experiments with high SPM-loads. By observation, these experiments show an "over-saturated" water column with regards to SPM. It is suggested that the implication of this is that the interactions between oil droplets and SPM become less effective, as particles will be so concentrated that their self-interaction can hinder the oil-SPM interactions. These concentrations (> 20 g SPM/L seawater) are also less realistic in an environmental perspective.

5.3.2 Sediment type

As demonstrated by Figure 4.7, the adsorption of oil varies with the type of sediments. Per gram of sediment, the clay from Buvika adsorbs 2-3 times more oil from a water column with 20 mg/L dispersed oil droplets, than the two sands applied in this study. There is no significant difference in adsorption between the carbonate sand from Grandefjæra and the quartz sand from Ranheim, and their grain size distributions (Figure 4.1) are not so different either.

The most apparent reason for the significant difference in adsorption of the oil is the size distribution of the sediments. For equivalent masses of sand and clay, clay will contain a

significantly greater proportion of individual particles, and hence have a significantly larger surface area for oil to adsorb to. In simulations of oil-SPM aggregation using a numerical model, Bandara et al. (2011) showed that sediment sizes > 0,5 mm led to less aggregate formation than smaller sizes (< 63 µm), and explained this by the reduction in number density of sediment in the water column. Natural waters are dominated by particles < 2 µm (Lee, 2002), so the results from the experiments with clay might be the most interesting in the environmental perspective. However, in high energy areas, particles of greater size are more likely to be suspended in the water column and influence the partitioning of oil.

The Ranheim sand was pre-rinsed with DCM before use in the experiments, and this will have lead to the removal of any organic residues coating the particles. This can have had an effect on the sorption of oil. In a review by Muschenheim and Lee (2002) it is presented that many studies have observed that organic coatings of the sediment particles have increased the sorption of hydrocarbons to the particles. Karickhoff et al. (1979) found that adsorption to particles of an isolated particle size depended upon the amount of organic substances associated with the particles. Hence, particles < 50 µm sorbed more hydrocarbons than particles > 50 µm, since the smaller particles were associated with more organic substances. In contrast, Meyers and Quinn (1973) found that organic coatings hindered the sorption of oil. Thus, it is not clear whether the rinsing of the sand has had any effect on the results of this study. The difference between sorption to Grandefjæra sand and Ranheim sand is not significant within the first standard deviation. It is therefore difficult to say whether the difference in mineral composition of the two sediments have had any influence on the adsorption process.

Stoffyn-Egli and Lee (2002) studied the influence of different clay types on oil-mineral aggregates and found that different clay types promoted aggregates of different shapes (droplet, flake, solid). Khelifa et al. (2005b) showed that while the concentration of oil-mineral aggregated droplets was determined mostly by oil type, the size droplet size was influenced by clay type and water salinity. Guyomarch et al. (2002) studied the effect of clay concentration on the size of formed oil-mineral aggregates and found that the largest aggregates were formed at a specific clay load. Lower or higher loads led to significantly smaller aggregates.

A number of studies focusing on oil-mineral aggregation, where the particulates are clay or other small mineral fines, have shown that the aggregates appear as oil droplets coated with fine particulates (Bragg and Owens, 1994, Guyomarch et al., 2002, Khelifa et al., 2002, Stoffyn-Egli and Lee, 2002, Ajijolaiya et al., 2006, Khelifa et al., 2005a, Khelifa et al., 2005b). It is therefore questionable whether the results of studies using clay can be directly extrapolated and compared to the current study which uses larger particles. It is possible that the larger sand particulates will be associated with oil droplets in a different manner than clay particles, but there is no existing evidence of this. Delvigne (2002), who found that oil in sediments had the appearance of droplets, also only looked at grains < 50 µm.

In the current study, the most important factor controlling the amount of oil adsorbed by SPM is the sediment grain size distribution, where smaller grains adsorb more oil than larger grains. Other studies have shown that mineral type can be an influence on the adsorption of oil to clay sediments. Further work is required to determine whether the mineral composition of sand is also an influence in the adsorption to these particulates. The physical appearance of oil adsorbed to larger particulates (~100 µm-2 mm) should also be investigated.

5.3.3 Amount of oil dissolved in water as function of sediment characteristics

There appears to be no significant difference in the amount of oil partitioning to the water phase when varying sediment characteristics (type, amount), as seen in Figures 4.13 and 4.14. This indicates that the process of dissolution of individual components is independent of the adsorption possibilities. Components with a log K_{OW} that favour dissolution in water will dissolve regardless of the SPM-loads in the water column. The compounds which will preferentially partition into the water phase from the oil droplets will not partition to the sediment at all. Therefore sediment type and concentration are non-influencing factors towards this equilibrium. The equilibrium will be based only on the partitioning of these compounds between the water phase and the oil droplets at the conditions of the experiments. It should be noted that other equilibria than that between oil component in water and SPM that might be of influence, given the experimental set-up (oil at surface, oil droplets, oil at glass wall).

5.4 Oil type

The degree of adsorption of the four studied oils to carbonate sand is shown in Figure 4. 8. The order below ranks the oils from highest (~15 mg) to lowest (~4 mg) adsorption to 15 g carbonate sand:

IF 380 Fresh > Avaldsnes 250+ > Troll 250+ > Kvitebjørn condensate 250+

In a study of oil-mineral aggregates, Guyomarch et al. (2002) found that the oil/clay ratio of four different oils increased with increasing asphaltenes content of the oils. The study also found that the heavy fuel oil adsorbed strongest (compared to two crudes and a HFO-crude mix), the asphaltenes content of the HFO was the highest of the oils. Asphaltene content can be seen as a measure of an oils polarity, and Guyomarch et al. (2002) suggests this as the explanation for the observed relationship between increased adsorption and asphaltene content of the oils. This is based upon their hypothesis that the formation of oil-mineral aggregates is caused by the interactions of polar oil compounds and the negatively charged clay particles. In the current study, the asphaltene content (See Table 3.1) of Avaldsnes oil is more than 10 times higher than the corresponding content in Troll and Kvitebjørn. The data therefore, seem to agree with the findings in Guyomarch et al. (2002), indicating that asphaltene content significantly influences the quantity of oil which partitions to sediment. In this study, the asphaltene content of the applied heavy fuel oil (IF 380) is unfortunately not known. In the study of (Guyomarch et al., 2002), the oil with highest asphaltene content was in fact the fuel oil (14 %). The recommended maximum content of asphaltenes in heavy fuel oil is 14 % (Wartsila, 2007). This indicate that the asphaltene content of heavy fuel oils may be higher than in the crude oils applied in this study (max 2,2 %). Should this assumption be correct, this would support the theory of asphaltene content being the dominant factor promoting oil-SPM interactions.

The viscosities of the oils used by Guyomarch et al. (2002) increased with increasing asphaltene content. In the present study this is not the case, as the Kvitebjørn condensate 250+ is the oil of highest viscosity. This may indicate that the asphaltene content is of greater importance than viscosity to the adsorption properties of an oil type.

In this study, the fuel oil IF 380 Fresh is demonstrated to adsorb to SPM in significantly greater quantities than some topped crude oils. It is known that significant amounts of fresh crude oil will be lost due to evaporation in the early hours following a spill (Wang and Stout,

2007). This clearly indicates that in the event of an oil spill, more oil will end up in the sediment if the spilled oil is a fuel oil than if it is a crude oil.

Variation in components dissolved in water as a function of oil type

Figure 4.15 shows the amount of each of the test oils which has partitioned into the aqueous phase. There appears to be relatively little difference in the total amount of each oil type in the aqueous phase and variation is less than an order of magnitude across all 4 oil types (~500-750 µg). A comparison of Figure 4.15 and Figure 4.8 shows that the difference between the least dissolved oil (Kvitebjørn condensate 250+) to the most dissolved oil (IF 380 Fresh) is relatively small when compared to the difference in adsorption to SPM of the same oils.

The GC-FID analysis (see Appendix F.2) of water extracts from the experiments where IF 380 Fresh is added stand out with “cleaner” chromatograms and less intense peaks than observed in other experiments. However, the quantification of GC-FID analysis show the water column from the experiment with IF 380 Fresh to be the most enriched in oil. The relative response factor used in the quantification for IF 380 Fresh (0,437) is lower than the one for Troll 250+ (0,748). Given that the water phase consists of individual components, the responses in the FID may not be dependent on the oils relative response factor, and hence the quantification overestimates the amount of oil in the water phase of IF 380 Fresh. The relative response factor of Avaldsnes 250+ is 0,591, and the relative response factor of Kvitebjørn condensate 250+ is 0,773. Figure 5.1 can be seen as a correction of Figure 4.15 from the results section, in which the quantification has used the same relative response factor (0,748) for all samples. This representation demonstrates that there is no significant difference between the dissolved components for Kvitebjørn condensate 250+, IF 380 Fresh and Avaldsnes 250+. The average amount of dissolved components for Troll 250+ is higher than for the rest, but the difference is not significant.

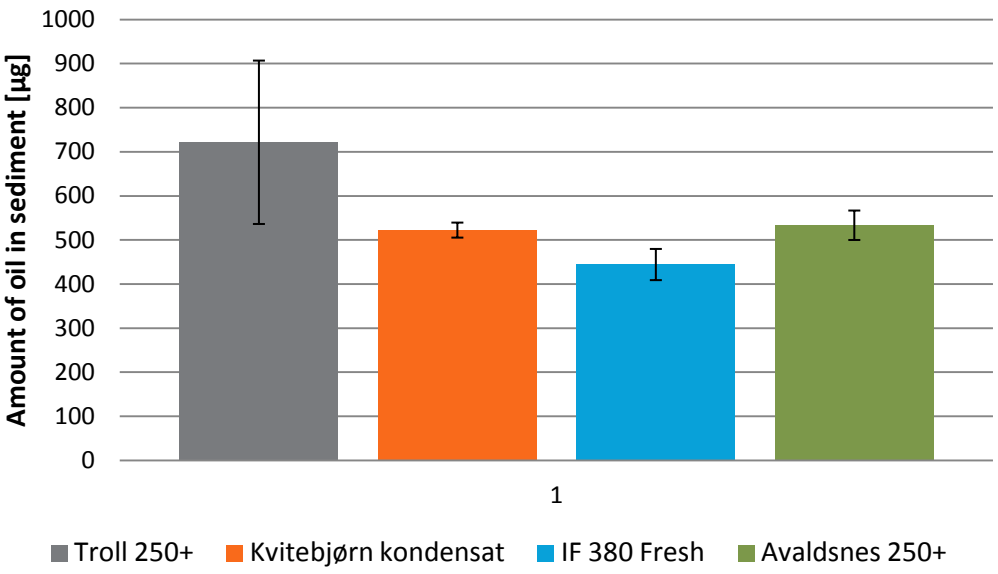

Figure 5.1 - Bar chart displaying the variation in oil in the water phase (µg) as a function of oil type. Calculations have used the same RRF for all samples (0,748). Error bars represent standard deviation.

GC-MS analyses of the water phase extracts (see Table 4.1) show that the sum of SVOC of IF 380 Fresh is lower (11±2 µg/sample) than the corresponding sum of SVOCs for Troll 250+ (77±22 µg/sample). This result is in contrast to the trend shown in Figure 5.1 and Figure 4.15, where no significant difference between the water partitioning of the different oils is observed.

When comparing the SVOC-profiles of Troll 250+ and IF 380 Fresh in Figure 4.19, it is seen that Troll 250+ is richer in naphthalenes than IF 380 Fresh. When considered in connection with Figure 4.21, this clearly demonstrates that naphthalenes are the main constituent of the dissolved fraction of SVOCs, irrespective of oil type. This could have explained why there appear to be more oil components in the water column of experiments using Troll 250+ than in the experiments using IF 380 Fresh. However, by referring to Table 4.1, it is also clearly seen that the sum of SVOCs is significantly lower in pure IF 380 Fresh (6±1 µg/sample) than in Troll 250+ (19±2 µg/sample). According to Raoult's law (Equation 2.2), a lower total concentration of SVOCs in the oil, would also lead to lower dissolution in the water phase. The results from this study also illustrate clearly that there are other water-soluble components from the oil (apart from the naphthalenes) that are predominantly dissolved in the water phase, but the identity of these was unfortunately not determined by the GC-MS analysis method used.

5.5 Temperature

The effect of varying the temperature (5, 10, 15, 20 °C) on oil adsorption to SPM is shown in Figure 4.9. The results demonstrate that the test oil (Troll 250+) adsorbs in the highest quantities at low temperatures (5 °C). The amounts adsorbed at 10, 15 and 20 °C are approximately the same (~6-7 mg), whilst the amount at 5 °C (~11 mg) is significantly higher than these values.

The viscosity of oil will increase at lower temperatures, and this might explain the higher adsorption at 5 °C. In the oil type experiments (see Figure 4.8), the oil type with the highest viscosity at 13 °C (Kvitebjørn condensate 250+), is actually the oil that adsorbs the least to SPM. But, it was also suggested (Chapter 5.4) that asphaltene content were of greater importance than viscosity in determining the adsorption properties of an oil type. Therefore, the adsorption properties of an individual oil type might be affected by viscosity changes induced by temperature changes. Stoffyn-Egli and Lee (2002) found a reduction in the oil content of oil-mineral aggregates at 0 °C when compared to 20 °C, and attributed this to the increased viscosity of oil at low temperature. This is the opposite trend of what is found in the current study.

In contrast to the findings of Stoffyn-Egli and Lee (2002), Meyers and Quinn (1973) found that sorption of hydrocarbons to sediment decreased with increasing temperature. The decrease in sorption was attributed to the increasing solubility of hydrocarbons with increasing temperature. This finding is supported by Tremblay et al. (2005), who investigated the partitioning of the PAHs phenanthrene and fluorene in estuarine environments, and found that the adsorption to SPM increased when the temperature of the water was lowered from 20 to 2 °C. The increase in sorption is attributed to the decreased water solubility of the PAHs at low temperature. In another study, Murray (1973) investigated the sorption of proteins to suspended sediments in Alaskan waters and found that varying the temperatures from 5-25 °C gave no significant change in amount protein sorbed. Zhao et al. (2001) also found that temperature did not influence the sorption of chlorobenzene to marine sediments. In general, the current study agrees with the results reported by Meyers and Quinn (1973) and Tremblay et al. (2005). However, in the present study, the dissolution of oil components does not increase significantly enough to explain the associated drop in adsorption (Figures 4.9 and 4.16) at low temperatures (5 °C). It is suggested that higher

temperatures increase the “bulk” solubility of oil droplets, and that dissolution of specific components from the droplets is a different, unlinked process. The viscosity of an oil also may be of influence, but to the authors knowledge there is nothing available in the current literature to support the findings of this study.

As the solubility of molecules increases with increasing temperature, it was expected that the amount of oil dissolved in the water phase would decrease in the experiments using lower temperature. This is not observed in the current study (Figure 4.16). One might therefore question if the proposed method used in this study (mixing for 1 hour followed by 24 hours settling time), allows sufficient time for the dissolution of oil compounds into the water phase to reach equilibrium. Faksness et al. (2008) investigated the effect of mixing time (of oil and seawater) in WAF experiments, and found that at lower temperatures, longer mixing times were necessary in order to achieve equilibrium. 48 hours is the recommended mixing time at 13 °C, but this was not sufficient at 2 °C. This indicates that the current study might have underestimated the amount of oil in the water phase, due to insufficient mixing times and failing to reach full equilibrium. In a study of petroleum hydrocarbon solubility, Page et al. (2000) found that naphthalenes equilibrated in the water column after 19 hours, but this observation may not be extrapolated to compounds of lower water-solubility.

5.6 Use of chemical dispersant

The results described in Chapter 4.3.5 clearly demonstrate how addition of dispersant decreases the adsorption of the test oil (Troll 250+) to suspended carbonate sand. Adding 1 % dispersant leads to an approximately 50 % reduction of the amount of oil adsorbed. Table 4.1 also shows that the total amount of SVOCs adsorbed to SPM is approximately halved by addition of 1 % dispersant to Troll 250+ oil. Increasing the dispersant amount to 5 % leads to an additional 50 % reduction (75 % reduction total) of the amount adsorbed. If one was to extrapolate this trend linearly, it would only take a dispersant to oil ratio of 6 % to ensure that no oil would adsorb to SPM. However, it is unlikely that the effect of increasing dispersant/oil ratio is linear. Mackay and Hossain (1982) also found that dispersants inhibited the adsorption of oil to sediments. They suggested a relationship expressed like this:

$$F_R = e^{-0,15D}$$

Where F_R is the ratio of oil settled with sediment and D is the dispersant to oil ratio (%).

Employing the same relationship with the data from this project, the equation would be (see Figure 4.10):

$$F_R = e^{-0,31D}$$

Interpreting the data as having an exponential trend would mean that there exists a minimum level of oil that will adsorb to SPMs no matter how much dispersant is added to the oil. From a practical point of view, adding dispersant cannot completely hinder oil droplets from interacting with suspended particulates in the water column. Figure 4.22 demonstrates how the SVOC distribution profile for sediment extracts is unrelated to the use of dispersant. This means that the chemically dispersed oil droplets will still adsorb as a bulk, only in smaller proportions than naturally dispersed droplets.

Lessard and DeMarco (2000) suggest it is less likely that a chemically dispersed oil will adhere to SPMs, as it is “less sticky” than a naturally dispersed oil. As discussed in Chapter 5.3.2, it is possible that the interaction mechanism of small (clay) particles and larger particles (e.g. sand) with oil droplets may be different. The difference is predominantly based upon the available surface area of the different particle sizes. However, Mackay and Hossain (1982) suggest a different explanation; smaller grains will reside longer in the water column and therefore have t he opportunity to interact more with dispersed oil. Irrespective of the process occuring, this does not explain why other previous studies have seen more association of oil-SPMs with dispersant added than without.

Chapter 1.6 reviews a number of previous studies which have focused on the effect of dispersants on oil-SPM interactions. These studies are in conflict with the findings of the current study and with the study of Mackay and Hossain (1982). Several of the studies found that chemical dispersants did not inhibit the formation of oil-SPM aggregates. Khelifa et al.

(2008) used clay particles and found that for low particle loads (< 25 mg/L) the chemical dispersant increased oil sedimentation by a factor of 3-5. For higher mineral loads, the adsorbed amount was equal for experiments with and without dispersant added. The reduction in oil droplet size, increase in concentration of oil droplets in the water column and the alteration of surface properties of the oil droplets are the reasons given for the observed increase in adsorption. Numerical model simulations by Bandara et al. (2011) showed that the presence of smaller oil droplets increased the predicted amounts of oil-SPM aggregates formed. The suggested explanation for this is that the droplet residence time in the water phase is prolonged due to the decreased buoyant velocity of smaller particles, and this allows for more interactions with suspended matter.

The current study looked at the effect of dispersant on adsorption to (carbonate) sand, whereas the studies showing increased adsorption when dispersant was added used fine clay particles. The increased total surface area of the chemically dispersed oil droplets might increase the adsorption of fine mineral particles on their surface. This would not be observed with sand particles. The reduction in adsorption to sand particles might therefore be explained by “less stickiness” of the oil, as suggested by Lessard and DeMarco (2000).

The results of this study show that adding dispersants to oil does not lead to an increase (or decrease) in amount of oil components dissolved in the water column (see Figure 4.17). Table 4.1 also shows how the total amount of SVOCs dissolved in the water column does not change when dispersant is added. Figure 4.23 shows how the addition of dispersant does not affect the SVOC profile of dissolved components. These observations indicate that dispersants do not directly affect the partitioning of individual components (or groups of components) to the water phase. This is in contrast to the impact on oil adsorption to SPM, which is clearly reduced in the presence of a dispersant. Wolfe et al. (1998) found that the concentration of naphthalene in water did not change with the addition of dispersant to a crude oil, and this supports the findings of current study (see Appendix I).

The observed reduction in oil adsorption to SPM when chemical dispersant is added is clearly not a direct result of increased dissolution of oil compounds into the water phase caused by the dispersant. A potential explanation may be that the surfactants of the dispersant stabilize the smaller oil droplets in the water column (and hence counteract adsorption to particulates). The stabilizing effect of dispersants on oil droplets is described by Fingas

(2011), Lessard and DeMarco (2000) and Fiocco and Lewis (1999). As the surfactants are structurally equal to detergents made to dissolve and stabilize household grease as droplets in wash water, this is not a surprising effect of the application of chemical dispersants on oil.

Effect of residence time

It has already been indicated that dispersant addition does not affect the amount of oil components, or component groups, that are dissolved in the water column. Therefore, it is not surprising that the experiments with a residence time of chemically dispersed oil droplets in water before addition of sediment show no difference in amount of oil dissolved (Figure 4.18).

The sediment phase extracts show a minimum concentration of oil adsorbed after a 10 minute residence time before interaction with SPM (Figure 4.11). In contrast, the concentration of oil in the samples following immediate interaction with sediment particles and interaction after 30 minutes, which both show similar amount of adsorption, are higher. However, the standard deviations mean that the differences between the different residence times are not significant. Furthermore, the amount of oil in all three sample types is in the range of 2500-3500 µg. It would be difficult to explain this observation, especially since there is little existing experience with the surface properties of chemically dispersed droplets in the marine environment. The reason for the interest in the effect of residence time is the potential for leaching of the dispersant surfactants from the droplets over time (Fingas, 2011, Lewis et al., 2010). This could potentially lead the droplets to be less stabilized after a given amount of time, and therefore start to behave like physically dispersed droplets. This trend is not observed in this study. It should also be noted that this study uses a closed system, and if the surfactants were to leave the oil droplets, they would still remain in the enclosed water-oil-SPM system, with the ability to re-interact with a new oil droplet.

5.7 Environmental implications

In this study, the effect of sediment type and concentration, oil type, temperature and use of chemical dispersant on the adsorption of oil to suspended sediment in seawater were studied. Three of the studied parameters stand out as most influential in affecting the

adsorption properties of oil droplets to SPM in seawater. First, sediment of smaller particulate size (clay) adsorbs more oil per gram than larger sediment (sand). Second, an oil characterised as being heavy and polar (higher content of asphaltenes) adsorbed more efficiently to suspended particulates than oils which were lighter and less polar oil. Finally, addition of chemical dispersant to the oil droplets decreased the sedimentation of oil in an exponential manner. 1 % dispersant halved the amount of oil sorbed to carbonate sand. GC-MS analysis revealed that the dispersant did not change the distribution of C_{10+} saturates, naphthalenes and 2-6 ring PAHs in the sediment, only the amount. The effect of varying temperature (5-20 °C) was not considerable compared to the other parameters in this study. Previous studies show conflicting results about the effect of temperature on adsorption. In this study, the adsorption was highest at the lowest temperature, and this is attributed to increased viscosity of the oil at lower temperature. GC-MS analysis revealed an absence of compounds with low log K_{OW} values (e.g. naphthalenes) in the oil adsorbed to sediment extract. No change in SVOC distribution was observed with the addition of 1 % dispersant.

The distribution and concentration of oil compounds dissolved in the water column was also monitored in every experiment. None of the parameters studied were found to alter the concentration or distribution of dissolved oil compounds significantly, and it is suggested that dissolution and adsorption are separate processes. Of the range of compounds studied by GC-MS, the naphthalenes exhibited the highest partitioning to the water phase. The C_0-C_3 naphthalenes are relatively volatile and represent some of the early-eluting components which were absent or reduced in the GC-FID chromatograms from the sediment extracts. In an oil spill scenario, the amount of oil sorbed to SPMs might therefore be related to the amount of dissolvable (and volatile) components in the spilled oil. However, there was no apparent influence from the studied parameters on the dissolution of specific oil. Dissolution is therefore regarded as an oil type dependent process.

Fate of chemically dispersed oil in the marine environment

The results from the current study show that chemically dispersed oil droplets adsorb less to suspended particulates in seawater than mechanically dispersed droplets. In a marine environment dominated by relatively high SPM-loads, this finding implies that the use of chemical dispersant will lead to more oil droplets being present in the water column over a

longer time period. As a result, the exposure time of marine organisms to oil will be correspondingly longer. Furthermore, the increased residence time of oil droplets in the water column might lead to increased dissolution of water-soluble components. Faksness et al. (2004) studied the partitioning of semi-soluble organic compounds between the water phase and dispersed oil droplets in produced water. It was found that there was a positive correlation between the concentration of dispersed oil in the water and the concentration of semi-soluble aromatics dissolved in the same water. The correlation varied for different groups of compounds, but the trend was especially clear for the PAHs. In the current study, an increase in oil components dissolved in the water phase from chemically dispersed oil droplets was not observed. This might be caused by the experimental conditions, where the stirring was switched off after an hour, allowing the droplets to float to the water surface. It is possible that the droplets will merge and significantly reduce the surface area of the oil in contact with the water. It is also likely given the short exposure period, that the system does not have the time to reach equilibrium for partitioning of compounds between the oil droplets and the water phase. In coastal regions, the energy of wave action may fluctuate, but turbulence in the water column will never subside completely. Therefore, the oil droplets are more likely to stay submerged in the water column and not reach the water surface. This might enhance the dissolution of components, and the same trend should be seen for physically dispersed droplets. It should be noted that the current study show that dispersant themselves do not enhance oil droplet dissolution.

Previous studies (Zahed et al., 2010, Venosa and Holder, 2007, Swannell et al., 1997) have shown increased weathering rates (especially biodegradation) for chemically dispersed oil droplets compared to naturally dispersed oil droplets. The smaller chemically dispersed droplets are more buoyant than the larger naturally dispersed droplets and therefore less likely to sink to bottom sediments without interactions with suspended materials. Previous studies and observations state that biodegradation of oil buried in sediments is slow (Muschenheim and Lee, 2002, Taylor and Reimer, 2008, Atlas, 1981, Garcia de Oteyza and Grimalt, 2006). Therefore, the use of chemical dispersant to disperse spilled oil in the marine environment should be considered carefully. Use of chemical dispersant will lead to a significantly increased lifetime of petroleum hydrocarbons in the water column and therefore increased exposure to pelagic species. In contrast, the mechanically dispersed oil

will most likely be adsorbed to SPMs and transported to the sea floor where it will be exposed to benthic organisms living in the sediment. For a given spill scenario in a given location, one must therefore determine what will be most detrimental, a short term increased exposure to oil for organisms in the water column, or an extensive exposure to oil for organisms at the sea bottom. In the last scenario, one should also take into account that the oil in bottom sediments may be re-distributed in the event of physical processes (wave action, erosion) affecting the sea floor.

The experiences from the Braer spill in 1993 (ESGOSS, 1994a, ESGOSS, 1994b) show that heavy weather will drastically effect the amount of oil stranded on shorelines. This is accounted to the formation of physically dispersed oil droplets by wind turbulence at the sea surface. Approximately 35 % of the oil is estimated to have ended up in the bottom sediments off the Shetland coast. Had the oil been chemically dispersed, less of the oil would have ended up in the sediments (according to the results from the current study), as less oil would adsorb to suspended sediments. The heavy weather conditions might have helped the chemically dispersed oil droplets spread and dilute.

The practical implication of the results from this study is that the increased amount of oil in the water column (dispersed droplets or dissolved components) must be taken into account when applying chemical dispersants in shallow waters. Wolfe et al. (1998), who found that the concentration of naphthalene in water did not change with the addition of dispersant to a crude oil, still found that the presence of dispersant increased the trophic transfer of the compound in primary levels of a marine food chain. In a recent study Jung et al. (2012) found a decrease in plankton assemblages due to higher oil (droplet) concentration in deeper water when the oil was chemically dispersed compared to situations with naturally dispersed oil.

6 Conclusion

The aim of this thesis was to study the adsorption of dispersed crude oil to seawater suspended particulate materials when oil is released into the marine environment. Laboratory experiments were conducted with simulated seawater conditions and mechanically generated oil droplets. The study attempted to determine which crude oil derived compounds preferentially adsorbed to the surface of particulate material and which remained in solution. A selection of parameters (sediment type and concentration, oil type, temperature and use of chemical dispersant) was varied to try to assess the individual parameters effects on the adsorption process.

It was shown that oil droplets adsorbed as a bulk to the sediment, not as individual components. An absence of the smaller, more water-soluble oil components was evidenced by the reduction of early eluting components in GC-FID profiles of sediment extracts. This was confirmed by comparing SVOC profiles (GC-MS analysis) of the pure oil and the oil extracted from sediment samples.

Particle size (surface area), oil characteristics (chemical composition) and presence of chemical dispersant were the three parameters which had the greater impact on the adsorption properties of oil droplets to SPM in seawater. In this study, smaller size sediments (e.g. clay) were capable of adsorbing up to 3 times more oil than sediment consisting mainly of larger grains (e.g. carbonate sand and quartz sand). This indicates that surface area has a primary role in controlling adsorption. Another important parameter in determining the adsorption is the chemical characteristics of oil. A heavy fuel oil (IF 380 Fresh) used in this study adsorbed 3 times more efficiently to suspended particulates than a Kvitebjørn condensate (topped 250+). The adsorption properties of oil appear to be related to the content of polar compounds (estimated by asphaltenes content). Finally, the addition of chemical dispersant to the seawater dispersed oil droplets decreased the sedimentation of oil in an exponential-like manner. Addition of just 1 % dispersant reduced the amount of oil sorbed to suspended carbonate sand by 50 %. However, the presence of dispersant did not change the distribution of compounds adsorbed to the sediment.

The effect of varying temperature (over the range 5-20 °C) was not considerable when compared to the influence of other parameters investigated in this study. Previous studies show conflicting results about the effect of temperature on adsorption. In this study, the

adsorption was highest at the lowest temperature, and this is attributed to increased viscosity of the oil at low temperatures.

The partitioning of oil components to the water column was also monitored in this study, and found not to be influenced significantly by any of the studied parameters. The use of chemical dispersant did not alter the concentration or distribution of oil components dissolved in water. It appears that the water partitioning of oil is dominated by the solubility of the individual components.

7 Further work

This thesis shows that there are several parameters that can significantly effect the adsorption properties of oil to suspended particulate material (SPM) present in the environment. In this study, sediment size, oil type and use of chemical dispersant are identified as the most important parameters governing the adsorption of oil to SPM.

The experimental work conducted for this thesis has formed part of the early stages of an ongoing large-scale research project at SINTEF Marine Environmental Technology. Based on the results generated in the present study, it is suggested that future work expands further on the role of particulate sizes in the lower sand-silt range. The influence of mineral composition in adsorption to larger particles should also be assessed. A planned next step of the SINTEF project includes the study of adsorption to algae species in seawater. It is suggested that chemical dispersant is used in these experiments, to see whether the trend of reducing adsorption is seen for biotic particles as well as the inorganic sediment particles used in this study.

It is seen as of special importance to determine the effect of cold water on the effectiveness of chemical dispersants. The described experimental set-up should be improved in order to achieve successful tests with dispersant at low temperatures. It is also seen as desirable to study the effect of dispersant on a greater variety of oil types. The effect of equilibrium time on the water dissolved compounds should also be assessed (see Chapter 5.5).

A scale up of the experimental dimensions, (e.g. with a more realistic wave action simulation), should also be conducted at a later stage in the project, in order to verify how realistic the small scale results are.

In future work, it is recommended to analyse more (preferentially all) samples by GC-MS to monitor the alterations in SVOC profiles by changing experimental parameters. In addition to supporting the findings from the GC-FID results, it will give the project a more developed understanding of which oil components are influenced most by altered parameters, and thus which oil components are the driving factors in oil-SPM aggregation. It should also be considered to include more components to the GC-MS profiling, such as the phenols (more polar compounds).

For future analysis of sediment extracts using GC-FID, one should find one or more additional surrogate internal standard (SIS-THC) to complement *o*-terphenyl in order to avoid the problems with co-elution that is seen in this study.

List of references

AJIJOLAIYA, L. O., HILL, P. S., KHELIFA, A., ISLAM, R. M. & LEE, K. 2006. Laboratory investigation of the effects of mineral size and concentration on the formation of oil-mineral aggregates. *Marine Pollution Bulletin,* 52**,** 920-927.

ALMÅS, K. 2011. KS 8016-11-102 Analyse og kvantifisering av hydrokarboner vha GC/FID. *SINTEF Internal procedure***,** 1-11.

ALMÅS, K. & RØNSBERG, M. U. 2012. *RE: Co-elution of C-19 and o-terphenyl.*

ATLAS, R. M. 1981. Microbial-Degradation of Petroleum-Hydrocarbons - An Environmental Perspective. *Microbiological Reviews,* 45**,** 180-209.

BANDARA, U. C., YAPA, P. D. & XIE, H. 2011. Fate and transport of oil in sediment laden marine waters. *Journal of Hydro-environment Research,* 5**,** 145-156.

BASSIN, N. J. & ICHIYE, T. 1977. Flocculation Behavior of suspended sediments and oil-emulsions. *Journal of Sedimentary Petrology,* 47**,** 671-677.

BJERKLI, K. 2011. *RE: Manager of GeoSubsea Kristian Bjerkli, addressing Alf Glein Melbye of SINTEF Materials and Chemistry.*

BOEHM, P. D. 1987. Transport and transformation processes regarding hydrocarbon and metal pollutants in offshore sedimentary environments. *In: Boesch, D.F., Rabalaias, N.N. (Eds), Long-Term Environmental Effects of Offshore Oil and Gas Development. Elsevier Applied Science, London & New York, pp. 233-287*.

BOEHM, P. D., BARAK, J. E., FIEST, D. L. & ELSKUS, A. A. 1982. A chemical investigation of the transport and fate of petroleum hydrocarbons in littoral and benthic environments: The TSESIS oil spill. *Marine Environmental Research,* 6**,** 157-188.

BOOTH, A. M. 2004. *Biodegradation, Water Solubility and Characterisation Studies of Unresolved Complex Mixtures (UCMs) of Aromatic Hydrocarbons.* PhD, University of Plymouth.

BOOTH, A. M., SUTTON, P. A., LEWIS, C. A., LEWIS, A. C., SCARLETT, A., CHAU, W., WIDDOWS, J. & ROWLAND, S. J. 2007. Unresolved complex mixtures of aromatic hydrocarbons: Thousands of overlooked persistent, bioaccumulative, and toxic contaminants in mussels. . *Environmental Science & Technology,* 41**,** 457-464.

BRAGG, J. R. & OWENS, E. H. 1994. Clay-Oil Flocculation as a Natural Cleansing Process Following Oil Spills .1. Studies of Shoreline Sediments and Residues From Past Spills. *Seventeenth Arctic and Marine Oil Spill Program (Amop) Technical Seminar, Vols 1 and 2***,** 1-23.

BRIGGS, G. G. 1981. Theoretical and Experimental Relationships Between Soil Adsorption, Octanol-Water Partition-Coefficients, Water Solubilites, Bioconcentration Factors, and the Parachor. *Journal of Agricultural and Food Chemistry,* 29**,** 1050-1059.

BRUNER, F. 1993. *Gas Chromatographic Environmental Analysis; Principles, Techniques, Instrumentation*, VCH Publishers, Inc.

CAREY, F. A. 2006. *Organic chemistry,* Boston, McGraw-Hill.

CARLS, M. G., HOLLAND, L., LARSEN, M., COLLIER, T. K., SCHOLZ, N. L. & INCARDONA, J. P. 2008. Fish embryos are damaged by dissolved PAHs, not oil particles. *Aquatic Toxicology,* 88**,** 121-127.

CEN 2006. Oil spill identification - Waterborne petroleum and petroleum products - Part 2: Analytical methodology and interpretation of results based on GC-FID and GC-MS low resolution analyses. CEN/TR 15522-2.

CHAPMAN, H., PURNELL, K., LAW, R. J. & KIRBY, M. F. 2007. The use of chemical dispersants to combat oil spills at sea: A review of practice and research needs in Europe. *Marine Pollution Bulletin,* 54**,** 827-838.

DALING, P. & BRANDVIK, P. J. 2010. *RE: Oil spill history and organization of Norwegian oil spill response.*

DALING, P. S., AAMO, O. M., LEWIS, A., STROM-KRISTIANSEN, T. & API 1997. *SINTEF/IKU oil-weathering model: Predicting oils' properties at sea*.

DALING, P. S., SINGSAAS, I., REED, M. & HANSEN, O. 2002. Experiences in Dispersant Treatment of Experimental Oil Spills. *Spill Science & Technology Bulletin,* 7**,** 201-213.

DALING, P. S. & STRØM, T. 1999. Weathering of Oils at Sea: Model/Field Data Comparisons. *Spill Science & Technology Bulletin,* 5**,** 63-74.

DELVIGNE, G. A. L. 2002. Physical Appearance of Oil in Oil-Contaminated Sediment. *Spill Science & Technology Bulletin,* 8**,** 55-63.

DHNRT. 2011. *Deepwater Horizon Oil Spill Phase I Early Restoration Plan and Environmental Assessment* [Online]. http://www.doi.gov/deepwaterhorizon/upload/Final-ERP-EA-ES-041812.pdf. [Accessed 18.04.2012].

EDGELL, N. 1994. The Braer tanker incident: Some lessons from the Shetland Islands. *Marine Pollution Bulletin,* 29**,** 361-367.

ESGOSS 1994a. Minimal impact from Braer spill. *Marine Pollution Bulletin,* 28**,** 467-468.

ESGOSS 1994b. Wreck of the tanker braer: The environmental impact of the oil spill. *Spill Science & Technology Bulletin,* 1**,** 101-107.

FAKSNESS, L.-G. 2000. KS 66-21-L-235 Extraction of water samples for petroleum analysis. *SINTEF Internal procedure***,** 1-7.

FAKSNESS, L.-G. 2001a. KS-66-21-A-211 Kromatografi/Bond-Elut, separasjon av hydrokarboner. *SINTEF Internal procedure***,** 1-3.

FAKSNESS, L.-G. 2001b. KS 66-21-A-204 Ekstraksjon og forsåpning av vått sediment. *SINTEF Internal procedure*.

FAKSNESS, L.-G., GRINI, P. G. & DALING, P. S. 2004. Partitioning of semi-soluble organic compounds between the water phase and oil droplets in produced water. *Marine Pollution Bulletin,* 48**,** 731-742.

FAKSNESS, L. G., BRANDVIK, P. J. & SYDNES, L. K. 2008. Composition of the water accommodated fractions as a function of exposure times and temperatures. *Marine Pollution Bulletin,* 56**,** 1746-1754.

FINGAS, M. 2011. Chapter 15 - Oil Spill Dispersants: A Technical Summary. *In:* MERVIN, F. (ed.) *Oil Spill Science and Technology.* Boston: Gulf Professional Publishing.

FIOCCO, R. J. & LEWIS, A. 1999. Oil spill dispersants. *Pure and Applied Chemistry,* 71**,** 27-42.

FRYSINGER, G. S., GAINES, R. B., XU, L. & REDDY, C. M. 2003. Resolving the unresolved complex mixture in petroleum-contaminated sediments. *Environmental Science & Technology,* 37**,** 1653-1662.

GARCIA DE OTEYZA, T. & GRIMALT, J. O. 2006. GC and GC–MS characterization of crude oil transformation in sediments and microbial mat samples after the 1991 oil spill in the Saudi Arabian Gulf coast. *Environmental Pollution,* 139**,** 523-531.

GREIBROKK, T., LUNDANES, E. & RASMUSSEN, K. 1984. *Kromatografi - Separasjon og deteksjon*, Universitetsforlaget AS.

GROSS, J. H. 2004. *Mass spectrometry: a textbook,* Berlin, Springer.

GUYOMARCH, J., LE FLOCH, S. & MERLIN, F.-X. 2002. Effect of Suspended Mineral Load, Water Salinity and Oil Type on the Size of Oil–Mineral Aggregates in the Presence of Chemical Dispersant. *Spill Science & Technology Bulletin,* 8**,** 95-100.

HELBÆK, M. & KJELSTRUP, S. 2006. *Fysikalsk kjemi,* Bergen, Fagbokforl.

HINSHAW, J. V. & ETTRE, L. S. 1994. *Introduction to Open-Tubular Column Gas Chromatography,* Cleveland, Ohio, Advanstar Communications.

HO, K. A. Y., PATTON, L., LATIMER, J. S., PRUELL, R. J., PELLETIER, M., MCKINNEY, R. & JAYARAMAN, S. 1999. The Chemistry and Toxicity of Sediment Affected by Oil from the North Cape Spilled into Rhode Island Sound. *Marine Pollution Bulletin,* 38**,** 314-323.

HOFFMANN, E. D. & STROOBANT, V. 2007. *Mass spectrometry: principles and applications,* Chichester, Wiley.

HUNT, J. M. 1996. *Petroleum geochemistry and geology,* New York, W. H. Freeman.

ITOPF. 2011. Statistics - Numbers and amounts spilt. [Accessed 15.03.2012].

JAMIALAHMADI, M., SOLTANI, B., MÜLLER-STEINHAGEN, H. & RASHTCHIAN, D. 2009. Measurement and prediction of the rate of deposition of flocculated asphaltene particles from oil. *International Journal of Heat and Mass Transfer,* 52**,** 4624-4634.

JOHANSSON, S., LARSSON, U. & BOEHM, P. 1980. The Tsesis oil spill impact on the pelagic ecosystem. *Marine Pollution Bulletin,* 11**,** 284-293.

JUNG, S. W., KWON, O. Y., JOO, C. K., KANG, J.-H., KIM, M., SHIM, W. J. & KIM, Y.-O. 2012. Stronger impact of dispersant plus crude oil on natural plankton assemblages in short-term marine mesocosms. *Journal of Hazardous Materials,* 217–218**,** 338-349.

KARICKHOFF, S. W., BROWN, D. S. & SCOTT, T. A. 1979. Sorption of hydrophobic pollutants on natural sediments. *Water Research,* 13**,** 241-248.

KHELIFA, A., FIELDHOUSE, B., WANG, Z., YANG, C., LANDRIAULT, M., E.;, B. C. & FINGAS, M. 2008. Effects of chemical dispersant on oil sedimentation due to oil-SPM flocculation: experiments with the NIST standard reference material 1941B. *2008 International Oil Spill Conference.*

KHELIFA, A., HILL, P. S. & LEE, K. 2005a. Chapter 10 The role of oil-sediment aggregation in dispersion and biodegradation of spilled oil. *In:* AL-AZAB, M. & EL-SHORBAGY, W. (eds.) *Developments in Earth and Environmental Sciences.* Elsevier.

KHELIFA, A., STOFFYN-EGLI, P., HILL, P. S. & LEE, K. 2002. Characteristics of oil droplets stabilized by mineral particles: Effects of oil type and temperature. *Spill Science & Technology Bulletin,* 8**,** 19-30.

KHELIFA, A., STOFFYN-EGLI, P., HILL, P. S. & LEE, K. 2005b. Effects of salinity and clay type on oil–mineral aggregation. *Marine Environmental Research,* 59**,** 235-254.

KILLOPS, S. D. & ALJUBOORI, M. 1990. Characterization of the Unresolved Complex Mixture (UCM) in the Gas Chromatograms of Biodegraded Petroleums. *Organic Geochemistry,* 15**,** 147-160.

LAW, R. J. & MOFFAT, C. F. 2011. Chapter 36 - The Braer Oil Spill, 1993. *In:* MERVIN, F. (ed.) *Oil Spill Science and Technology.* Boston: Gulf Professional Publishing.

LEE, K. 2002. Oil-particle interactions in aquatic environments: Influence on the transport, fate, effect and remediation of oil spills. *Spill Science & Technology Bulletin,* 8**,** 3-8.

LESSARD, R. R. & DEMARCO, G. 2000. The Significance of Oil Spill Dispersants. *Spill Science & Technology Bulletin,* 6**,** 59-68.

LEWIS, A., KEN TRUDEL, B., BELORE, R. C. & MULLIN, J. V. 2010. Large-scale dispersant leaching and effectiveness experiments with oils on calm water. *Marine Pollution Bulletin,* 60**,** 244-254.

LI, M. & GARRETT, C. 1998. The relationship between oil droplet size and upper ocean turbulence. *Marine Pollution Bulletin,* 36**,** 961-970.

LI, Z., KEPKAY, P., LEE, K., KING, T., BOUFADEL, M. C. & VENOSA, A. D. 2007. Effects of chemical dispersants and mineral fines on crude oil dispersion in a wave tank under breaking waves. *Marine Pollution Bulletin,* 54**,** 983-993.

LI, Z. K., LEE, K., KING, T., BOUFADEL, M. C. & VENOSA, A. D. 2009. Evaluating Chemical Dispersant Efficacy in an Experimental Wave Tank: 2-Significant Factors Determining In Situ Oil Droplet Size Distribution. *Environmental Engineering Science,* 26**,** 1407-1418.

LI, Z. K., LEE, K., KING, T., BOUFADEL, M. C. & VENOSA, A. D. 2010. Effects of temperature and wave conditions on chemical dispersion efficacy of heavy fuel oil in an experimental flow-through wave tank. *Marine Pollution Bulletin,* 60**,** 1550-1559.

LUQUE DE CASTRO, M. D. & LUQUE-GARCIA, J. L. 2002. Acceleration and Automation of Solid Sample Treatment. *Elsevier, Amsterdam*.

LUQUE DE CASTRO, M. D. & PRIEGO-CAPOTE, F. 2010. Soxhlet extraction: Past and present panacea. *Journal of Chromatography A,* 1217**,** 2383-2389.

LØVÅS, G. G. 2004. *Statistikk for universiteter og høgskoler,* Oslo, Universitetsforl.

MACKAY, D. & HOSSAIN, K. 1982. An Exploratory Study of Sedimentation of Naturally and Chemically Dispersed Oil. EE Environment Canada.

MANAHAN, S. E. 2005. *Environmental chemistry,* Boca Raton, Fla., CRC Press.

MELBYE, A. G., BRAKSTAD, O. G., HOKSTAD, J. N., GREGERSEN, I. K., HANSEN, B. H., BOOTH, A. M., ROWLAND, S. J. & TOLLEFSEN, K. E. 2009. Chemical and Toxicological Characterization of an Unresolved Complex Mixture-Rich Biodegraded Crude Oil. *Environmental Toxicology and Chemistry,* 28**,** 1815-1824.

MEYERS, P. A. & QUINN, J. G. 1973. Association of Hydrocarbons and Mineral Particles in Saline Solution. *Nature,* 244**,** 23-24.

MURRAY, A. P. 1973. Protein adsorption by suspended sediments: Effects of pH, temperature, and concentration. *Environmental Pollution (1970),* 4**,** 301-312.

MUSCHENHEIM, D. K. & LEE, K. 2002. Removal of Oil from the Sea Surface through Particulate Interactions: Review and Prospectus. *Spill Science & Technology Bulletin,* 8**,** 9-18.

NEFF, J. M. 1979. *Polycyclic aromatic hydrocarbons in the aquatic environment: sources, fates and biological effects,* London, Applied Science Publ.

NEFF, J. M., COX, B. A., DIXIT, D. & ANDERSON, J. W. 1976. Accumulation and release of petroleum-derived aromatic hydrocarbons by four species of marine animals. *Marine Biology,* 38**,** 279-289.

NORDTUG, T. & VANG, S.-H. 2011. *RE: Instructions on the oil-droplet generator.*

OLSEN, T. 2012. *RE: Oil droplet generator.*

PAGE, C. A., BONNER, J. S., SUMNER, P. L. & AUTENRIETH, R. L. 2000. Solubility of petroleum hydrocarbons in oil/water systems. *Marine Chemistry,* 70**,** 79-87.

PAYNE, J. R., CLAYTON JR, J. R. & KIRSTEIN, B. E. 2003. Oil/Suspended Particulate Material Interactions and Sedimentation. *Spill Science & Technology Bulletin,* 8**,** 201-221.

PAYNE, J. R., CLAYTON JR, J. R., MCNABB JR., G. D., KIRSTEIN, B. E., CLARY, C., REDDING, R., EVANS, J. S., REIMNITZ, E. & KEMPEMA, E. W. 1989. Oil-ice-sediment interactions during freezeup and breakup. Outer Continental Shelf Environmental Assessment Program, Final Reports of Principal Investigators, US Department of Commerce, NOAA, OCSEAP Final Rep. 64, pp. 1-382.

PAYNE, J. R. & MCNABB, G. D. 1984. Weathering of petroleum in the marine-environment. *Marine Technology Society Journal,* 18**,** 24-42.

PIPKIN, B. W., TRENT, D. D. & HAZLETT, R. 2005. *Geology and the environment,* Belmont, Calif., Thomson Brooks/Cole.

POOLE, C. F. 2003. *The essence of chromatography*, Elsevier.

REED, M., AAMO, O. M. & DALING, P. S. 1995. Quantitative analysis of alternate oil spill response strategies using OSCAR. *Spill Science & Technology Bulletin,* 2**,** 67-74.

SAEED, T. & AL-MUTAIRI, M. 2000. Comparative composition of polycyclic aromatic hydrocarbons (PAHs) in the sea water-soluble fractions of different Kuwaiti crude oils. *Advances in Environmental Research,* 4**,** 141-145.

SCHMID, R. 2010. *RE: IV. Gasskromatografi.* Type to NTNU.

SILVERSTEIN, R. M., WEBSTER, F. X. & KIEMLE, D. J. 2005. *Spectrometric identification of organic compounds,* Hoboken, N.J., Wiley.

SKOOG, D. A. 2004. *Fundamentals of analytical chemistry,* Belmont, Calif., Thomson Brooks/Cole.

SPEIGHT, J. G. 2007. *The chemistry and technology of petroleum,* Boca Raton, Fla., CRC Press.

STERLING JR, M. C., BONNER, J. S., PAGE, C. A., FULLER, C. B., ERNEST, A. N. S. & AUTENRIETH, R. L. 2003. Partitioning of crude oil polycyclic aromatic hydrocarbons in aquatic systems. *Environmental Science and Technology,* 37**,** 4429-4434.

STOFFYN-EGLI, P. & LEE, K. 2002. Formation and Characterization of Oil–Mineral Aggregates. *Spill Science & Technology Bulletin,* 8**,** 31-44.

STUMM, W. & MORGAN, J. J. 1996. *Aquatic chemistry: chemical equilibria and rates in natural waters,* New York, Wiley.

SUN, J., KHELIFA, A., ZHENG, X., WANG, Z., SO, L. L., WONG, S., YANG, C. & FIELDHOUSE, B. 2010. A laboratory study on the kinetics of the formation of oil-suspended particulate matter aggregates using the NIST-1941b sediment. *Marine Pollution Bulletin,* 60**,** 1701-1707.

SWANNELL, R. P. J., DANIEL, F., CROFT, B. C., ENGELHARDT, M. A., WILSON, S., MITCHELL, D. J., LUNEL, T. & EC 1997. *Influence of physical and chemical dispersion on the biodegradation of oil under simulated marine conditions,* Ottawa, Environment Canada.

SØRHEIM, K. R. 2005. KS 66-21-A-248 Prøveopparbeiding av jord og partikulært materiale med soxhlet - ultralyd. *SINTEF Internal procedure***,** 1-4.

TAYLOR, E. & REIMER, D. 2008. Oil persistence on beaches in Prince William Sound - A review of SCAT surveys conducted from 1989 to 2002. *Marine Pollution Bulletin,* 56**,** 458-474.
THORPE, S. A. 1995. Vertical dispersion of oil droplets in strong winds; the Braer oil spill. *Marine Pollution Bulletin,* 30**,** 756-758.
TISSOT, B. P. & WELTE, D. H. 1984. *Petroleum formation and occurrence,* Berlin, Springer.
TOLLS, J., VAN DIJK, J., VERBRUGGEN, E. J. M., HERMENS, J. L. M., LOEPRECHT, B. & SCHUURMANN, G. 2002. Aqueous solubility-molecular size relationships: A mechanistic case study using C-10- to C-19-alkanes. *Journal of Physical Chemistry A,* 106**,** 2760-2765.
TREMBLAY, L., KOHL, S. D., RICE, J. A. & GAGNÉ, J.-P. 2005. Effects of temperature, salinity, and dissolved humic substances on the sorption of polycyclic aromatic hydrocarbons to estuarine particles. *Marine Chemistry,* 96**,** 21-34.
TURRELL, W. R. 1994. Modelling the Braer oil spill—A retrospective view. *Marine Pollution Bulletin,* 28**,** 211-218.
VENOSA, A. D. & HOLDER, E. L. 2007. Biodegradability of dispersed crude oil at two different temperatures. *Marine Pollution Bulletin,* 54**,** 545-553.
WANG, Z. & FINGAS, M. 1997. Developments in the analysis of petroleum hydrocarbons in oils, petroleum products and oil-spill-related environmental samples by gas chromatography. *Journal of Chromatography A,* 774**,** 51-78.
WANG, Z. & STOUT, S. A. 2007. *Oil spill environmental forensics: fingerprinting and source identification,* Amsterdam, Elsevier.
WARTSILA. 2007. *Quality requirements and recommendations for heavy fuel oil* [Online]. [Accessed 08.05.2012.
WOLFE, M. F., SCHLOSSER, J. A., SCHWARTZ, G. J. B., SINGARAM, S., MIELBRECHT, E. E., TJEERDEMA, R. S. & SOWBY, M. L. 1998. Influence of dispersants on the bioavailability and trophic transfer of petroleum hydrocarbons to primary levels of a marine food chain. *Aquatic Toxicology,* 42**,** 211-227.
XING, B. 1997. The effect of the quality of soil organic matter on sorption of naphthalene. *Chemosphere,* 35**,** 633-642.
ZAHED, M. A., AZIZ, H. A., ISA, M. H. & MOHAJERI, L. 2010. Effect of Initial Oil Concentration and Dispersant on Crude Oil Biodegradation in Contaminated Seawater. *Bulletin of Environmental Contamination and Toxicology,* 84**,** 438-442.
ZHAO, X.-K., YANG, G.-P., WU, P. & LI, N.-H. 2001. Study on Adsorption of Chlorobenzene on Marine Sediment. *Journal of Colloid and Interface Science,* 243**,** 273-279.
ZURCHER, F. & THUER, M. 1978. Rapid weathering processes of fuel oil in natural-waters - analyses and interpretations. *Environmental Science & Technology,* 12**,** 838-843.

Appendices

Appendix A Experimental series and data for experiments

Table A.1 – Data for all experiments

Experiment ID	Main variable(s)	Weight of sediment added [g]	Weight of sediment extracted [g]	Volume of oil added [µL]	Weight of oil added [mg]	Date of experiment
LIS001_1	Sediment concentration 5 g/L	7,49	7,17	34,3	31,9	10.10.2011
LIS001_2		7,48	7,14	34,3	31,9	10.10.2011
LIS001_3		7,52	6,97	34,3	31,9	10.10.2011
LIS001_4		7,51	6,29	34,3	31,9	04.01.2012
LIS002_1	Sediment concentration 10 g/L	15,08	14,51	34,3	31,9	10.10.2011
LIS002_2		15,07	13,43	34,3	31,9	10.10.2011
LIS002_3		15,07	13,59	34,3	31,9	10.10.2011
LIS002_4		15,12	14,52	34,3	31,9	04.01.2012
LIS002_5		15,15	14,66	34,3	31,9	04.01.2012
LIS002_6		15,05	14,53	34,3	31,9	06.03.2012
LIS002_7		15,01	14,36	34,3	31,9	06.03.2012
LIS003_1	Sediment concentration 20 g/L	30,39	29,66	34,3	31,9	17.10.2011
LIS003_2		30,53	29,76	34,3	31,9	17.10.2011
LIS003_3		30,21	29,03	34,3	31,9	17.10.2011
LIS003_4		30,16	29,11	34,3	31,9	04.01.2012
LIS004_1	Sediment concentration 40 g/L	60,13	59,25	34,3	31,9	24.10.2011
LIS004_2		60,10	58,34	34,3	31,9	24.10.2011
LIS004_3		60,08	N/A	34,3	31,9	24.10.2011

LIS005_1	Sediment concentration 80 g/L	120,00	121,54	34,3	31,9	24.10.2011
LIS005_2		120,13	120,38	34,3	31,9	24.10.2011
LIS005_3		120,14	120,87	34,3	31,9	24.10.2011
LIS006_1	Temperature 4-5 °C	15,11	14,59	34,3	31,9	03.11.2011
LIS006_2		15,13	14,38	34,3	31,9	03.11.2011
LIS006_3		15,14	14,34	34,3	31,9	03.11.2011
LIS006_6		15,06	13,48	34,3	31,9	01.02.2012
LIS006_7		15,06	14,37	34,3	31,9	01.02.2012
LIS007_1	Temperature 10-11 °C	15,15	14,59	34,3	31,9	07.11.2011
LIS007_2		15,05	14,56	34,3	31,9	07.11.2011
LIS007_3		15,10	14,54	34,3	31,9	07.11.2011
LIS007_4		14,99	14,53	34,3	31,9	11.01.2012
LIS007_5		15,04	14,56	34,3	31,9	11.01.2012
LIS008_1	Oil type Kvitebjørn condensate 250+	15,27	14,76	37,4	31,9	10.11.2011
LIS008_2		15,08	14,50	37,4	31,9	10.11.2011
LIS008_3		14,98	14,33	37,4	31,9	10.11.2011
LIS009_1	Oil type; IF380 Fresh	15,10	14,60	33,1	31,9	14.11.2011
LIS009_2		15,10	14,53	33,1	31,9	14.11.2011
LIS009_3		15,14	14,49	33,1	31,9	14.11.2011
LIS010_1	Dispersant 1 %	15,18	14,27	34,3	31,9	22.11.2011
LIS010_2		15,05	13,59	34,3	31,9	22.11.2011
LIS010_3		15,09	14,17	34,3	31,9	22.11.2011
LIS010_4		15,09	14,22	34,3	31,9	07.02.2012
LIS010_5		15,05	3,27	34,3	31,9	07.02.2012

Table A.1 continued

Experiment ID	Main variable(s)	Weight of sediment added [g]	Weight of sediment extracted [g]	Volume of oil added [µL]	Weight of oil added [mg]	Date of experiment
LIS011_1	Dispersant 5 %	15,10	14,60	34,3	31,9	22.11.2011
LIS011_2		15,07	14,37	34,3	31,9	22.11.2011
LIS011_3		15,18	14,16	34,3	31,9	22.11.2011
LIS011_4		15,06	14,16	34,3	31,9	07.02.2012
LIS011_5		15,04	13,59	34,3	31,9	07.02.2012
LIS012_1	Dispersant 1 % 10 min residence time	15,14	14,54	34,3	31,9	29.11.2011
LIS012_2		15,10	14,47	34,3	31,9	29.11.2011
LIS012_3		15,09	14,55	34,3	31,9	29.11.2011
LIS013_1	Dispersant 1 % 30 min residence time	15,00	14,47	34,3	31,9	29.11.2011
LIS013_2		15,15	N/A	34,3	31,9	29.11.2011
LIS013_3		15,10	N/A	34,3	31,9	29.11.2011
LIS014_1	Temperature; 10 °C Dispersant 1 %	15,17	14,26	34,3	31,9	12.01.2012
LIS014_2		15,03	14,40	34,3	31,9	12.01.2012
LIS014_3		15,03	14,13	N/A	N/A	12.01.2012
LIS014_4		15,16	14,45	34,3	31,9	12.01.2012
LIS015_1	Temperature; 5 °C Dispersant 1 %	15,10	14,12	34,3	31,9	31.01.2012
LIS015_2		15,02	14,55	34,3	31,9	31.01.2012
LIS015_3		15,05	14,19	34,3	31,9	31.01.2012
LIS015_4		15,10	14,20	34,3	31,9	31.01.2012
LIS016_1	Temperature; 14-15 °C	14,97	14,45	34,3	31,9	21.02.2012
LIS016_2		15,02	14,27	34,3	31,9	21.02.2012
LIS016_3		15,05	14,44	34,3	31,9	21.02.2012
LIS016_4		15,08	14,14	34,3	31,9	21.02.2012

LIS017_1	Sediment type; Clay from Buvika	15,12	14,94	34,3	31,9	23.02.2012
LIS017_2		15,09	14,88	34,3	31,9	23.02.2012
LIS017_3		15,03	15,03	34,3	31,9	23.02.2012
LIS017_4		15,06	14,81	34,3	31,9	23.02.2012
LIS018_1	Oil type; Avaldsnes 250+	15,13	14,57	34,1	31,9	28.02.2012
LIS018_2		15,09	14,31	34,1	31,9	28.02.2012
LIS018_4		15,06	14,42	34,1	31,9	29.02.2012
LIS018_5		15,07	14,14	34,1	31,9	29.02.2012
LIS019_1	Sediment type; Sand from Ranheim	15,00	14,74	34,3	31,9	06.03.2012
LIS019_2		15,06	14,53	34,3	31,9	06.03.2012
LIS019_3		15,03	14,53	34,3	31,9	06.03.2012
LIS019_4		15,07	14,32	34,3	31,9	06.03.2012
B1	Procedural blank	15,15	14,37	-	-	17.10.2011
B2		15,27	14,44	-	-	07.11.2011
B3		15,02	14,41	-	-	14.11.2011
Lab blank 1	Lab blank Carbonate sand from Grandefjæra	15,02	15,02	-	-	-
Lab blank 2		14,97	14,97	-	-	-
Lab blank 3		15,00	14,94	-	-	-
Lab blank 4		15,04	14,98	-	-	-
Lab blank 5	Lab blank Clay from Buvika	15,09	14,98	-	-	-
Lab blank 6		15,11	15,04	-	-	-
Lab blank 7		15,00	14,84	-	-	-
Lab blank 8	Lab blank Sand from Ranheim	15,01	14,92	-	-	-
Lab blank 9		15,03	14,96	-	-	-
Lab blank 10		15,02	14,98	-	-	-

Appendix B Parameters for the syringe pump

The syringe used on the syringe pump had a volume of 1 mL and a length of 6 cm. Hence, the internal diameter of the syringe was 0,4608 cm. This number was used to set the pump rate correctly.

The rate of the water valve pump was 160 mL/min, and the desired concentration of oil was 20 mg/L. This, along with the densities of the respective oil was used to calculate the necessary rate of the oil syringe for each oil, by equation B.1. The calculation results are given in Table B.1.

$$Rate_{oilpump}[\mu L/\min] = \frac{Rate_{waterpump}[mL/\min] \times Concentration_{oil}[mg/L] \times 10^{-6}}{Density_{oil}[g/mL]} \quad \text{(B.1)}$$

Table B.1 – Rate of oil output from the syringe pump

Oil type	Rate of seawater [mL/min]	Concentration of oil [mg/L]	Density oil [kg/L]	Rate of oil [µL/min]
Troll 250+	160	20	0,92962	3,442
Avaldsnes 250+	160	20	0,93534	3,421
Kvitebjørn condensate 250+	160	20	0,85337	3,750
IF380 Fresh	160	20	0,9631	3,323

When dispersants were added to the oil, a different rate of the syringe pump was necessary. This was calculated using equation B.2, and the results are given in Table B.2.

$$Rate_{oilpump}[\mu L/\min] = \frac{Rate_{waterpump}[mL/\min] \times Concentration_{oil}[mg/L] \times 10^{-6}}{Density_{oil}[g/mL]} \times (1 + \frac{DOR(\%)}{100}) \quad \text{(B.2)}$$

Table B.2 – Rate of oil and dispersant on the syringe pump

Oil type	Rate of seawater [mL/min]	Concentration of oil [mg/L]	Density of oil [kg/L]	Amount of oil [µL/min]	Mengde dispersant (%)	Oil + dispersant [µL/min]
Troll 250+	160	20	0,92962	3,442	1	3,477
Troll 250+	160	20	0,92962	3,442	5	3,614

B.1 Test of syringe pump stability

The stability in output of the syringe pump was tested by allowing it to pump 5 repeated parallels of 34,3 µL Troll 250+ into a pre-weighed GC-glass, and weighing the glass again for each parallel. The first parallel was disregarded since the amount of oil was significantly lower than for the rest of the parallels, and this can be explained by that the oil didn't yet fill the entire syringe tip.

Given the density of Troll 250 + (Table B.1), the expected mass of 34,3 µL would be 31,9 mg. The syringe pumps output when set to 24,3 µL was (31,7 ± 1,2) mg. The relative standard deviation for the repeated parallels were 3,9 %.

Table B.3 – Stability in oil mass output of syringe pump

Nominal volume of oil added [µL]	Weight of GC-glass with oil [g]	Weight of nominal 34,3 µL oil [mg]
0	2,345	0
34,3	2,374	28,7 (Disregarded)
68,6	2,405	31,6
102,9	2,437	31,8
137,2	2,468	31,4
171,5	2,500	32,1
	Average [mg]	31,7
	Standard deviation [mg]	1,2
	Relative standard deviation (%)	3,9

Appendix C Grain size distribution

This appendix presents the results from the determination of grain size distribution of the sediment, as described in Chapter 3, and in SINTEF procedure KS 66-21-A-220.

Tables C.1 and C.2 show the grain size distributions for the sediments from Grandefjæra and Ranheim. Three parallels of both sediments were sieved, and average and standard deviations are calculated.

Table C.1 – Grain size distribution of the carbonate sand from Grandefjæra

	Grandefjæra					
	G1 [g]	**G2 [g]**	**G3 [g]**	**Average [g]**	**Standard deviation [g]**	**Relative standard deviation (%)**
Total mass	20,01	20,01	20,00	20,01	0,00	0,0
> 2000 µm	0,23	0,17	0,19	0,20	0,03	16,0
1000-2000 µm	1,25	1,73	1,42	1,46	0,24	16,7
500-1000 µm	1,43	1,54	1,29	1,42	0,13	8,8
355-500 µm	0,92	0,95	1,06	0,98	0,07	7,5
250-355 µm	4,70	5,00	2,48	4,06	1,38	34,0
180-250 µm	7,96	5,76	9,53	7,75	1,89	24,4
125-180 µm	2,71	3,98	3,08	3,25	0,66	20,2
90-125 µm	0,40	0,45	0,48	0,44	0,04	9,2
63-90 µm	0,27	0,26	0,26	0,26	0,00	1,0
< 63 µm	0,08	0,07	0,10	0,08	0,01	16,1

Table C.2 - Grain size distribution of the sand from Ranheim

	Ranheim					
	R1 [g]	**R2 [g]**	**R3 [g]**	**Average [g]**	**Standard deviation [g]**	**Relative standard deviation (%)**
Total mass	20,00	20,01	20,01	20,01	0,00	0,0
> 2000 µm	-	-	-	-	-	-
1000-2000 µm	3,33	3,80	3,91	3,68	0,31	8,4
500-1000 µm	3,19	3,41	3,26	3,28	0,11	3,3
355-500 µm	3,38	2,93	3,52	3,28	0,31	9,4
250-355 µm	6,74	6,69	6,24	6,56	0,28	4,3
180-250 µm	2,19	2,12	2,06	2,12	0,07	3,2
125-180 µm	0,89	0,82	0,77	0,83	0,06	7,4
90-125 µm	0,16	0,16	0,14	0,15	0,01	9,3
63-90 µm	0,03	0,03	0,02	0,02	0,00	18,4

Appendix D Relative response factors of the oil types for GC-FID

As described in Chapter 3 of the main text, four calibration standards of each oil was prepared and analyzed by GC-FID in order to determine the relative response factor (RRF) of the oil type. The calibration standards were made from a primary standard of 20 mg oil dissolved in 10 mL of DCM. The standards held concentrations of 10, 5, 2,5 and 1 mg/mL. The equation for calculating RRF is given in Chapter 3 of the main text.

D.1 Troll 250+

An overlay of the chromatograms of the calibration standards for Troll 250+ is given in Figure D.1.

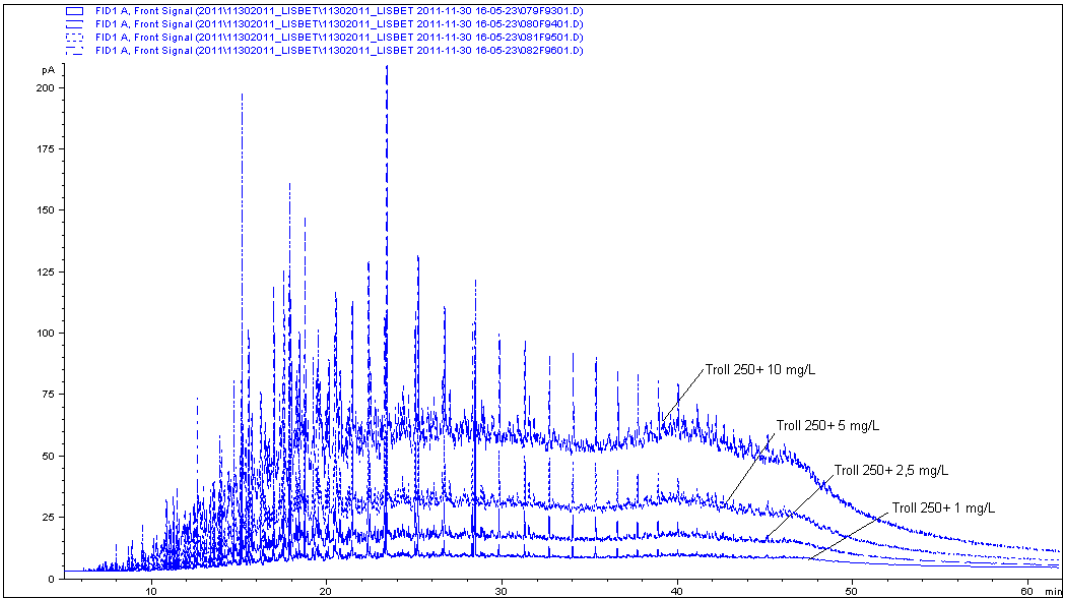

Figure D.1 – Overlay of GC-FID chromatograms for the calibration standards of Troll 250+

The analytical data for the GC-FID analysis of the Troll 250+ standards are given in Table D.1. The concentration of the primary standard was 20,64 mg/mL.

A calibration curve is plotted in Figure D.2, and this demonstrates that the response for of Troll 250+ is linear in the investigated concentration range.

Table D.1 - Calibration data for Troll 250+

Total area [pA]	Area of α-androstane [pA]	Area-DCM [pA]	Concentration of oil [mg/mL]	Relative response factor RRF
15 631	156	12 810	1,03	0,802
32 370	153	29 550	2,58	0,754
60 977	152	58 156	5,16	0,749
118 073	164	115 252	10,32	0,689
			Average RRF	**0,748**
Average area of DCM blanks in the run [pA]	2 821		Standard deviation RRF	0,047
Concentration of α-androstane [mg/mL]	0,01008		Relative standard deviation RRF (%)	6,218

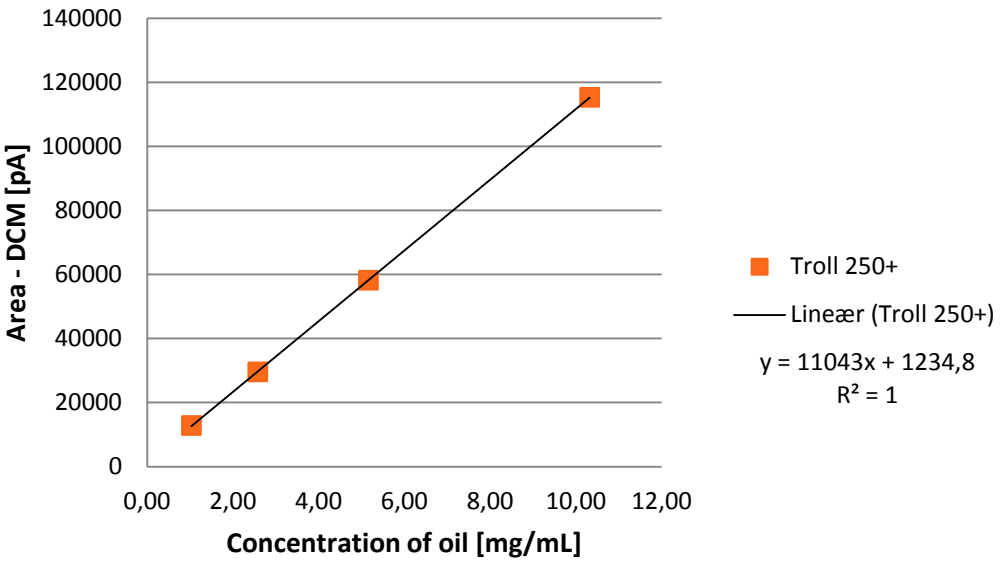

Figure D.2 - Calibration curve for Troll 250+

D.2 Avaldsnes 250+

An overlay of the chromatograms of the calibration standards for Avaldsnes 250+ is given in Figure D.3.

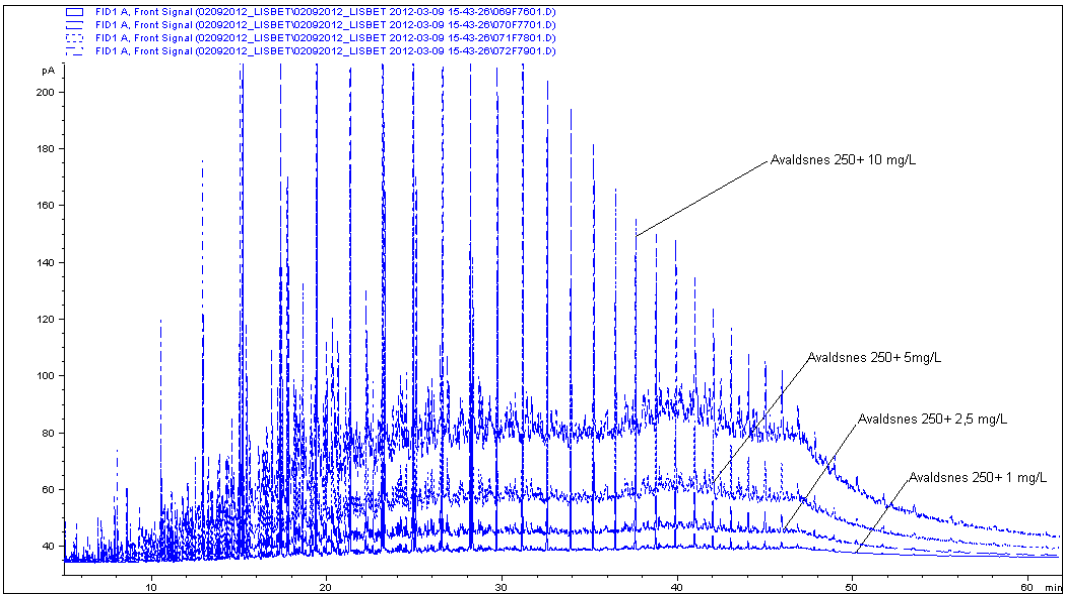

Figure D.3 - Overlay of GC-FID chromatograms for the calibration standards of Avaldsnes 250+

The analytical data for the GC-FID analysis of the Avaldsnes 250+ standards are given in Table D.2. The concentration of the primary standard was 20,22 mg/mL.

A calibration curve is plotted in Figure D.4, and this demonstrates that the response for of Avaldsnes 250+ is linear in the investigated concentration range.

Table D.2 – Calibration data for Avaldsnes 250+

Total area [pA]	**Area of α-androstane [pA]**	**Area-DCM [pA]**	**Concentration of oil [mg/mL]**	**Relative response factor RRF**
12 923	180	9 830	1,01	0,544
26 271	167	23 178	2,53	0,555
54 747	162	51 654	5,05	0,635
105 775	163	102 682	10,11	0,630
Average area of DCM blanks in the run [pA]	3 093		**Average RRF**	**0,591**
Concentration of α-androstane [mg/mL]	0,01008		Standard deviation RRF	0,048
			Relative standard deviation RRF (%)	8,134

.

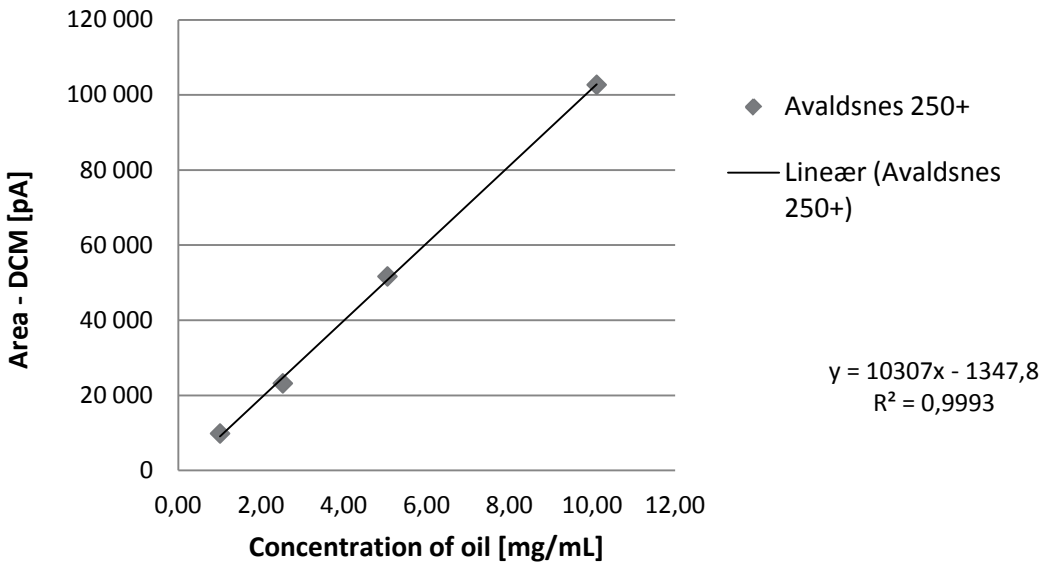

Figure D.4 – Calibration curve for Avaldsnes 250+

D.3 Kvitebjørn condensate 250+

An overlay of the chromatograms of the calibration standards for Kvitebjørn condensate 250+ is given in Figure D.5.

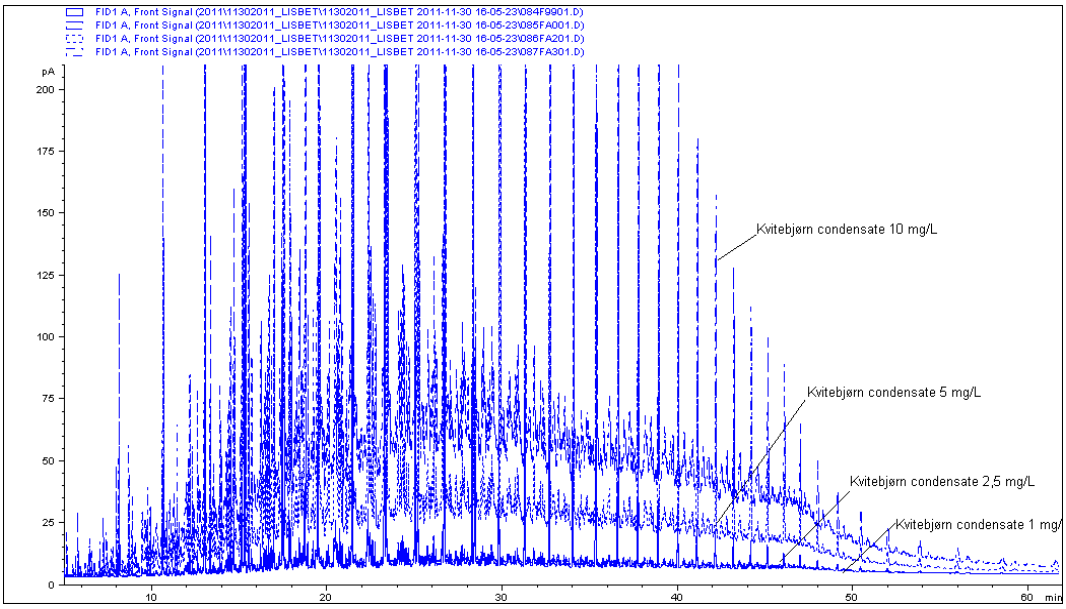

Figure D.5 - Overlay of GC-FID chromatograms for the calibration standards of Kvitebjørn condensate 250+

The analytical data for the GC-FID analysis of the Kvitebjørn condensate 250+ standards are given in Table D.3. The concentration of the primary standard was 20,68 mg/mL. As seen from the overlay in Figure D.5, the standard supposed to be of concentration 2,5, demonstrates unexplainable low response. The data for this standard is therefore omitted from the calculation of RRF.

A calibration curve is plotted in Figure D.6, and this demonstrates that the response for of Kvitebjørn condensate 250+ is linear in the investigated concentration range.

Table D.3 - Calibration data for Kvitebjørn condensate 250+

Total area [pA]	**Area of α-androstane [pA]**	**Area-DCM [pA]**	**Concentration of oil [mg/mL]**	**Relative response factor RRF**
17 170	170	14 349	1,03	0,824
73 559	190	70 738	5,17	0,727
149 476	186	146 655	10,34	0,769
			Average RRF	**0,773**
Average area of DCM blanks in the run [pA]	2 821		Standard deviation RRF	0,049
Concentration of α-androstane [mg/mL]	0,01008		Relative standard deviation RRF (%)	6,327

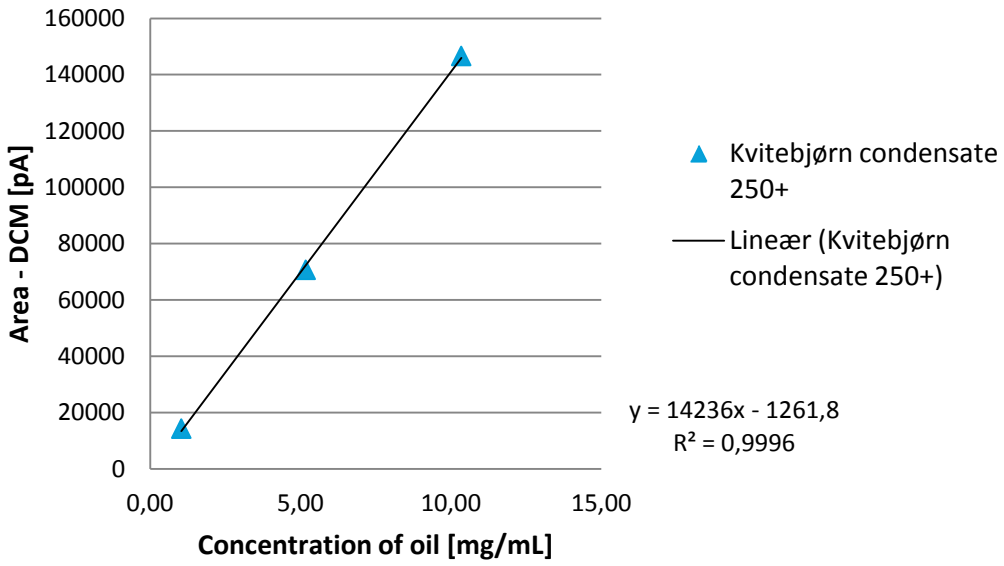

Figure D.6 - Calibration curve for Kvitebjørn condensate 250+

D.4 IF380 Fresh

An overlay of the chromatograms of the calibration standards for IF380 Fresh is given in Figure D.7.

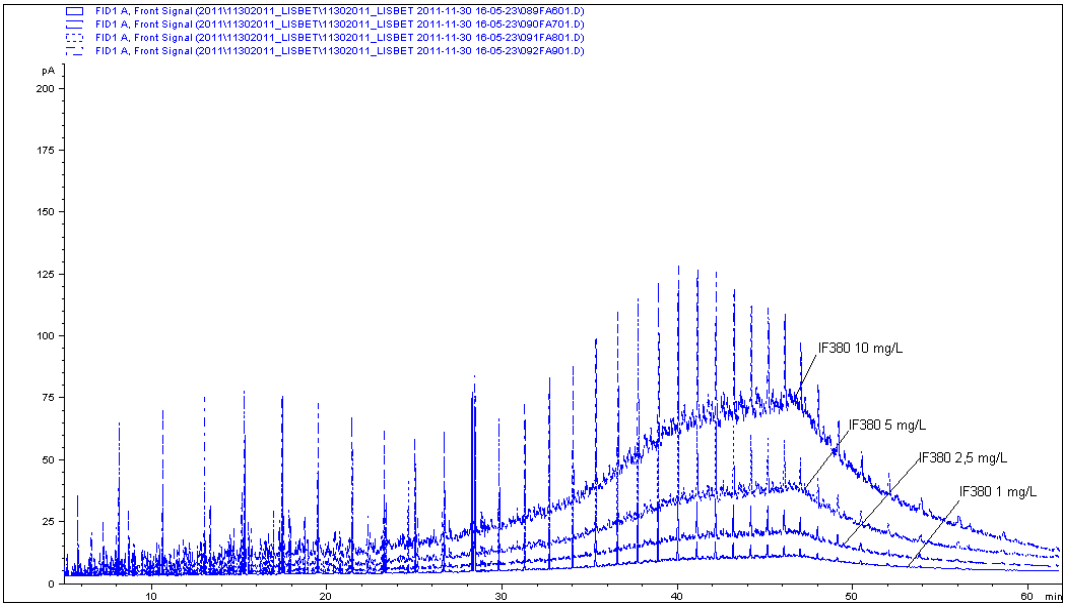

Figure D.7 - Overlay of GC-FID chromatograms for the calibration standards of IF380 Fresh

The analytical data for the GC-FID analysis of the IF380 Fresh standards are given in Table D.4. The concentration of the primary standard was 20,57 mg/mL.

A calibration curve is plotted in Figure D.8, and this demonstrates that the response for of IF380 Fresh is linear in the investigated concentration range.

Table D.4 – Calibration data for IF380 Fresh

Total area [pA]	Area of α-androstane [pA]	Area-DCM [pA]	Concentration of oil [mg/mL]	Relative response factor RRF
10 730	165	7 910	1,03	0,470
20 715	167	17 894	2,57	0,421
39 456	163	36 635	5,14	0,440
72 587	163	69 766	10,29	0,418
			Average RRF	**0,437**
Average area of DCM blanks in the run [pA]	2 821		Standard deviation RRF	0,024
Concentration of α-androstane [mg/mL]	0,01008		Relative standard deviation RRF (%)	5,500

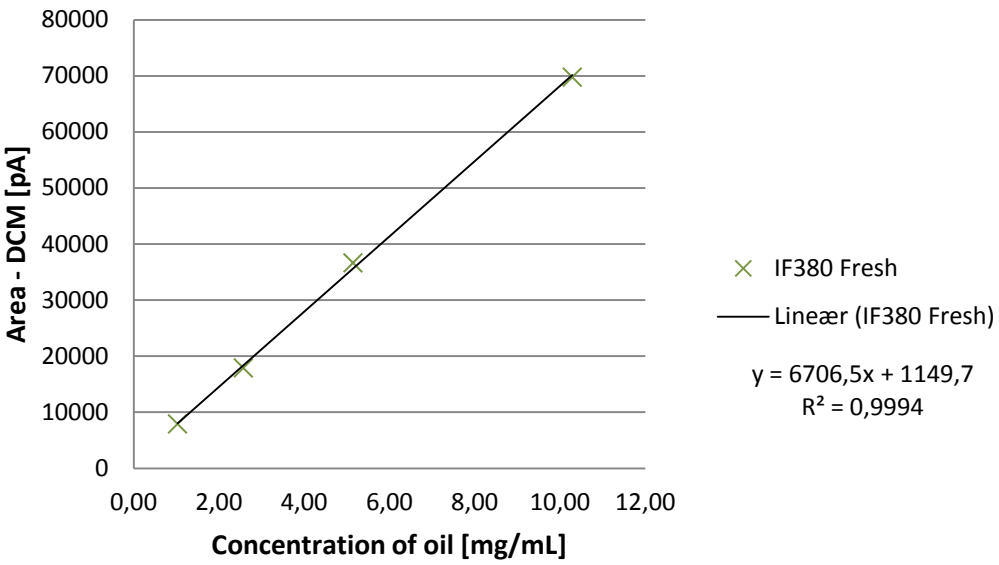

Figure D.8 – Calibration curve for IF 380 Fresh

Appendix E Method development

E.1 Comparison of extraction techniques

Table E.1 show the experimental data for the six experiments used to compare Soxhlet extraction and alkaline saponification.

Table E.1 – Data of samples for comparison of extraction techniques

Experiment ID	Extraction method	Weight of sediment [g]	Volume of oil added [µL]	Weight of oil added [mg]
M1_1	Soxhlet extraction	7,55	N/A	N/A
M1_2		7,61	31,82	29,58
M1_3		7,65	30,15	28,03
M2_1	Alkaline saponification	7,60	30,07	27,95
M2_2		7,53	30,18	28,06
M2_3		7,64	30,04	27,93

The results from GC-FID analysis of the extracts are shown in Table E.2 and Figures E.1 – E.6.

Figure E.7 is an overlay of the two quantifiable chromatograms for each extraction.

Table E.2 – Results from GC-FID analysis of method development samples

Sample ID	A_{tot}	A_{DCM}	A_{otp}	$A_{5\alpha\text{-and}}$	A_{THC}	C_{RIS} [µg]	RRF (oil)	THC [µg/ extract]	C_{SIS} [µg]	THC [µg/ sample]
M1_1	46 153	10579	136	194	35 244	10	0,748	2 424	10	3467
M1_2	42 478	10579	109	178	31 612	10	0,748	2 372	10	3877
M2_2	27 724	10579	107	184	16 854	10	0,748	1 223	10	2106
M2_3	22 991	10579	189	218	12 006	10	0,748	738	10	848

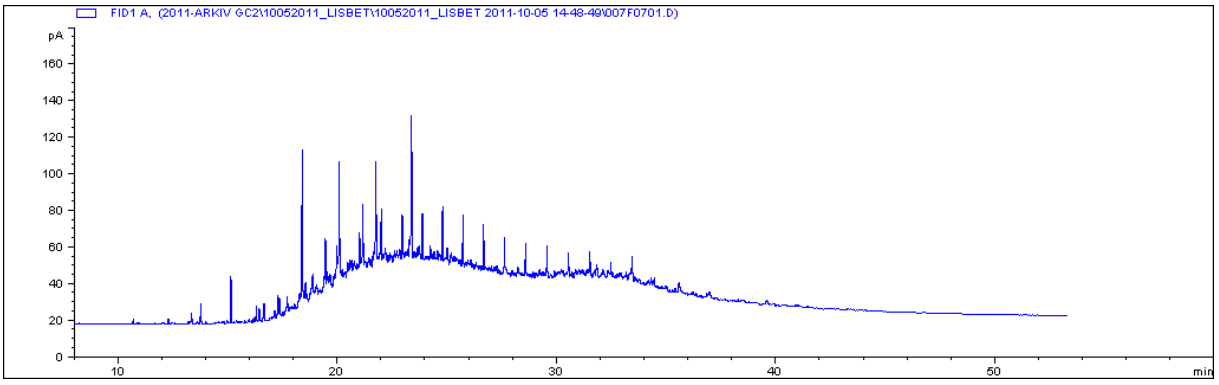

Figure E.1 - M1_1 Soxhlet extraction

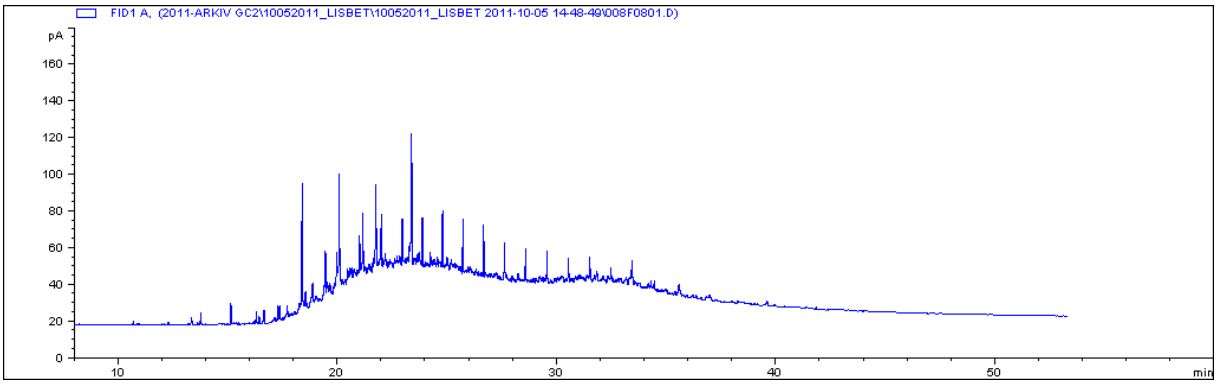

Figure E.2 - M1_2 Soxhlet extraction

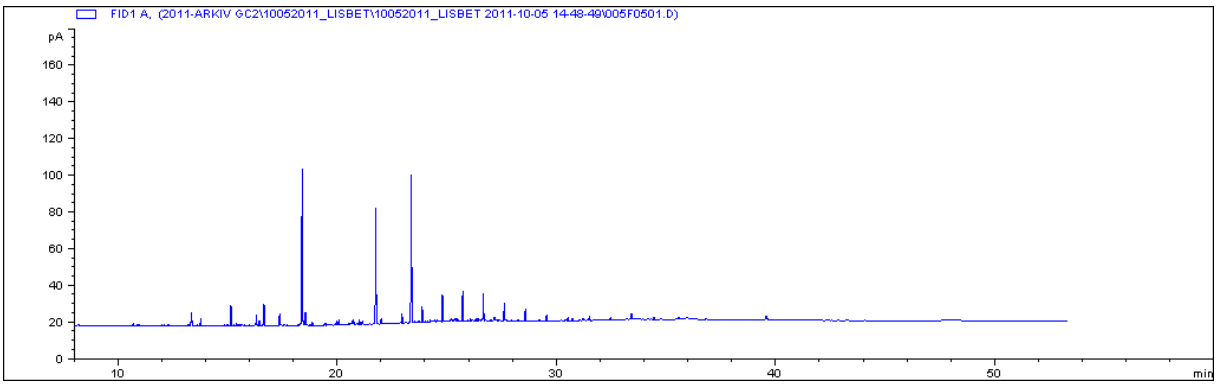

Figure E.3 - M1_3 Soxhlet extraction

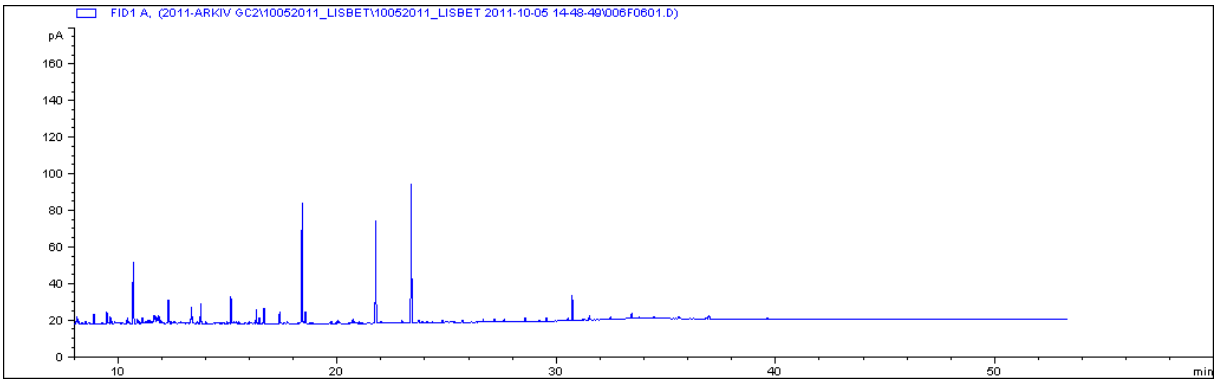

Figure E.4 – M2_1 Alkaline saponification

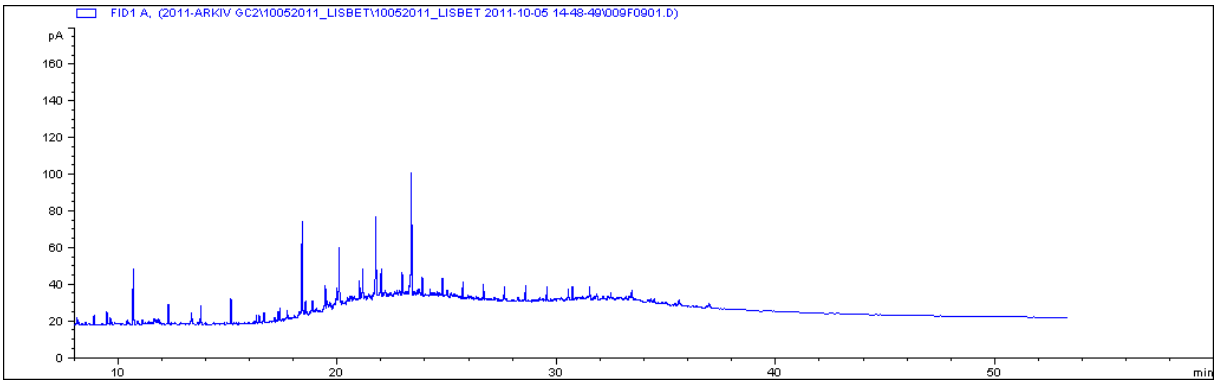

Figure E.5 - M2_2 Alkaline saponification

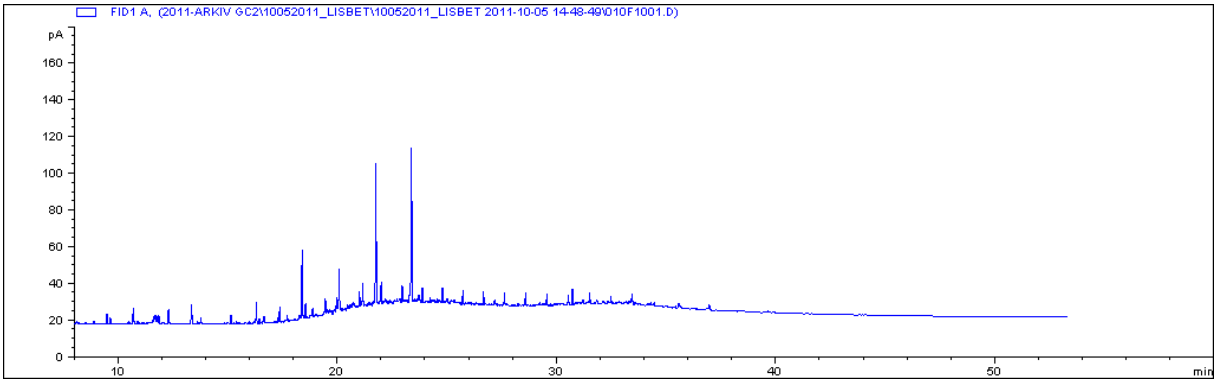

Figure E.6 - M2_3 Alkaline saponification

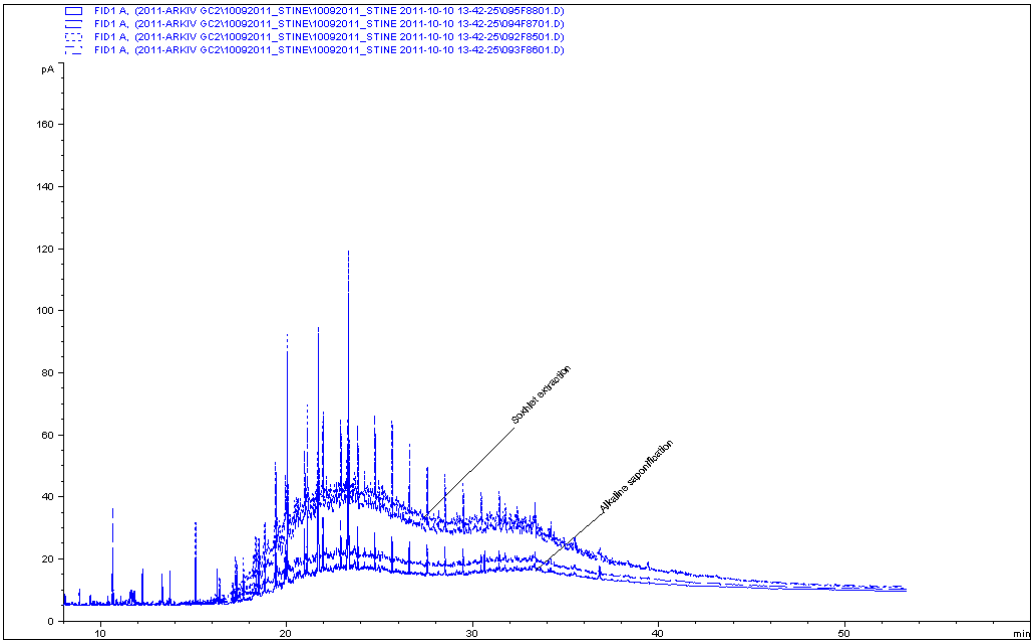

Figure E.7 - Overlay of M1_1, M1_2, M2_2, and M2_3. Comparison of Soxhlet extraction and alkaline saponification.

Appendix F GC-FID Chromatograms

This appendix will present all chromatograms obtained by GC-FID analysis of sediment extracts, water extracts, procedural blanks and laboratory blanks. Values on x-axis is in minutes, values on y-axis is in pA.

F.1 GC-FID Chromatograms of sediment extracts

The following will present the chromatograms for all samples of sediment extracts.

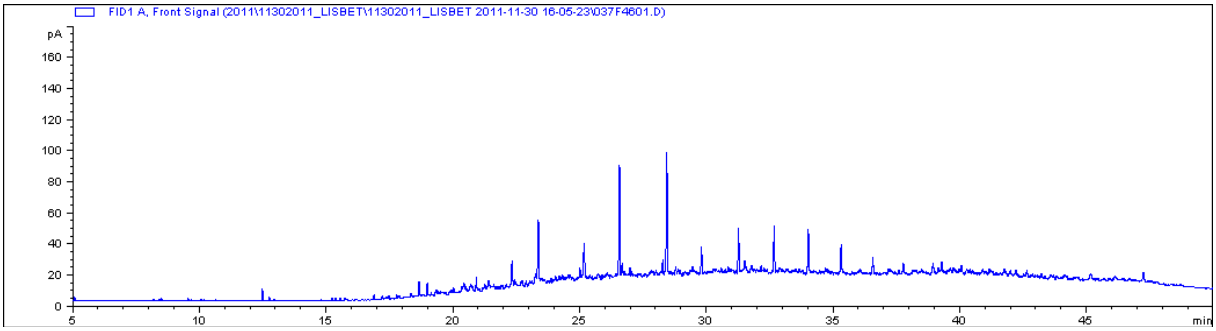

Figure F.1 - LIS001_1 Sediment

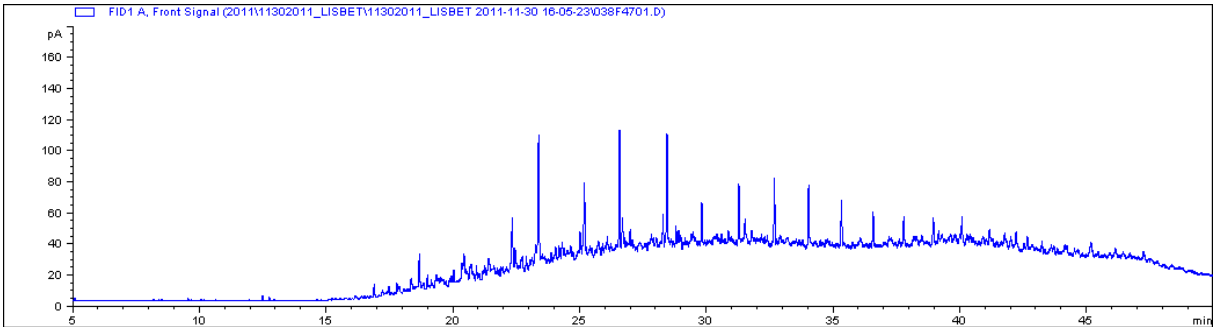

Figure F.2 - LIS001_2 Sediment

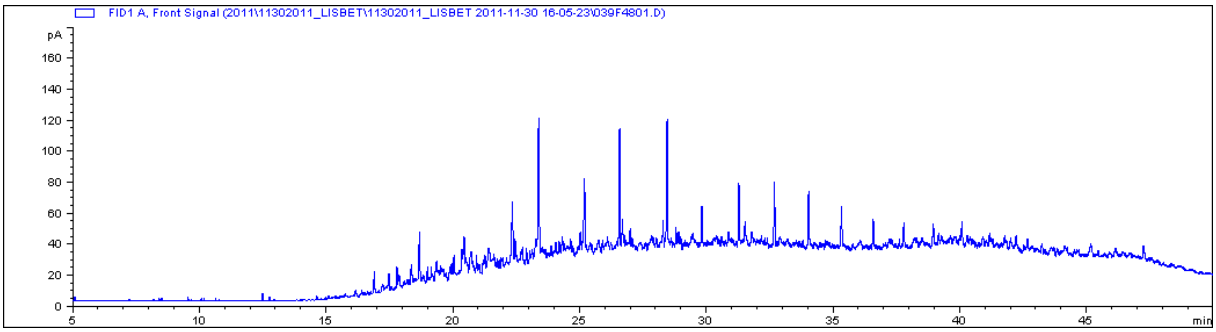

Figure F.3 - LIS001_3 Sediment

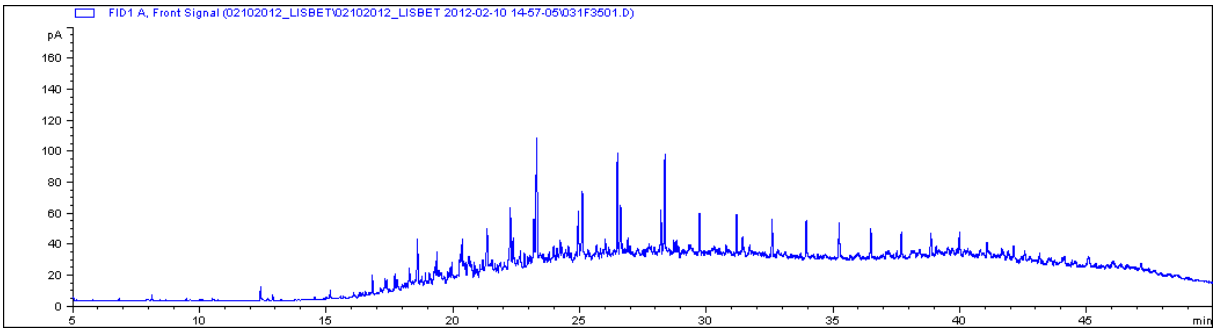

F.4 - **LIS001_4 Sediment**

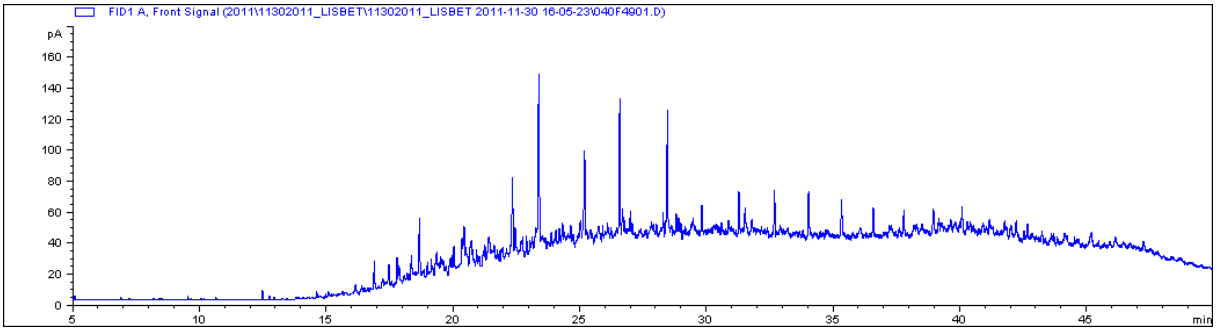

Figure F.5 - LIS002_1 Sediment

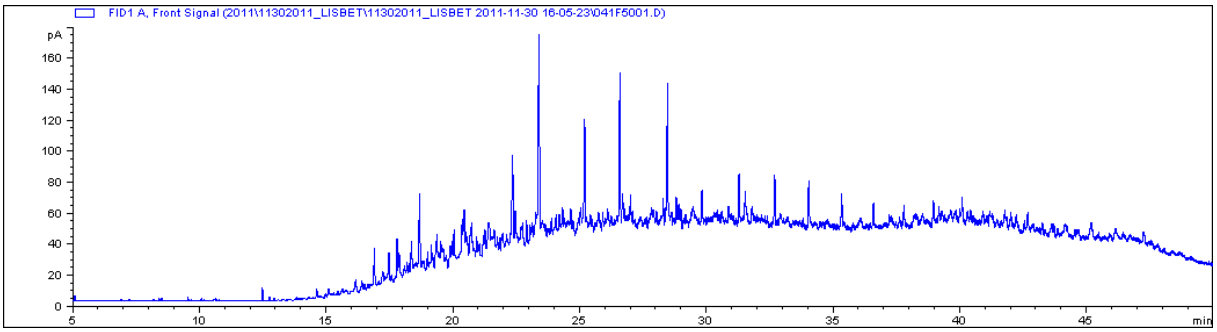

Figure F.6 - LIS002_2 Sediment

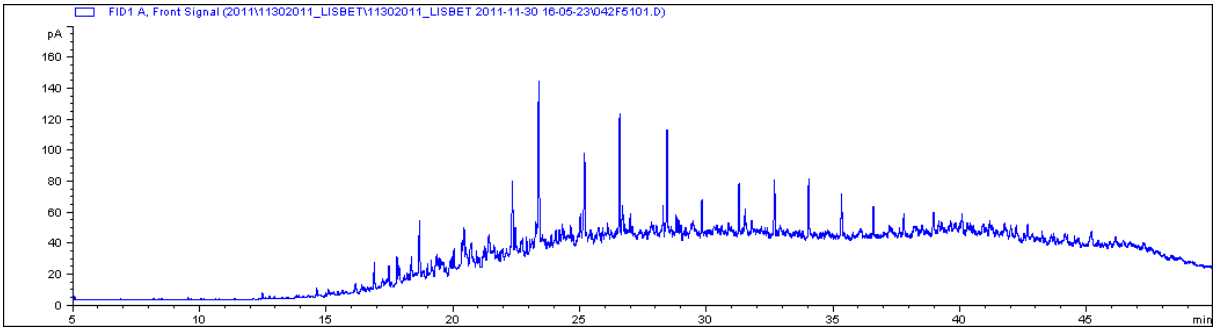

Figure F.7 - LIS002_3 Sediment

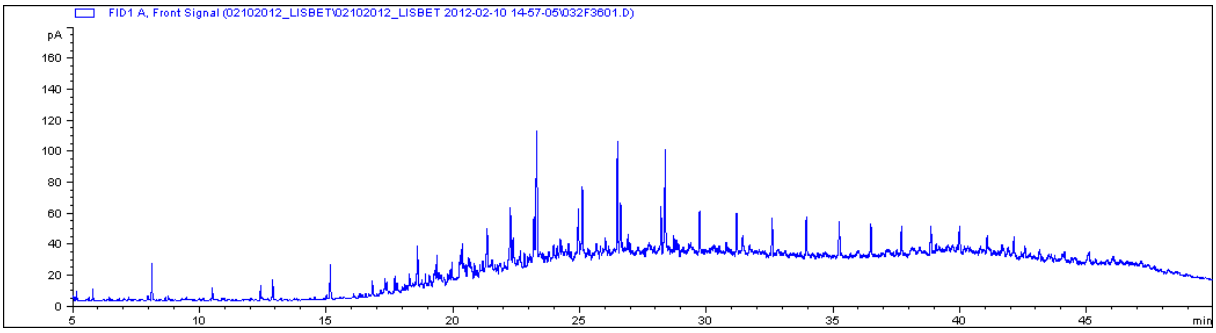

Figure F.8 - LIS002_4 Sediment

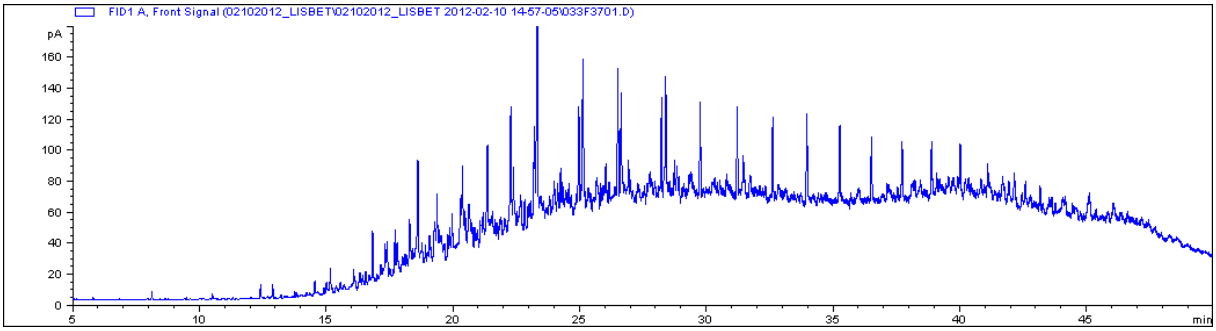

Figure F.9 - LIS002_5 Sediment

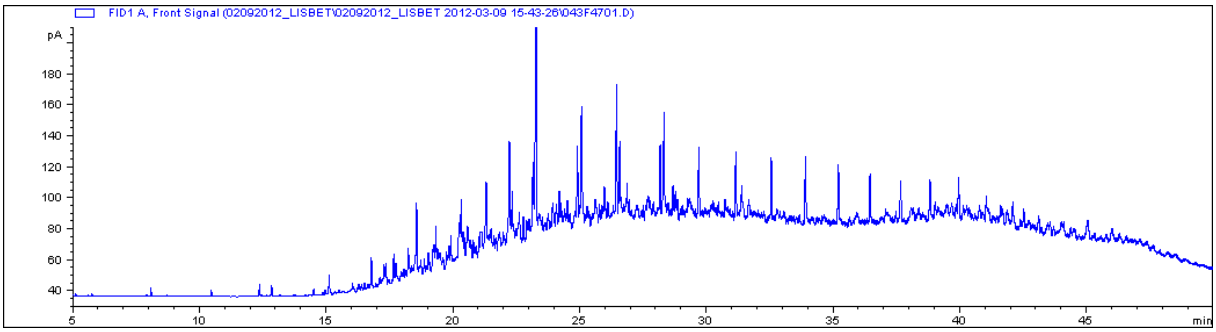

Figure F.10 - LIS002_6 Sediment

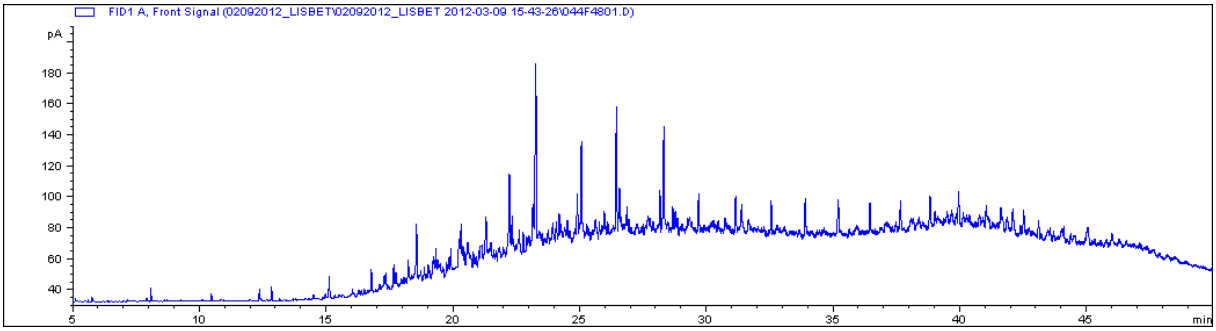

Figure F.11 - LIS002_7 Sediment

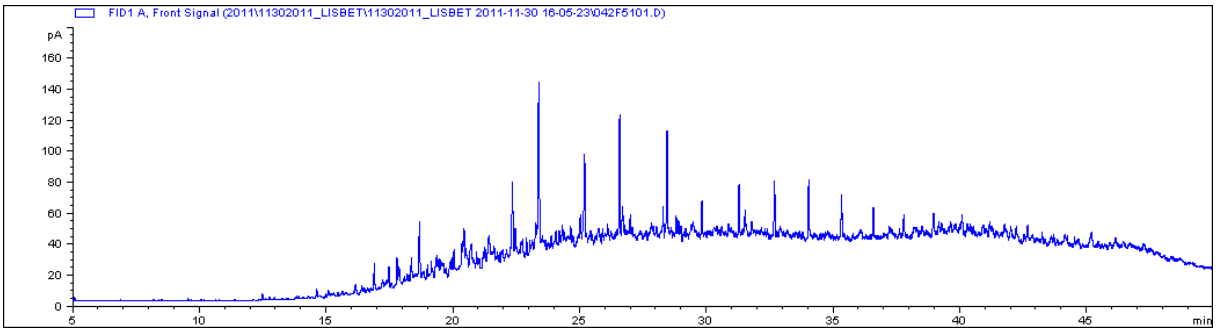

Figure F.12 - LIS003_1 Sediment

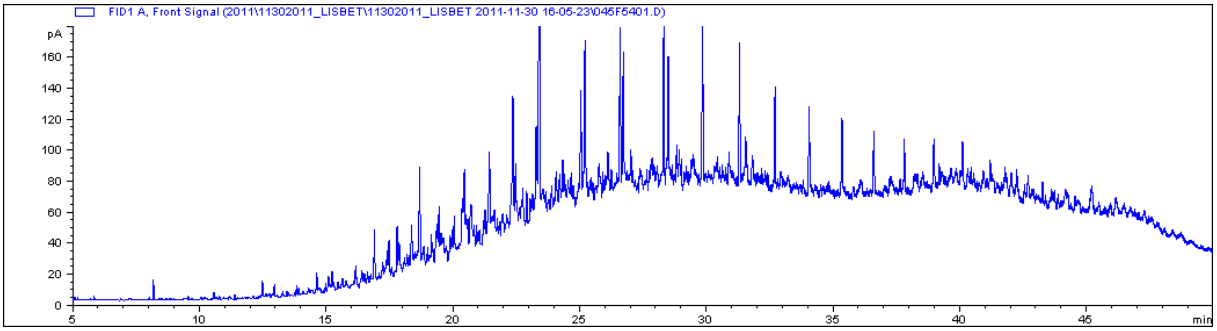

Figure F.13 -LIS003_2 Sediment

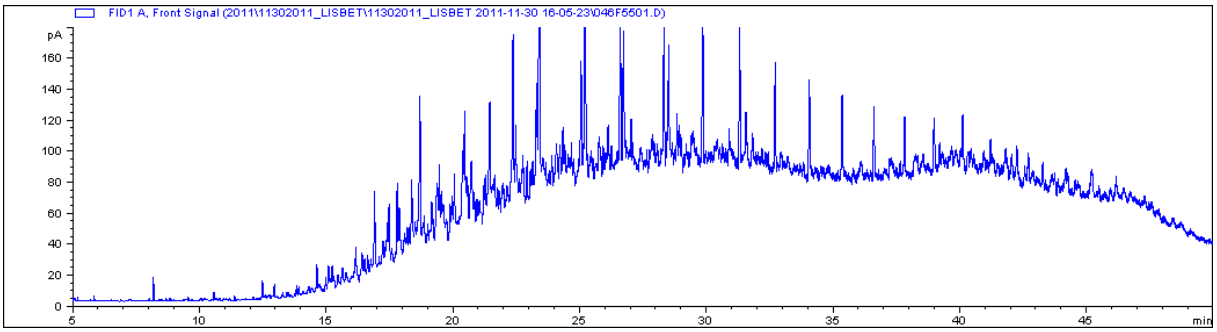

Figure F.14 - LIS003_3 Sediment

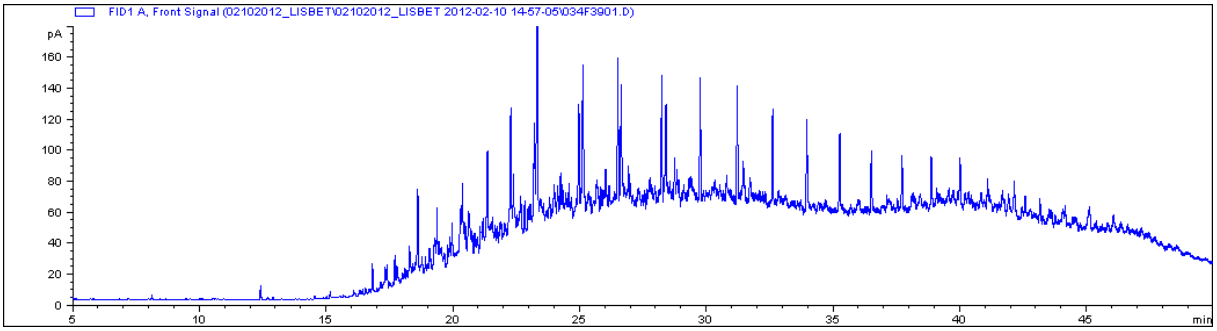

Figure F.15 - LIS003_4 Sediment

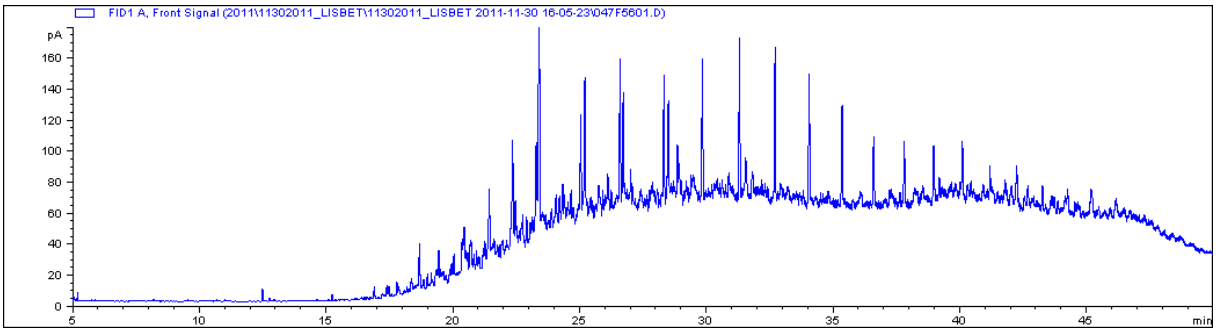

Figure F.16 - LIS004_1 Sediment

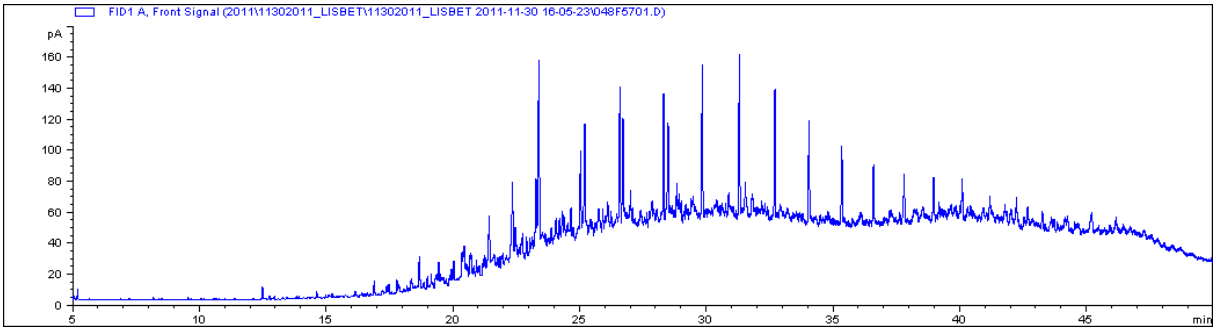

Figure F.17 - LIS004_2 Sediment

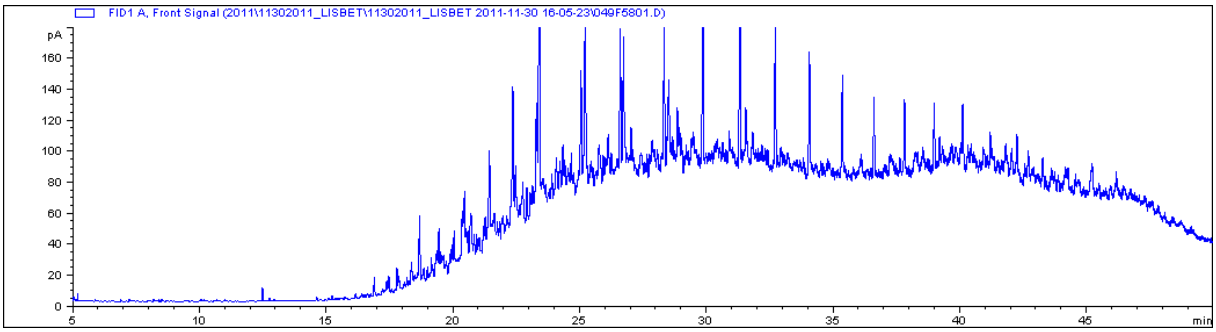

Figure F.18 - LIS004_3 Sediment

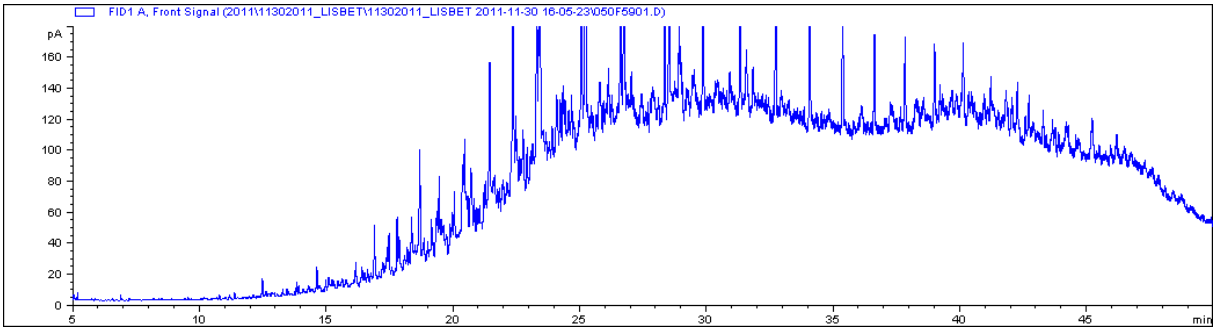

Figure F.19 - LIS005_1 Sediment

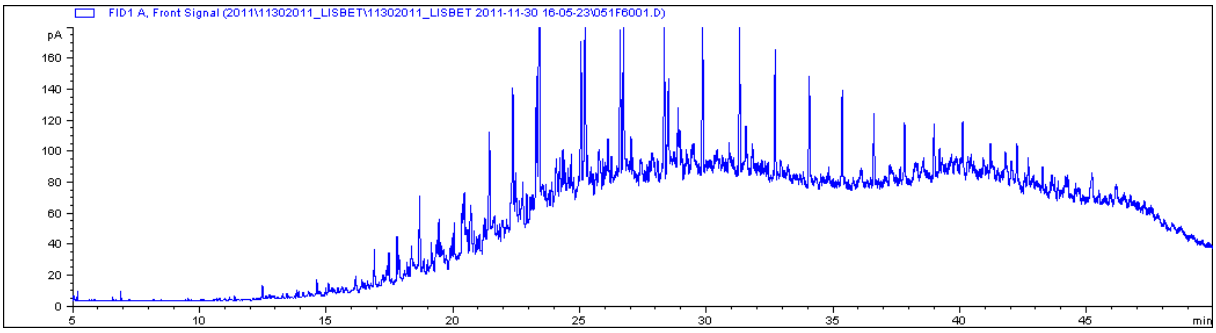

Figure F.20 - LIS005_2 Sediment

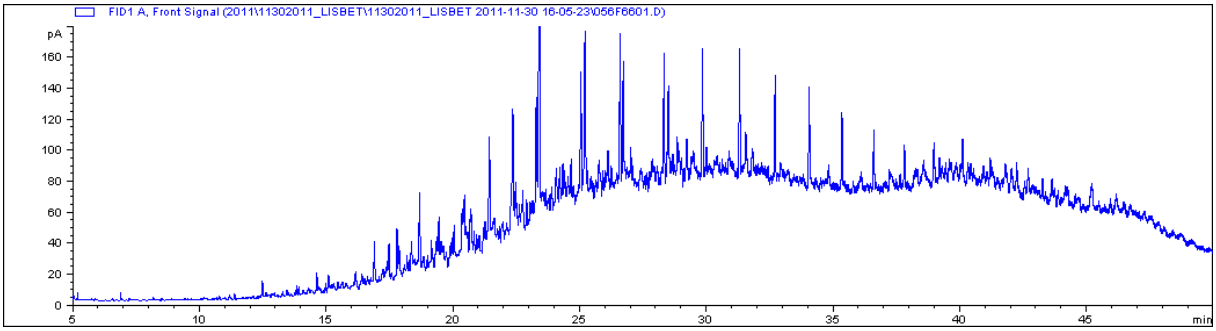

Figure F.21 - LIS005_3 Sediment

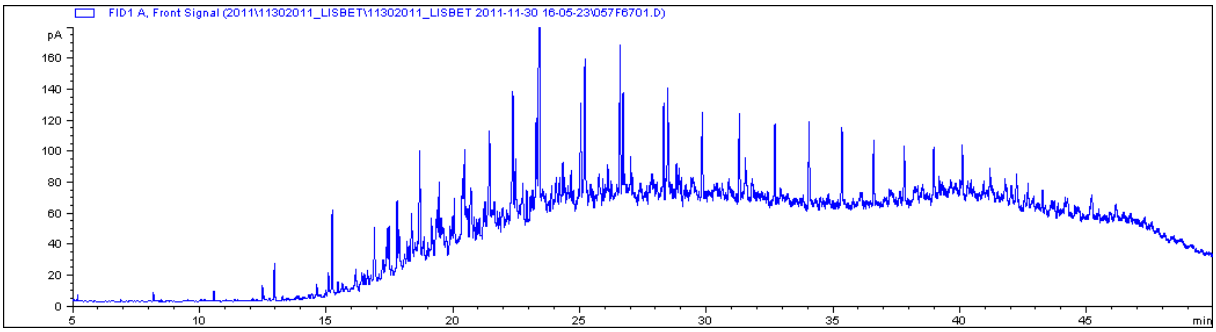

Figure F.22 - LIS006_1 Sediment

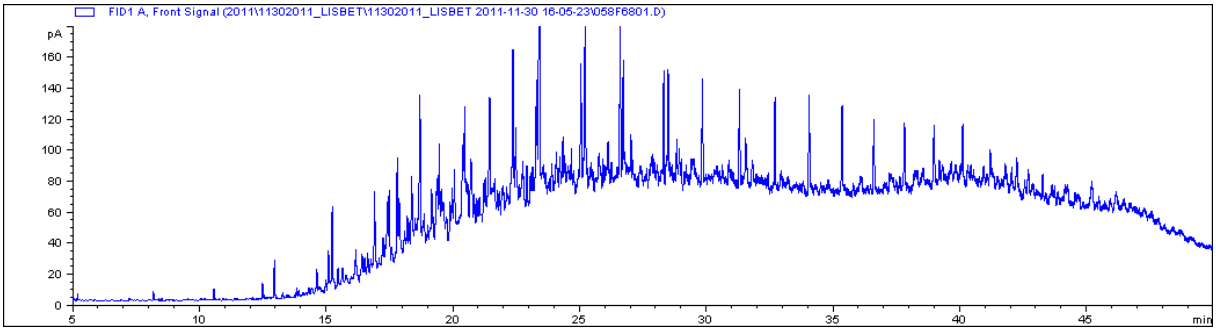

Figure F.23 - LIS006_2 Sediment

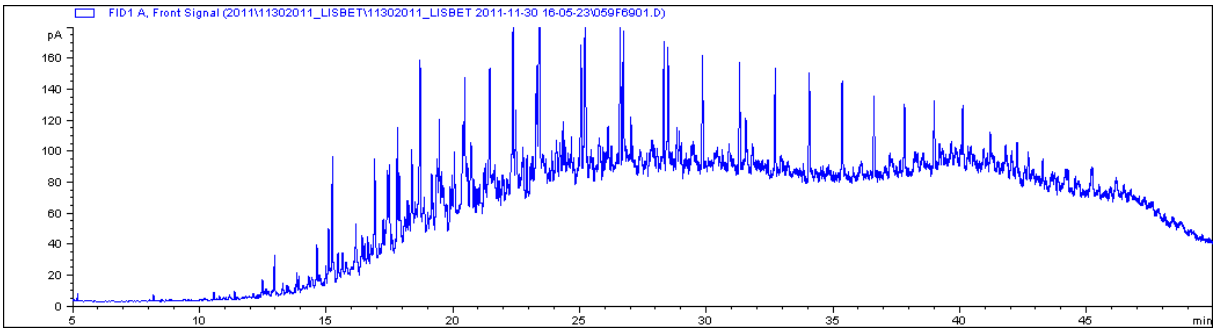

Figure F.24 - LIS006_3 Sediment

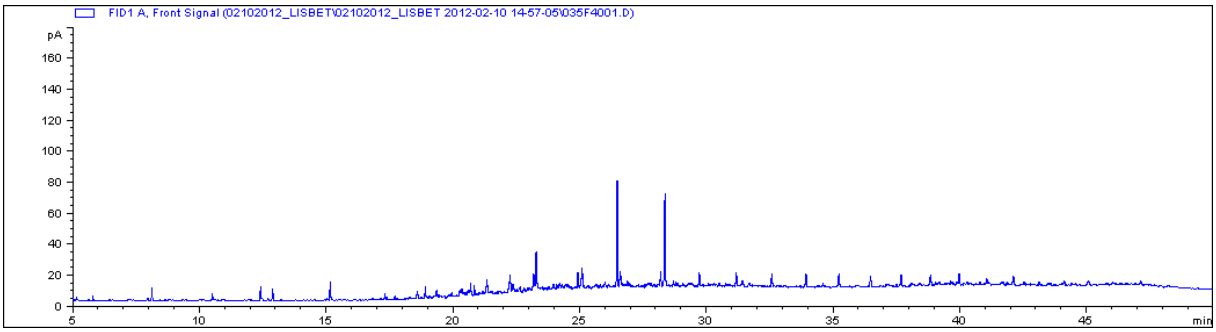

Figure F.25 - LIS006_6 Sediment

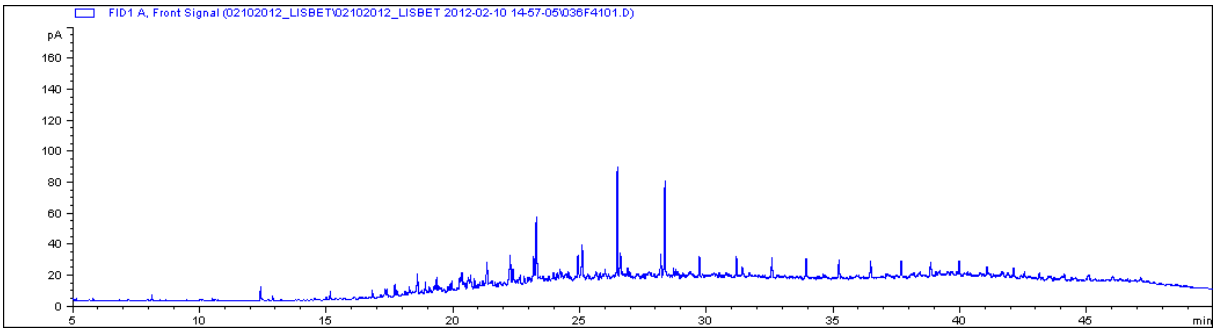

Figure F.26 - LIS006_7 Sediment

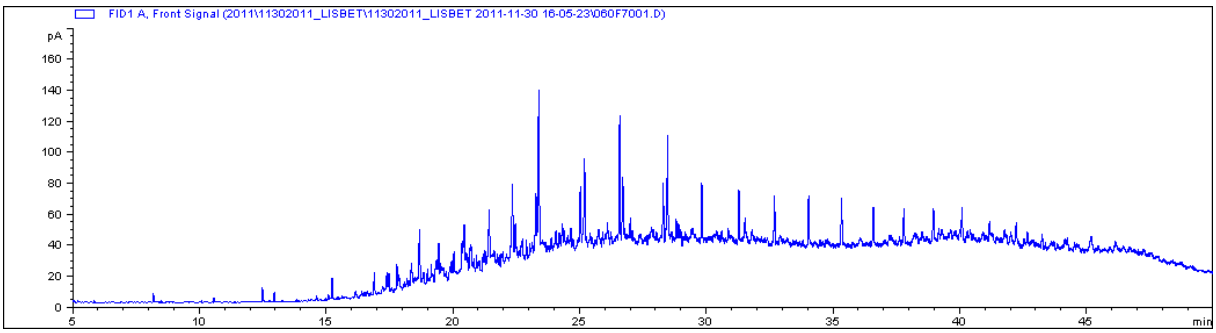

Figure F.27 - LIS007_1 Sediment

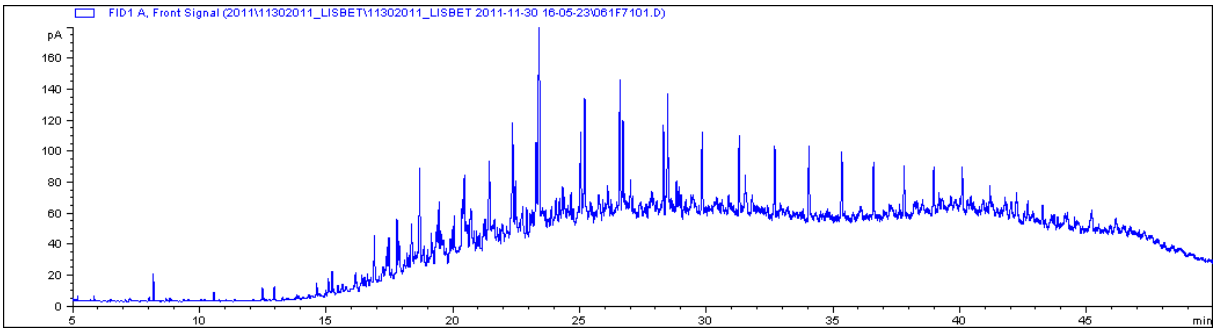

Figure F.28 - LIS007_2 Sediment

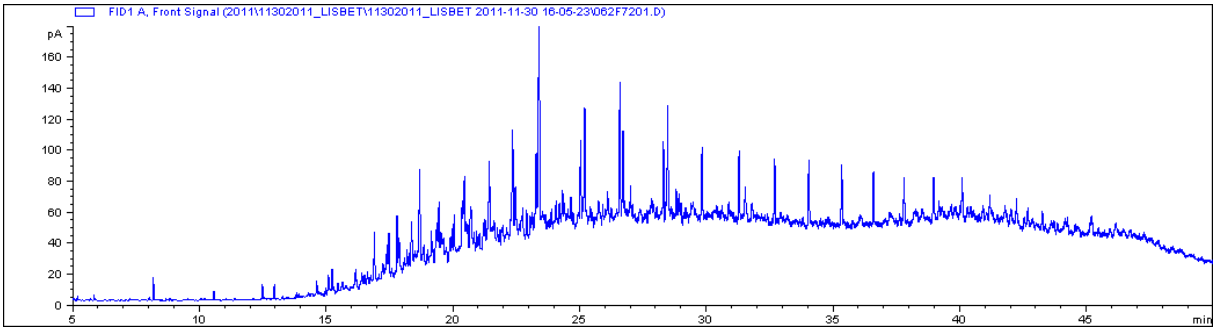

Figure F.29 - LIS007_3 Sediment

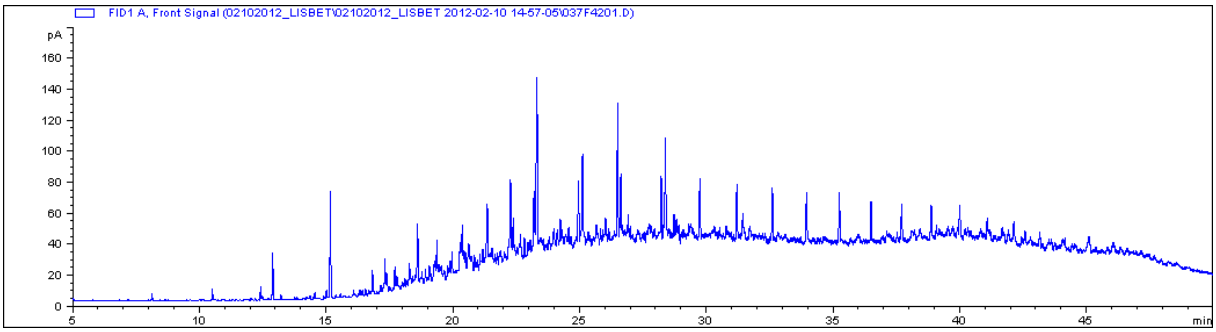

Figure F.30 - LIS007_4 Sediment

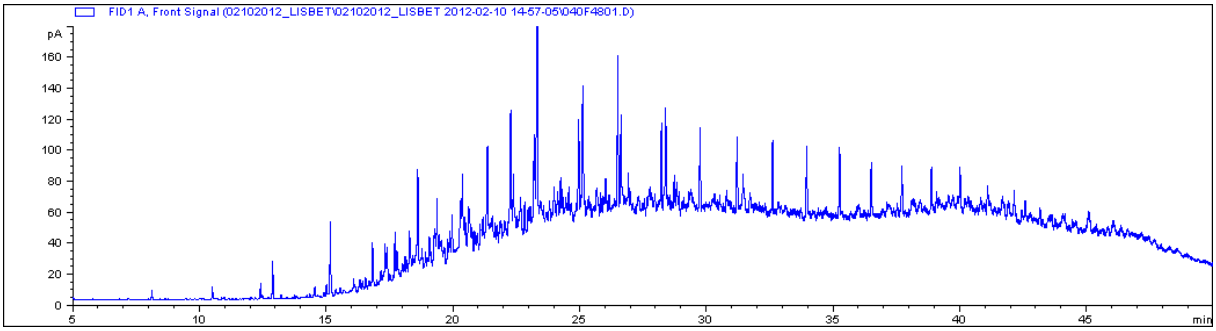

Figure F.31 - LIS007_5 Sediment

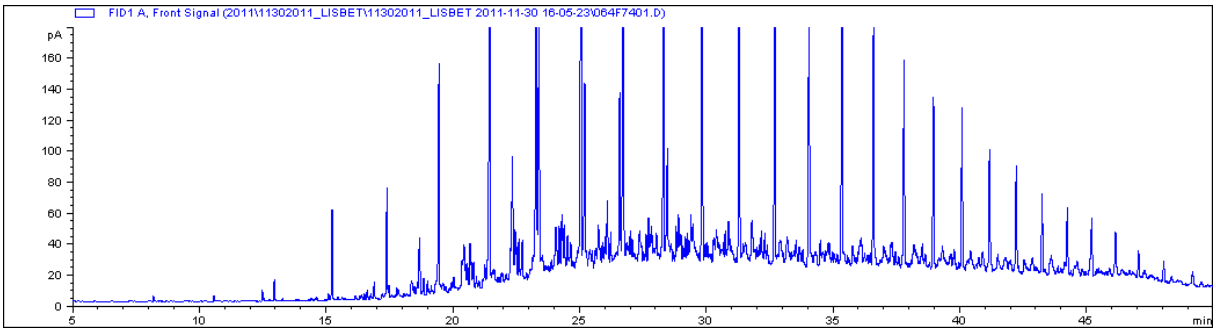

Figure F.32 - LIS008_1 Sediment

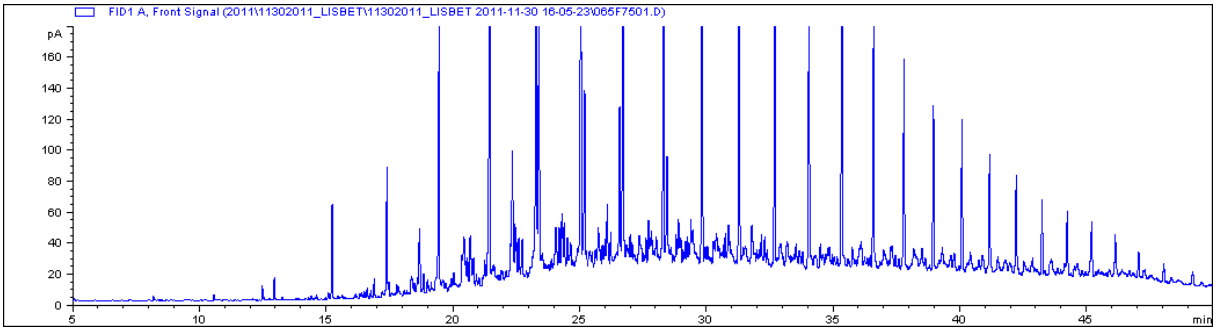

Figure F.33 - LIS008_2 Sediment

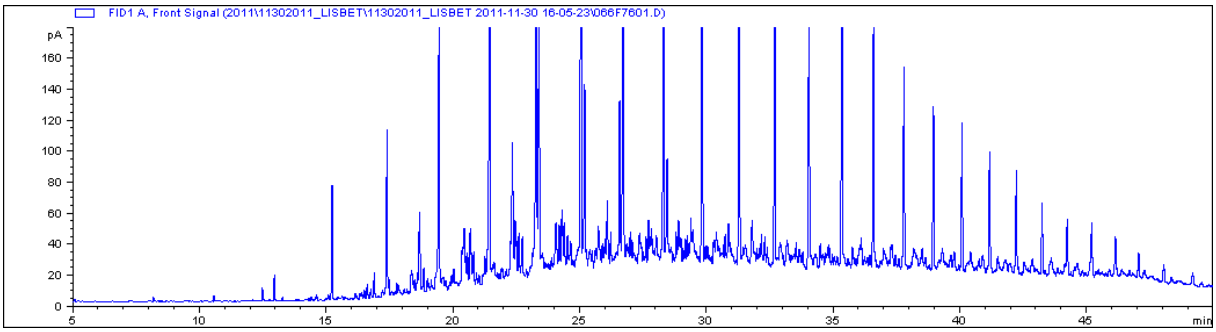

Figure F.34 - LIS008_3 Sediment

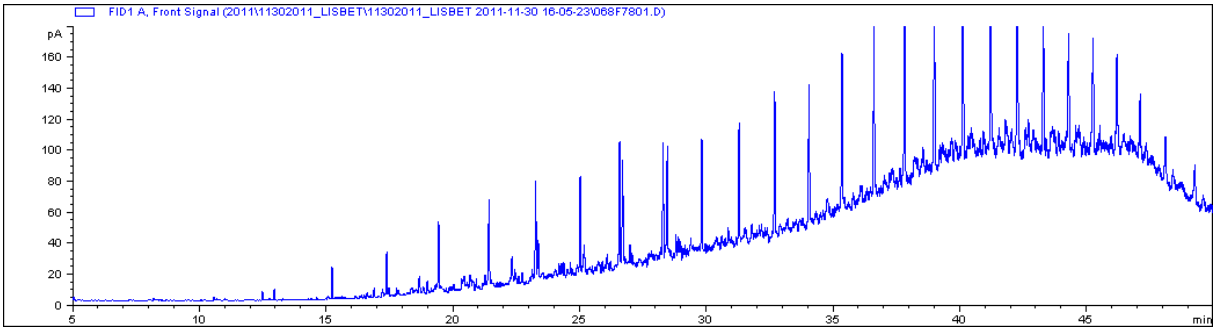

Figure F.35 - LIS009_1 Sediment

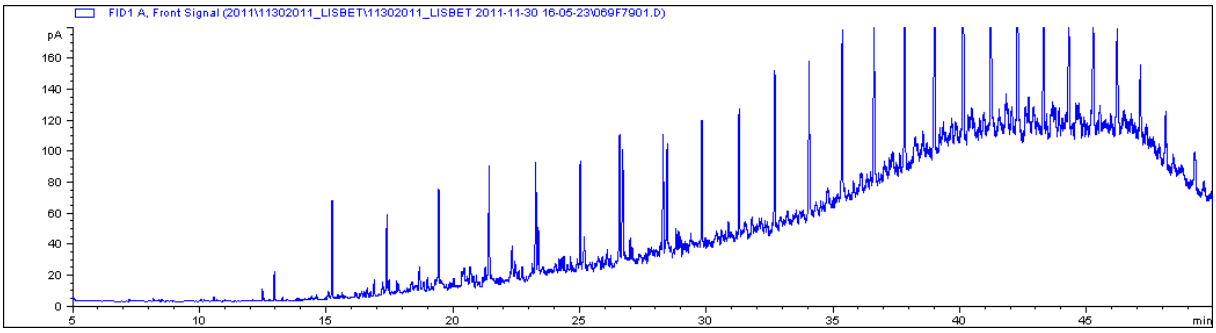

Figure F.36 - LIS009_2 Sediment

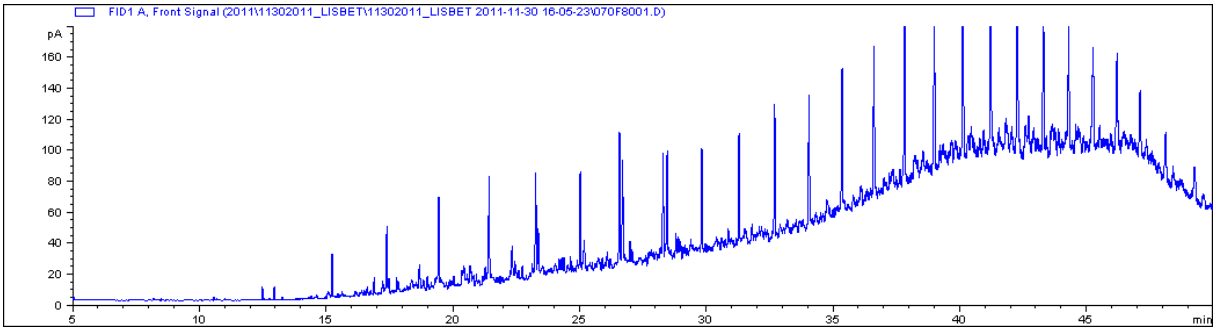

Figure F.37 - LIS009_3 Sediment

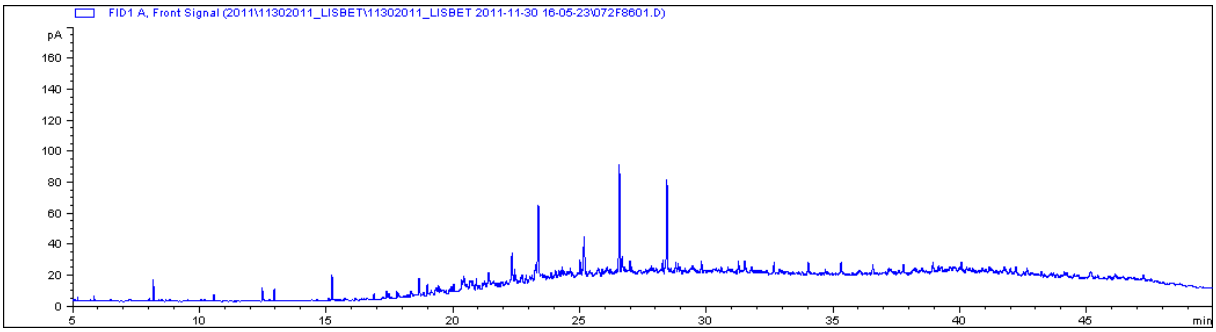

Figure F.38 - LIS010_1 Sediment

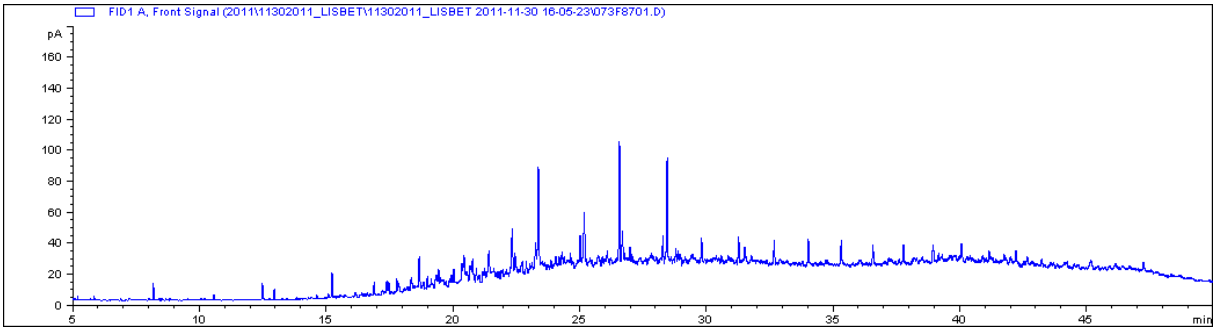

Figure F.39 - LIS010_2 Sediment

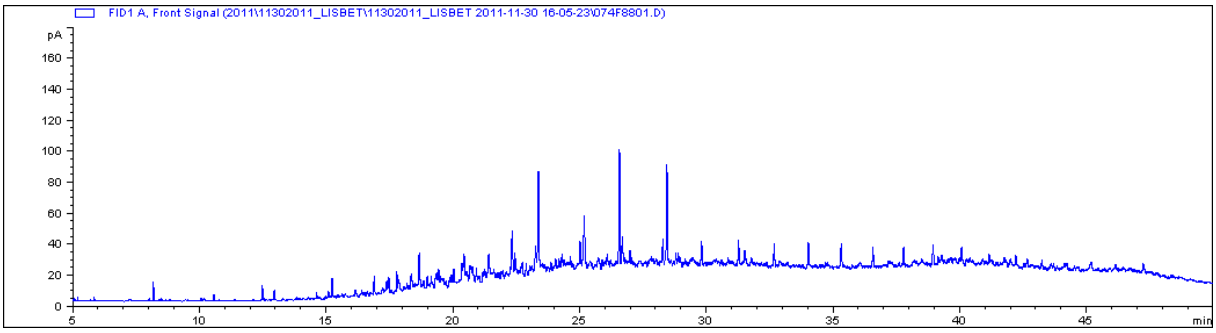

Figure F.40 - LIS010_3 Sediment

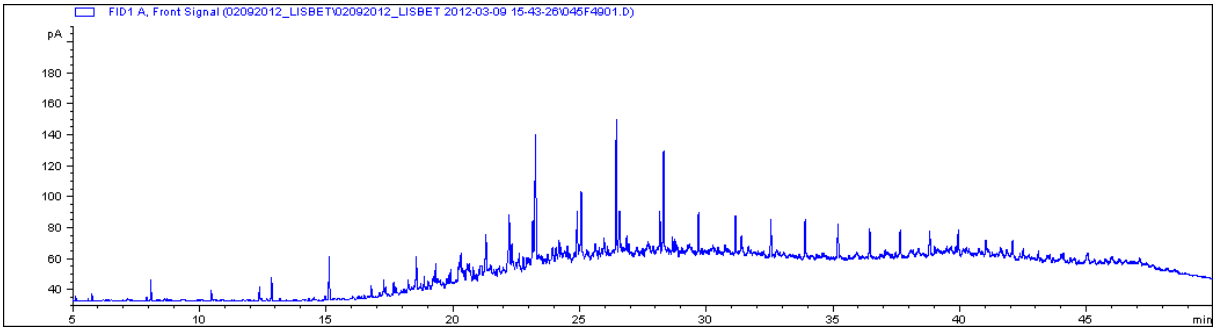

Figure F.41 - LIS010_4 Sediment

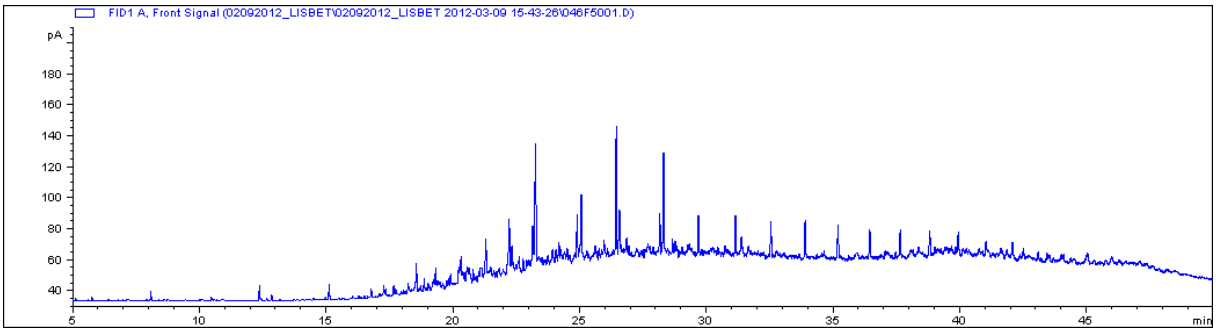

Figure F.42 - LIS010_5 Sediment

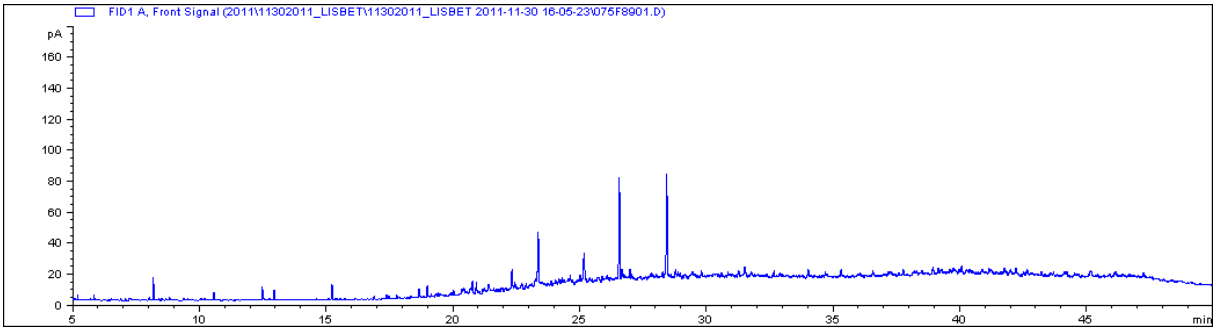

Figure F.43 - LIS011_1 Sediment

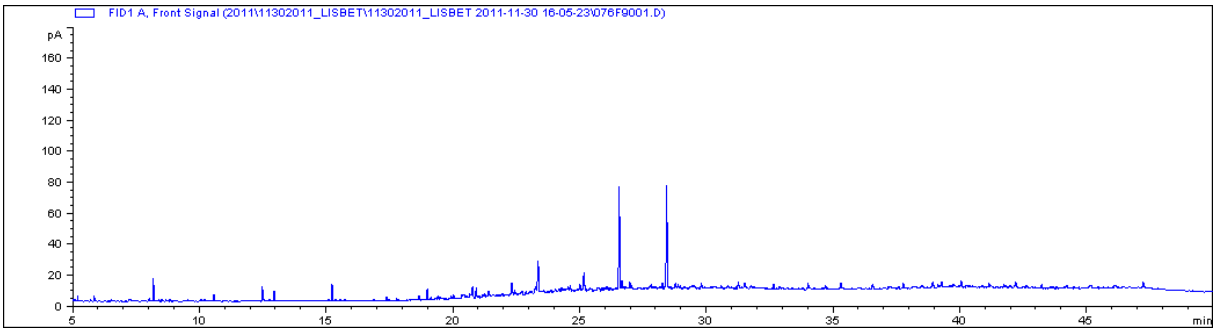

Figure F.44 - LIS011_2 Sediment

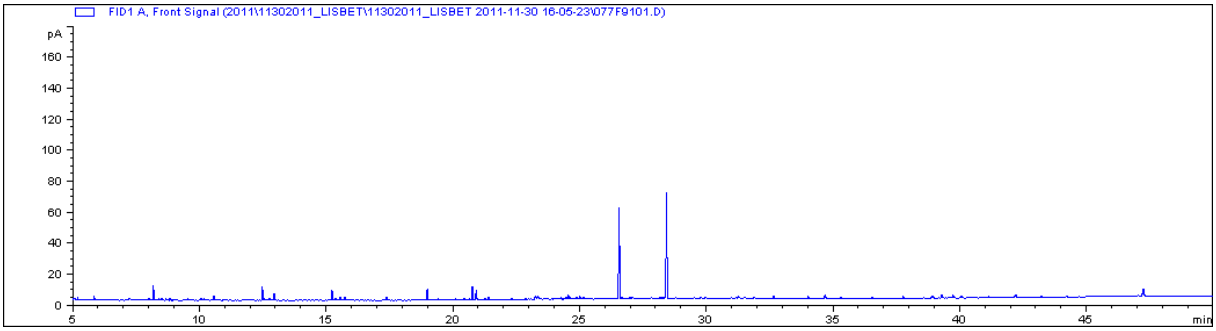

Figure F.45 - LIS011_3 Sediment

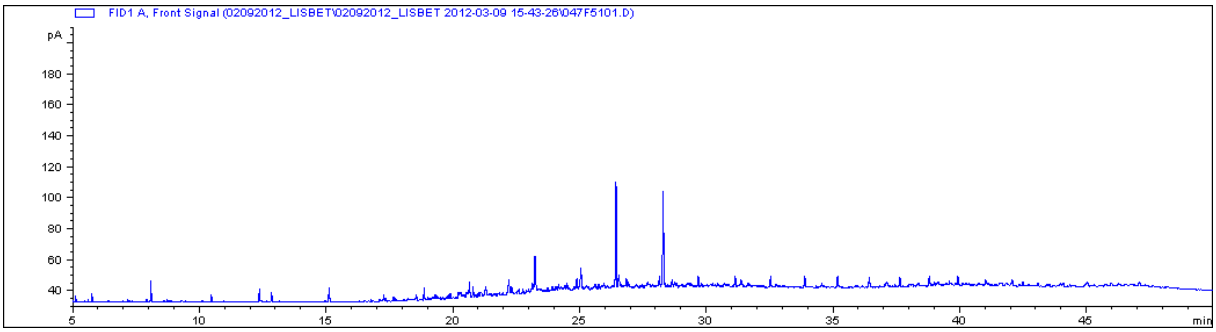

Figure F.46 - LIS011_4 Sediment

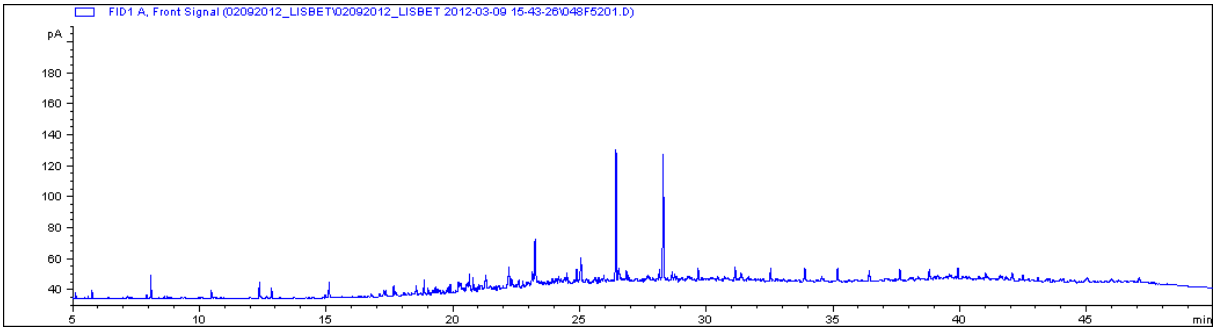

Figure F.47 - LIS011_5 Sediment

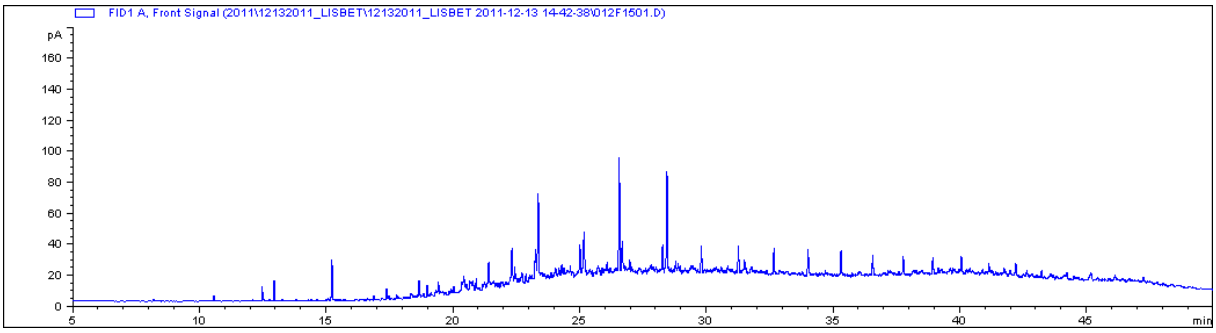

Figure F.48 - LIS012_1 Sediment

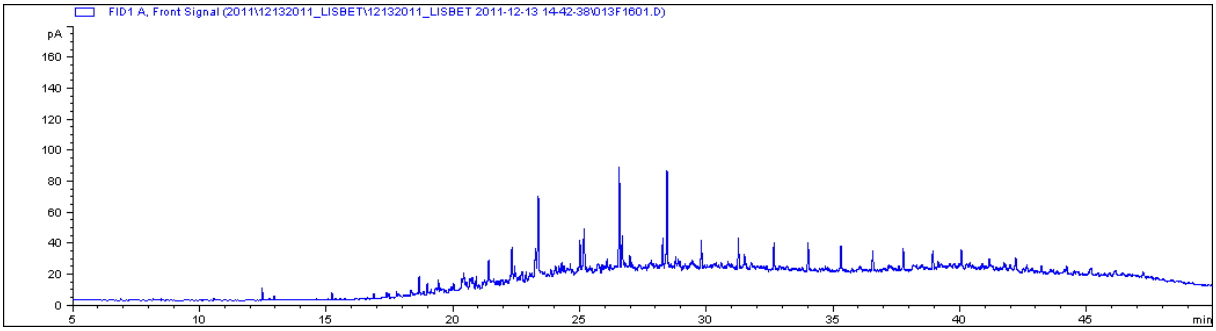

Figure F.49 -LIS012_2 Sediment

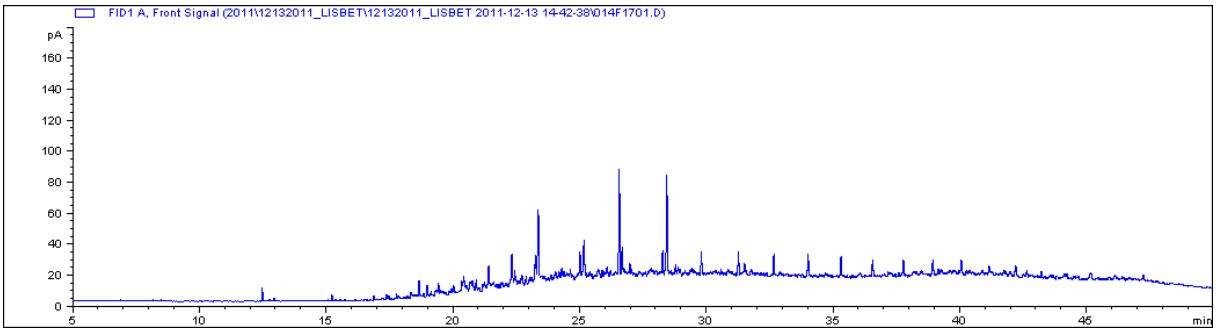

Figure F.50 - LIS012_3 Sediment

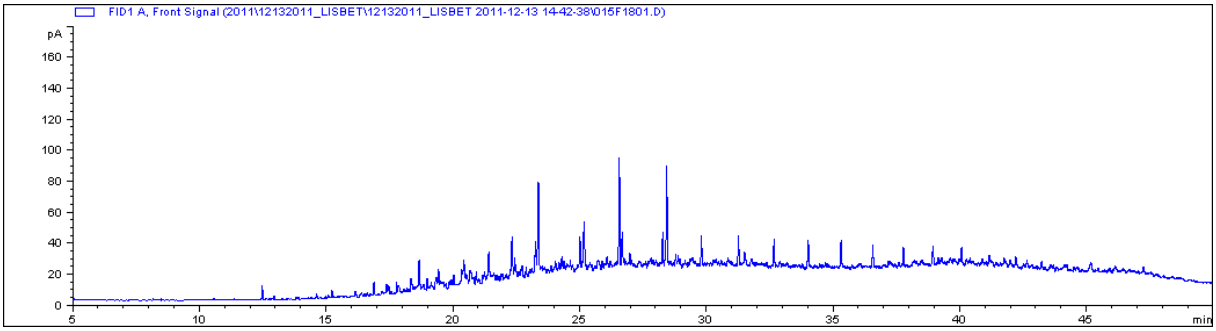

Figure F.51 - LIS013_1 Sediment

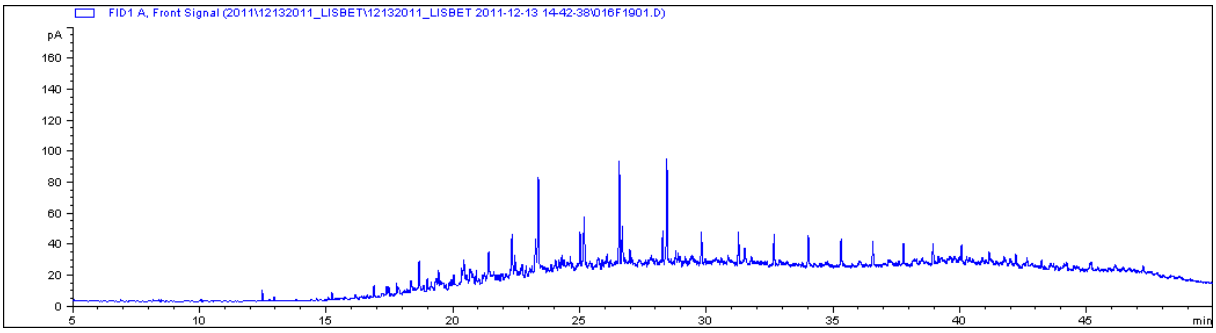

Figure F.52 - LIS013_2 Sediment

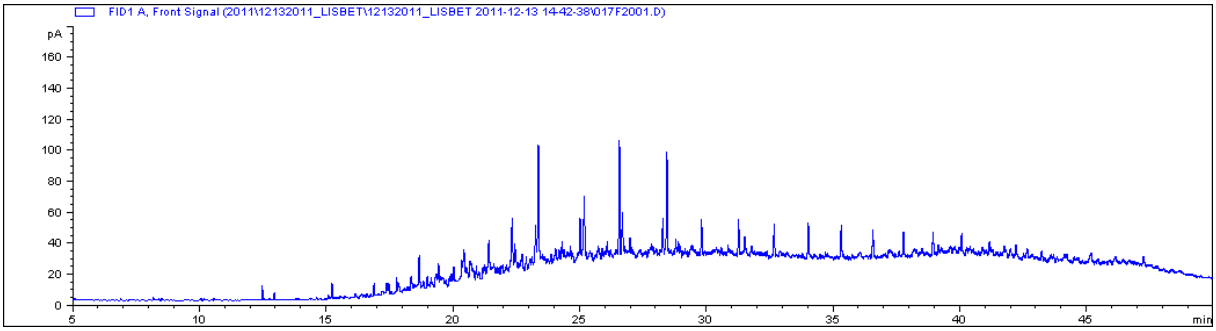

Figure F.53 - LIS013_3 Sediment

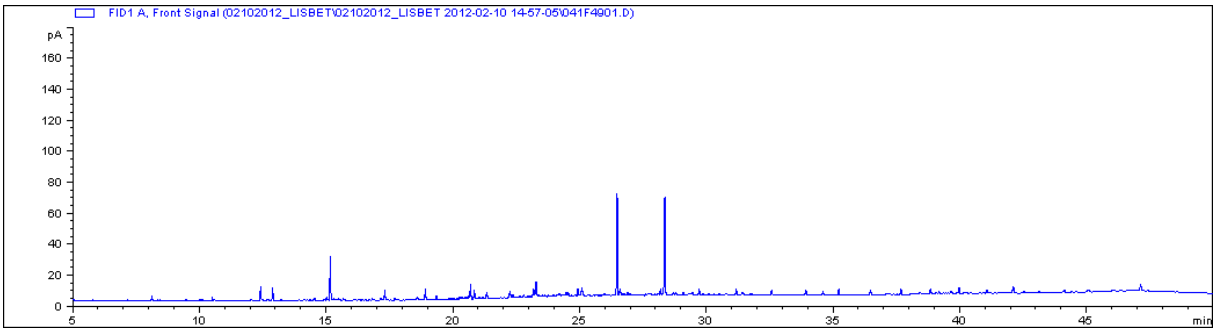

Figure F.54 - LIS014_1 Sediment

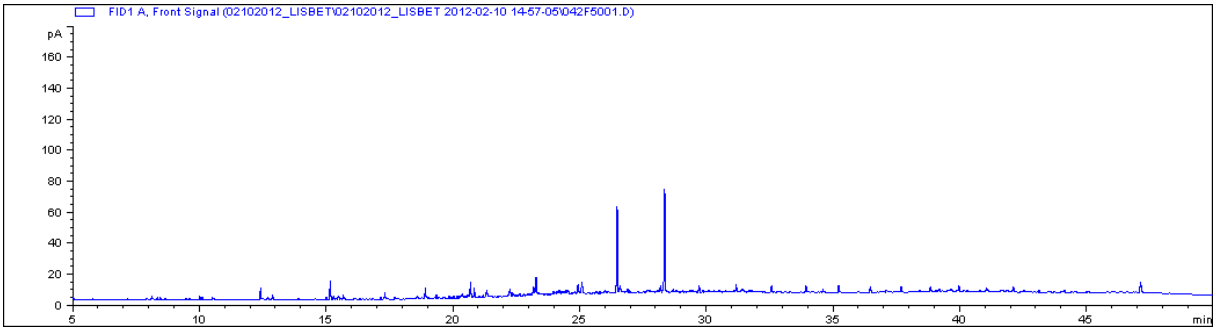

Figure F.55 - LIS014_2 Sediment

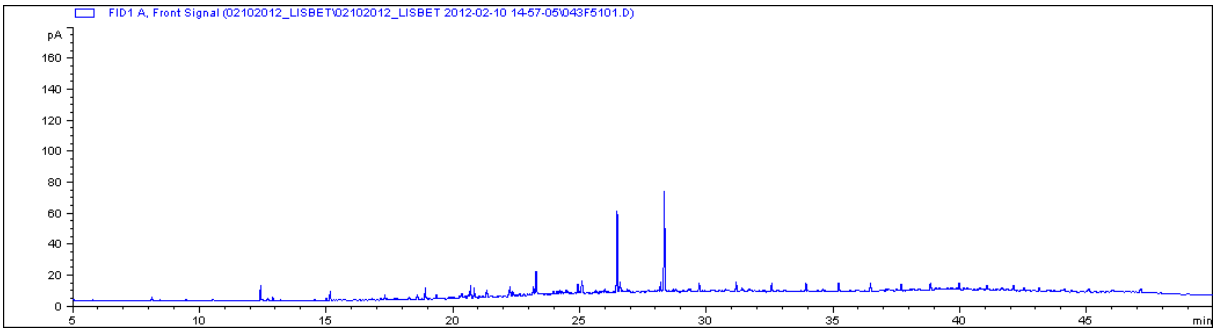

Figure F.56 - LIS014_3 Sediment

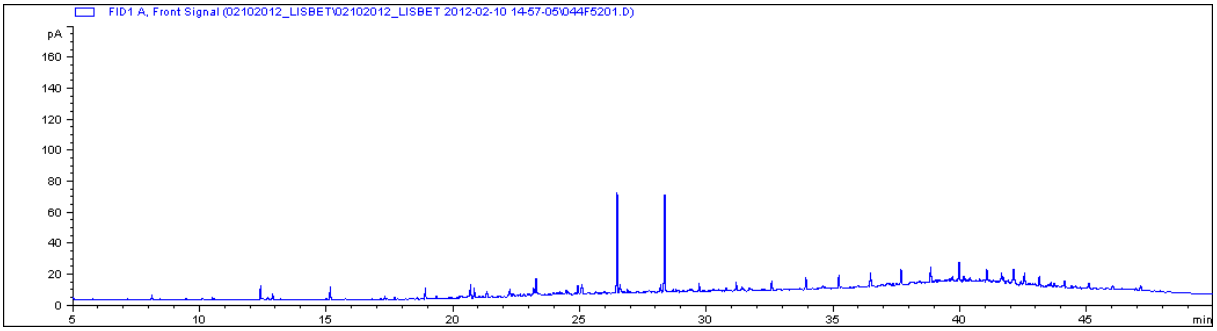

Figure F.57 - LIS014_4 Sediment

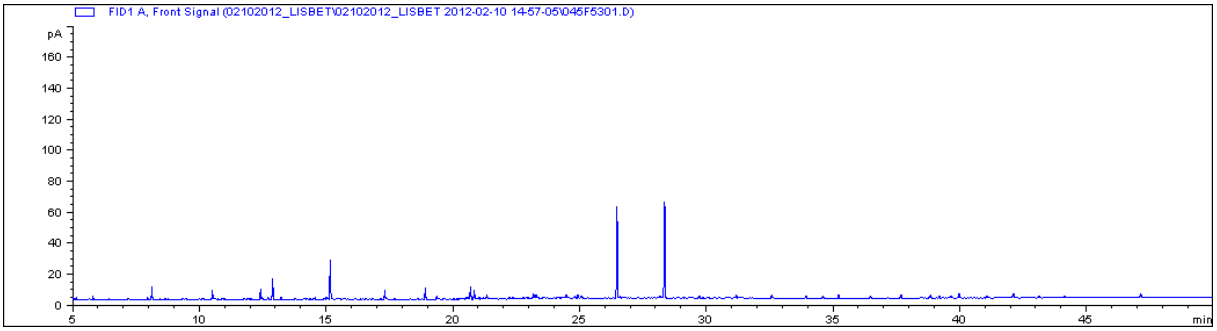

Figure F.58 - LIS015_1 Sediment

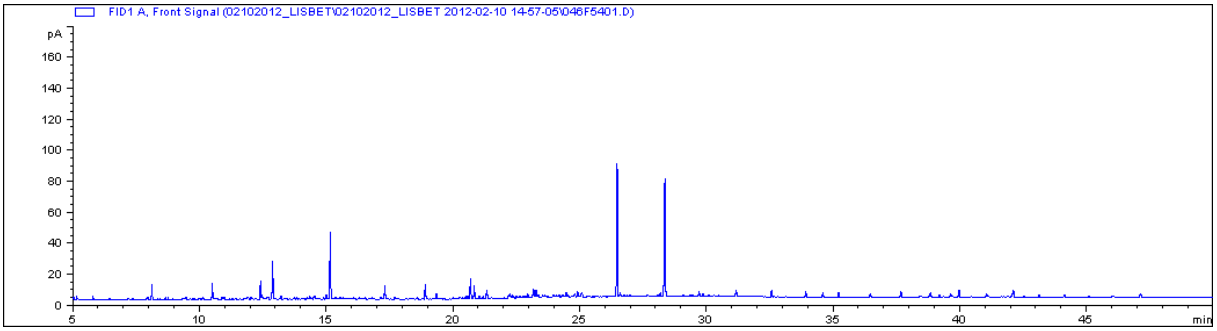

Figure F.59 - LIS015_2 Sediment

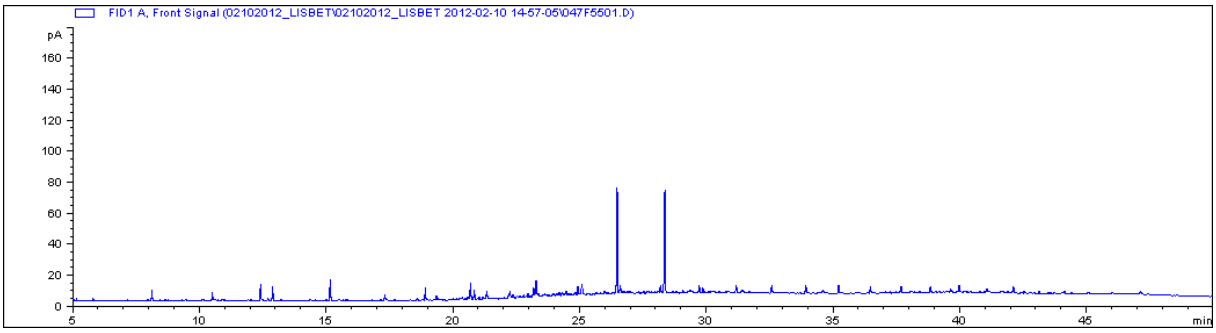

Figure F.60 - LIS015_3 Sediment

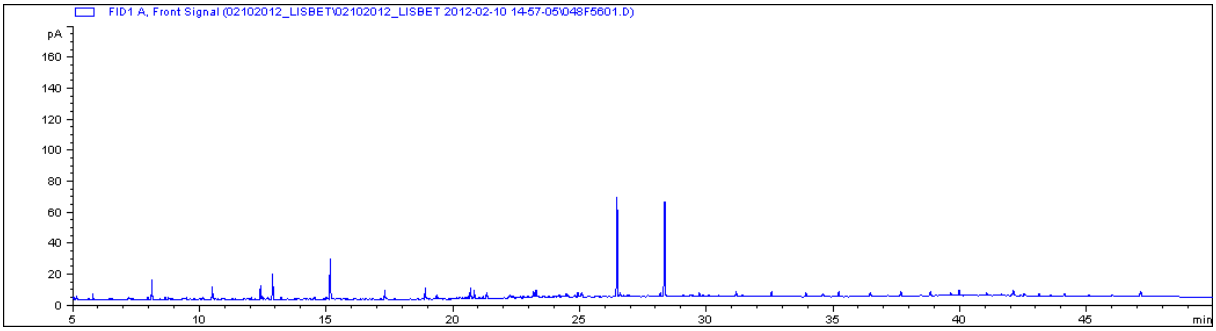

Figure F.61 - LIS015_4 Sediment

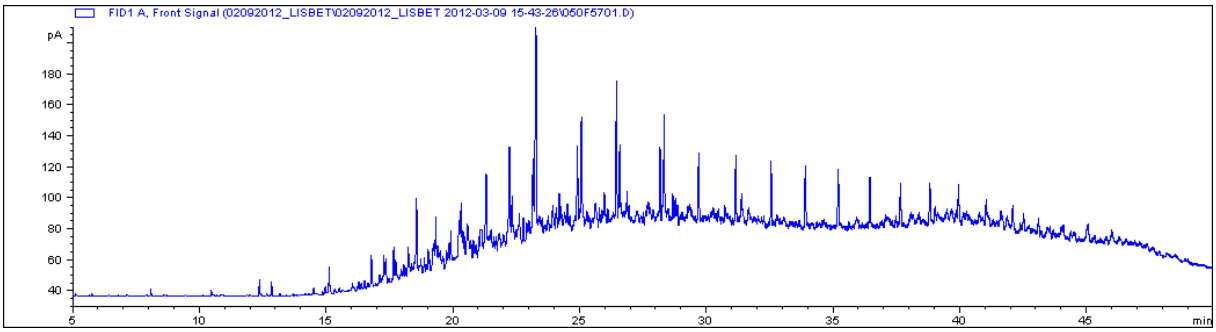

Figure F.62 - LIS016_1 Sediment

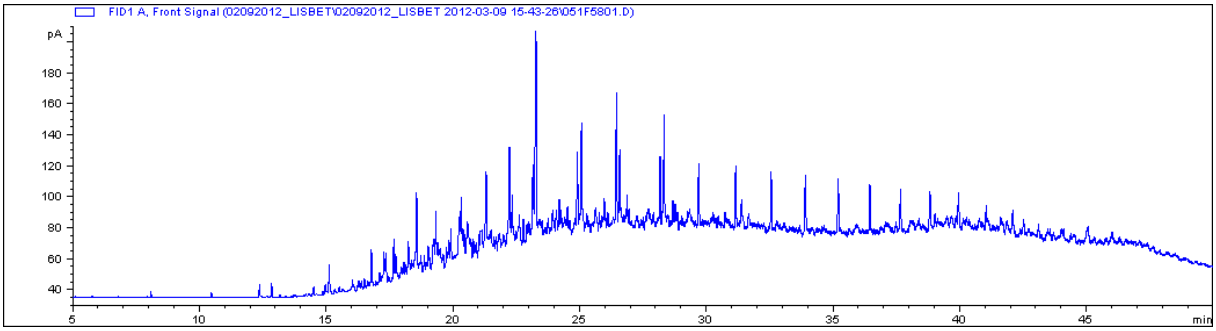

Figure F.63 - LIS016_2 Sediment

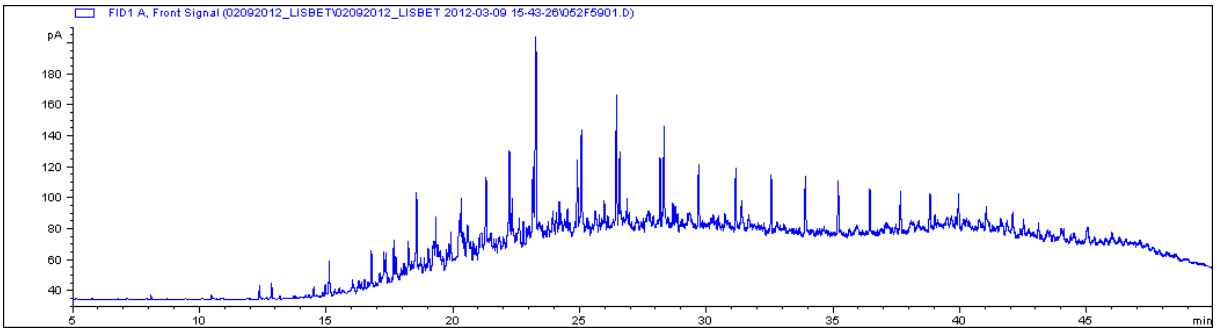

Figure F.64 - LIS016_3 Sediment

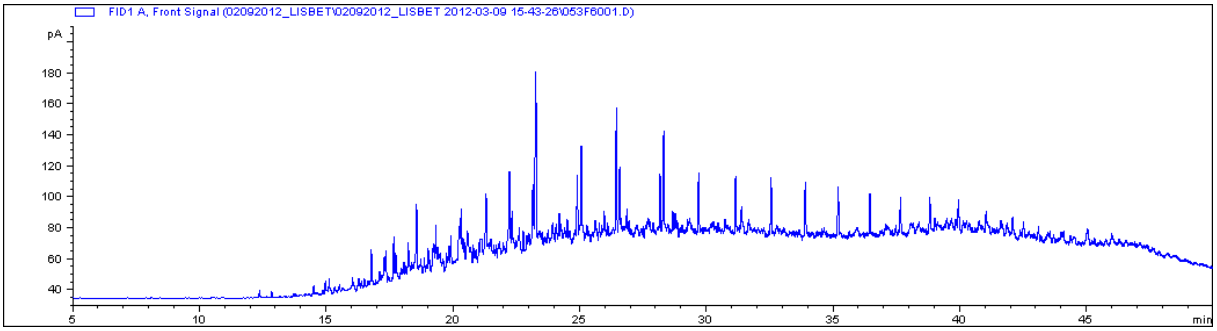

Figure F.65 - LIS016_4 Sediment

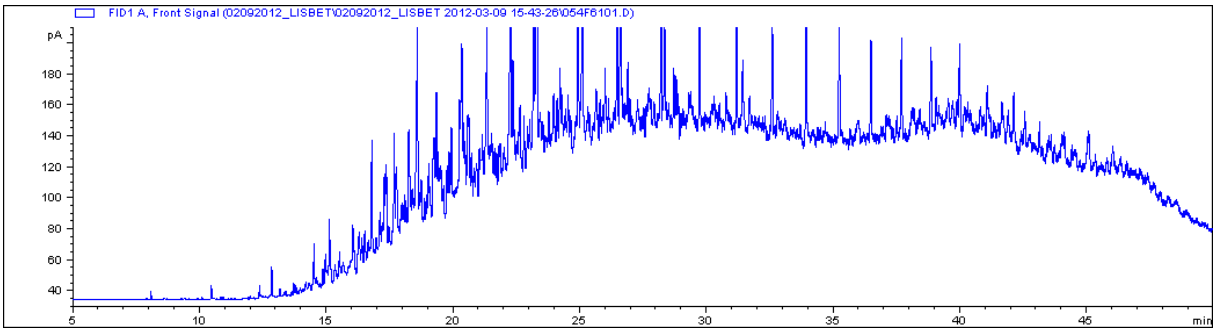

Figure F.66 - LIS017_1 Sediment

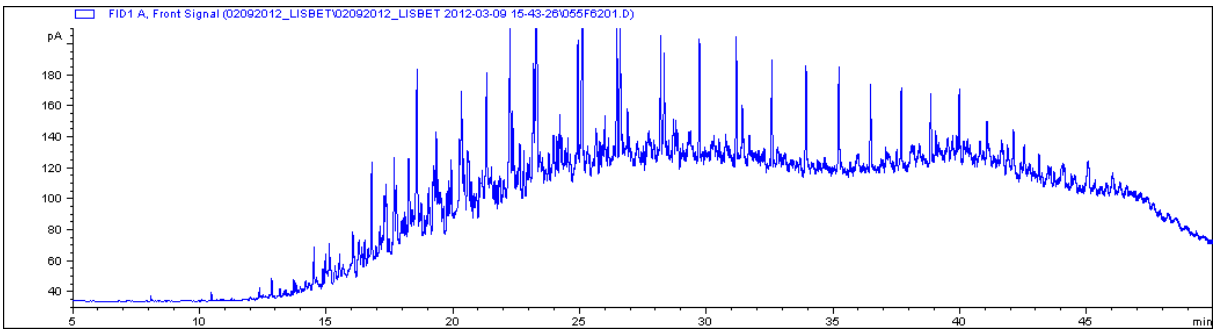

Figure F.67 - LIS017_2 Sediment

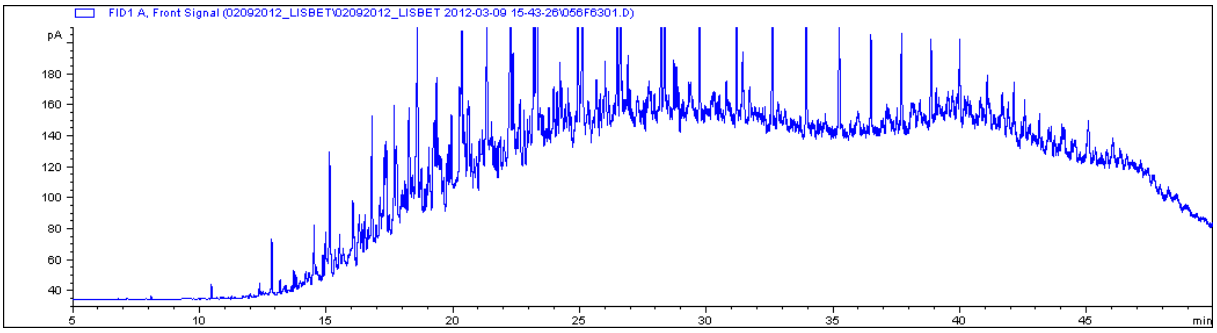

Figure F.68 - LIS017_3 Sediment

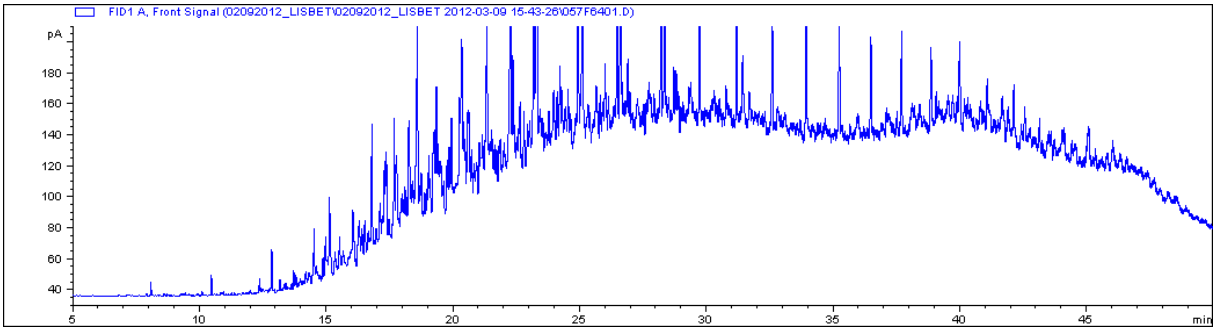

Figure F.69 - LIS017_4 Sediment

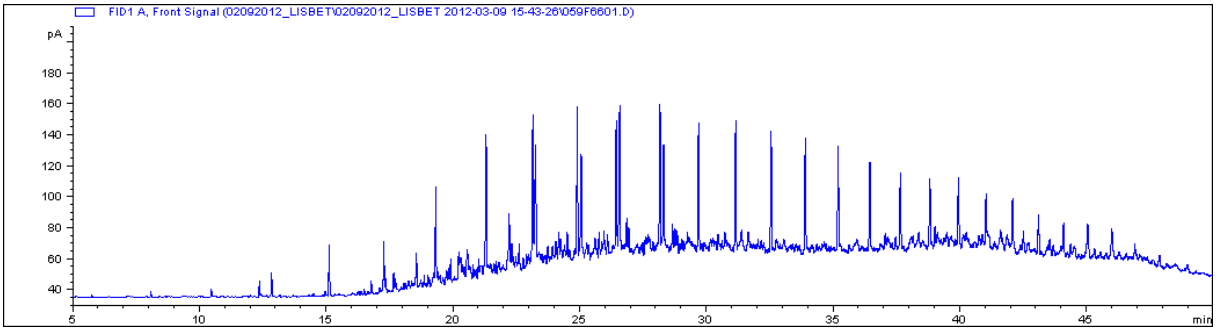

Figure F.70 - LIS018_1 Sediment

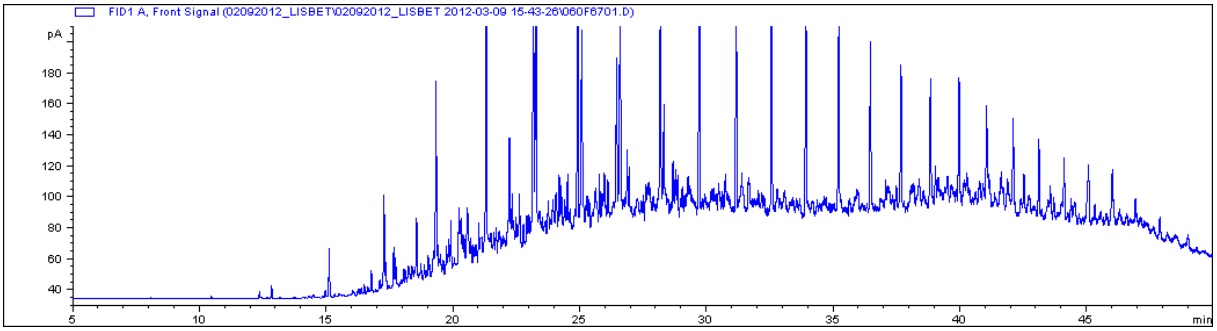

Figure F.71 - LIS018_2 Sediment

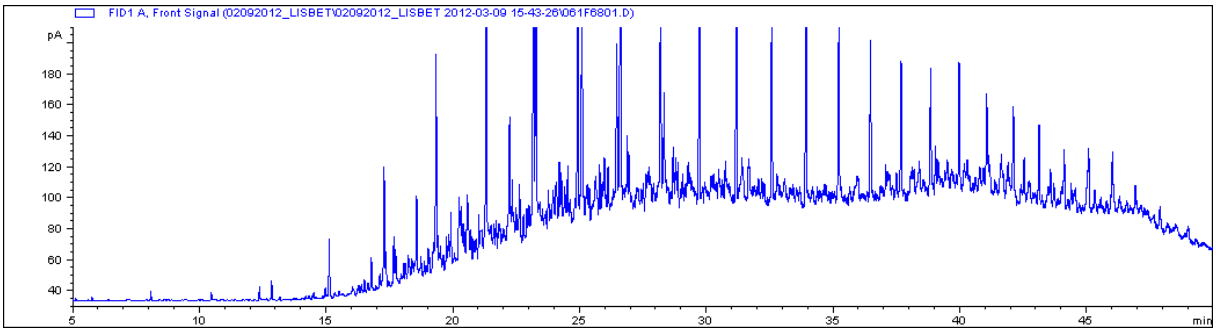

Figure F.72 - LIS018_4 Sediment

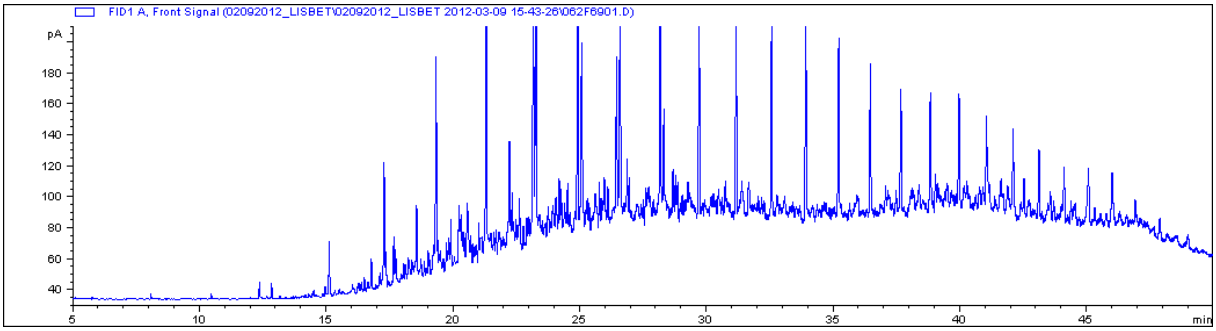

Figure F.73 - LIS018_5 Sediment

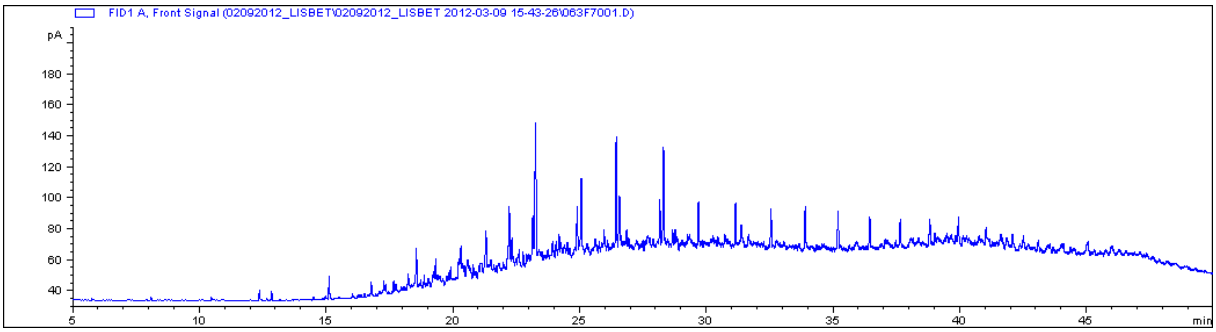

Figure F.74 - LIS019_1 Sediment

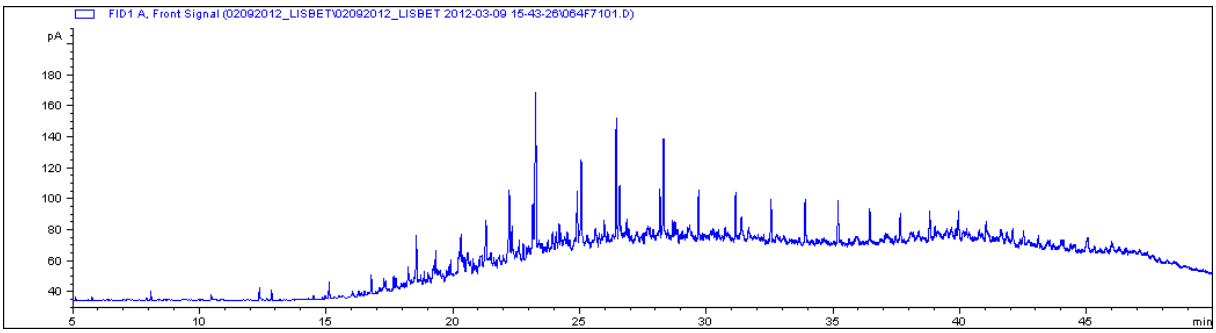

Figure F.75 - LIS019_2 Sediment

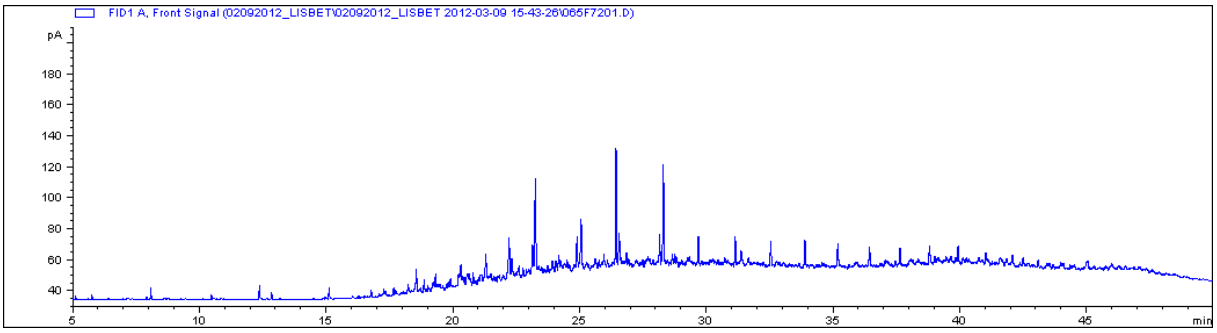

Figure F.76 - LIS019_3 Sediment

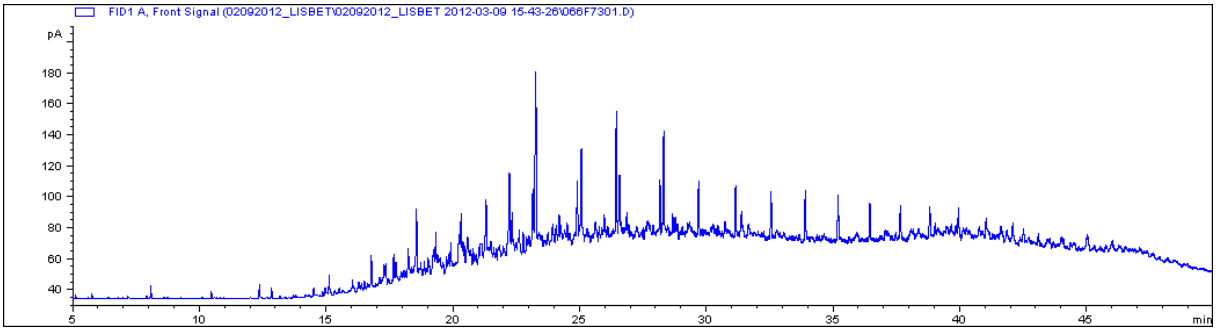

Figure F.77 -LIS019_4 Sediment

F.1.1 GC-FID Chromatograms of extracts of procedural blanks for sediment

These are the chromatograms of extracts of the sediment fraction of the three procedural blanks.

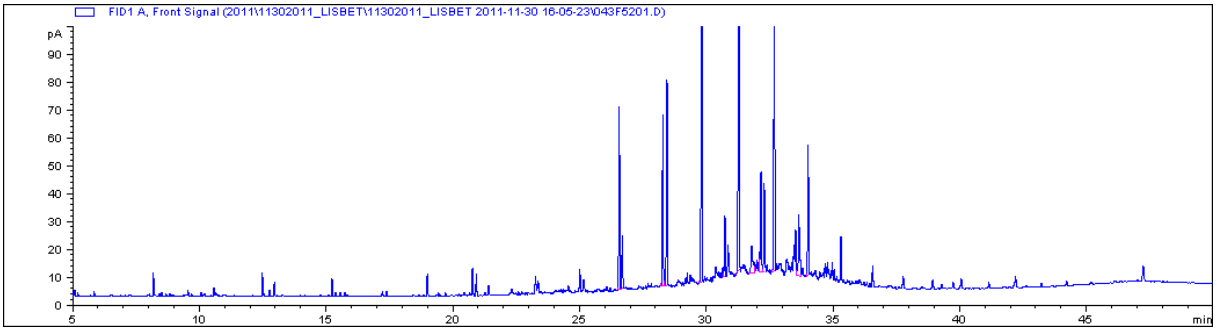

Figure F.78 - Procedural blank 1 Sediment

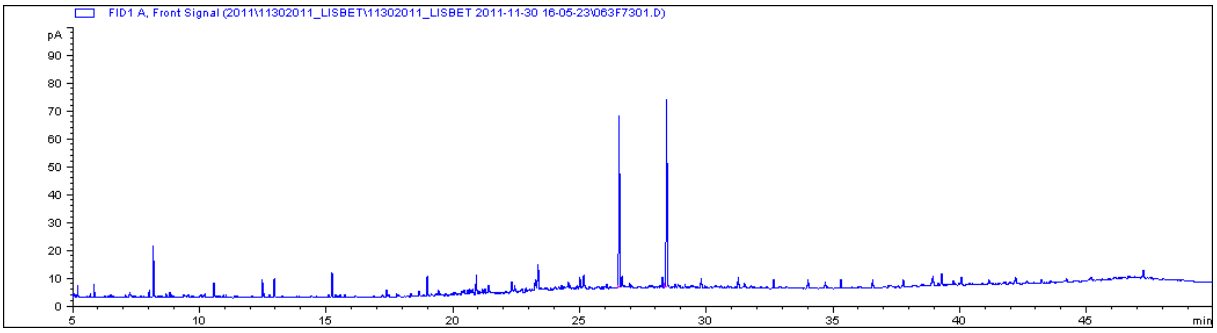

Figure F.79 - Procedural blank 2 Sediment

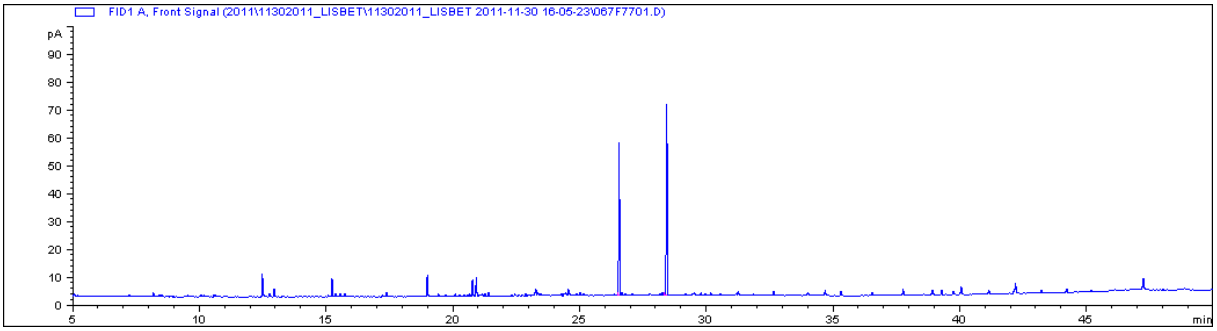

Figure F.80 - Procedural blank 3 Sediment

F.1.2 GC-FID Chromatograms of extracts of laboratory blanks for sediment

The first four chromatograms are for analysis of “blank” sediment from Grandefjæra (carbonate sand).

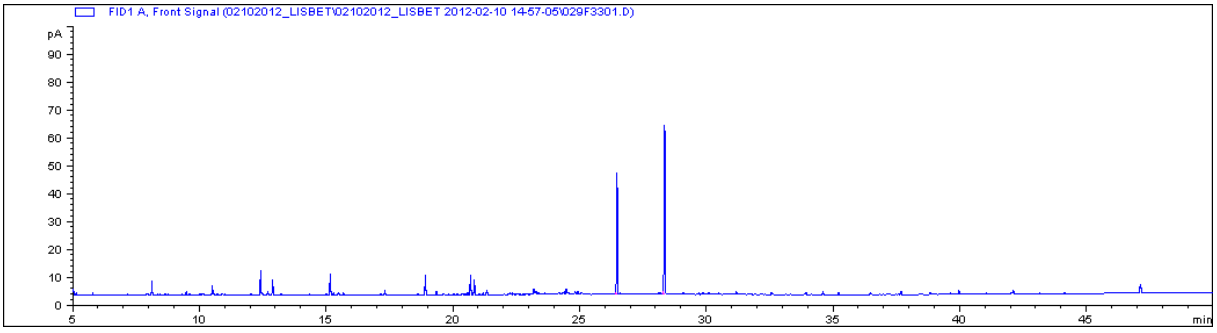

Figure F.81 - Laboratory blank 1 Sediment Grandefjæra

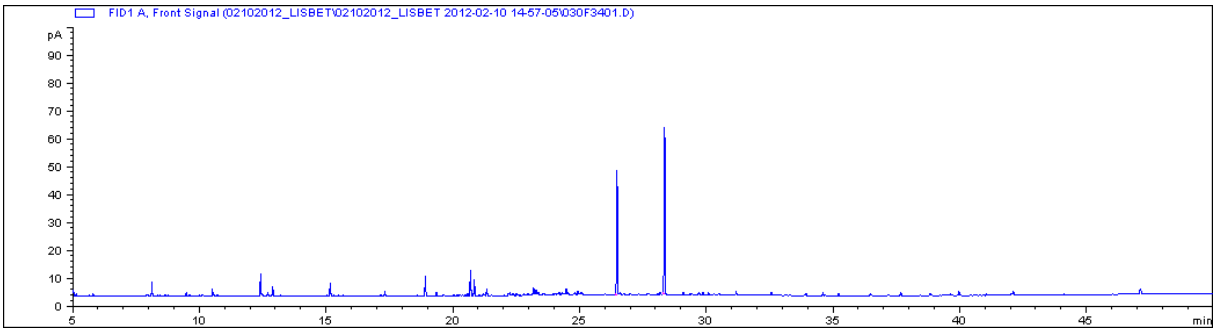

Figure F.82 - Laboratory blank 2 Sediment Grandefjæra

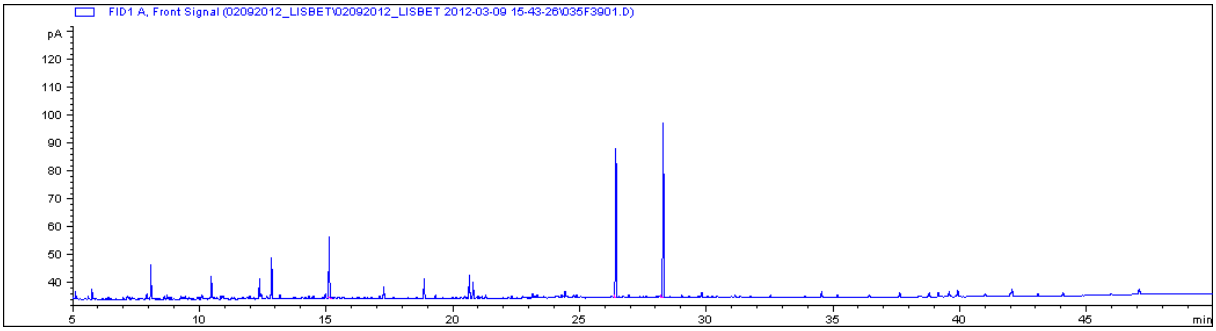

Figure F.83 - Laboratory blank 3 Sediment Grandefjæra

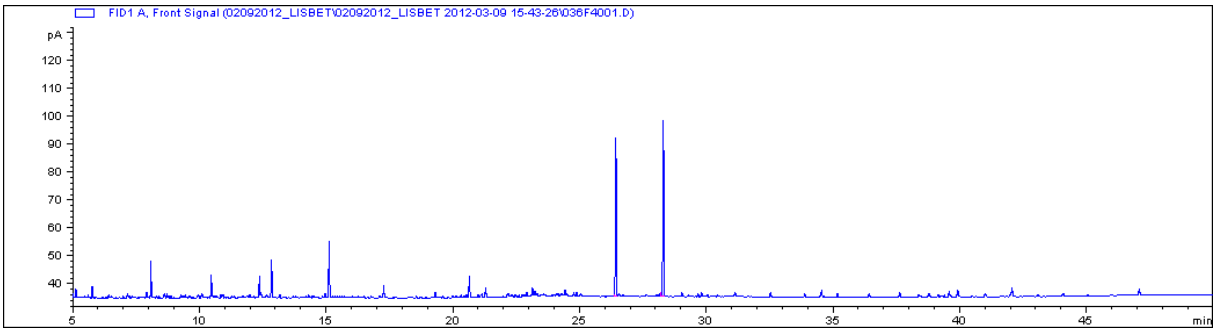

Figure F.84 - Laboratory blank 4 Sediment Grandefjæra

The following three chromatograms are for analysis of “blank” sediment from Buvika (clay).

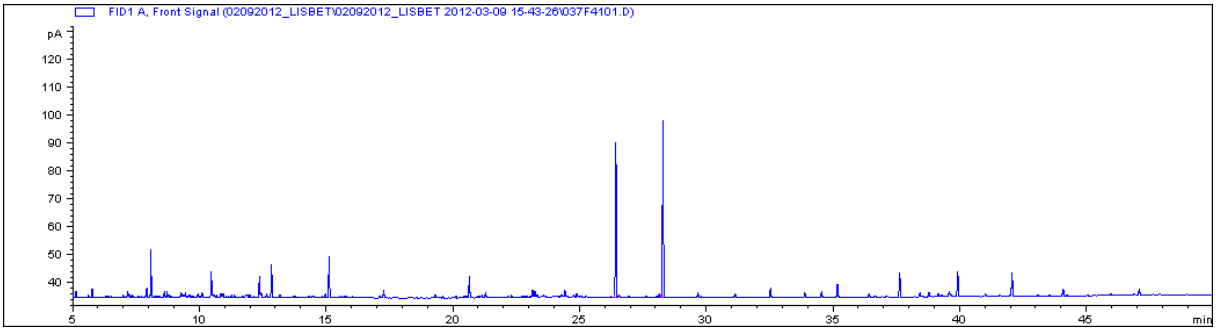

Figure F.85 - Laboratory blank 5 Sediment Buvika

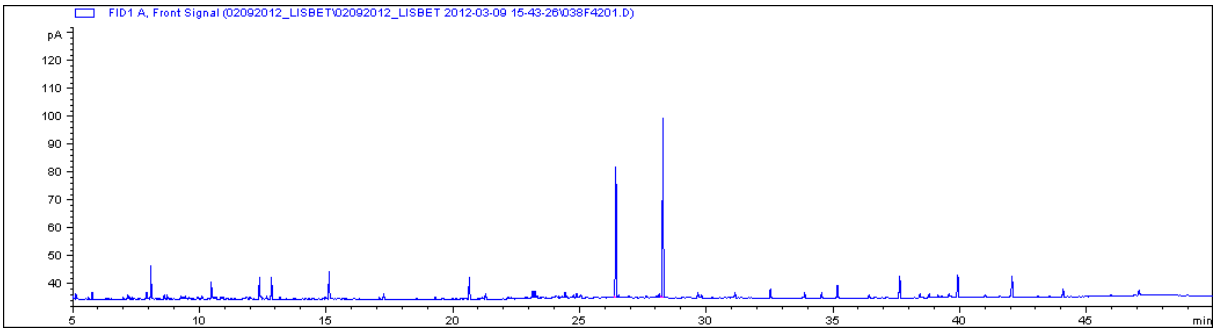

Figure F.86 - Laboratory blank 6 Sediment Buvika

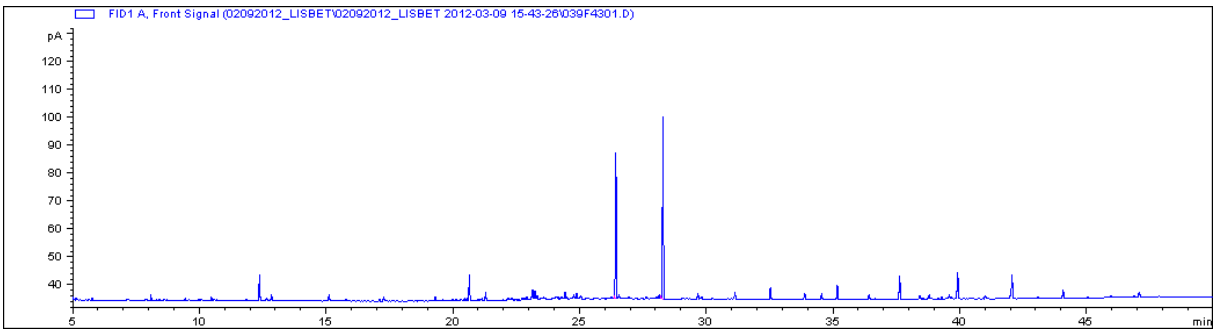

Figure F.87 - Laboratory blank 7 Sediment Buvika

The following three chromatograms are for analysis of “blank” sediment from Ranheim (sand).

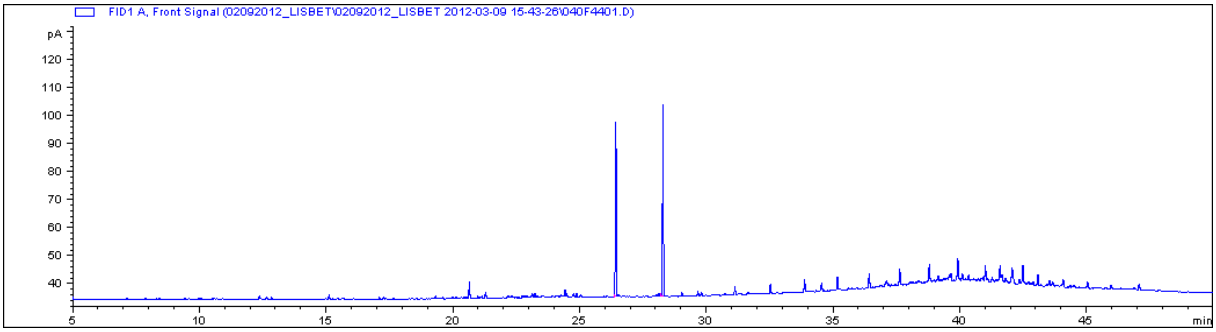

Figure F.88 - Laboratory blank 8 Sediment Ranheim

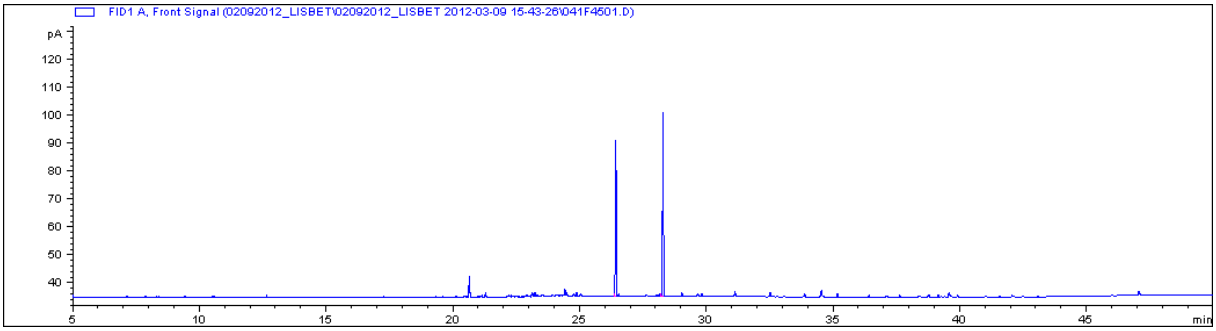

Figure F.89 - Laboratory blank 9 Sediment Ranheim

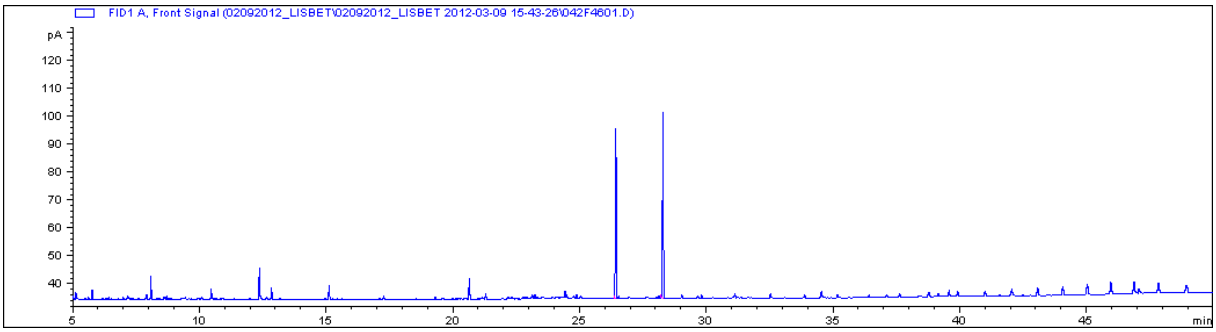

Figure F.90 - Laboratory blank 10 Sediment Ranheim

F.2 GC-FID Chromatograms of water extracts

The following will present the chromatograms for all samples of water extracts.

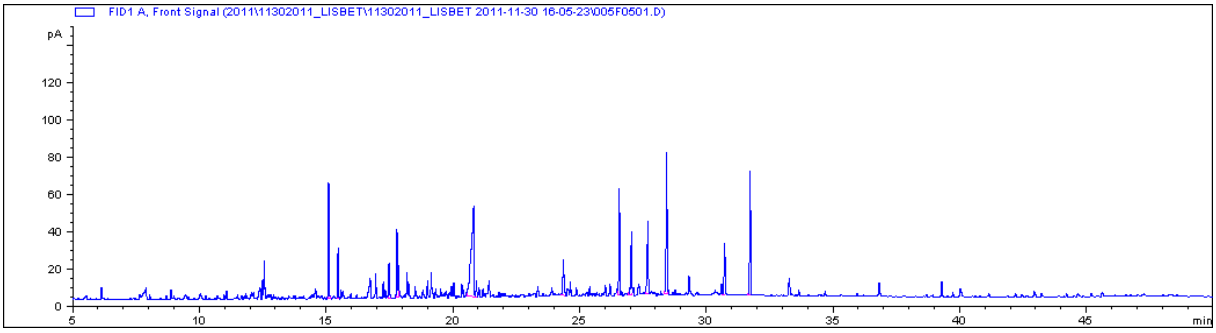

Figure F.91 - LIS001_1 Water

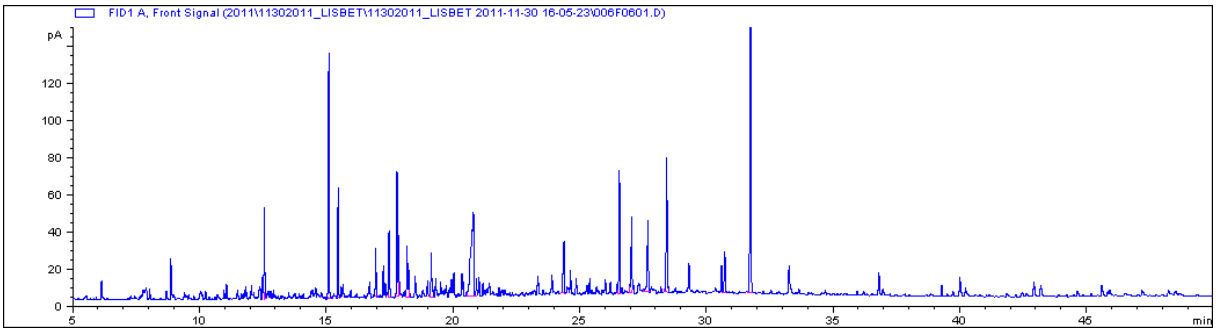

Figure F.92 - LIS001_2 Water

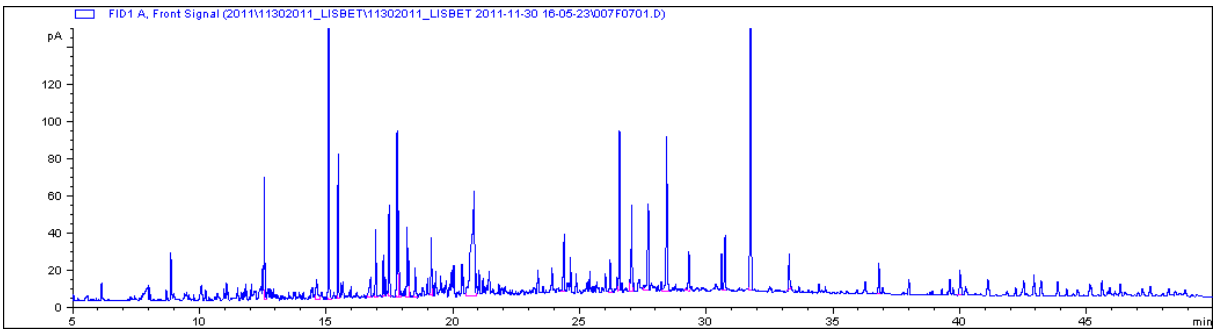

Figure F.93 - LIS001_3 Water

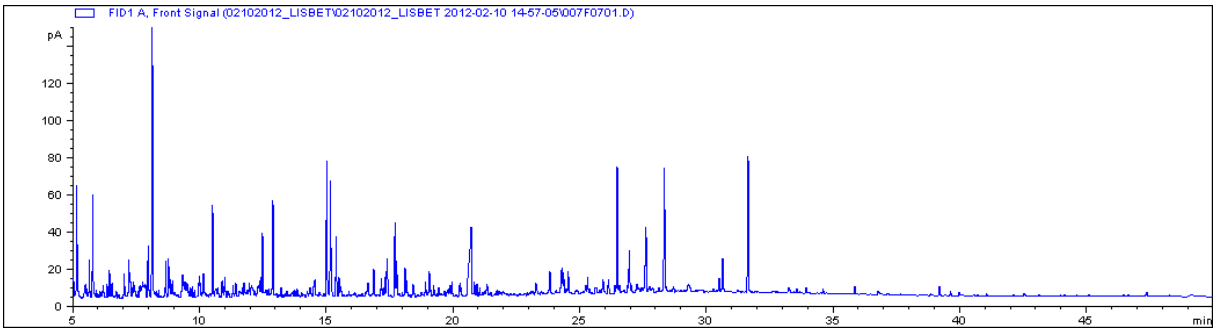

Figure F.94 - LIS001_4 Water

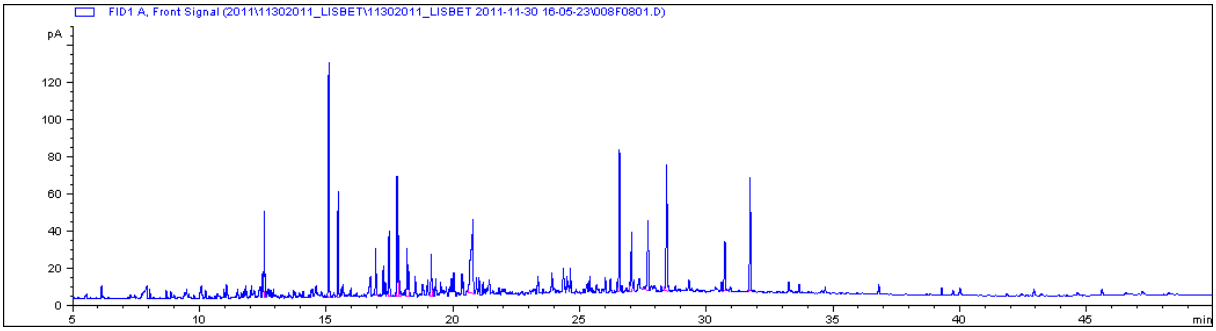

Figure F.95 - LIS002_1 Water

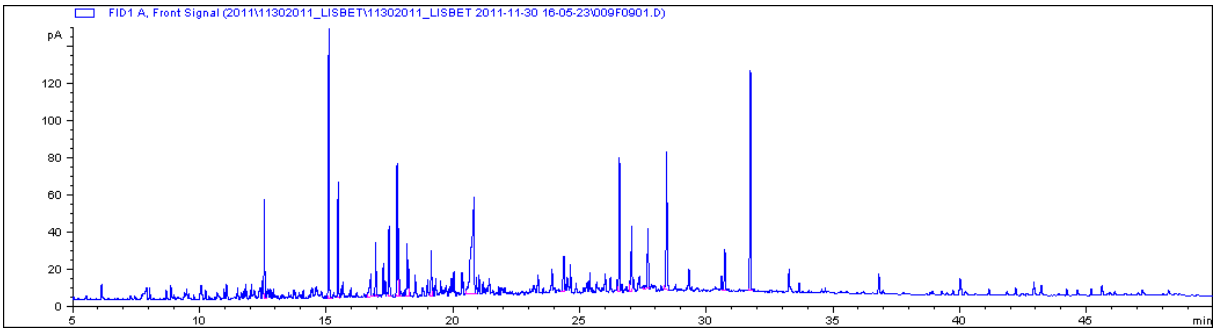

Figure F.96 - LIS002_2 Water

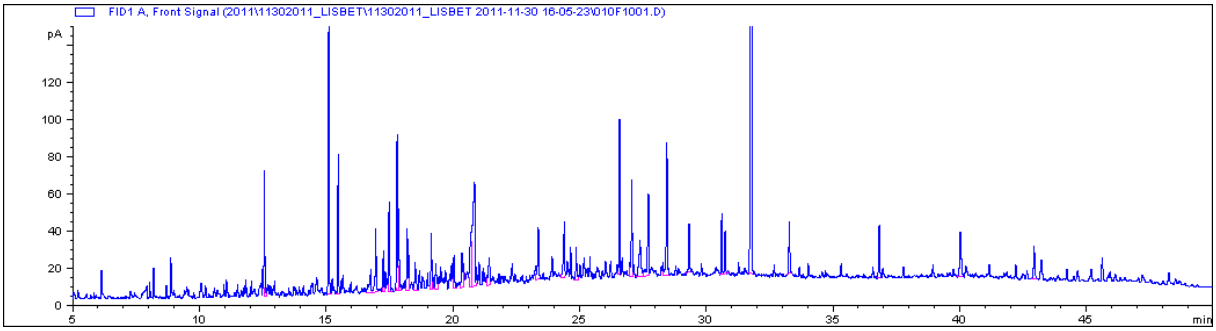

Figure F.97 - LIS002_3 Water

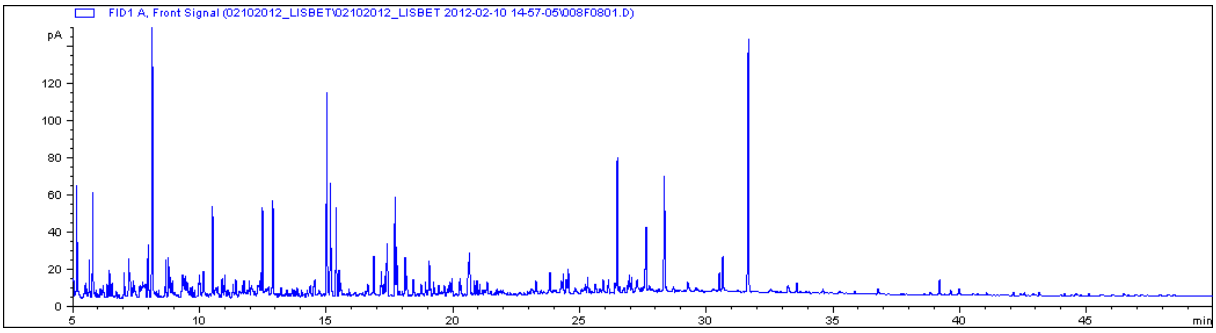

Figure F.98 - LIS002_4 Water

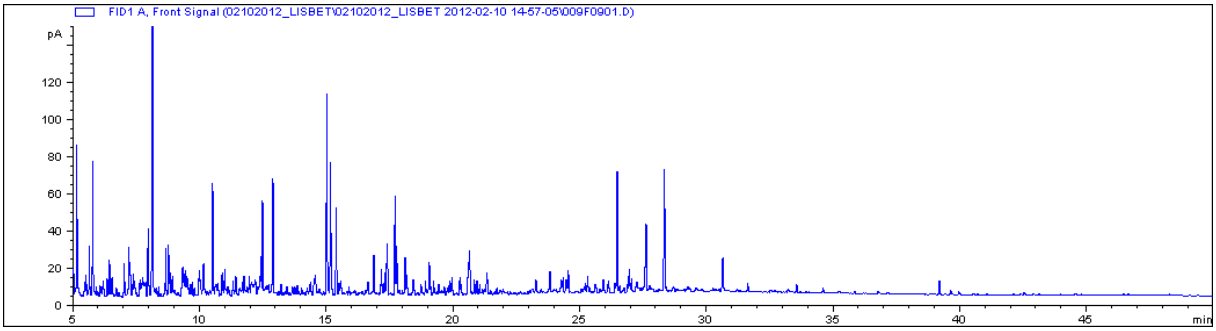

Figure F.99 - LIS002_5 Water

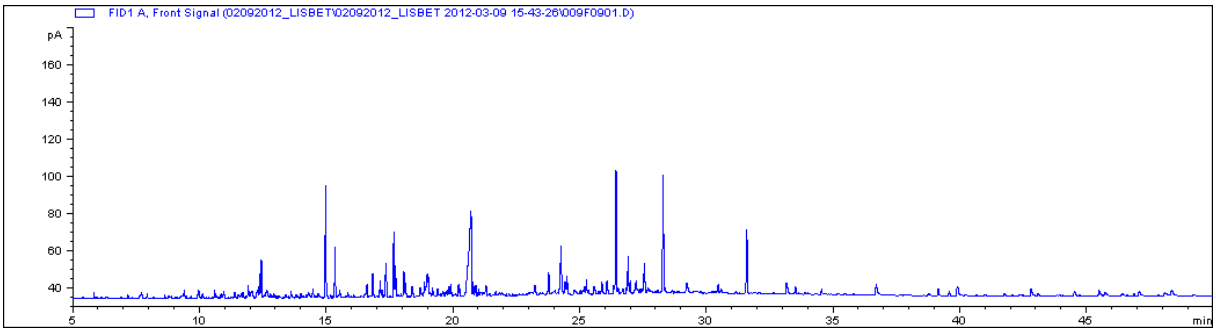

Figure F.100 - LIS002_6 Water

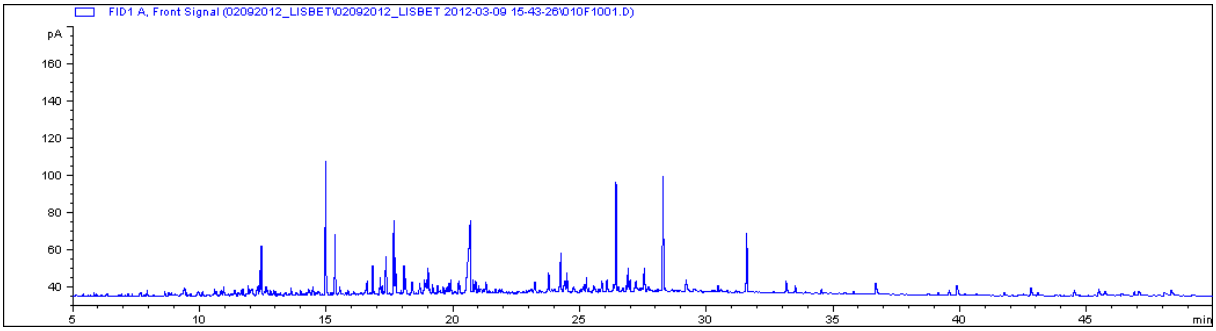

Figure F.101 - LIS002_7 Water

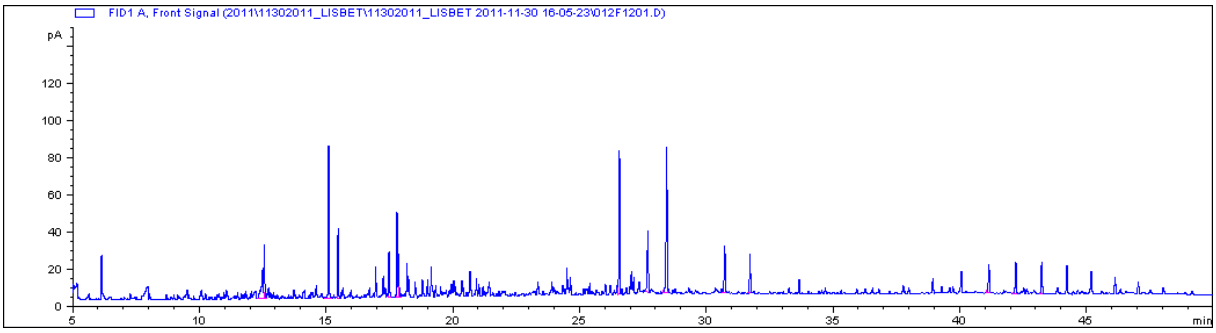

Figure F.102 - LIS003_1 Water

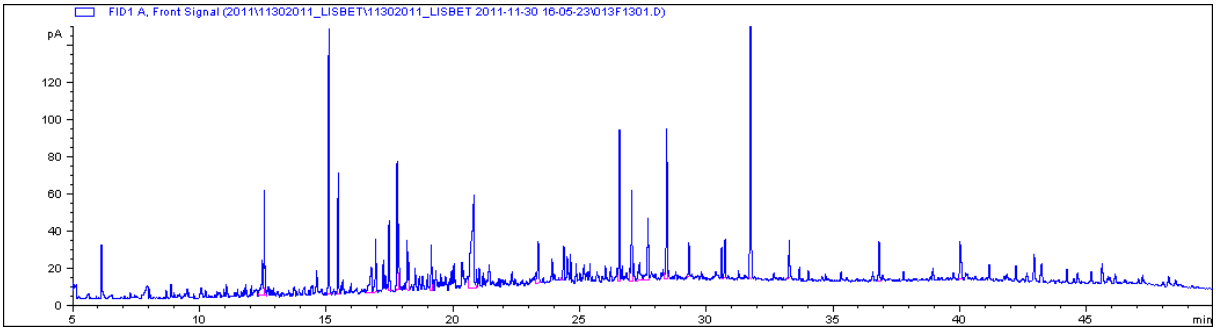

Figure F.103 - LIS003_2 Water

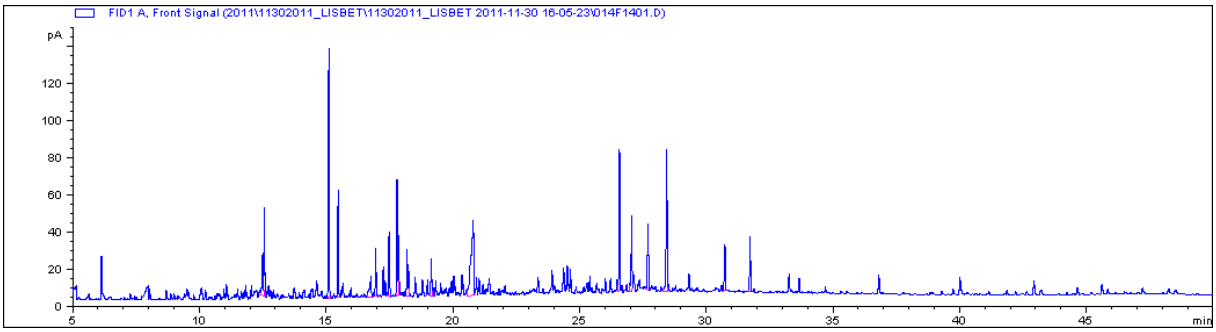

Figure F.104 - LIS003_3 Water

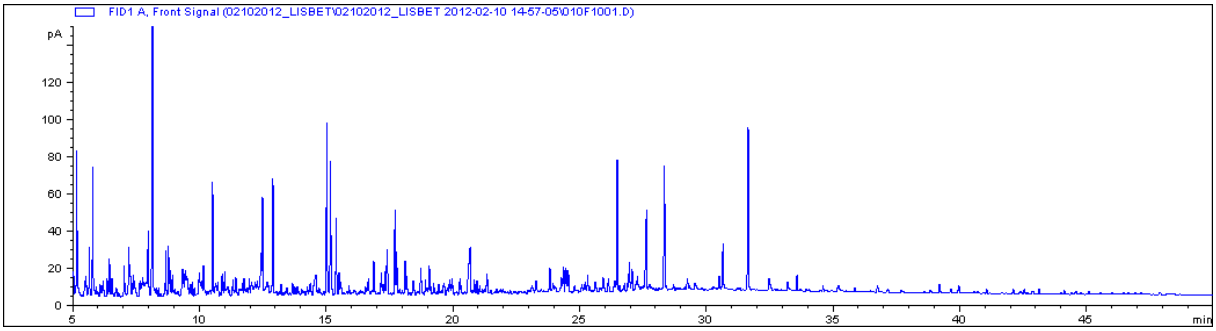

Figure F.105 - LIS003_4 Water

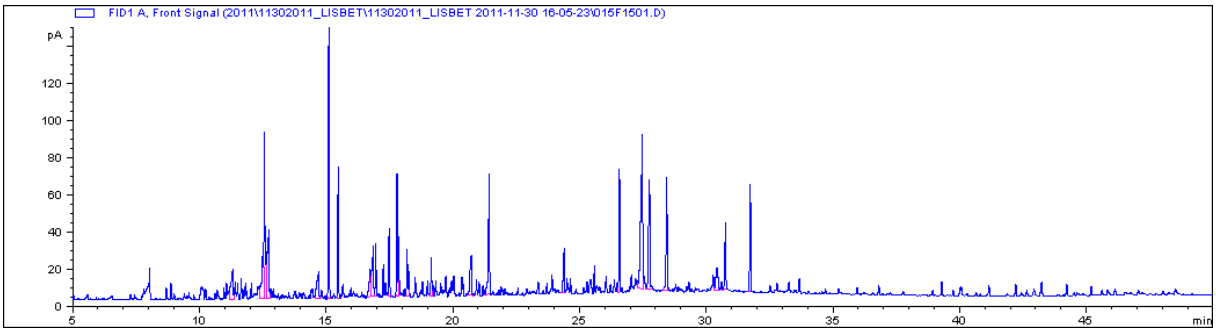

Figure F.106 - LIS006_1 Water

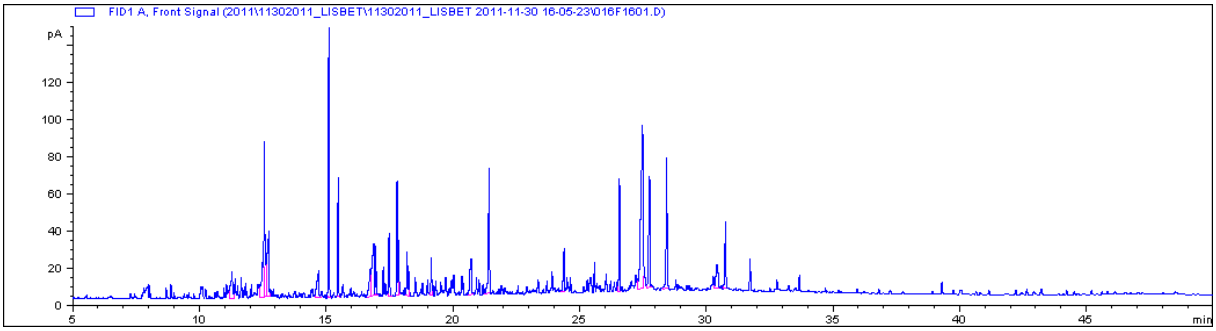

Figure F.107 - LIS006_2 Water

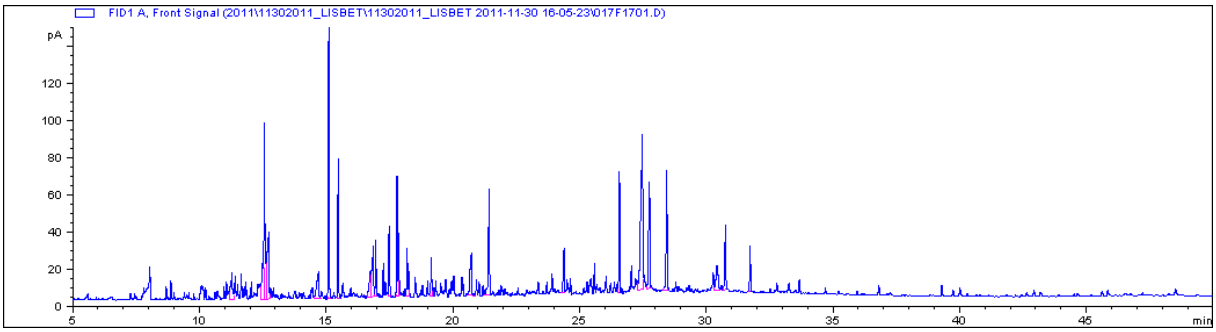

Figure F.108 - LIS006_3 Water

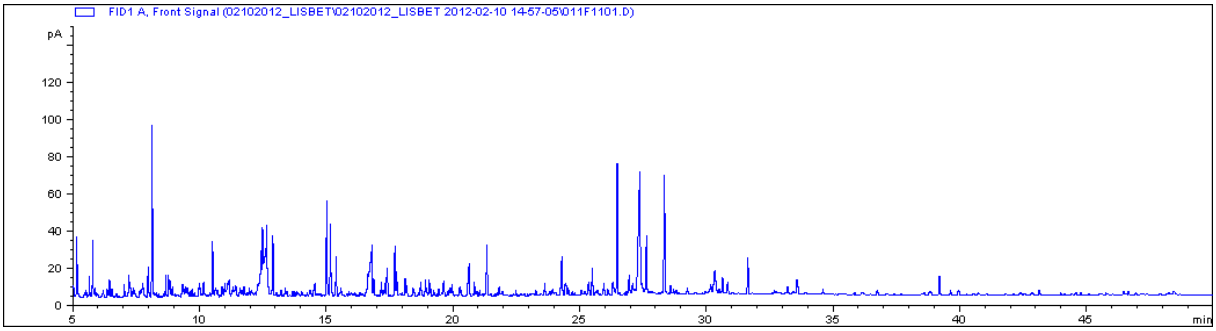

Figure F.109 - LIS006_6 Water

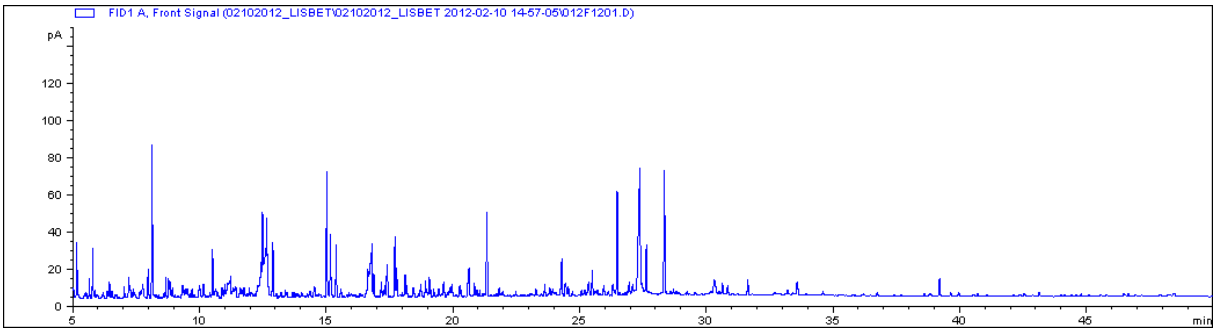

Figure F.110 - LIS006_7 Water

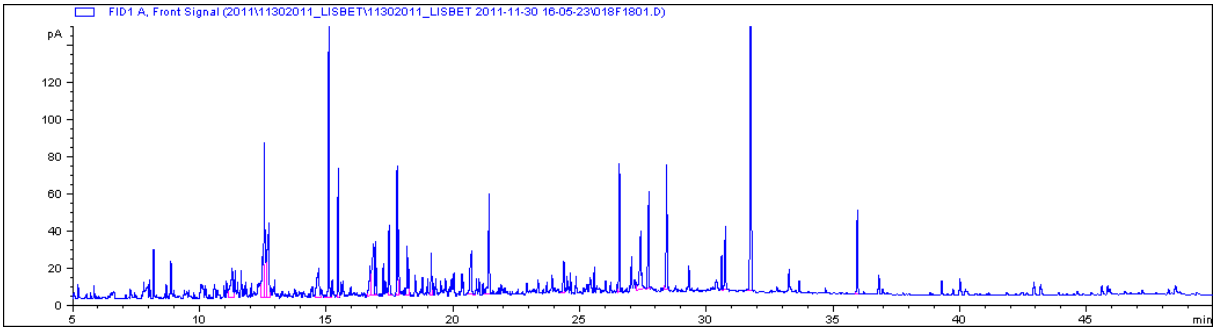

Figure F.111 - LIS007_1 Water

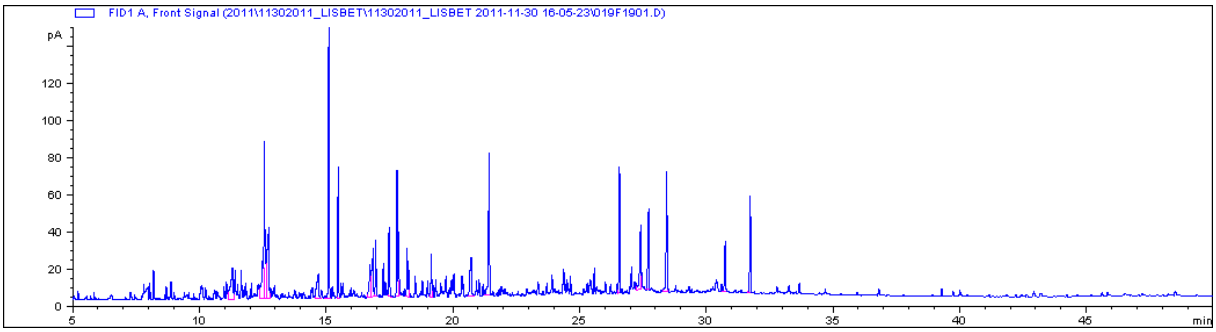

Figure F.112 - LIS007_2 Water

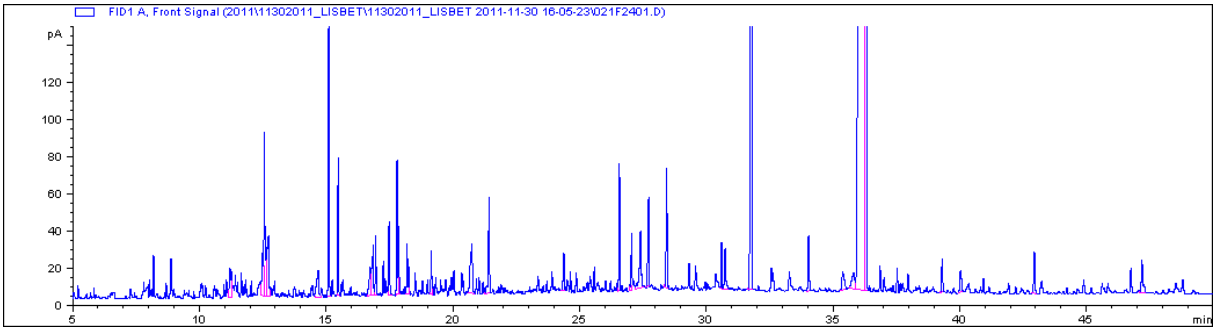

Figure F.113 - LIS007_3 Water

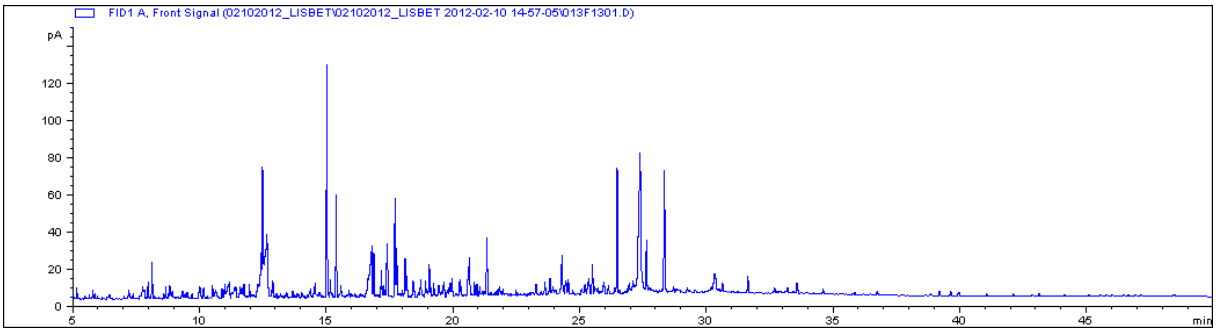

Figure F.114 - LIS007_4 Water

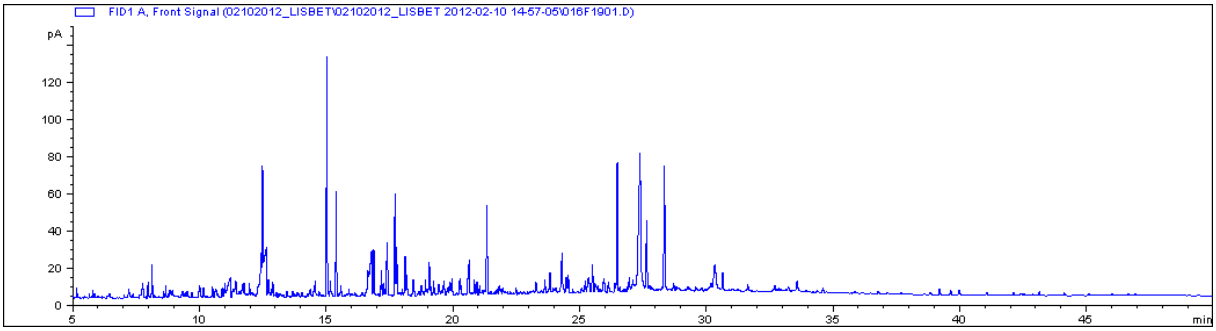

Figure F.115 - LIS007_5 Water

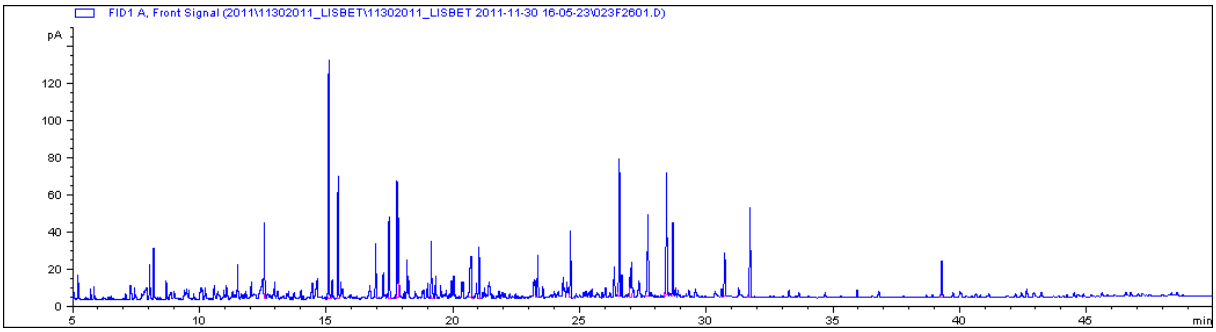

Figure F.116 - LIS008_1 Water

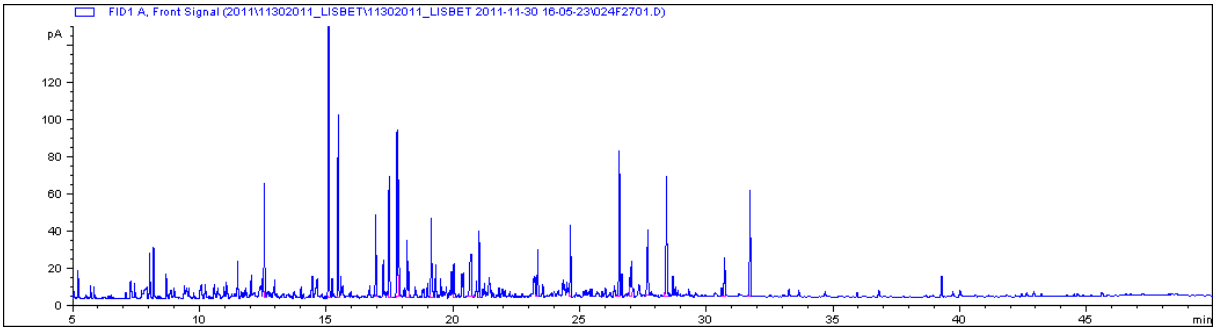

Figure F.117 - LIS008_2 Water

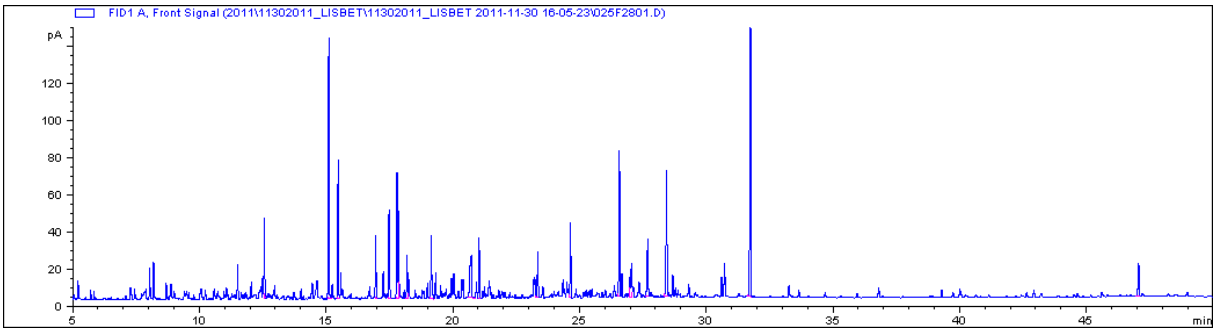

Figure F.118 - LIS008_3 Water

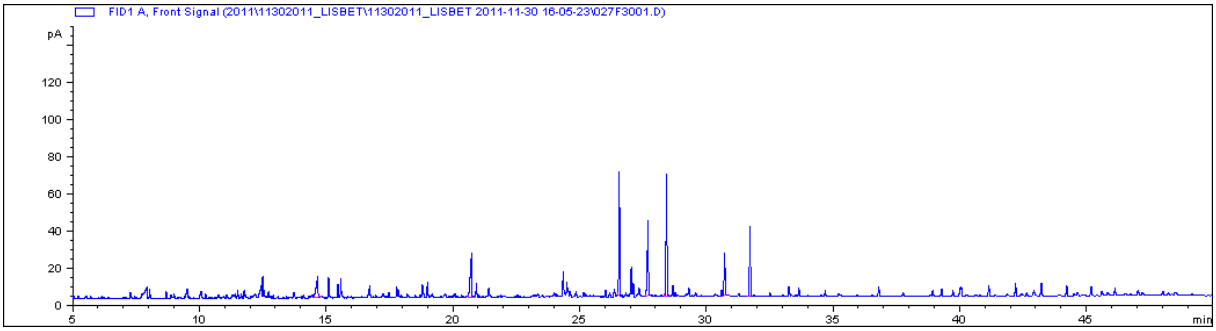

Figure F.119 - LIS009_1 Water

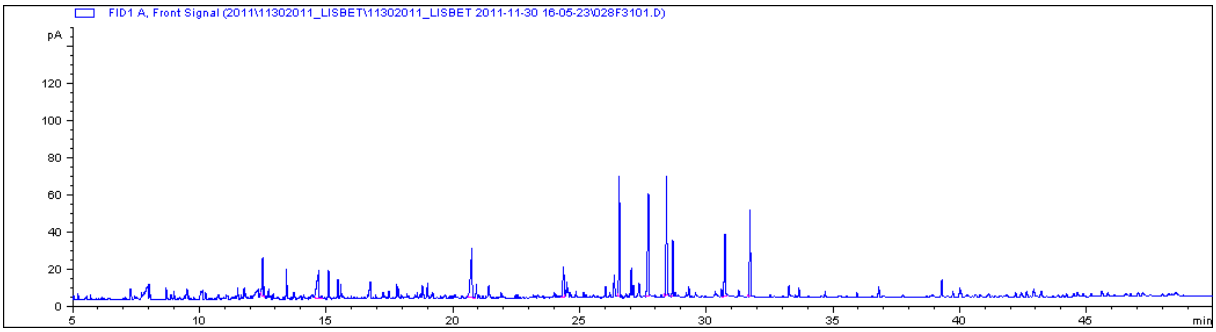

Figure F.120 - LIS009_2 Water

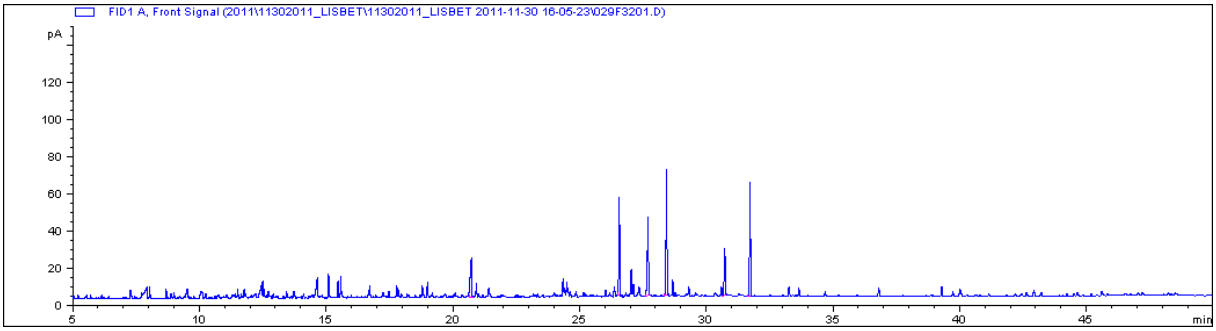

Figure F.121 - LIS009_3 Water

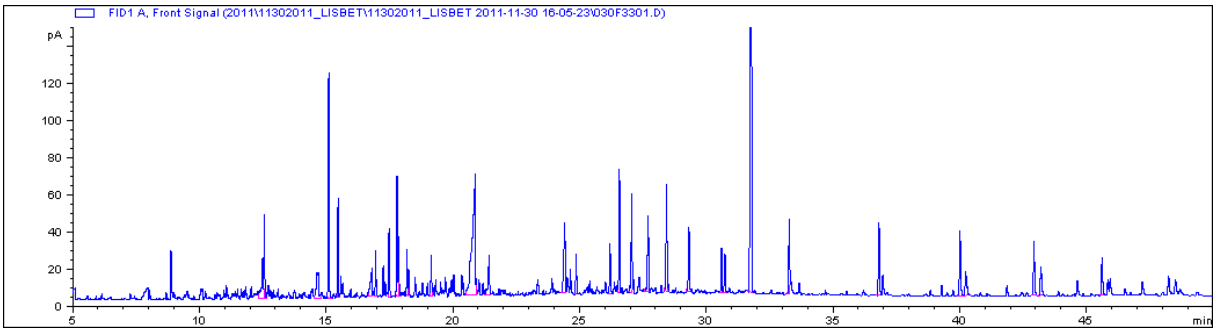

Figure F.122 - LIS010_1 Water

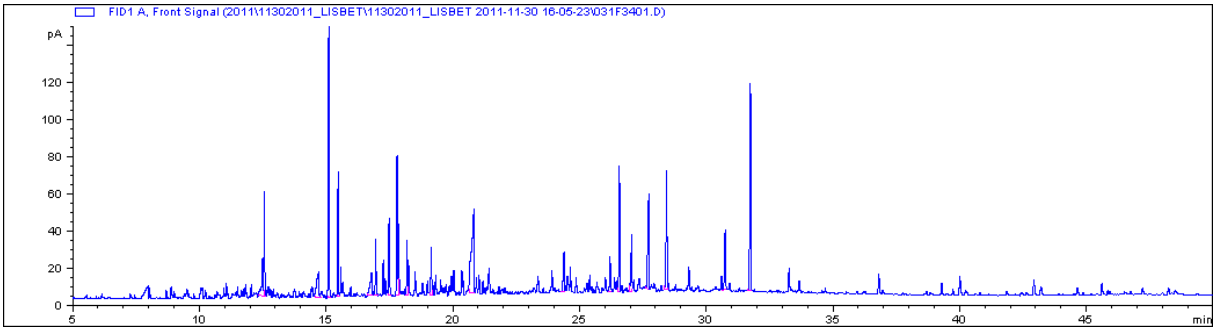

Figure F.123 - LIS010_2 Water

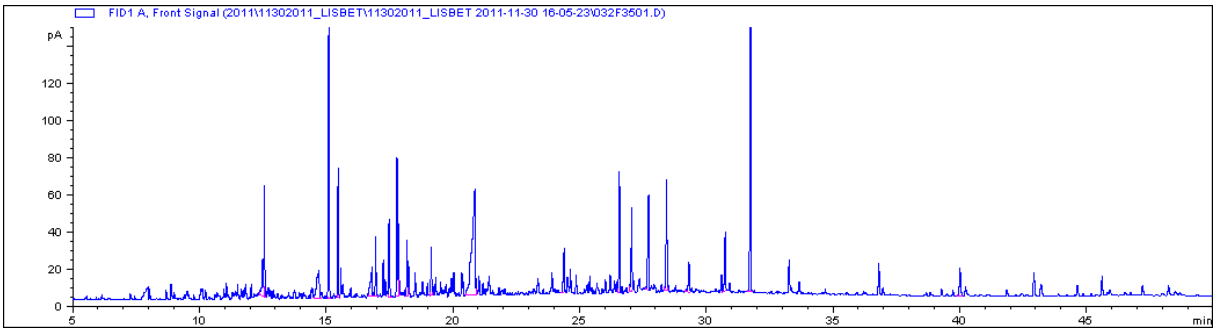

Figure F.124 - LIS010_3 Water

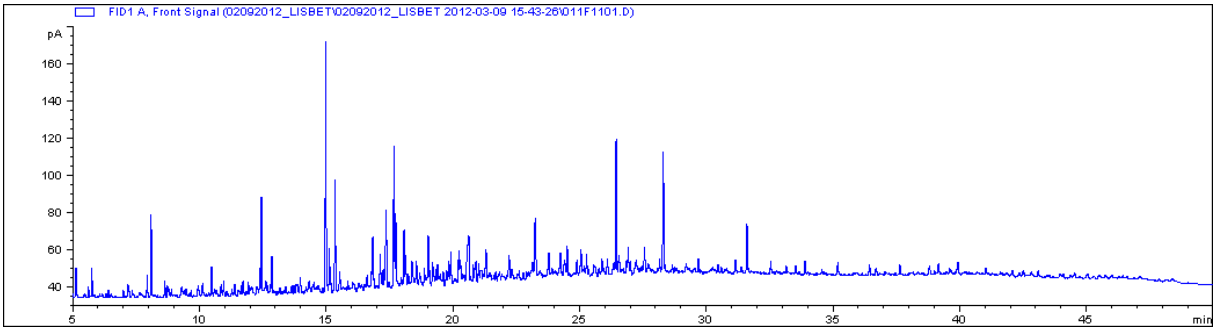

Figure F.125 - LIS010_4 Water

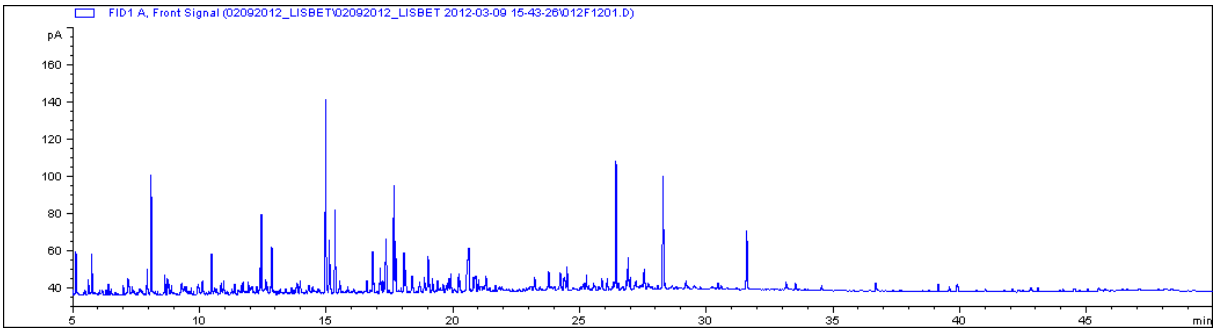

Figure F.126 - LIS010_5 Water

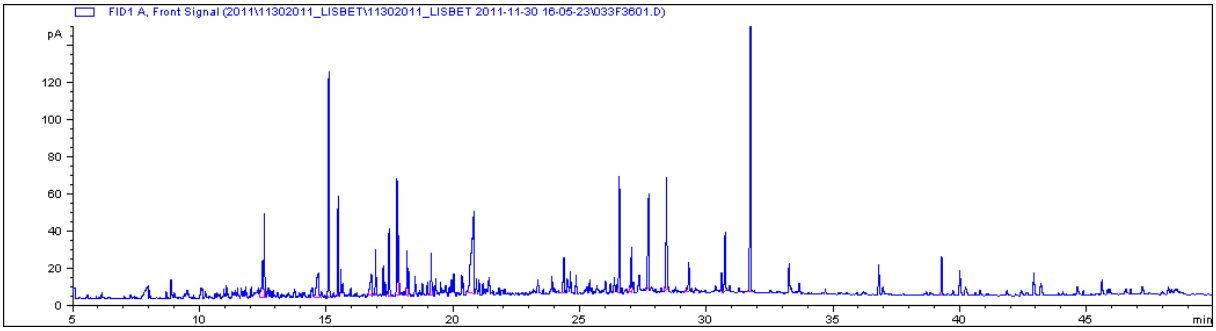

Figure F.127 - LIS011_1 Water

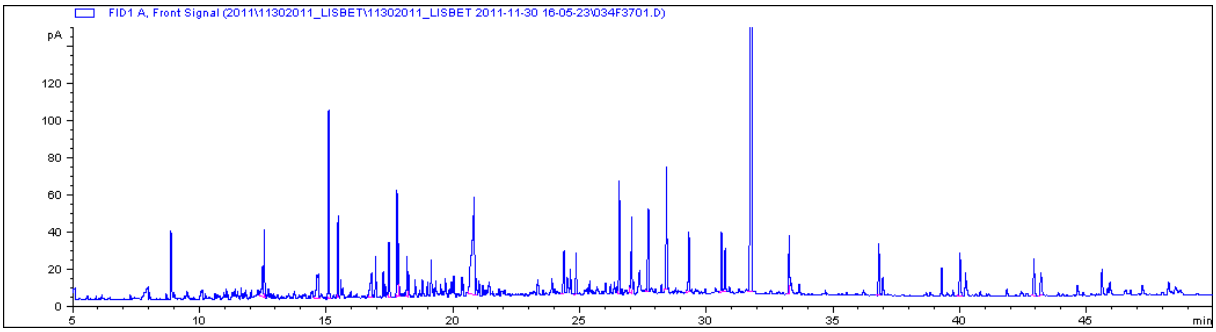

Figure F.128 - LIS011_2 Water

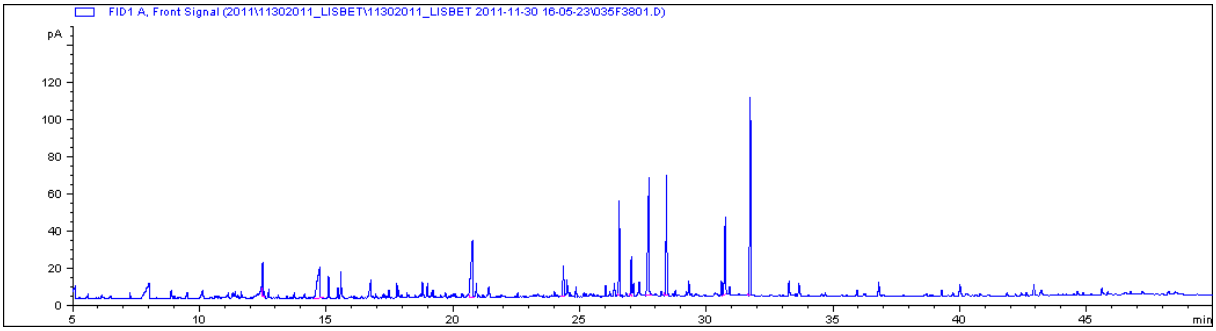

Figure F.129 - LIS011_3 Water

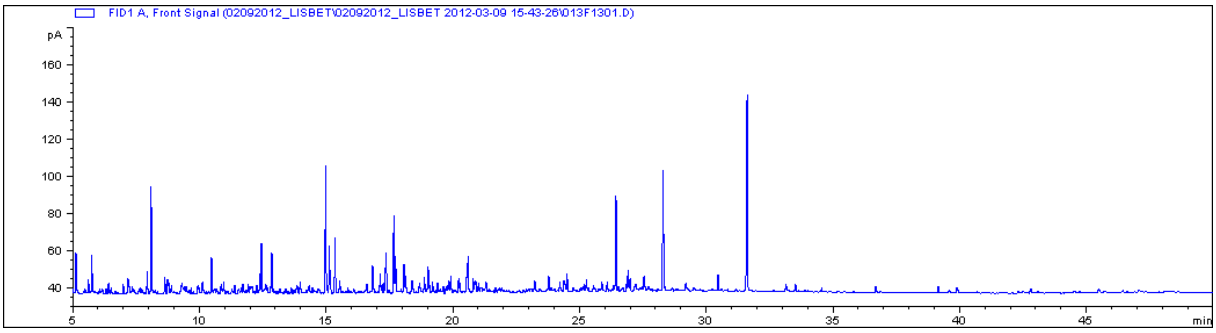

Figure F.130 - LIS011_4 Water

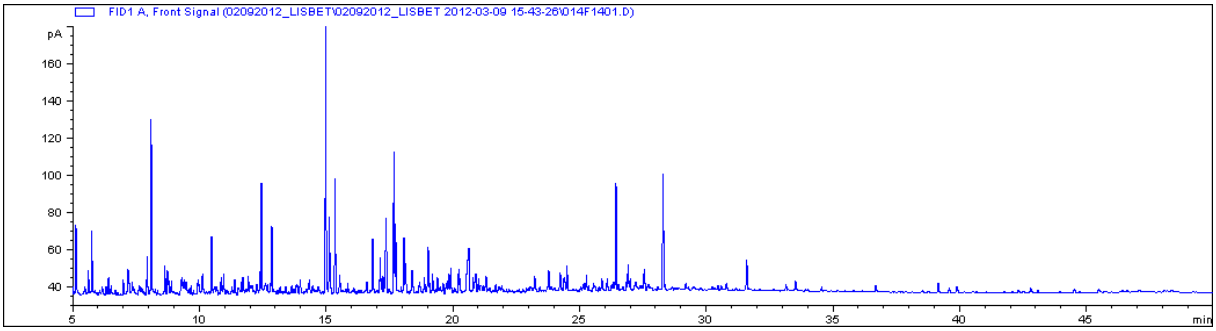

Figure F.131 - LIS011_5 Water

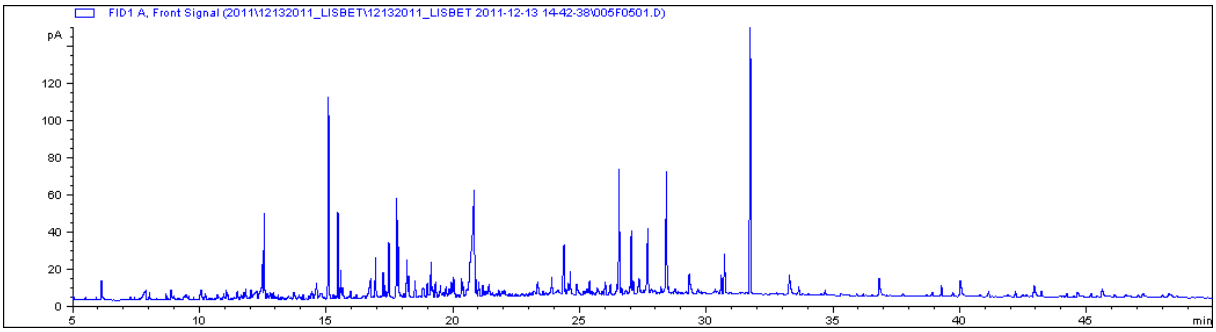

Figure F.132 - LIS012_1 Water

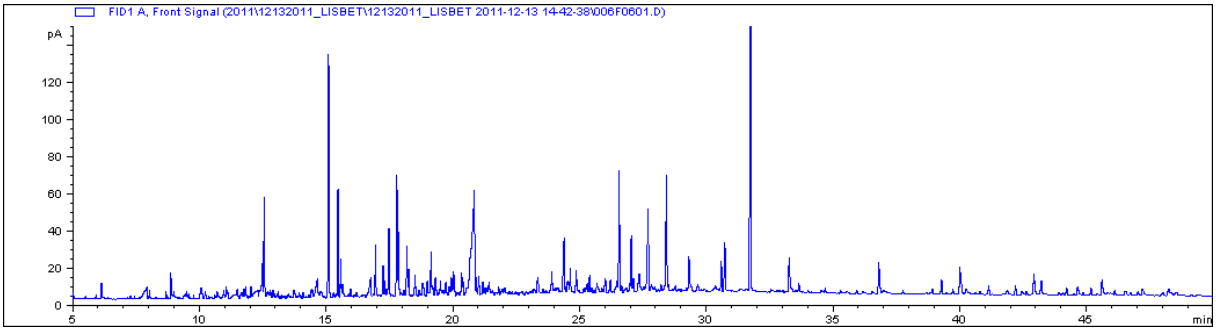

Figure F.133 - LIS012_2 Water

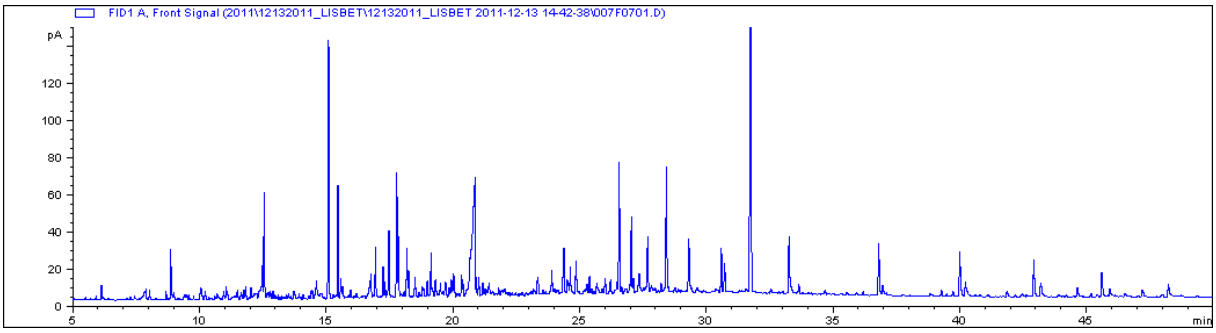

Figure F.134 - LIS012_3 Water

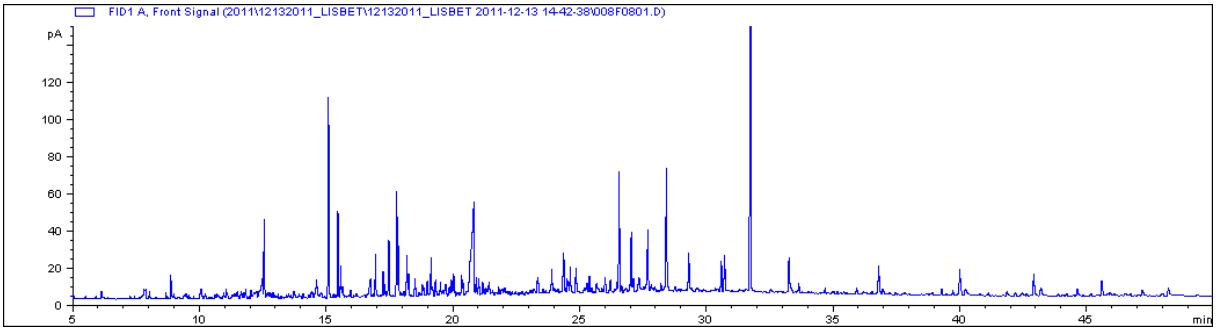

Figure F.135 - LIS013_1 Water

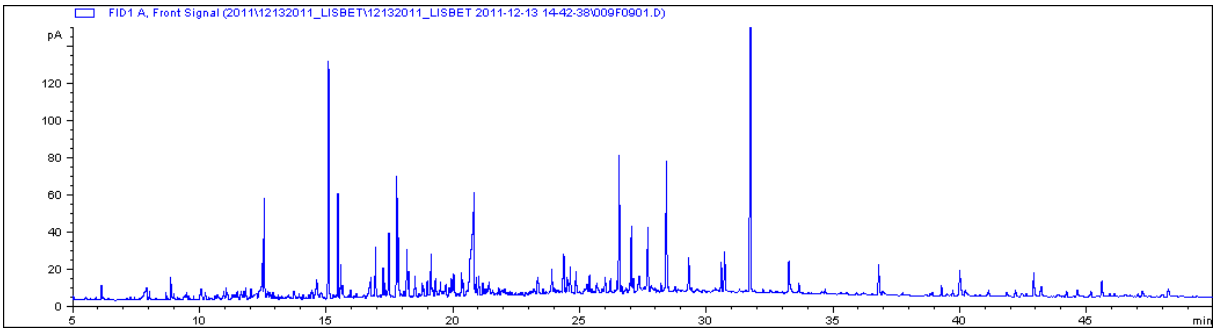

Figure F.136 - LIS013_2 Water

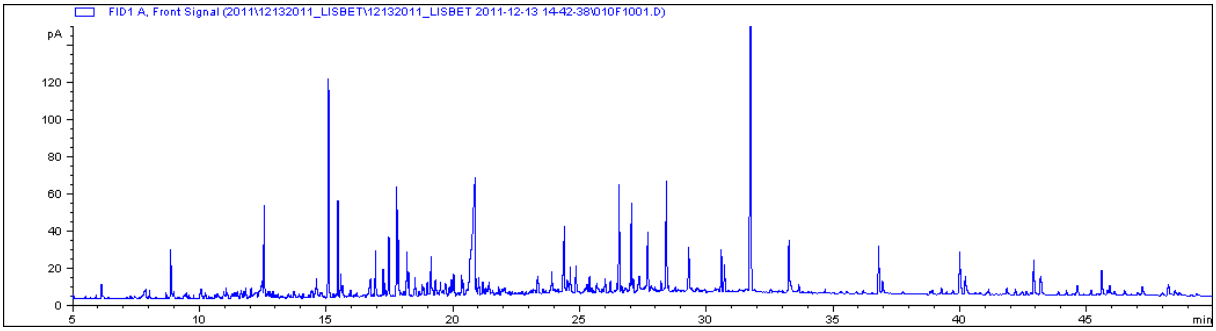

Figure F.137 - LIS013_3 Water

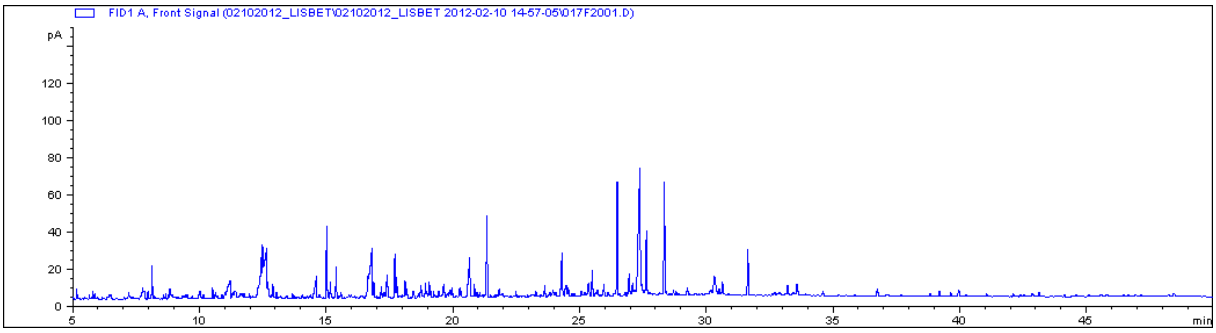

Figure F.138 - LIS014_1 Water

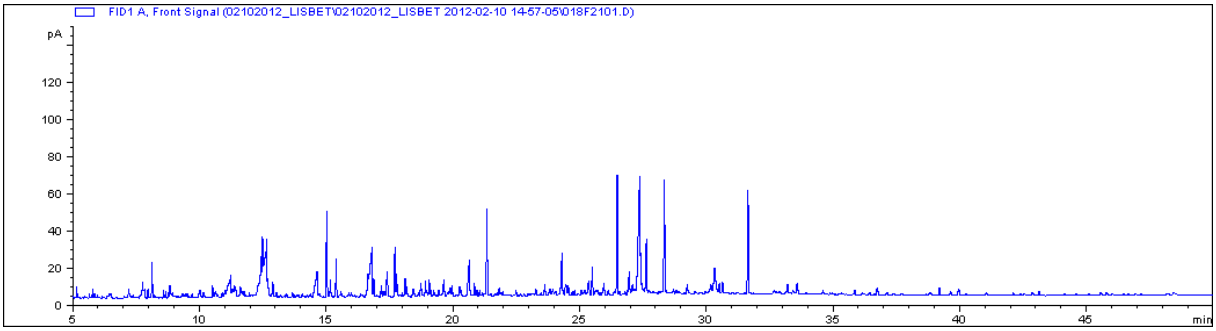

Figure F.139 - LIS014_2 Water

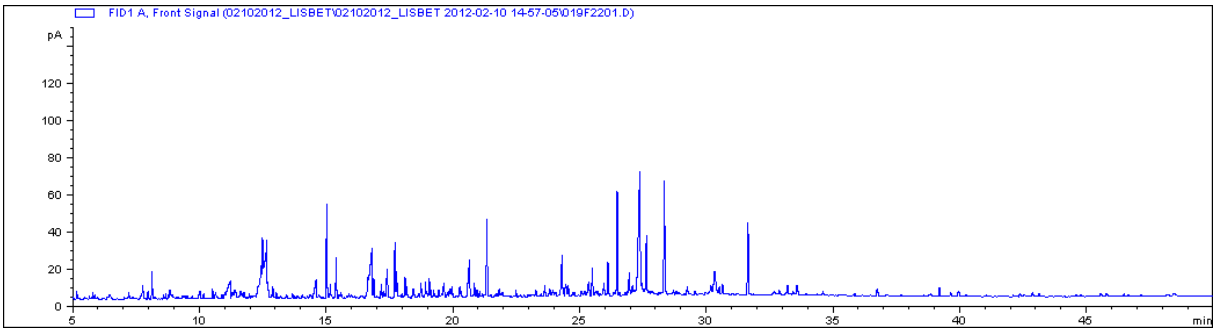

Figure F.140 - LIS014_3 Water

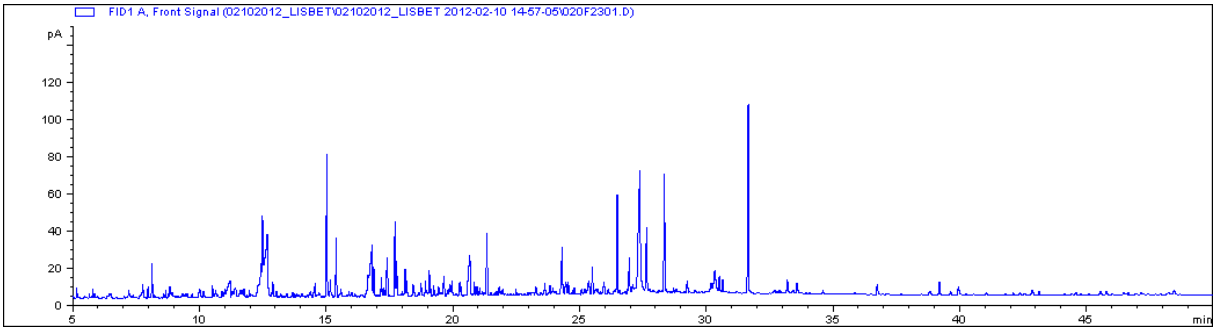

Figure F.141 - LIS014_4 Water

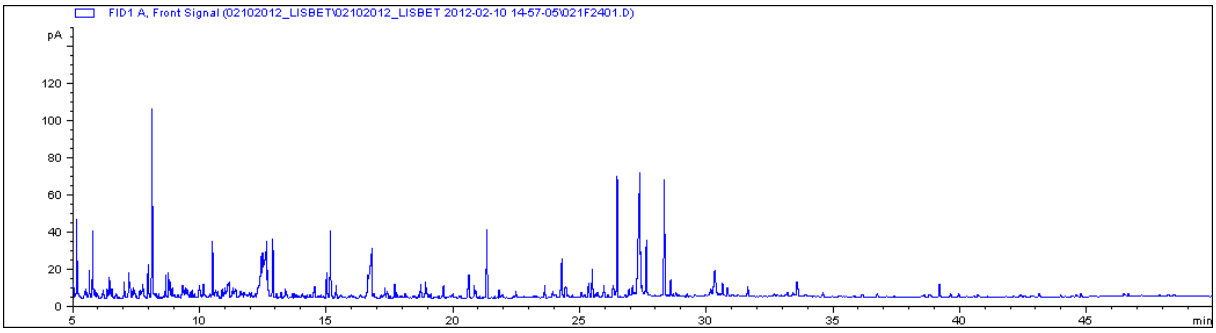

Figure F.142 - LIS015_1 Water

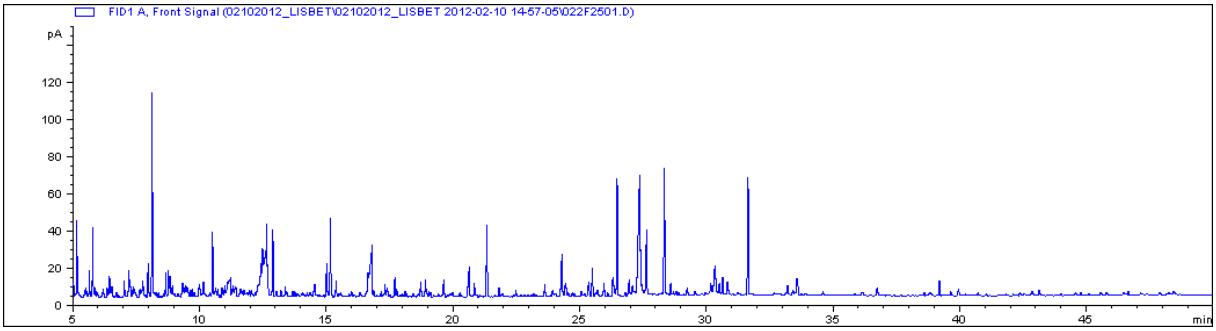

Figure F.143 - LIS015_2 Water

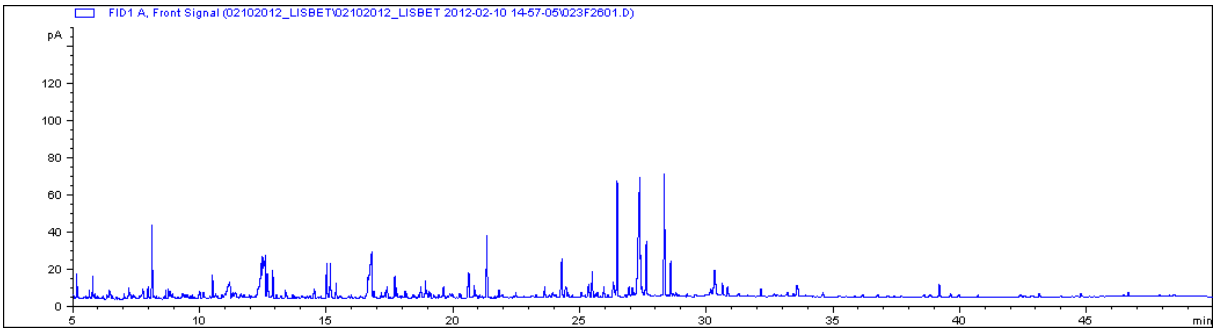

Figure F.144 - LIS015_3 Water

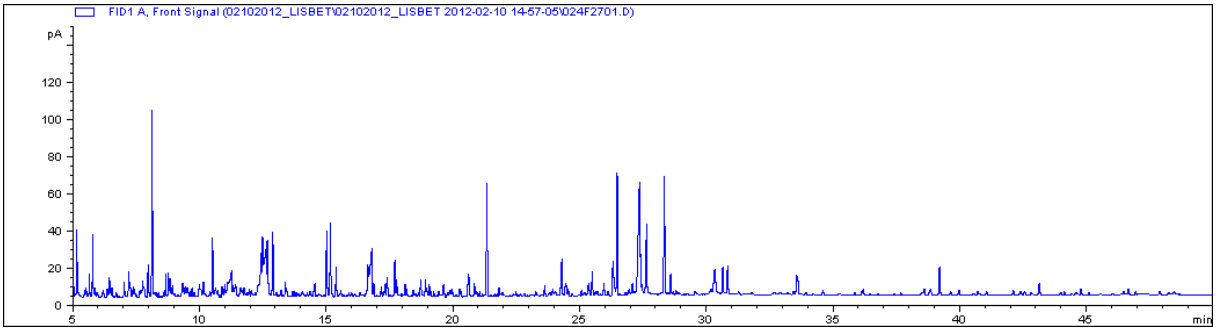

Figure F.145 - LIS015_4 Water

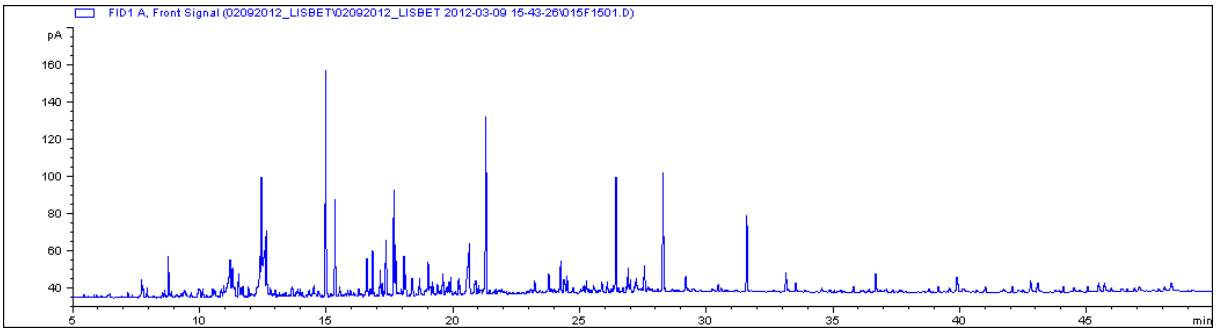

Figure F.146 - LIS016_1 Water

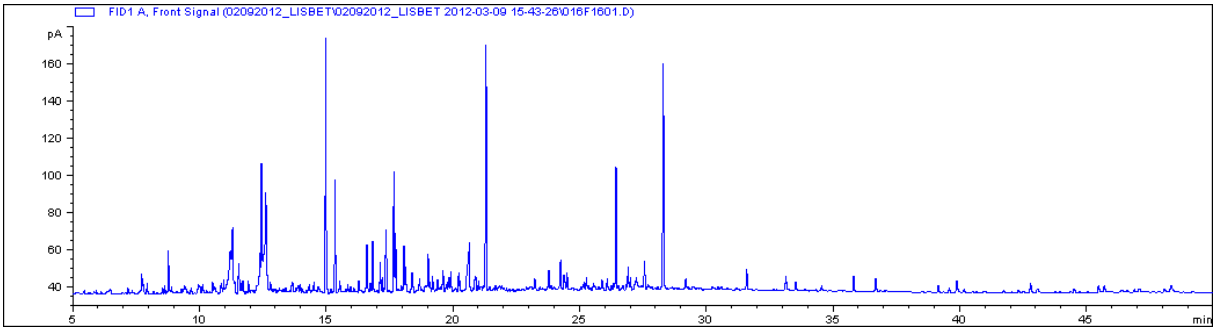

Figure F.147 - LIS016_2 Water

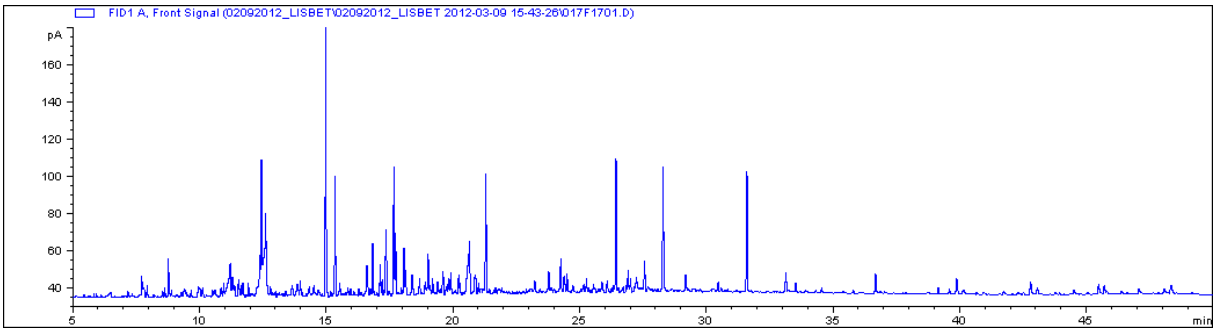

Figure F.148 - LIS016_3 Water

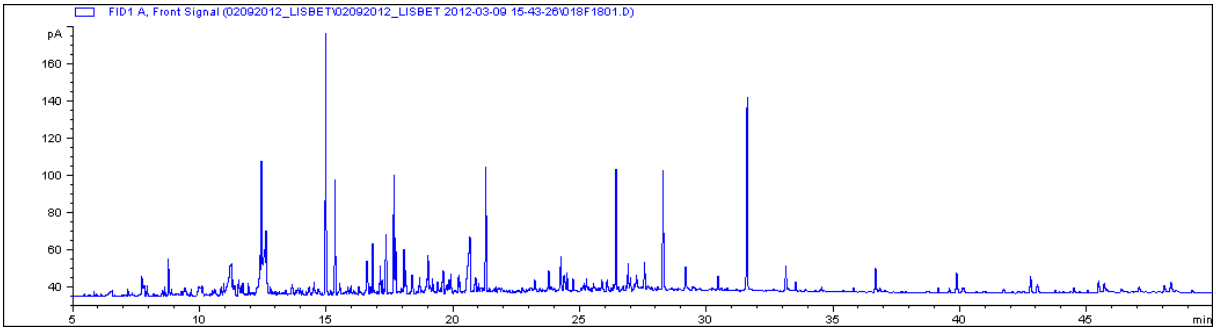

Figure F.149 - LIS016_4 Water

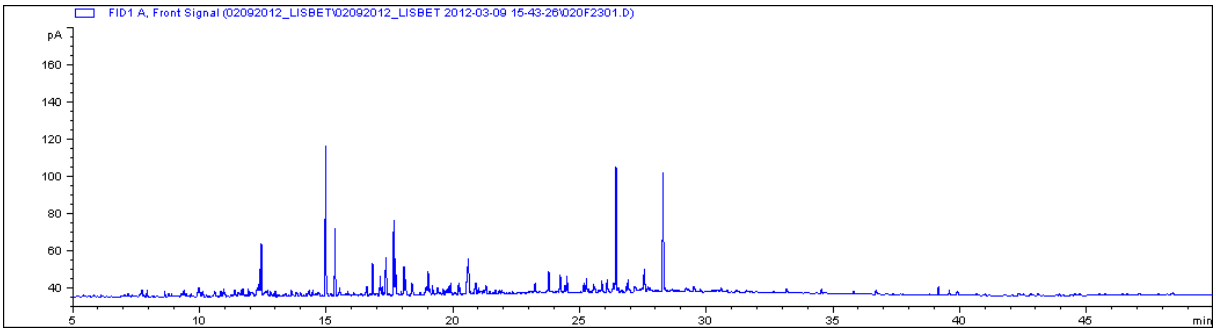

Figure F.150 - LIS017_1 Water

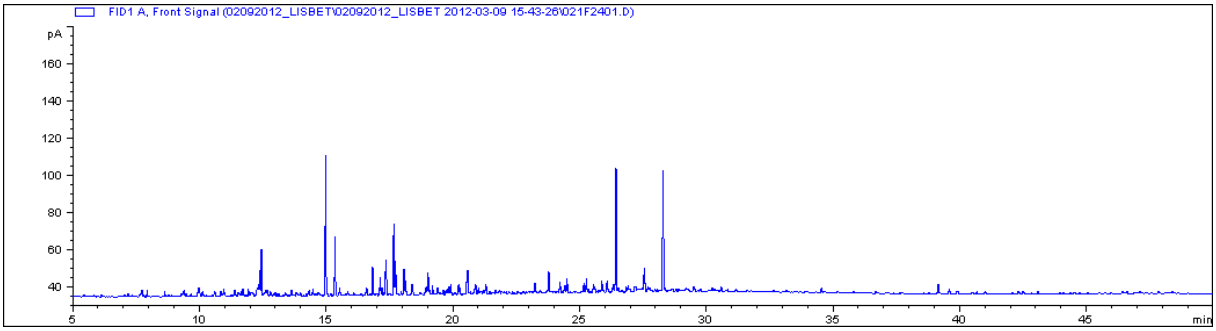

Figure F.151 - LIS017_2 Water

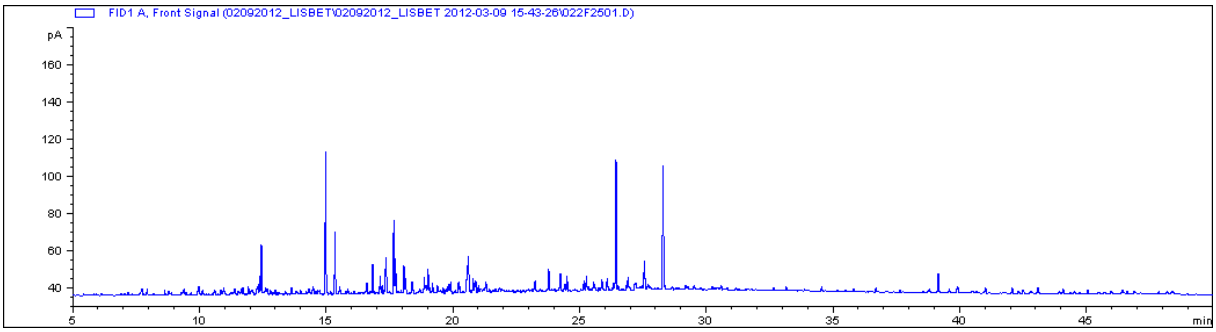

Figure F.152 - LIS017_3 Water

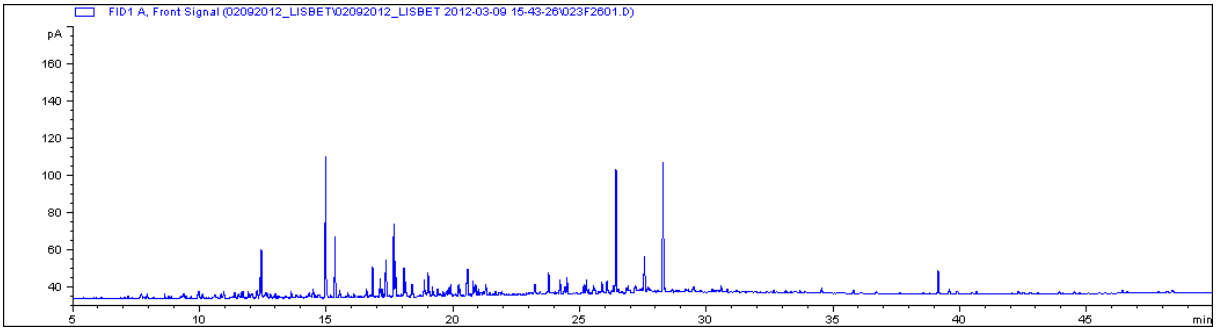

Figure F.153 - LIS017_4 Water

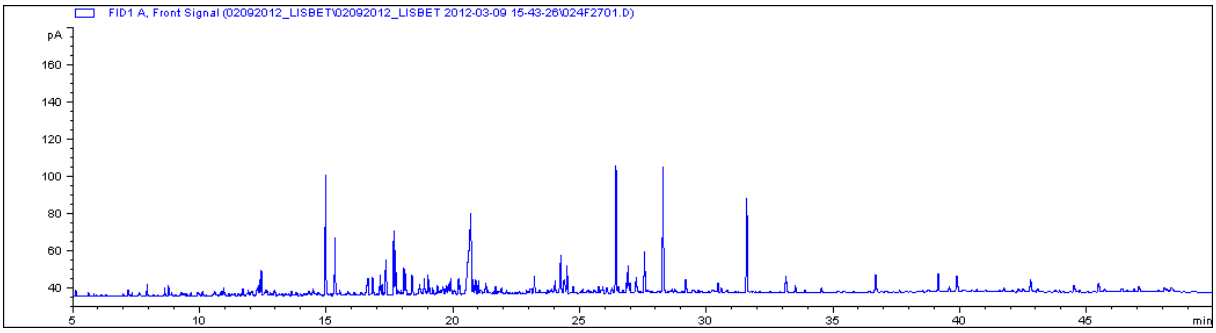

Figure F.154 - LIS018_1 Water

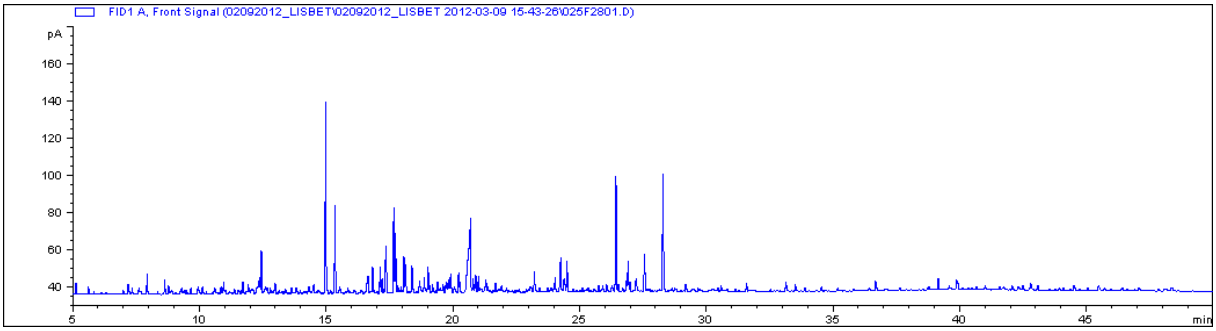

Figure F.155 - LIS018_2 Water

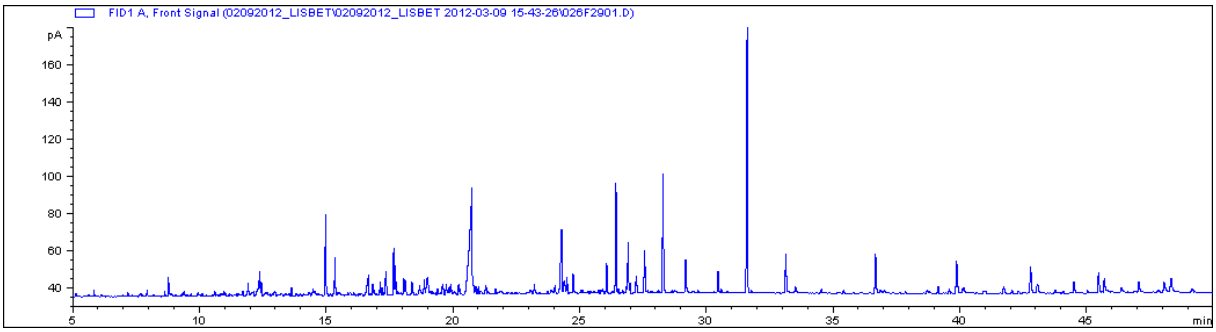

Figure F.156 - LIS018_4 Water

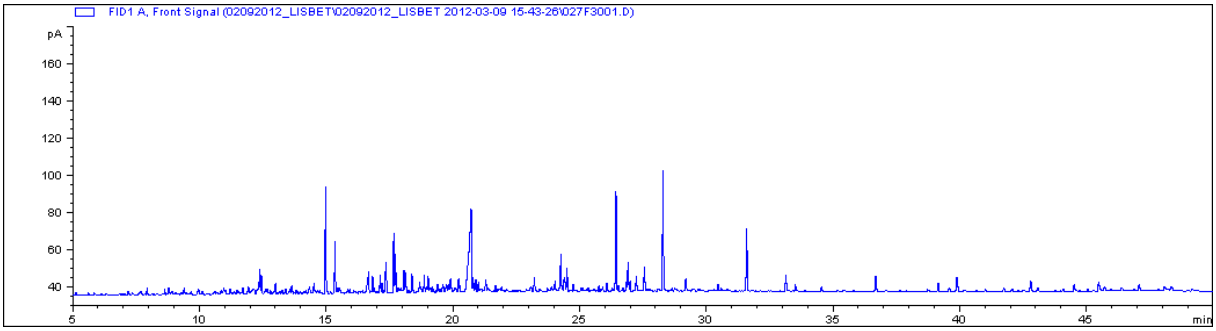

Figure F.157 - LIS018_5 Water

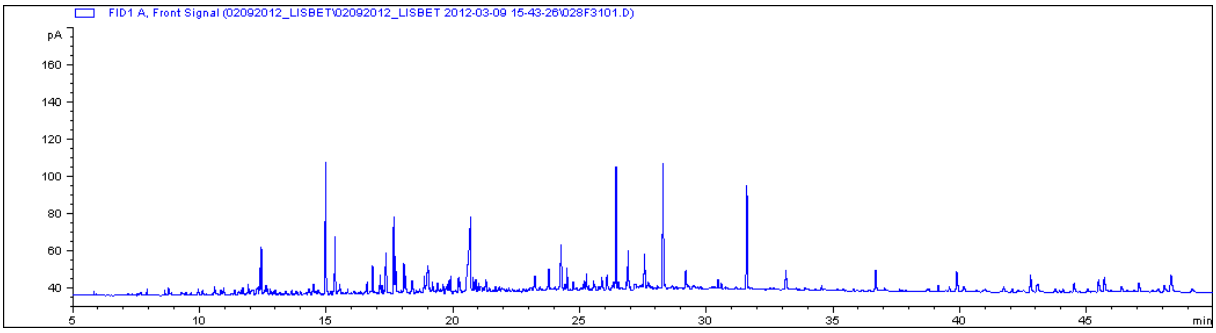

Figure F.158 - LIS019_1 Water

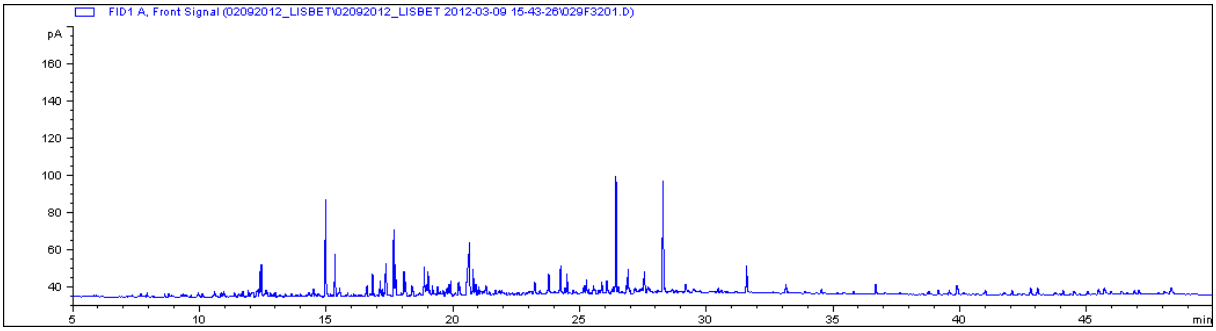

Figure F.159 - LIS019_2 Water

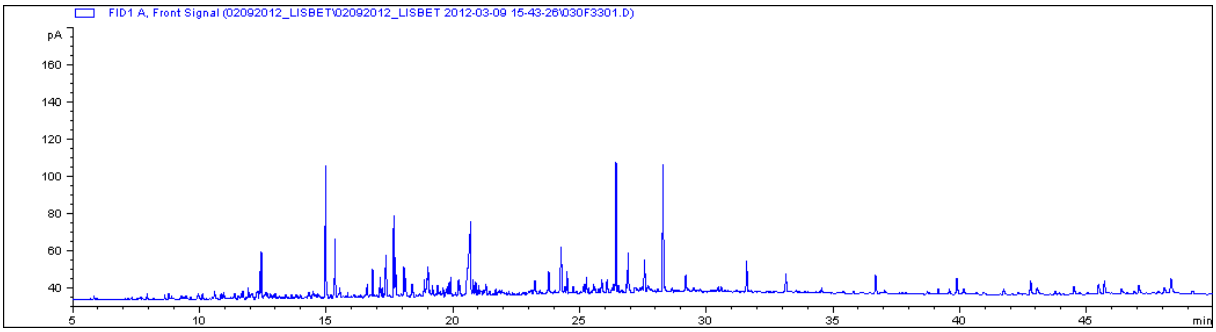

Figure F.160 - LIS019_3 Water

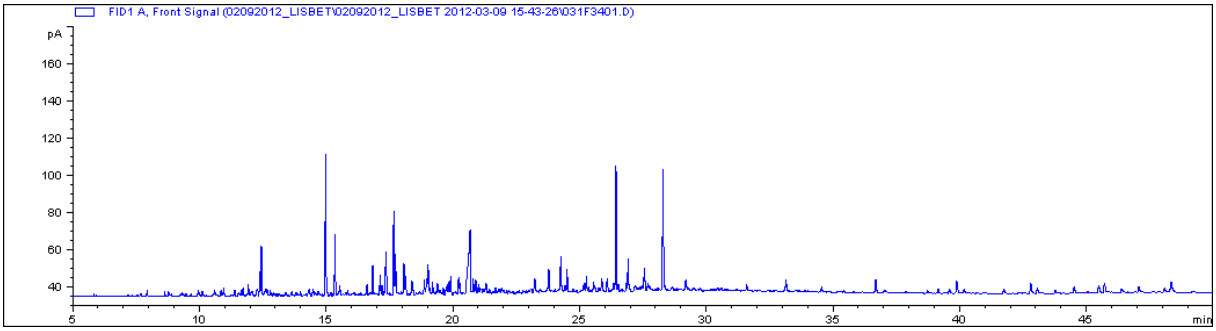

Figure F.161 - LIS019_4 Water

F.2.1 GC-FID Chromatograms of extracts of procedural blanks for water

These are the chromatograms of extracts of the water fraction of the three procedural blanks.

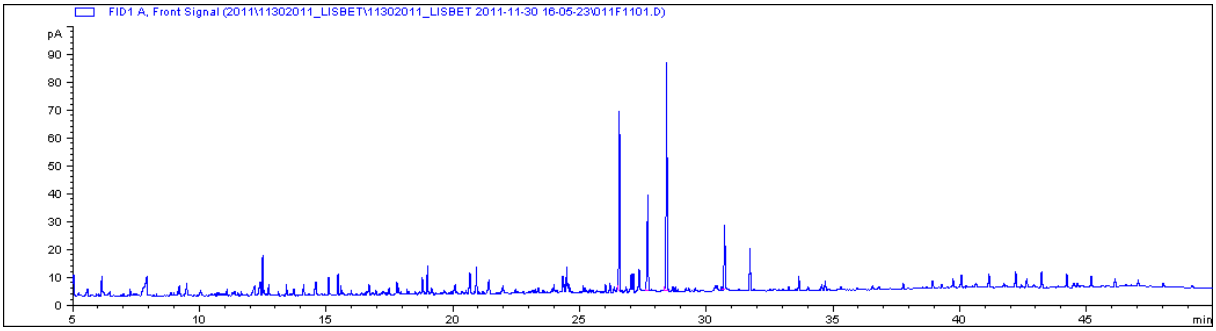

Figure F.162 - Procedural blank 1 Water

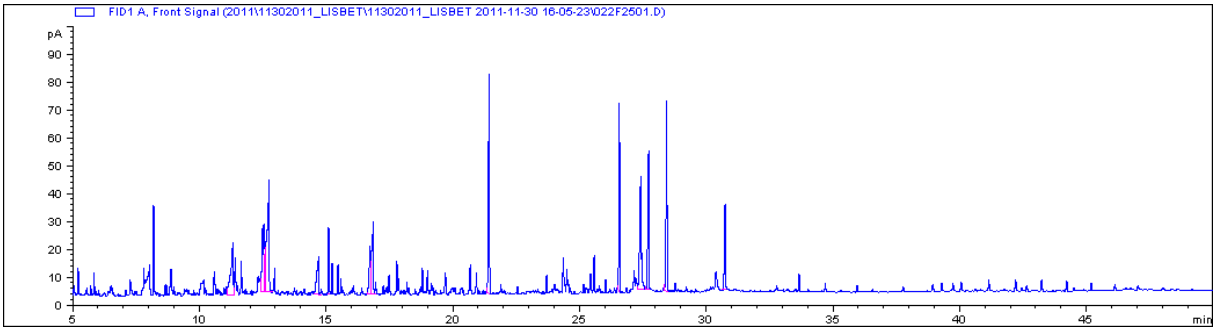

Figure F.163 – Procedural blank 2 Water

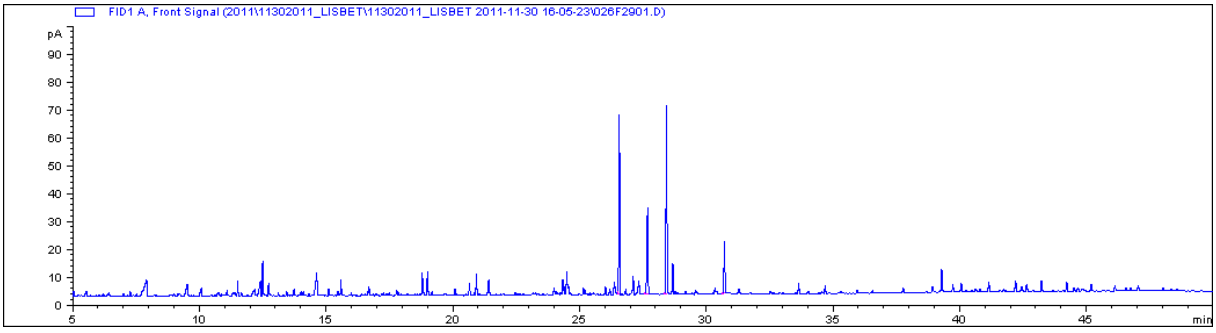

Figure F.164 – Procedural blank 3 Water

F.2.2 GC-FID Chromatograms of extracts of laboratory blanks for water

These are the chromatograms of six laboratory blanks of sea water from the same supply as used in the experiments.

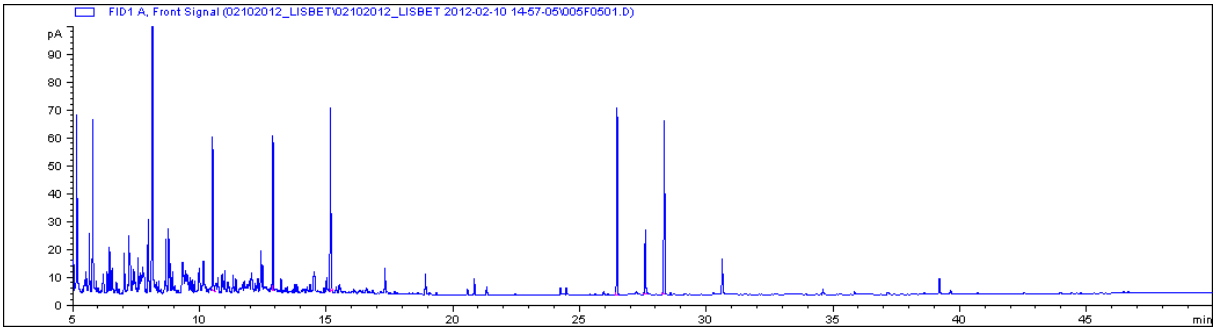

Figure F.165 - Laboratory blank 1 Water

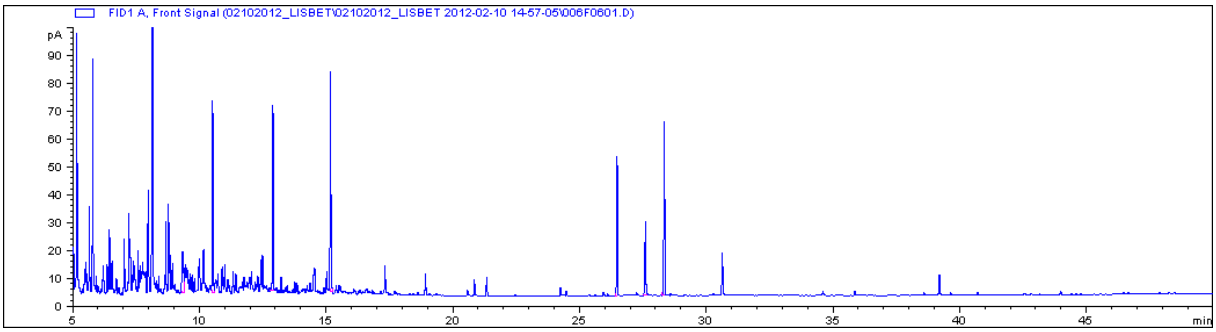

Figure F.166 - Laboratory blank 2 Water

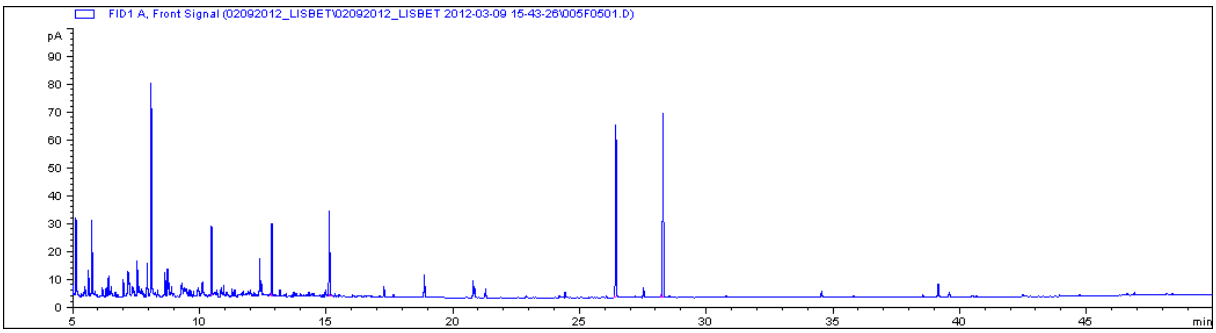

Figure F.167 - Laboratory blank 3 Water

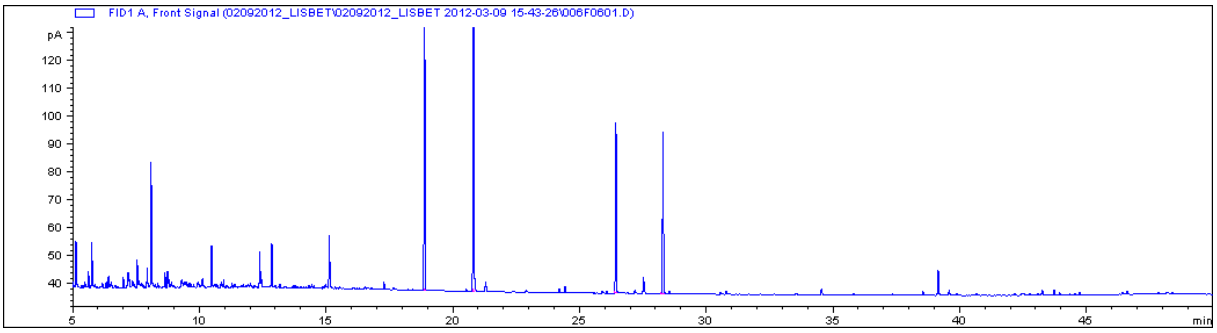

Figure F.168 - Laboratory blank 4 Water

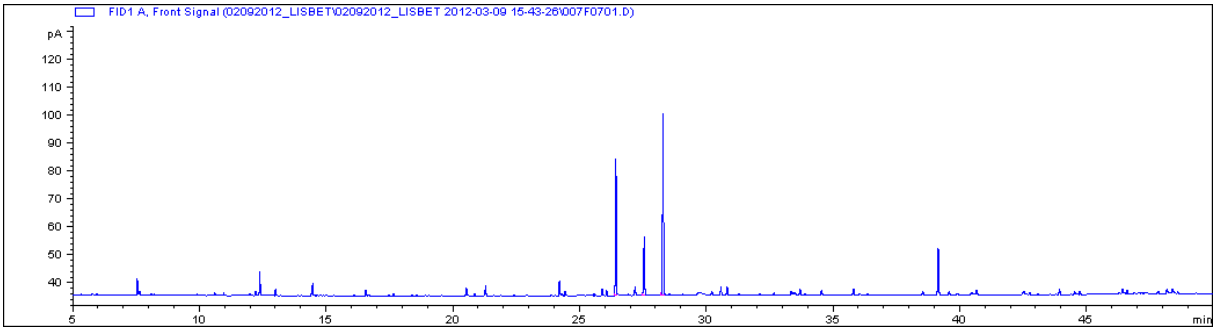

Figure F.169 - Laboratory blank 5 Water

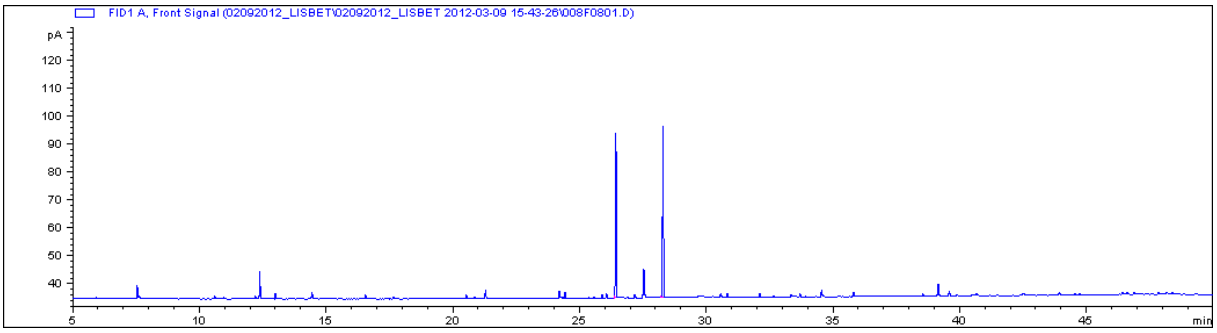

Figure F.170 - Laboratory blank 6 Water

F.3 Overlay of chromatograms for comparison of experiments with/without dispersant

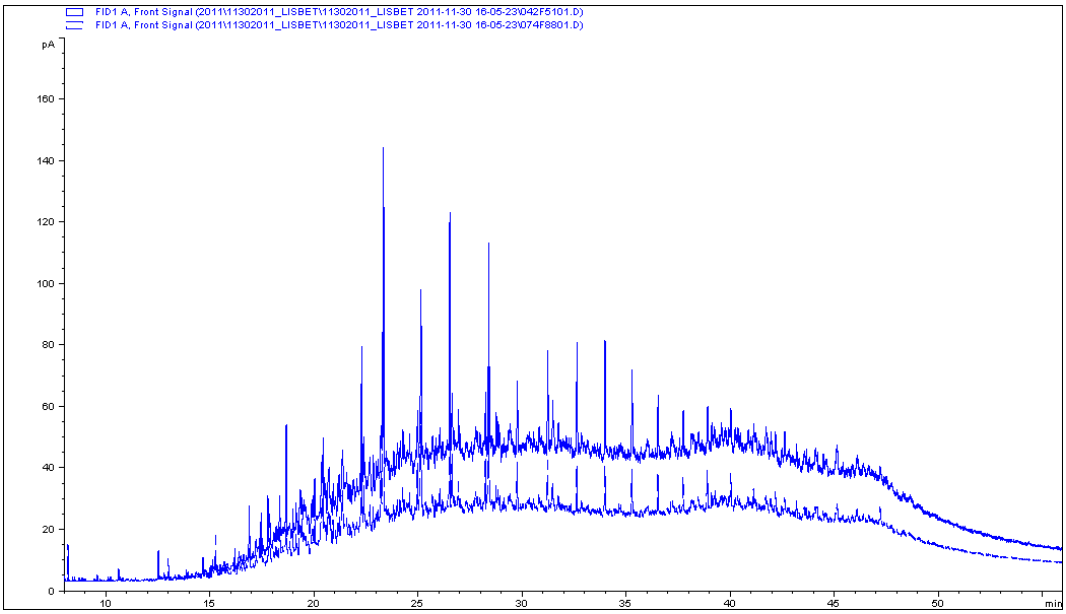

Figure F.171 - LIS002_3 Sediment (no dispersant) (most intensive) overlaid with LIS010_3 (1 % dispersant).

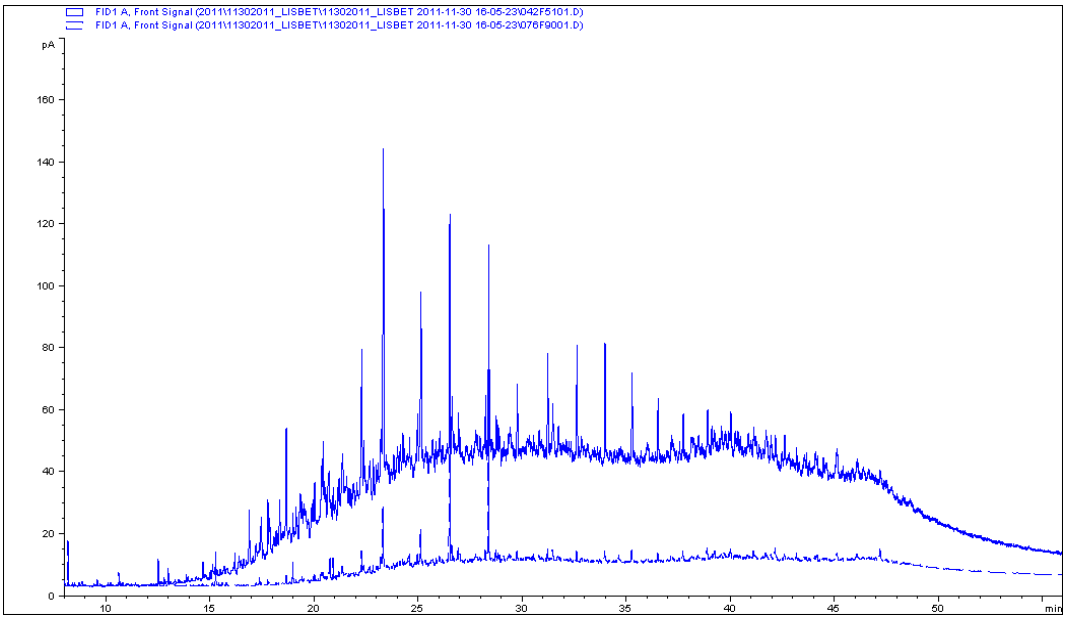

Figure F.172 - LIS002_3 Sediment (no dispersant) (most intensive) overlaid with LIS011_2 Sediment (1 % dispersant).

Appendix G GC-FID Results

Table G.1 – Quantification of GC-FID results for sediment extracts. Areas of SIS-component (A_{otp}) written in bold italic are estimated values (see Table G.3, refer also to Chapter 3.4.2 of the main text). Samples marked * are not used for calculations.

Sample ID	A_{tot}	A_{hexane}	A_{otp}	$A_{5\alpha\text{-and}}$	A_{THC}	C_{RIS} [µg]	RRF (oil)	THC [µg/ extract]	C_{SIS} [µg]	Recovery	THC [µg/ sample]
LIS001_1 Sed*	31 545	2 501	177	214	28 653	10	0,748	1 792	10	0,8	2167
LIS001_2 Sed	62 367	2 501	193	203	59 471	10	0,748	3 926	10	1,0	4126
LIS001_3 Sed	64 541	2 501	199	224	61 616	10	0,748	3 682	10	0,9	4135
LIS001_4 Sed	54 207	3 621	164	173	50 248	10	0,748	3 876	10	0,9	4089
LIS002_1 Sed	76 555	2 501	***166***	197	73 691	10	0,748	5 001	10	0,8	5935
LIS002_2 Sed	90 863	2 501	***166***	246	87 950	10	0,748	4 776	10	0,7	7083
LIS002_3 Sed	76 286	2 501	***166***	197	73 421	10	0,748	4 975	10	0,8	5913
LIS002_4 Sed	56 232	3 621	***166***	181	52 264	10	0,748	3 867	10	0,9	4209
LIS002_5 Sed	120 548	3 621	***166***	199	116 562	10	0,748	7 819	10	0,8	9387
LIS002_6 Sed	90 234	3 699	***166***	175	86 194	10	0,748	6 581	10	0,9	6942
LIS002_7 Sed	81 896	3 699	***166***	183	77 847	10	0,748	5 681	10	0,9	6270
LIS003_1 Sed*	72 752	2 501	***166***	200	69 884	10	0,748	4 667	10	0,8	5628
LIS003_2 Sed	130 562	2 501	***166***	239	127 656	10	0,748	7 138	10	0,7	10281
LIS003_3 Sed	158 146	2 501	***166***	213	155 266	10	0,748	9 736	10	0,8	12504
LIS003_4 Sed	109 483	3 621	***166***	189	105 507	10	0,748	7 459	10	0,9	8497

Table G.1 continued

Sample ID	A_{tot}	A_{hexane}	A_{otp}	$A_{5\alpha\text{-and}}$	A_{THC}	C_{RIS} [µg]	RRF (oil)	THC [µg/extract]	C_{SIS} [µg]	Recovery	THC [µg/sample]
LIS004_1 Sed	110 764	2 501	***166***	185	107 912	10	0,748	7 819	10	0,9	8691
LIS004_2 Sed	89 538	2 501	***166***	218	86 653	10	0,748	5 312	10	0,8	6979
LIS004_3 Sed	145 815	2 501	***166***	236	142 912	10	0,748	8 113	10	0,7	11510
LIS005_1 Sed	201 489	2 501	***166***	263	198 559	10	0,748	10 097	10	0,6	15991
LIS005_2 Sed	139 650	2 501	***166***	205	136 778	10	0,748	8 933	10	0,8	11016
LIS005_3 Sed	132 860	2 501	***166***	225	129 968	10	0,748	7 729	10	0,7	10467
LIS006_1 Sed	121 750	2 501	***166***	176	118 906	10	0,748	9 012	10	0,9	9576
LIS006_2 Sed	142 083	2 501	***166***	198	139 218	10	0,748	9 405	10	0,8	11212
LIS006_3 Sed	162 326	2 501	***166***	195	159 464	10	0,748	10 950	10	0,9	12843
LIS006_6 Sed*	20 377	3 621	***166***	165	16 425	10	0,748	1 333	10	1,0	1323
LIS006_7 Sed*	30 587	3 621	***166***	161	26 639	10	0,748	2 218	10	1,0	2145
LIS007_1 Sed	71 407	2 501	***166***	179	68 561	10	0,748	5 115	10	0,9	5522
LIS007_2 Sed	104 367	2 501	***166***	200	101 500	10	0,748	6 788	10	0,8	8174
LIS007_3 Sed	97 311	2 501	***166***	193	94 451	10	0,748	6 553	10	0,9	7607
LIS007_4 Sed	73 117	3 621	***166***	180	69 150	10	0,748	5 150	10	0,9	5569
LIS007_5 Sed	105 194	3 621	***166***	187	101 219	10	0,748	7 221	10	0,9	8152
LIS008_1 Sed	59 373	2 501	***166***	191	56 515	10	0,773	3 832	10	0,9	4404
LIS008_2 Sed	56 966	2 501	***166***	213	54 086	10	0,773	3 285	10	0,8	4215
LIS008_3 Sed	59 772	2 501	***166***	196	56 909	10	0,773	3 760	10	0,8	4435

LIS009_1 Sed	105 386	2 501	***166***	175	102 543	10	0,437	13 386	10	0,9	14136
LIS009_2 Sed	120 110	2 501	***166***	195	117 248	10	0,437	13 759	10	0,9	16163
LIS009_3 Sed	107 783	2 501	***166***	198	104 918	10	0,437	12 150	10	0,8	14463
LIS010_1 Sed	33 489	2 501	***166***	150	30 671	10	0,748	2 734	10	1,1	2470
LIS010_2 Sed	45 283	2 501	***166***	174	42 442	10	0,748	3 261	10	1,0	3418
LIS010_3 Sed	44 509	2 501	***166***	165	41 676	10	0,748	3 379	10	1,0	3356
LIS010_4 Sed	54 469	3 699	***166***	172	50 431	10	0,748	3 911	10	1,0	4062
LIS010_5 Sed	52 408	3 699	***166***	184	48 359	10	0,748	3 512	10	0,9	3895
LIS011_1 Sed*	28 277	2 501	***166***	174	25 436	10	0,748	1 958	10	1,0	2055
LIS011_2 Sed	16 803	2 501	159	162	13 981	10	0,748	1 156	10	1,0	1176
LIS011_3 Sed*	5 306	2 501	145	161	2 499	10	0,748	208	10	0,9	231
LIS011_4 Sed	20 353	3 699	163	169	16 322	10	0,748	1 292	10	1,0	1335
LIS011_5 Sed	23 750	3 699	212	213	19 626	10	0,748	1 234	10	1,0	1238
LIS012_1 Sed	33 004	2 528	***166***	169	30 141	10	0,748	2 382	10	1,0	2427
LIS012_2 Sed	36 389	2 528	170	175	33 515	10	0,748	2 560	10	1,0	2629
LIS012_3 Sed	31 393	2 528	167	179	28 519	10	0,748	2 131	10	0,9	2286
LIS013_1 Sed	41 685	2 528	***166***	173	38 818	10	0,748	3 005	10	1,0	3126
LIS013_2 Sed	43 864	2 528	***166***	171	40 999	10	0,748	3 202	10	1,0	3302
LIS013_3 Sed	52 826	2 528	***166***	171	49 961	10	0,748	3 906	10	1,0	4024
LIS014_1 Sed*	11 192	3 621	154	165	7 252	10	0,748	588	10	0,9	630
LIS014_2 Sed*	11 934	3 621	136	167	8 009	10	0,748	641	10	0,8	788
LIS014_3 Sed*	13 880	3 621	127	161	9 970	10	0,748	827	10	0,8	1046

Table G.1 continued

Sample ID	A_{tot}	A_{hexane}	A_{otp}	$A_{5\alpha\text{-and}}$	A_{THC}	C_{RIS} [µg]	RRF (oil)	THC [µg/extract]	C_{SIS} [µg]	Recovery	THC [µg/sample]
LIS014_4 Sed*	15 676	3 621	160	166	11 729	10	0,748	945	10	1,0	978
LIS015_1 Sed*	5 833	3 621	137	162	1 913	10	0,748	158	10	0,8	186
LIS015_2 Sed*	7 530	3 621	200	224	3 486	10	0,748	208	10	0,9	233
LIS015_3 Sed*	11 825	3 621	167	173	7 864	10	0,748	607	10	1,0	631
LIS015_4 Sed*	7 745	3 621	151	159	3 814	10	0,748	320	10	0,9	338
LIS016_1 Sed	85 871	3 699	***166***	177	81 829	10	0,748	6 191	10	0,9	6590
LIS016_2 Sed	84 005	3 699	***166***	187	79 953	10	0,748	5 719	10	0,9	6439
LIS016_3 Sed	84 594	3 699	***166***	176	80 552	10	0,748	6 108	10	0,9	6487
LIS016_4 Sed	78 526	3 699	***166***	179	74 482	10	0,748	5 554	10	0,9	5998
LIS017_1 Sed	202 542	3 699	***166***	163	198 514	10	0,748	16 312	10	1,0	15988
LIS017_2 Sed	166 980	3 699	***166***	151	162 964	10	0,748	14 435	10	1,1	13124
LIS017_3 Sed	213 362	3 699	***166***	187	209 310	10	0,748	14 956	10	0,9	16857
LIS017_4 Sed	204 203	3 699	***166***	187	200 151	10	0,748	14 325	10	0,9	16119
LIS018_1 Sed*	59 268	3 699	***166***	164	55 239	10	0,591	5 703	10	1,0	5631
LIS018_2 Sed	111 438	3 699	***166***	176	107 397	10	0,591	10 353	10	0,9	10947
LIS018_4 Sed	126 732	3 699	***166***	186	122 681	10	0,591	11 160	10	0,9	12505
LIS018_5 Sed	108 077	3 699	***166***	183	104 029	10	0,591	9 613	10	0,9	10604
LIS019_1 Sed	62 255	3 699	***166***	173	58 217	10	0,748	4 504	10	1,0	4689
LIS019_2 Sed	69 333	3 699	***166***	177	65 290	10	0,748	4 926	10	0,9	5258

LIS019_3 Sed*	41 408	3 699	***166***	174	37 369	10	0,748	2 870	10	1,0	3010
LIS019_4 Sed	74 204	3 699	***166***	181	70 158	10	0,748	5 185	10	0,9	5650
Procedure blank 1	12 216	2 501	161	201	9 353	10	0,748	621	10	0,8	776
Procedure blank 2	10 086	2 501	149	171	7 265	10	0,748	568	10	0,9	654
Procedure blank 3	4 169	2 501	132	176	1 360	10	0,773	100	10	0,7	134
Lab blank 1 (Grandefjæra)	4 544	3 621	105	155	663	10	0,748	57	10	0,7	84
Lab blank 2	4 585	3 621	108	158	699	10	0,748	59	10	0,7	87
Lab blank 3*	5 001	3 699	134	159	1 009	10	0,748	85	10	0,8	101
Lab blank 4	4 264	3 699	145	166	254	10	0,748	20	10	0,9	23
Lab blank 5 (Buvika)	3 629	3 699	137	166	-373	10	0,748	-30	10	0,8	-36
Lab blank 6	4 109	3 699	120	164	126	10	0,748	10	10	0,7	14
Lab blank 7	4 278	3 699	124	168	287	10	0,748	23	10	0,7	31
Lab blank 8 (Ranheim)	8 411	3 699	153	173	4 386	10	0,748	339	10	0,9	384
Lab blank 9*	3 770	3 699	134	170	-233	10	0,748	-18	10	0,8	-23
Lab blank 10	4 706	3 699	151	173	684	10	0,748	53	10	0,9	61

Table G.2 - Quantification of GC-FID results for water extracts. Samples marked * are not used for calculations.

Sample ID	A_{tot}	A_{DCM}	A_{otp}	$A_{5\alpha\text{-and}}$	A_{THC}	C_{RIS} [µg]	RRF (oil)	THC [µg/extract]	C_{SIS} [µg]	Recovery	THC [µg/sample]
LIS001_1 Water*	9 809	2 688	133	207	6 781	10	0,748	437	10	0,6	680
LIS001_2 Water	13 044	2 688	158	199	9 999	10	0,748	672	10	0,8	846
LIS001_3 Water	17 387	2 688	211	225	14 262	10	0,748	847	10	0,9	902
LIS001_4 Water	13 567	3 390	160	171	9 846	10	0,748	769	10	0,9	824
LIS002_1 Water	12 034	2 688	178	193	8 975	10	0,748	620	10	0,9	674
LIS002_2 Water	14 509	2 688	169	183	11 469	10	0,748	836	10	0,9	908
LIS002_3 Water*	31 623	2 688	198	184	28 553	10	0,748	2 077	10	1,1	1 925
LIS002_4 Water	14 709	3 390	171	169	10 979	10	0,748	871	10	1,0	858
LIS002_5 Water	14 217	3 390	154	165	10 509	10	0,748	854	10	0,9	915
LIS002_6 Water	9 609	3 093	157	167	6 192	10	0,748	496	10	0,9	526
LIS002_7 Water	8 223	3 093	144	160	4 827	10	0,748	404	10	0,9	449
LIS003_1 Water*	12 476	2 688	188	210	9 390	10	0,748	597	10	0,9	668
LIS003_2 Water	26 771	2 688	193	212	23 677	10	0,748	1 491	10	0,9	1 640
LIS003_3 Water	14 029	2 688	180	187	10 975	10	0,748	785	10	1,0	816
LIS003_4 Water	16 078	3 390	165	174	12 349	10	0,748	950	10	0,9	1 000
LIS006_1 Water	14 993	2 688	155	164	11 986	10	0,748	976	10	0,9	1 033
LIS006_2 Water	14 671	2 688	147	171	11 665	10	0,748	910	10	0,9	1 059
LIS006_3 Water	14 450	2 688	150	164	11 448	10	0,748	931	10	0,9	1 024
LIS006_6 Water*	12 015	3 390	164	166	8 295	10	0,748	669	10	1,0	676
LIS006_7 Water*	12 062	3 390	131	164	8 377	10	0,748	685	10	0,8	854
LIS007_1 Water	15 198	2 688	158	166	12 185	10	0,748	981	10	1,0	1 028
LIS007_2 Water	13 620	2 688	159	168	10 605	10	0,748	842	10	0,9	890
LIS007_3 Water*	44 357	2 688	158	176	41 336	10	0,748	3 147	10	0,9	3 498
LIS007_4 Water	13 209	3 390	157	172	9 490	10	0,748	739	10	0,9	806
LIS007_5 Water	13 583	3 390	164	175	9 854	10	0,748	751	10	0,9	806

LIS008_1 Water	10 148	2 688	180	177	7 103	10	0,773	519	10	1,0	510
LIS008_2 Water	10 411	2 688	182	169	7 372	10	0,773	566	10	1,1	524
LIS008_3 Water	10 170	2 688	190	180	7 111	10	0,773	510	10	1,1	484
LIS009_1 Water	7 579	2 688	155	174	4 562	10	0,437	599	10	0,9	676
LIS009_2 Water	8 531	2 688	158	171	5 514	10	0,437	738	10	0,9	797
LIS009_3 Water	7 609	2 688	130	177	4 613	10	0,437	596	10	0,7	810
LIS010_1 Water	15 200	2 688	157	158	12 198	10	0,748	1 033	10	1,0	1 041
LIS010_2 Water	13 804	2 688	160	173	10 783	10	0,748	834	10	0,9	904
LIS010_3 Water	14 330	2 688	155	162	11 325	10	0,748	936	10	1,0	977
LIS010_4 Water*	30 372	3 093	176	166	26 938	10	0,748	2 175	10	1,1	2 050
LIS010_5 Water	11 188	3 093	160	163	7 772	10	0,748	638	10	1,0	649
LIS011_1 Water	13 025	2 688	150	161	10 026	10	0,748	831	10	0,9	893
LIS011_2 Water	14 584	2 688	144	173	11 578	10	0,748	894	10	0,8	1 072
LIS011_3 Water	8 406	2 688	120	170	5 429	10	0,748	428	10	0,7	606
LIS011_4 Water	8 103	3 093	119	168	4 723	10	0,748	376	10	0,7	532
LIS011_5 Water	10 792	3 093	144	168	7 388	10	0,748	590	10	0,9	688
LIS012_1 Water	11 880	2 748	160	177	8 795	10	0,748	664	10	0,9	736
LIS012_2 Water	14 197	2 748	151	161	11 137	10	0,748	925	10	0,9	985
LIS012_3 Water	14 353	2 748	167	177	11 261	10	0,748	851	10	0,9	899
LIS013_1 Water	12 935	2 748	146	171	9 869	10	0,748	770	10	0,9	903
LIS013_2 Water	13 743	2 748	175	181	10 639	10	0,748	786	10	1,0	812
LIS013_3 Water	14 113	2 748	138	151	11 076	10	0,748	978	10	0,9	1 074
LIS014_1 Water*	10 598	3 390	148	160	6 900	10	0,748	578	10	0,9	624
LIS014_2 Water*	11 159	3 390	152	158	7 458	10	0,748	631	10	1,0	658
LIS014_3 Water*	11 060	3 390	139	162	7 368	10	0,748	607	10	0,9	708
LIS014_4 Water*	12 162	3 390	130	160	8 482	10	0,748	711	10	0,8	872
LIS015_1 Water*	9 990	3 390	155	161	6 284	10	0,748	523	10	1,0	542
LIS015_2 Water*	11 011	3 390	151	172	7 298	10	0,748	568	10	0,9	644
LIS015_3 Water*	9 226	3 390	152	164	5 520	10	0,748	450	10	0,9	487

Table G.2 continued

Sample ID	A_{tot}	A_{DCM}	A_{otp}	$A_{5\alpha\text{-and}}$	A_{THC}	C_{RIS} [µg]	RRF (oil)	THC [µg/extract]	C_{SIS} [µg]	Recovery	THC [µg/sample]
LIS015_4 Water*	11 661	3 390	156	166	7 949	10	0,748	640	10	0,9	683
LIS016_1 Water	12 606	3 093	153	166	9 194	10	0,748	739	10	0,9	805
LIS016_2 Water	10 327	3 093	154	163	6 916	10	0,748	567	10	0,9	600
LIS016_3 Water	11 780	3 093	167	174	8 346	10	0,748	640	10	1,0	668
LIS016_4 Water	12 020	3 093	154	169	8 604	10	0,748	681	10	0,9	745
LIS017_1 Water	8 082	3 093	156	171	4 662	10	0,748	366	10	0,9	400
LIS017_2 Water	8 624	3 093	159	175	5 197	10	0,748	397	10	0,9	438
LIS017_3 Water	8 658	3 093	161	172	5 232	10	0,748	408	10	0,9	433
LIS017_4 Water	9 948	3 093	159	177	6 519	10	0,748	492	10	0,9	549
LIS018_1 Water	9 448	3 093	161	169	6 025	10	0,591	604	10	1,0	632
LIS018_2 Water	9 121	3 093	151	163	5 714	10	0,591	594	10	0,9	639
LIS018_4 Water	9 591	3 093	143	166	6 189	10	0,591	630	10	0,9	734
LIS018_5 Water	9 199	3 093	141	164	5 802	10	0,591	600	10	0,9	697
LIS019_1 Water	10 645	3 093	157	175	7 221	10	0,748	553	10	0,9	617
LIS019_2 Water	8 167	3 093	149	166	4 759	10	0,748	384	10	0,9	426
LIS019_3 Water	11 993	3 093	166	185	8 550	10	0,748	619	10	0,9	689
LIS019_4 Water	9 768	3 093	153	168	6 355	10	0,748	505	10	0,9	557
Procedure blank 1	8269	2 688	159	215	5 207	10	0,748	323	10	0,7	439
Procedure blank 2	9034	2 688	158	177	6 011	10	0,748	453	10	0,9	507
Procedure blank 3	5861	2 688	156	173	2 844	10	0,773	212	10	0,9	236
Lab blank 1 SW	6848	3 390	153	163	3 142	10	0,748	258	10	0,9	275
Lab blank 2 SW	7421	3 390	121	161	3 749	10	0,748	311	10	0,7	415
Lab blank 3 SW	4190	3 093	149	169	779	10	0,748	62	10	0,9	70
Lab blank 4 SW	7279	3 093	150	150	3 885	10	0,748	345	10	1,0	346
Lab blank 5 SW	3605	3 093	117	170	225	10	0,748	18	10	0,7	26
Lab blank 6 SW	4263	3 093	136	161	872	10	0,748	72	10	0,8	85

Table G.3 – Estimated area of *o*-terphenyl peak in sediment extracts from samples without co-elution

Sample ID	A_{otp}	Recovery
LIS001_1 Sed	177	0,83
LIS001_2 Sed	193	0,95
LIS001_3 Sed	199	0,89
LIS001_4 Sed	164	0,95
LIS011_1 Sed	166	0,95
LIS011_2 Sed	159	0,98
LIS011_4 Sed	163	0,97
LIS012_2 Sed	170	0,97
LIS012_3 Sed	167	0,93
LIS014_1 Sed	154	0,93
LIS014_4 Sed	160	0,97
LIS015_2 Sed	200	0,90
LIS015_3 Sed	167	0,96
LIS015_4 Sed	151	0,95
Proc blank 1 Sed	161	0,80
Proc. blank 2 Sed	149	0,87
Lab blank 4 Sed	145	0,87
Lab blank 8 Sed	153	0,88
Lab blank 10 Sed	151	0,87
Average area	**166**	0,92
Standard deviation	**16**	0,05
Relative standard deviation (%)	**10**	6

Appendix H Target ions in GC-MS SIM mode

Table H.1 – Target ions in GC-MS SIM mode

Component	Component group	Target ion
Decalin	C-10 saturates	138
C1-decalins	C-10 saturates	152
C2-decalins	C-10 saturates	166
C3-decalins	C-10 saturates	180
C4-decalins	C-10 saturates	194
Naphthalene	Naphthalenes	128
C1-naphthalenes	Naphthalenes	142
C2-naphthalenes	Naphthalenes	156
C3-naphthalenes	Naphthalenes	170
C4-naphthalenes	Naphthalenes	184
Biphenyl	2-3 ring PAHs	164
Acenaphthylene	2-3 ring PAHs	152
Acenaphthene	2-3 ring PAHs	154
Dibenzofuran	2-3 ring PAHs	168
Fluorene	2-3 ring PAHs	166
C1-fluorenes	2-3 ring PAHs	180
C2-fluorenes	2-3 ring PAHs	194
C3-fluorenes	2-3 ring PAHs	208
Phenanthrene	2-3 ring PAHs	178
Anthracene	2-3 ring PAHs	178
C1-phenanthrenes/anthracenes	2-3 ring PAHs	192
C2-phenanthrenes/anthracenes	2-3 ring PAHs	206
C3-phenanthrenes/anthracenes	2-3 ring PAHs	220
C4-phenanthrenes/anthracenes	2-3 ring PAHs	234
Dibenzothiophene	2-3 ring PAHs	184
C1-dibenzothiophenes	2-3 ring PAHs	198
C2-dibenzothiophenes	2-3 ring PAHs	212
C3-dibenzothiophenes	2-3 ring PAHs	226
C4-dibenzothiophenes	2-3 ring PAHs	240
Fluoranthene	4-6 ring PAHs	202
Pyrene	4-6 ring PAHs	202
C1-fluoranthrenes/pyrenes	4-6 ring PAHs	216
C2-fluoranthenes/pyrenes	4-6 ring PAHs	230
C3-fluoranthenes/pyrenes	4-6 ring PAHs	244
Benz(a)anthracene	4-6 ring PAHs	228
Chrysene	4-6 ring PAHs	228
C1-chrysenes	4-6 ring PAHs	242
C2-chrysenes	4-6 ring PAHs	256
C3-chrysenes	4-6 ring PAHs	270
C4-chrysenes	4-6 ring PAHs	284

Table H.1 continued

Component	Component group	Target ion
Benzo(b)fluoranthene	4-6 ring PAHs	252
Benzo(k)fluoranthene	4-6 ring PAHs	252
Benzo(e)pyrene	4-6 ring PAHs	252
Benzo(a)pyrene	4-6 ring PAHs	252
Perylene	4-6 ring PAHs	252
Indeno(1,2,3-c,d)pyrene	4-6 ring PAHs	276
Dibenz(a,h)anthracene	4-6 ring PAHs	278
Benzo(g,h,i)perylene	4-6 ring PAHs	276
Internal standards		
Flurorene-d10 (RIS)		176
Naphthalene-d8 (SIS)		136
Phenanthrene-d10 (SIS)		188
Chrysene-d12 (SIS)		240
Perylene-d12 (RIS)		264

Appendix I GC-MS Results

Table I.1 – GC-MS quantification results for pure oil samples

Sample ID	RRF	Troll 1 µg/mL	Troll 2,5 µg/mL	Troll 5 µg/mL	Troll 10 µg/mL	IF380 1 µg/mL	IF380 2,5 µg/mL	IF380 5 µg/mL	IF380 10 µg/mL
d8 naftalen		*0,891*	*0,883*	*0,847*	*0,783*	*0,975*	*0,959*	*0,943*	*0,899*
d10 fenatren		*0,909*	*0,909*	*0,889*	*0,83*	*0,988*	*0,968*	*0,968*	*0,929*
d12 crysene		*0,956*	*0,956*	*0,956*	*0,916*	*0,996*	*1,016*	*1,036*	*1,056*
Decalin	0,262	0,47	1,04	2,05	3,99	0,11	0,23	0,46	0,91
C1-decalins	0,262	1,40	3,17	6,12	11,94	0,17	0,37	0,73	1,41
C2-decalins	0,262	1,33	2,95	5,96	11,72	0,17	0,37	0,82	1,36
C3-decalins	0,262	1,47	3,18	6,53	12,70	0,18	0,43	0,87	1,70
C4-decalins	0,262	1,41	2,78	5,26	11,58	0,00	0,25	0,70	1,30
Benzo(b)thiophene	2,045	0,00	0,02	0,03	0,06	0,00	0,01	0,02	0,05
Naphthalene	1,792	0,86	1,88	3,68	7,13	0,12	0,25	0,51	0,99
C1-naphthalenes	1,792	2,39	5,21	10,24	19,81	0,38	0,84	1,68	3,33
C2-naphthalenes	1,792	3,18	6,89	13,37	25,69	0,54	1,18	2,33	4,60
C3-naphthalenes	1,792	2,41	5,13	9,98	18,91	0,50	1,02	1,94	3,77
C4-naphthalenes	1,792	1,31	2,68	5,68	10,49	0,25	0,56	1,15	2,16
Biphenyl	2,31	0,30	0,66	1,27	2,43	0,03	0,06	0,11	0,22
Acenaphthylene	1,764	0,02	0,00	0,00	0,00	0,00	0,00	0,01	0,00
Acenaphthene	0,997	0,05	0,08	0,17	0,32	0,02	0,04	0,07	0,14
Dibenzofuran	2,564	0,04	0,08	0,15	0,30	0,01	0,01	0,03	0,05
Fluorene	1,259	0,14	0,27	0,57	1,09	0,04	0,08	0,17	0,32
C1-fluorenes	1,259	0,32	0,68	1,33	2,47	0,12	0,24	0,49	0,94
C2-fluorenes	1,259	0,46	1,35	2,53	5,51	0,19	0,39	0,83	1,65
C3-fluorenes	1,259	0,64	1,46	2,98	4,36	0,18	0,45	0,78	1,82
Phenanthrene	2,011	0,32	0,68	1,34	2,61	0,20	0,27	4,58	1,05

Anthracene	1,766	0,00	0,00	0,00	0,00	0,02	0,04	0,00	0,14
C1-phenanthrenes/anthracenes	2,011	0,73	1,56	2,93	5,74	0,33	0,74	1,49	2,98
C2-phenanthrenes/anthracenes	2,011	0,75	1,63	3,27	6,33	0,44	0,99	2,05	4,13
C3-phenanthrenes/anthracenes	2,011	0,56	1,25	2,38	4,88	0,33	0,72	1,59	3,01
C4-phenanthrenes/anthracenes	2,011	0,31	1,14	2,06	3,91	0,21	0,41	0,93	2,01
Dibenzothiophene	2,804	0,03	0,06	0,12	0,24	0,02	0,03	0,10	0,14
C1-dibenzothiophenes	2,804	0,10	0,21	0,42	0,82	0,06	0,15	0,28	0,59
C2-dibenzothiophenes	2,804	0,13	0,26	0,52	0,98	0,12	0,26	0,53	1,05
C3-dibenzothiophenes	2,804	0,11	0,21	0,04	0,88	0,11	0,25	0,48	1,03
C4-dibenzothiophenes	2,804	0,05	0,13	0,22	0,46	0,07	0,15	0,31	0,60
Fluoranthene	2,146	0,02	0,05	0,10	0,19	0,01	0,02	0,04	0,08
Pyrene	2,221	0,04	0,00	0,12	0,22	0,03	0,07	0,13	0,24
C1-fluoranthrenes/pyrenes	2,221	0,17	0,36	0,74	1,38	0,14	0,32	0,55	1,13
C2-fluoranthenes/pyrenes	2,221	0,22	0,49	0,97	1,80	0,20	0,45	0,90	1,73
C3-fluoranthenes/pyrenes	2,221	0,20	0,40	1,00	1,47	0,20	0,45	0,93	1,75
Benz(a)anthracene	1,83	0,01	0,02	0,04	0,07	0,02	0,05	0,10	0,19
Chrysene	1,839	0,05	0,10	0,21	0,40	0,08	0,17	0,34	0,64
C1-chrysenes	1,839	0,12	0,23	0,48	0,87	0,19	0,43	0,88	1,72
C2-chrysenes	1,839	0,12	0,28	0,55	0,95	0,21	0,50	1,06	2,00
C3-chrysenes	1,839	0,00	0,27	0,41	0,84	0,16	0,40	0,76	1,45
C4-chrysenes	1,839	0,00	0,00	0,00	0,67	0,00	0,24	0,41	0,94
Benzo(b)fluoranthene	2,021	0,00	0,02	0,04	0,07	0,02	0,03	0,07	0,13
Benzo(k)fluoranthene	2,023	0,00	0,00	0,00	0,00	0,00	0,00	0,00	0,00
Benzo(e)pyrene	3,138	0,01	0,02	0,03	0,07	0,02	0,05	0,09	0,19
Benzo(a)pyrene	1,867	0,00	0,01	0,01	0,03	0,01	0,02	0,04	0,08
Perylene	2,994	0,01	0,01	0,03	0,05	0,01	0,02	0,05	0,10
Indeno(1,2,3-c,d)pyrene	1,683	0,00	0,00	0,00	0,00	0,00	0,01	0,02	0,03
Dibenz(a,h)anthracene	1,558	0,00	0,00	0,00	0,02	0,01	0,02	0,03	0,07
Benzo(g,h,i)perylene	1,957	0,00	0,01	0,02	0,03	0,01	0,03	0,06	0,11

Table I.1 continued

Sample ID	RRF	Troll 1 µg/mL	Troll 2,5 µg/mL	Troll 5 µg/mL	Troll 10 µg/mL	IF380 1 µg/mL	IF380 2,5 µg/mL	IF380 5 µg/mL	IF380 10 µg/mL
Fluorene-d10 concentration	1,003								
Sum all compounds		*22*	*49*	*96*	*186*	*6*	*14*	*32*	*56*
C10-saturates		*6*	*13*	*26*	*52*	*1*	*2*	*4*	*7*
Naphthalenes		*10*	*22*	*43*	*82*	*2*	*4*	*8*	*15*
2-3 ring PAHs		*5*	*12*	*22*	*43*	*2*	*5*	*15*	*22*
4-6 ring PAHs		*1*	*2*	*5*	*9*	*1*	*3*	*6*	*13*

Table I.2 – GC-MS Quantification results of sediment extracts

Sample ID	RRF	LIS-002-1	LIS-002-2	LIS-002-7	LIS-009-1	LIS-009-2	LIS-009-3	LIS-010-2	LIS-010-3	LIS-010-5
d8 naftalen		*0,273*	*0,297*	*0,405*	*0,289*	*0,381*	*0,393*	*0,546*	*0,482*	*0,494*
d10 fenatren		*0,692*	*0,613*	*0,83*	*0,731*	*0,712*	*0,81*	*0,81*	*0,81*	*0,87*
d12 crysene		*0,857*	*0,737*	*0,956*	*1,016*	*0,956*	*0,996*	*0,976*	*0,916*	*1,036*
Decalin	0,262	0,03	0,02	0,22	0,04	0,04	0,03	0,14	0,21	0,11
C1-decalins	0,262	0,20	0,12	0,48	0,00	0,00	0,00	0,39	0,59	0,24
C2-decalins	0,262	0,64	0,54	0,53	0,00	0,63	0,33	0,50	0,84	0,23
C3-decalins	0,262	2,68	2,14	1,19	0,00	1,18	0,74	0,91	1,34	0,43
C4-decalins	0,262	6,07	6,51	2,66	0,00	1,03	1,65	1,61	2,48	1,32
Benzo(b)thiophene	2,045	0,00	0,00	0,00	0,00	0,00	0,00	0,00	0,00	0,00
Naphthalene	1,792	0,07	0,05	0,38	0,27	0,53	0,20	0,25	0,31	0,15
C1-naphthalenes	1,792	0,88	1,11	0,77	0,66	1,34	0,97	0,51	0,96	0,28
C2-naphthalenes	1,792	4,29	5,90	3,63	1,60	2,62	2,56	2,35	3,23	1,46
C3-naphthalenes	1,792	8,56	10,70	8,10	3,11	4,31	4,09	4,78	5,14	4,14
C4-naphthalenes	1,792	7,04	8,38	7,49	2,80	3,61	3,33	4,05	4,13	4,04
Biphenyl	2,31	0,14	0,21	0,13	0,05	0,10	0,07	0,10	0,15	0,05
Acenaphthylene	1,764	0,00	0,00	0,05	0,01	0,02	0,02	0,03	0,04	0,02
Acenaphthene	0,997	0,00	0,00	0,00	0,06	0,09	0,09	0,00	0,04	0,00
Dibenzofuran	2,564	0,05	0,07	0,07	0,03	0,04	0,04	0,04	0,05	0,04
Fluorene	1,259	0,28	0,36	0,30	0,24	0,35	0,31	0,22	0,22	0,16
C1-fluorenes	1,259	1,65	1,95	1,82	1,22	1,61	1,40	1,03	0,92	0,96
C2-fluorenes	1,259	2,96	3,58	3,16	2,79	3,46	3,18	1,74	1,51	1,98
C3-fluorenes	1,259	2,44	3,14	2,89	3,86	3,63	3,48	1,63	1,45	1,63
Phenanthrene	2,011	1,82	2,11	2,02	1,37	1,60	1,44	1,19	1,15	1,25
Anthracene	1,766	0,00	0,00	0,00	0,21	0,27	0,23	0,00	0,00	0,00
C1-phenanthrenes/anthracenes	2,011	5,62	5,89	5,60	5,65	6,28	5,54	3,29	2,98	3,80
C2-phenanthrenes/anthracenes	2,011	6,27	6,96	6,65	8,43	9,62	7,87	3,75	3,41	4,29

Table I.2 continued

Sample ID	RRF	LIS-002-1	LIS-002-2	LIS-002-7	LIS-009-1	LIS-009-2	LIS-009-3	LIS-010-2	LIS-010-3	LIS-010-5
C3-phenanthrenes/anthracenes	2,011	4,54	5,34	4,83	6,69	7,21	6,02	2,63	2,40	3,05
C4-phenanthrenes/anthracenes	2,011	3,25	4,01	3,79	4,15	5,06	4,08	1,83	1,86	2,32
Dibenzothiophene	2,804	0,15	0,17	0,16	0,18	0,21	0,19	0,10	0,09	0,10
C1-dibenzothiophenes	2,804	0,76	0,85	0,82	1,00	1,15	1,04	0,45	0,40	0,50
C2-dibenzothiophenes	2,804	1,00	1,14	1,02	2,08	2,30	1,97	0,58	0,55	0,68
C3-dibenzothiophenes	2,804	0,84	0,94	0,93	2,05	2,48	1,81	0,51	0,50	0,57
C4-dibenzothiophenes	2,804	0,45	0,48	0,49	1,29	1,39	1,22	0,27	0,24	0,31
Fluoranthene	2,146	0,26	0,27	0,30	0,25	0,27	0,23	0,20	0,27	0,34
Pyrene	2,221	0,24	0,29	0,31	0,50	0,56	0,50	0,20	0,25	0,35
C1-fluoranthrenes/pyrenes	2,221	1,14	1,42	1,35	2,04	2,23	2,05	0,73	0,73	0,88
C2-fluoranthenes/pyrenes	2,221	1,23	1,37	1,33	3,12	3,48	3,11	0,71	0,71	0,88
C3-fluoranthenes/pyrenes	2,221	0,70	1,03	1,17	2,74	3,92	3,30	0,41	0,59	0,45
Benz(a)anthracene	1,83	0,10	0,09	0,10	0,38	0,45	0,37	0,07	0,12	0,34
Chrysene	1,839	0,43	0,45	0,45	1,21	1,36	1,20	0,26	0,34	0,60
C1-chrysenes	1,839	0,80	0,86	0,76	2,86	0,00	2,92	0,45	0,46	0,62
C2-chrysenes	1,839	0,84	0,97	0,83	3,27	3,56	3,59	0,54	0,46	0,66
C3-chrysenes	1,839	0,57	0,67	0,48	2,57	3,32	2,88	0,35	0,33	0,44
C4-chrysenes	1,839	0,38	0,42	0,32	1,56	1,78	1,92	0,25	0,25	0,30
Benzo(b)fluoranthene	2,021	0,12	0,11	0,11	0,28	0,29	0,26	0,07	0,16	0,42
Benzo(k)fluoranthene	2,023	0,07	0,06	0,07	0,11	0,12	0,08	0,05	0,13	0,42
Benzo(e)pyrene	3,138	0,08	0,08	0,09	0,32	0,36	0,31	0,05	0,10	0,22
Benzo(a)pyrene	1,867	0,08	0,07	0,08	0,20	0,22	0,17	0,05	0,15	0,51
Perylene	2,994	0,05	0,05	0,05	0,19	0,21	0,19	0,03	0,04	0,11
Indeno(1,2,3-c,d)pyrene	1,683	0,05	0,05	0,05	0,09	0,09	0,07	0,04	0,11	0,36
Dibenz(a,h)anthracene	1,558	0,01	0,00	0,00	0,00	0,00	0,00	0,01	0,00	0,05
Benzo(g,h,i)perylene	1,957	0,06	0,07	0,07	0,25	0,26	0,23	0,04	0,12	0,33

Fluorene-d10 concentration (µg/mL)	1,003									
Sum all compounds		70	81	68	72	85	77	39	43	42
C10-saturates		10	9	5	0	3	3	4	5	2
Naphthalenes		21	26	20	8	12	11	12	14	10
2-3 ring PAHs		32	37	35	41	47	40	19	18	22
4-6 ring PAHs		7	8	8	22	22	23	5	5	8

Table I.3 – GC-MS Quantification results of water extracts

Sample ID	RRF	LIS-002-1-VANN	LIS-002-2-VANN	LIS-002-7-VANN	LIS-009-1-VANN	LIS-009-2-VANN	LIS-009-3-VANN	LIS-010-2-VANN	LIS-010-3-VANN	LIS-010-5-VANN
d8 naftalen		*0,55*	*0,401*	*0,63*	*0,53*	*0,622*	*0,397*	*0,542*	*0,574*	*0,682*
d10 fenatren		*0,81*	*0,593*	*0,771*	*0,791*	*0,81*	*0,593*	*0,751*	*0,771*	*0,83*
d12 crysene		*0,936*	*0,797*	*0,896*	*0,996*	*0,956*	*0,777*	*0,896*	*0,896*	*0,976*
Decalin	0,262	0,17	0,28	0,10	0,00	0,00	0,00	0,16	0,14	0,90
C1-decalins	0,262	0,18	0,32	0,11	0,00	0,00	0,00	0,17	0,00	1,24
C2-decalins	0,262	0,08	0,14	0,06	0,00	0,00	0,00	0,07	0,00	0,69
C3-decalins	0,262	0,00	0,00	0,00	0,00	0,00	0,00	0,00	0,00	0,39
C4-decalins	0,262	0,00	0,00	0,00	0,00	0,00	0,00	0,00	0,00	0,21
Benzo(b)thiophene	2,045	0,03	0,04	0,02	0,05	0,06	0,07	0,03	0,03	0,02
Naphthalene	1,792	7,79	12,33	4,97	0,92	1,19	1,35	10,57	11,23	7,30
C1-naphthalenes	1,792	21,70	33,29	13,49	2,41	2,98	3,59	27,88	29,14	17,71
C2-naphthalenes	1,792	14,50	21,71	11,15	1,49	1,96	2,16	19,58	20,23	14,56
C3-naphthalenes	1,792	5,83	8,58	4,64	0,85	0,86	1,13	7,39	7,49	6,04
C4-naphthalenes	1,792	1,38	2,84	1,35	0,24	0,27	0,34	1,82	1,70	1,46
Biphenyl	2,31	2,12	3,23	1,63	0,12	0,17	0,18	2,87	3,05	2,12
Acenaphthylene	1,764	0,00	0,06	0,04	0,01	0,00	0,01	0,05	0,05	0,04
Acenaphthene	0,997	0,28	0,43	0,22	0,07	0,10	0,11	0,36	0,39	0,29
Dibenzofuran	2,564	0,29	0,44	0,23	0,03	0,04	0,05	0,37	0,39	0,30
Fluorene	1,259	1,12	1,73	0,91	0,21	0,24	0,30	1,41	1,44	1,16
C1-fluorenes	1,259	1,31	1,97	1,13	0,32	0,32	0,43	1,54	1,50	1,32
C2-fluorenes	1,259	3,50	6,68	4,65	0,30	0,32	0,42	5,05	0,00	2,96
C3-fluorenes	1,259	2,97	3,74	3,24	0,18	0,16	0,18	3,18	3,08	2,84
Phenanthrene	2,011	1,88	2,86	1,74	0,45	0,46	0,62	2,23	2,20	2,08
Anthracene	1,766	0,00	0,00	0,00	0,05	0,05	0,07	0,00	0,00	0,00
C1-phenanthrenes/anthracenes	2,011	1,70	2,53	1,59	0,64	0,63	0,86	1,82	1,87	1,85

C2-phenanthrenes/anthracenes	2,011	0,86	1,14	0,78	0,33	0,32	0,47	0,72	0,79	0,82
C3-phenanthrenes/anthracenes	2,011	0,41	0,72	0,43	0,11	0,09	0,13	0,47	0,39	0,30
C4-phenanthrenes/anthracenes	2,011	0,22	0,42	0,00	0,00	0,00	0,00	0,33	0,28	0,24
Dibenzothiophene	2,804	0,19	0,29	0,18	0,06	0,07	0,09	0,23	0,23	0,21
C1-dibenzothiophenes	2,804	0,24	0,38	0,25	0,13	0,13	0,18	0,28	0,26	0,26
C2-dibenzothiophenes	2,804	0,12	0,19	0,12	0,09	0,08	0,12	0,12	0,14	0,12
C3-dibenzothiophenes	2,804	0,04	0,00	0,00	0,04	0,04	0,05	0,00	0,00	0,00
C4-dibenzothiophenes	2,804	0,00	0,00	0,00	0,00	0,00	0,00	0,00	0,00	0,00
Fluoranthene	2,146	0,05	0,06	0,05	0,03	0,03	0,03	0,06	0,05	0,06
Pyrene	2,221	0,04	0,05	0,04	0,04	0,04	0,05	0,04	0,04	0,04
C1-fluoranthrenes/pyrenes	2,221	0,14	0,17	0,13	0,06	0,06	0,08	0,15	0,14	0,15
C2-fluoranthenes/pyrenes	2,221	0,29	0,37	0,28	0,05	0,04	0,06	0,00	0,22	0,21
C3-fluoranthenes/pyrenes	2,221	0,25	0,23	0,24	0,00	0,00	0,00	0,26	0,23	0,26
Benz(a)anthracene	1,83	0,02	0,03	0,00	0,01	0,01	0,01	0,01	0,01	0,00
Chrysene	1,839	0,02	0,03	0,02	0,02	0,02	0,03	0,02	0,03	0,02
C1-chrysenes	1,839	0,03	0,03	0,03	0,02	0,02	0,02	0,12	0,03	0,03
C2-chrysenes	1,839	0,00	0,00	0,00	0,00	0,00	0,00	0,00	0,00	0,00
C3-chrysenes	1,839	0,00	0,00	0,00	0,00	0,00	0,00	0,00	0,00	0,00
C4-chrysenes	1,839	0,00	0,00	0,00	0,00	0,00	0,00	0,00	0,00	0,00
Benzo(b)fluoranthene	2,021	0,00	0,00	0,00	0,00	0,00	0,00	0,00	0,00	0,00
Benzo(k)fluoranthene	2,023	0,00	0,00	0,00	0,00	0,00	0,00	0,00	0,00	0,00
Benzo(e)pyrene	3,138	0,00	0,00	0,00	0,00	0,00	0,00	0,00	0,00	0,00
Benzo(a)pyrene	1,867	0,00	0,00	0,00	0,00	0,00	0,00	0,00	0,00	0,00
Perylene	2,994	0,00	0,00	0,00	0,00	0,00	0,00	0,00	0,00	0,00
Indeno(1,2,3-c,d)pyrene	1,683	0,00	0,00	0,00	0,00	0,00	0,00	0,00	0,00	0,00
Dibenz(a,h)anthracene	1,558	0,00	0,00	0,00	0,00	0,00	0,00	0,00	0,00	0,00
Benzo(g,h,i)perylene	1,957	0,00	0,00	0,00	0,00	0,00	0,00	0,00	0,00	0,00
Fluorene-d10 concentration (µg/mL)	1,003									

Table I.3 continued

Sample ID	RRF	LIS-002-1-VANN	LIS-002-2-VANN	LIS-002-7-VANN	LIS-009-1-VANN	LIS-009-2-VANN	LIS-009-3-VANN	LIS-010-2-VANN	LIS-010-3-VANN	LIS-010-5-VANN
Sum all compounds		70	107	54	9	11	13	89	87	68
C10-saturates		0	1	0	0	0	0	0	0	3
Naphthalenes		51	79	36	6	7	9	67	70	47
2-3 ring PAHs		17	27	17	3	3	4	21	16	17
4-6 ring PAHs		1	1	1	0	0	0	1	1	1